Loss of LasR function reshapes inter-species interactions in a polymicrobial cystic fibrosis airway model

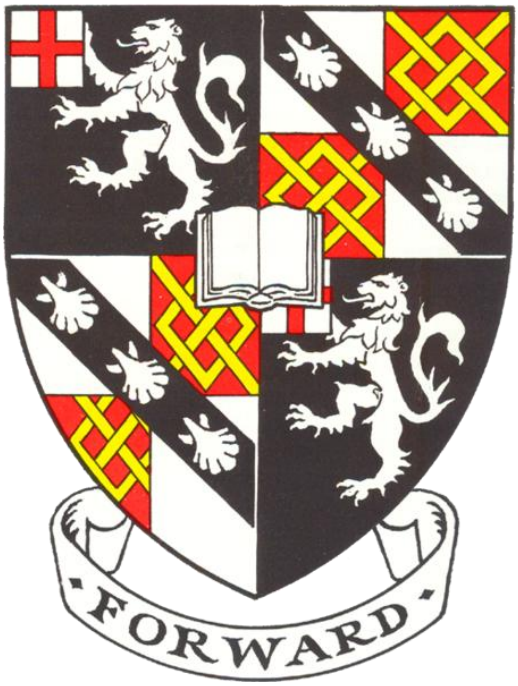

Dr Éva Bernadett Bényei

Churchill College

October 2024

This thesis is submitted for the degree of Doctor of Philosophy.

Declaration

This thesis is the result of my own work and includes nothing which is the outcome of work done in collaboration except as declared in the preface and specified in the text.

It is not substantially the same as any work that has already been submitted, or, is being concurrently submitted, for any degree, diploma or other qualification at the University of Cambridge or any other University or similar institution except as declared in the preface and specified in the text.

It does not exceed the prescribed word limit for the relevant Degree Committee.

Preface

This dissertation presents an overview of the four years of research I conducted in the Welch Laboratory. It has been an incredibly formative experience, and I believe I have gained invaluable knowledge and skills throughout this journey. The completion of this work, including the writing of this document, would not have been possible without the support and contributions of many individuals and initiatives, for which I express my heartfelt gratitude in the Acknowledgement. However, there are a few key individuals and programs that I wish to mention here, as their specific collaborations played an important role in shaping my project.

My collaboration with Anastasios Galanis was essential in allowing me to delve deeply into RNA sequencing data analysis. He introduced me to the fundamentals, from accessing the high-performance computing (HPC) facility to constructing a pipeline for analysis. Over the course of two weeks of daily meetings, he took a step-by-step approach to guide me in building a custom analysis pipeline for my data, offering continuous feedback on my ideas. His support extended beyond those initial sessions, as he remained readily available for additional guidance and kindly reviewed the final versions of the relevant sections. An equally significant contribution came from Rahan Nazeer, who generated the mutants for this project. The *Pseudomonas aeruginosa* mutants he created include the ΔPA3904-08 mutant, the Δ*lasR*+PA3904-08 mutant, and the Δ*lasR*+Empty mutant. Collaboration of this kind is a hallmark of the host laboratory, where I also had the opportunity to contribute to other projects by sharing my expertise about, for example, the continuous-flow experimental setup and preparation of ASM. Another key contributor was my colleague, Pok-Man Ho, whose expertise in R and other computational tools proved invaluable. His guidance, coupled with his constant availability, not only benefited me but also helped many other members of the lab to improve their precision and efficiency in computational approaches. Dr Leonardo Mancini was also a great help, particularly in organising the whole genome sequencing (WGS), coordinating with MicrobesNG, and providing guidance during the sample collection process.

In addition to my colleagues, I would also like to acknowledge a few programs that have been instrumental in helping me communicate my ideas and results more effectively. First, BioRender offered an exceptional platform for creating visuals that truly speak louder than words. Additionally, GraphPad Prism allowed for seamless customisation of graphs, ensuring both clarity and consistency across my work. Finally, I would like to acknowledge the use of

large language models for assisting with proofreading and polishing the final version of my dissertation. This was done in full compliance with university guidelines, following a detailed discussion with my Supervisor, and in line with the recommendations from the "*Introduction to Ethical AI for Academic Writing and Research*" workshop. I used Grammarly to address spelling, punctuation, and word choice, while ChatGPT-4o was employed to suggest enhancements in grammar, sentence structure, clarity, and coherence. Crucially, throughout these processes, the content remained unchanged, ensuring that the writing reflected my own work and ideas.

Overall, the various forms of support described here enhanced my work, helping me achieve outcomes that would have been challenging to reach on my own.

Acknowledgement

Many people contributed to my journey in Cambridge, and I am deeply grateful for all the discussions and shared experiences I had the privilege to be part of.

First and foremost, I owe immense thanks to the Welch lab. I am especially grateful to my Supervisor, Professor Martin Welch, for offering me this invaluable opportunity, for his insightful suggestions and feedback, and for fostering a joyful atmosphere in the lab.

I would like to thank all the past and present members of the Welch lab, not only for the countless laughs we shared and stimulating discussions we had but also for their patience and assistance over the years. I would like to especially express my gratitude to the following people: Dr Thomas O'Brien (a true pioneer) for showing me how the 'system' works and for all the advice that helped me settle in; Rahan Nazeer (an exceptional scientific talent) for our collaborations, his treasured suggestions and providing the mutants for this project; Pok-Man Ho (an extraordinary computer wizard) for all the programming assistance and help with computational queries; Dr Meng Wang (a role model of scientific professionalism) for her guidance and for being my "late-night buddy"; Dr Isabel Askenasy Flores (a proficient scientific expert) for her smiles, technical help, and friendly chats; Jemima Swain (a master of both science and baking) for her company and delightful discussions; Dr Leonardo Mancini (who masterfully blends biology and physics) for the collaborative work and organising the WGS; Dr Stephen Trigg (who always lands on his feet with great success) for his wisdom and thoughts about work and life; Joshua Western (the calmest person I have ever met) for the last-minute orders and helping hands; Dr Wendy Figueroa Chavez (an icon) for her encouragement and warm, welcoming attitude; Dr Yue Yuan On (a fantastic scientist) for the welcoming friendly and fun discussions; and Dr Sivan Nir (a true superwoman) for her uplifting personality and great conversations.

I would also like to thank Anastasios Galanis from the Maori Group for teaching me about transcriptomic data analysis and collaboratively designing the used pipeline; Caia D.S. Duncan from the Mata Group for her assistance and insights regarding RNA purification; Dr Ashraf Zarkan from the Zarkan Group for all the constructive feedback and useful advices; and Dr Camilla Godlee from the Godlee Group for her wonderful personality and thoughtful comments.

I would like to extend my thanks to all members and staff of Churchill College. A special thanks goes to Rebecca Sawalmeh and Dr Elizabeth DeMarrais for always being there and for their support and assistance.

I could not have completed this journey without the support of my friends and family. I am incredibly grateful to the following people: my housemates from 70 Storey's Way – especially Andreas, Richard, Cathy, and Renato – who not only welcomed me but also shared the "COVID experience" with me, turning it into an enjoyable time that created lifelong bonds; Greicy, who became my true friend in the lab and beyond, offering me her unconditional support; Michaela, with whom we experienced both the highs and lows of the MCR Executive Committee, while always remaining dear friends; Amila and Hasini, great friends who have constantly provided supported and have been there to both help and celebrate together; Ana Sofia, who always brightened discussions with her fantastic insights; and Fran, who brought new perspectives into every conversation.

I am also endlessly grateful to my friends in Hungary and around the world. Thank you for staying connected and relentlessly flourishing our friendships despite the geographical distances.

I am also deeply grateful for my family – especially Mom, Dad and my brother, Daniel – who always provided unwavering support and encouragement throughout this project. I could not have succeeded without their love, help, and constant reassurance.

My heartfelt thanks go to Soma for his unshakable love, boundless patience, and constant inspiration every day.

Finally, I would like to express my sincere gratitude to my funding bodies, the Oliver Gatty PhD Studentship and the Laszlo Solyom Studentship, for enabling me to work on this PhD project. I am also thankful to the Microbiology Society, Churchill College, the Cambridge Philosophical Society, and other organisations for their generous support for my many conference attendances.

Abstract

The airways of people with cystic fibrosis (CF) exhibit a particular predilection for infection by certain opportunistic pathogens. One such interloper is *Pseudomonas aeruginosa*, a WHO high-priority pathogen, infamous for its ability to evade antibiotic clearance. However, *P. aeruginosa* often has to share the airway environment with a variety of other microbes: these are polymicrobial infections. We now know that the interactions between co-habiting Gram-negative, Gram-positive, and fungal species can significantly impact the outcomes of these airway infections. Factors like intra-species genetic variation and (potentially existential) environmental challenges such as antibiotic treatment further complicate the situation. However, our understanding of the biology underpinning the microbial responses in such complex environments remains limited.

In this study, I investigate the impact of loss-of-function of a gene (*lasR*) that is frequently mutated in CF isolates of *P. aeruginosa*, and also the impact of anti-pseudomonal drugs on a polymicrobial ecosystem populated by a representative selection of CF-associated microbes. To do this, I utilise an *in vitro* continuous-flow system that faithfully captures many of the microbial dynamics seen in CF patients. Using artificial sputum medium, this robust experimental platform enables the stable co-culture of *P. aeruginosa* alongside two other CF airway pathogens: *Staphylococcus aureus* and *Candida albicans*.

I demonstrate that *P. aeruginosa* has the highest abundance in the studied polymicrobial community. Unexpectedly, the transcriptome of 'wild-type' *P. aeruginosa* was only minorly altered in the presence of other species, whereas the transcriptome of a *lasR* mutant showed substantial changes in the polymicrobial scenario. Furthermore, I found that the population dynamics of the *lasR* mutant, in co-culture with the 'wild-type', were very similar to those seen in people with CF (with the *lasR* mutant never exceeding ca. 10% of the overall *P. aeruginosa* titres). One key LasR-regulated gene cluster that was affected in the *lasR* mutant was the *tseT* operon, which encodes a component of the Type VI Secretion System. However, I found that this secretion system apparently plays little obvious role in constraining *lasR* mutant titres. I also investigated the susceptibility of *P. aeruginosa* to clinically-deployed antibiotics. I found that *P. aeruginosa* exhibits reduced susceptibility to ciprofloxacin in the presence of other co-habiting species and that treatment with ciprofloxacin and colistin combined leads to a long-

term increase in titres of the fungus, *C. albicans*. This “fungal blooming” was linked with expression of the *tseT* operon.

In summary, my work shows the importance of considering not only inter-species variation in the response to antibiotic challenge, but also intra-species variation. This is important because although CF-associated infections are often associated with single clones of *P. aeruginosa*, these clonally-derived populations often display significant genetic diversity.

Abbreviations

AHL	Acyl-homoserine lactone
ASM	Artificial Sputum Media
BHL	*N*-butanoyl-L-homoserine lactone or C4-HSL
BiGGY agar	Bismuth Glycine Glucose Yeast agar
CDI	Contact-dependent Inhibition
CDS	Coding Sequences
CF	Cystic Fibrosis
CFTR	Cystic Fibrosis Transmembrane Conductance Regulator
CFU	Colony-forming unit
DMSO	Dimethyl sulfoxide
FC	Fold Change
FEV_1	Forced Expiratory Volume in 1 second
GlcNAc	*N*-acetyl glucosamine
HAQs	4-hydroxy-2-alkylquinolines
HHQ	2-heptyl-4-hydroxyquinoline
HPC	High-performance Computing
HQNO	2-heptyl-4-hydroxyquinoline *N*-oxide
IPTG	Isopropyl β-D-1-thiogalactopyranoside
IV	Intravenous
LB	Luria-Bertani
MCL	Markov Cluster Algorithm
MIC	Minimum Inhibitory Concentration
MSA	Mannitol Salt Agar
OD	Optical Density
OdDHL	*N*-(3-oxododecanoyl)-L-homoserine lactone or 3-oxo-C12-HSL
PBS	Phosphate-buffered Saline
PCA	Principal Component(s) Analysis
PEx	Pulmonary Exacerbations

PIA	Pseudomonas Isolation Agar
PQS	2-heptyl-3-hydroxy-4(1H)-quinolone or Pseudomonas quinolone signal
pwCF	People with CF
QC	Quality Control
QS	Quorum Sensing
RIN	RNA Integrity Number
ROS	reactive oxygen species
SCFM	Synthetic Cystic Fibrosis Sputum
SCVs	Small-colony variants
T6SS	Type VI Secretion System
WGS	Whole Genome Sequencing
WHO	World Health Organization
WT	Wild type

Table of Contents

Introduction 15

1.1. Cystic fibrosis 15

1.1.1. Pathophysiology and lung-associated infections 15

1.1.2. Diversity of microbial communities in the airways 18

1.2. *Pseudomonas aeruginosa* 22

1.2.1. General characteristics 22

1.2.2. Quorum sensing 23

1.2.3. Type VI Secretions Systems 26

1.2.4. Iron homeostasis 29

1.3. Clinical relevance of *Pseudomonas aeruginosa* in cystic fibrosis 30

1.3.1. Common mutant derivates in clinical samples 30

1.3.2. Anti-pseudomonal treatment 33

1.4. Investigating polymicrobial infection scenarios 36

1.4.1. Considerations and challenges in research design 36

1.4.2. Models of CF lung microbiology 39

1.5. Polymicrobial interactions in the cystic fibrosis lung 43

1.5.1. Examples of bacterial interactions 43

1.5.2. Examples of interkingdom interactions: bacteria and fungi 45

Thesis 49

Materials and methods 51

3.1. Microbial strains and routine culture conditions 51

3.2. Growth media and solutions 51

3.3. Whole genome sequencing 60

3.4. Growth in the continuous-flow culture model 60

3.4.1. Setup 61

3.4.2. Inoculation and growth 61
3.5. Sample collection and processing 63
3.5.1. Colony-forming unit enumeration 63
3.5.2. Processing and storage 63
3.5.3. Imaging 66
3.6. Transcriptomic analysis 66
3.6.1. RNA extraction 68
3.6.2. Library preparation and sequencing 68
3.6.3. Data analysis 69
3.7. Quorum sensing molecule quantification 70
3.8. Co-culturing of *Pseudomonas aeruginosa* genetic variants in the continuous-flow system 71
3.9. Co-culturing of microbes in microtiter plate-based cultures 71
3.10. Antibiotic challenge 72
3.10.1. Minimum inhibitory concentration 72
3.10.2. Antimicrobial perturbation of steady-state cultures 72
3.10.3. Susceptibility of isolates from polymicrobial culture 73
3.11. Statistical analysis 73
Transcriptional profile of *Pseudomonas aeruginosa* genetic variants 76
4.1. Background and rationale 76
4.2. Non-disturbed polymicrobial cultures 77
4.2.1. 'Wild-type' *Pseudomonas aeruginosa* $PAO1_{MW}$ 77
4.2.2. Δ*lasR* mutant 80
4.3. Whole genome sequencing 80
4.4. Transcriptome profiling 83
4.4.1. Comparative analysis of $PAO1_{MW}$ mono- and polymicrobial culture samples 86

4.4.2. Comparative analysis of Δ*lasR* mutant mono- and polymicrobial culture 91
4.4.3. Comparative analysis of $PAO1_{MW}$ and Δ*lasR* mutant cultures 98
4.4.4. Transcriptomic landscape in the literature 104
4.5. QS molecules 105
4.6. Discussion 107
Polyclonal co-cultures of *Pseudomonas aeruginosa* strains 112
5.1. Background and rationale 112
5.2. Co-cultures of 'wild-type' $PAO1_{MW}$ and Δ*lasR* mutant 114
5.3. Role of the *tseT* operon in co-cultures 114
5.3.1. ΔPA3904-08 mutant 116
5.3.2. Little role in policing mechanisms 116
5.4. *tseT* operon affecting polymicrobial dynamics 122
5.5. Discussion 126
Polymicrobial cultures and anti-pseudomonal challenge 131
6.1. Background and rationale 131
6.2. Antibiotics and minimal inhibitory concentration 132
6.3. Antibiotic monotherapy 134
6.3.1. *Pseudomonas aeruginosa* $PAO1_{MW}$ 134
6.3.2. *Pseudomonas aeruginosa* Δ*lasR* mutant 136
6.4. Combined antibiotic therapy 139
6.4.1. Changing community dynamics 139
6.4.2. Fungal bloom 141
6.4.3. Impact of Δ*lasR* mutants 146
6.5. Investigating the background of the blooming phenomenon 148
6.5.1. Absence of *tseT* operon prevents *Candida* blooming 150
6.5.2. Verification of results using Δ*lasR*+PA3904-08 mutant 150

6.6. Discussion 153

Final conclusion 157

7.1. *lasR* is a keystone gene for *P. aeruginosa* 157

7.2. Limitations of the project 160

7.3. Future directions 161

References 163

Appendix 214

Supplementary Table A. 214

Supplementary Table B. 217

Supplementary Table C. 238

Supplementary Table D. 238

Chapter 1

Introduction

1.1. Cystic fibrosis

1.1.1. Pathophysiology and lung-associated infections

Cystic fibrosis (CF) is a recessive inherited genetic disease affecting the respiratory, gastrointestinal, and other systems, as illustrated in *Figure 1.1* (Cystic Fibrosis Foundation, 2024; Shteinberg *et al.*, 2021). Globally, over 100,000 individuals have already been diagnosed with CF, including approximately 11,000 people in the UK and 40,000 people in the United States (Cystic Fibrosis Foundation, 2024; Cystic Fibrosis Trust, 2024). CF affects individuals of all racial and ethnic backgrounds, although it is often described as more common among Caucasians (McGarry & McColley, 2021; Naito *et al.*, 2023).

CF is caused by mutations in the cystic fibrosis transmembrane conductance regulator (CFTR) gene (Riordan *et al.*, 1989). Over 2,000 mutations have been identified, displaying various molecular, cellular, and functional phenotypes (CFTR2, 2023; Veit *et al.*, 2016). There have been several different classifications over the years. Currently, these mutations are categorised into five groups, representing various aspects of malfunctioning or mistargeting the epithelial chloride/bicarbonate pump, CFTR (McGarry & McColley, 2021). The details of the mutation classes are shown in *Figure 1.2*. Notably, an individual can have more than one mutation. The most common CFTR genotype is the ΔF508 variant of Class II, present in 85-90% of CF alleles (Françoise & Héry-Arnaud, 2020; Veit *et al.*, 2016).

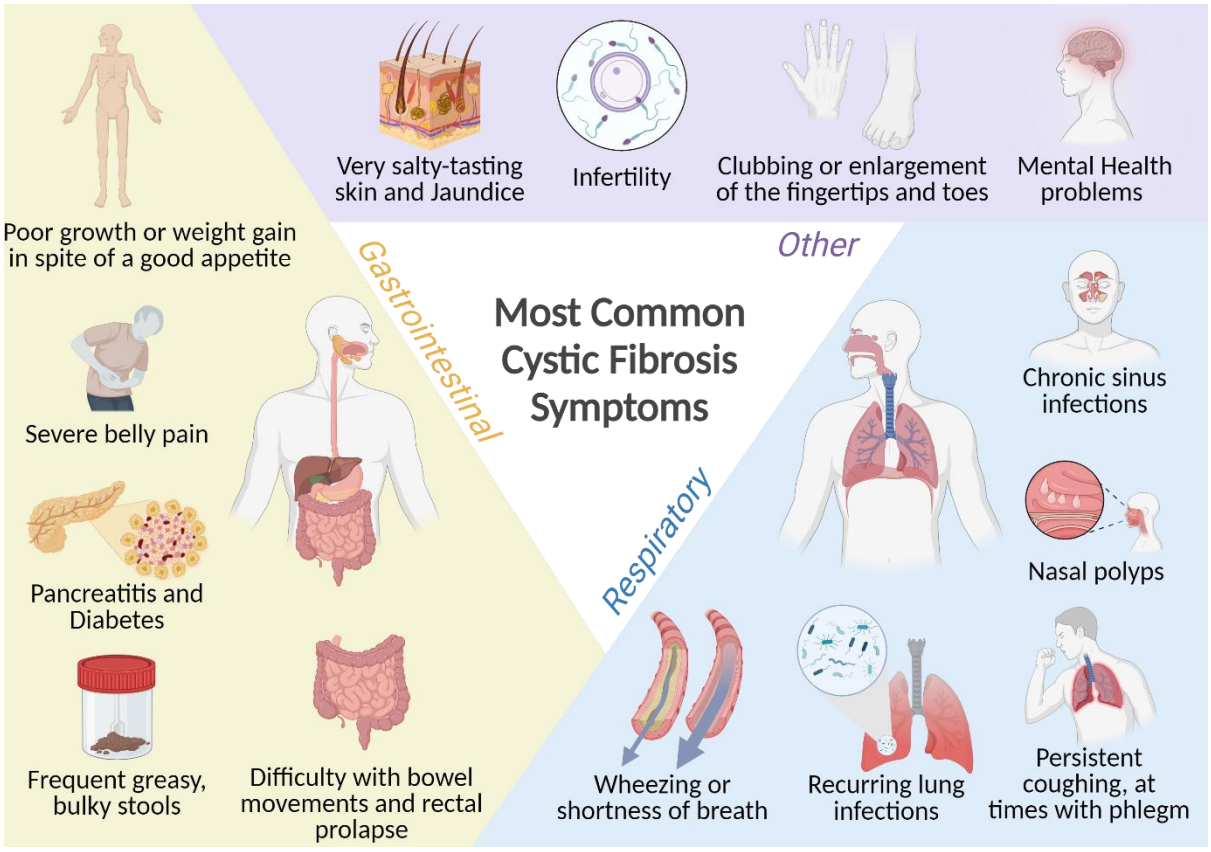

Figure 1.1. **Illustration of the most common symptoms of cystic fibrosis.** CF is a multisystemic disease that affects multiple organs in the human body. According to the CF Foundation, clinical symptoms can vary between individuals (Cystic Fibrosis Foundation, 2024). The most common symptoms occur in the respiratory (blue background) and the gastrointestinal (yellow background) systems, whereas some affect other organs (purple background). Created with *BioRender.com*.

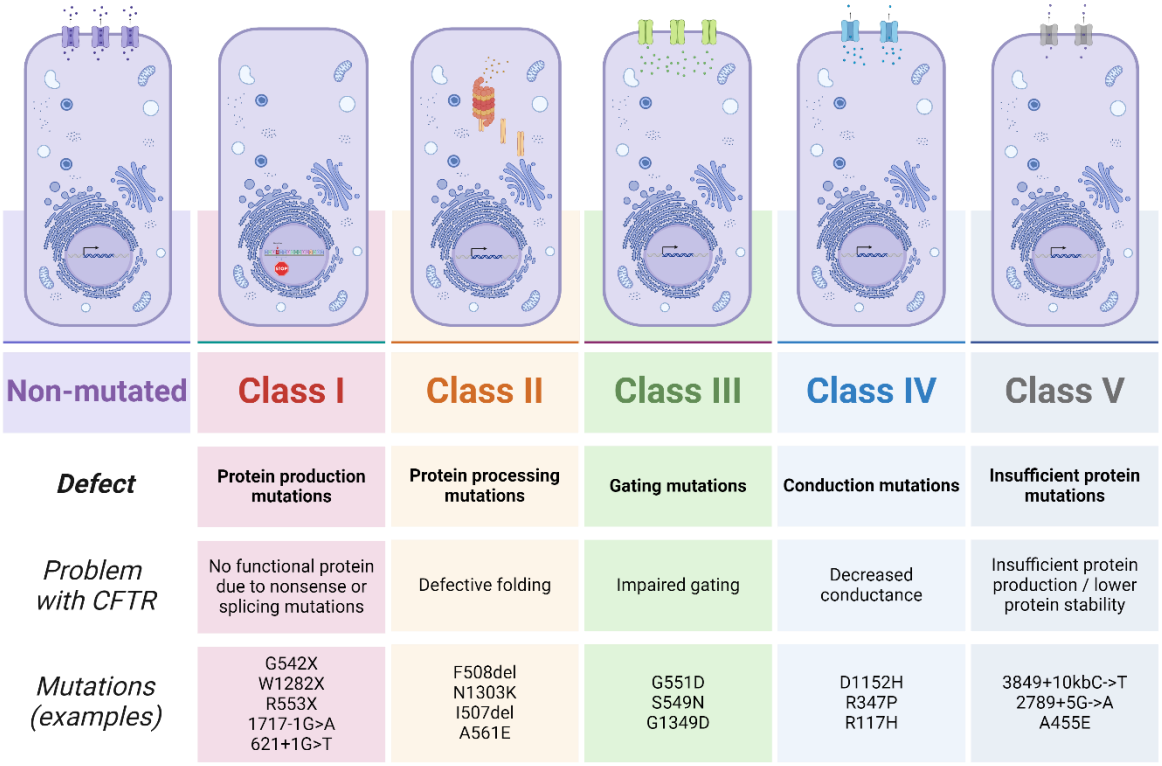

	Non-mutated	Class I	Class II	Class III	Class IV	Class V
Defect		**Protein production mutations**	**Protein processing mutations**	**Gating mutations**	**Conduction mutations**	**Insufficient protein mutations**
Problem with CFTR		No functional protein due to nonsense or splicing mutations	Defective folding	Impaired gating	Decreased conductance	Insufficient protein production / lower protein stability
Mutations (examples)		G542X W1282X R553X 1717-1G>A 621+1G>T	F508del N1303K I507del A561E	G551D S549N G1349D	D1152H R347P R117H	3849+10kbC->T 2789+5G->A A455E

Figure 1.2. **Classification of cystic fibrosis transmembrane conductance regulator mutations.** In a healthy individual, the CFTR protein is produced and then transported to the apical surface of epithelial cells, where it functions as a bicarbonate and chloride channel. Mutations causing CF lead to reduced or non-functional CFTR protein and are classified into five groups based on their specific impact on CFTR protein production. The illustration of the epithelial cell demonstrates the abnormality of the CFTR protein compared with its normal state. The columns also include information about the associated issues with the CFTR protein and provide examples of mutations. Created with *BioRender.com*.

CF manifests across a broad spectrum of health conditions, with most morbidity and mortality linked to the respiratory tract (King *et al.*, 2022). The production of thicker airway mucus and impaired mucociliary clearance makes people with CF (pwCF) more susceptible to microbial colonisation of the airways. The significant increase in biomass and abundance of potential pathogens leads to severe, potentially life-threatening infections (Mika *et al.*, 2016; Moran Losada *et al.*, 2016). During childhood, *Staphylococcus aureus* and *Haemophilus influenzae* are the most prevalent species in the CF lungs. Later, mainly during school age or young adulthood, most pwCF experience their first *Pseudomonas aeruginosa* colonisation, leading to more than 60% of adults being affected (McGarry & McColley, 2021). Despite groundbreaking medical advancements in CF management and care, lung infections remain a leading cause of mortality (Françoise & Héry-Arnaud, 2020). Notably, the introduction of CFTR modulator therapies has brought significant hope for most pwCF; however, their long-term effect on the airway microbiome is yet to be determined (Saluzzo *et al.*, 2022). Thus, studying microbes in CF-like environments remains crucial for gaining a better understanding and providing improved medical care.

1.1.2. Diversity of microbial communities in the airways

The application of culture-independent technologies has revealed that various microorganisms, including bacteria, fungi, viruses, and archaea, make up the lung microbiota in both healthy individuals and those with underlying conditions (Charlson *et al.*, 2011; Dickson *et al.*, 2015; Moffatt & Cookson, 2017). During the course of a disease like CF, changes take place in the abundance of individual species and the overall microbial mass of the airways (Bassis *et al.*, 2015; Bittinger *et al.*, 2014; Charlson *et al.*, 2011; Martinsen *et al.*, 2021; Van Woerden *et al.*, 2013). Moreover, the composition and diversity of the airway microbiota in pwCF vary from person to person and even between different lobes of the same lung (Magurran & Henderson, 2003; Surette, 2014). This variability, along with changes due to age and environmental factors, present challenges in defining a consistent “core” microbiota of CF. However, certain trends can be identified, as illustrated in *Figure 1.3*.

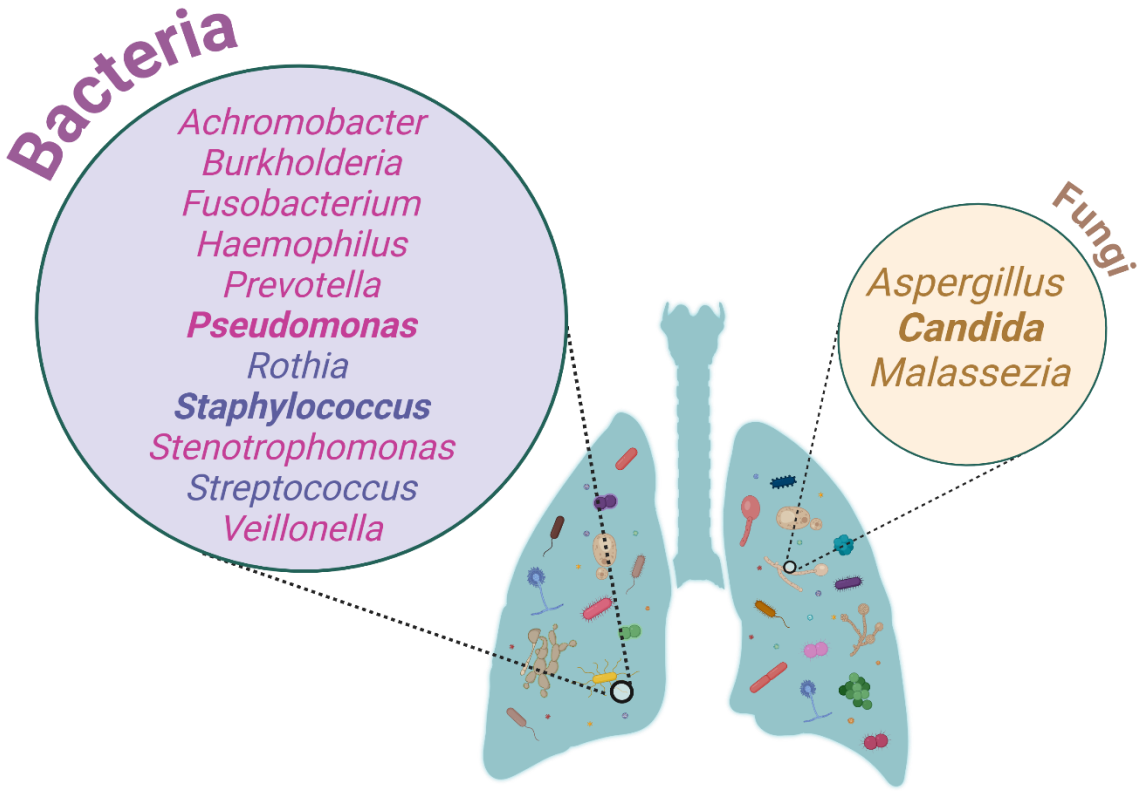

Figure 1.3. **Illustration of bacteria and fungi genera commonly found in cystic fibrosis airways.** In individuals with CF, increased mucus production and decreased clearance mechanisms create a favourable environment for microbial colonisation. Aerobic and anaerobic bacteria, along with various fungal species, have been identified as resident organisms in the CF lung. The most common ones are listed in the figure, with bacteria categorised by Gram staining: Gram-negative (pink) and Gram-positive (purple). This work focuses explicitly on the Gram-negative bacterium, *P. aeruginosa*, the Gram-positive bacterium, *S. aureus*, and the fungus, *C. albicans*, as highlighted in bold. Created with *BioRender.com*.

Commonly found inhabiting bacteria include species from the genera *Pseudomonas, Streptococcus*, *Staphylococcus*, *Burkholderia*, *Stenotrophomonas*, *Achromobacter*, *Rothia*, and *Haemophilus*. Unexpectedly, despite being an aerobic organ, the CF lung microbiota often also includes anaerobes such as *Prevotella*, *Veillonella*, and *Fusobacterium* (Cuthbertson *et al.*, 2016; Lamoureux *et al.*, 2021; Lamoureux *et al.*, 2019; Turner *et al.*, 2015; Van Der Gast *et al.*, 2011). Of all bacteria, *P. aeruginosa* is the most problematic when it comes to causing infections, as discussed later and in *Section 1.3*.

In addition to the complex bacterial composition, common respiratory viruses also have a higher prevalence in individuals with CF compared with the general healthy population. Among these, Rhinoviruses are the most frequently detected, but Respiratory syncytial virus and Influenza viruses are also common. Other respiratory viruses, such as Coronaviruses, Parainfluenza viruses, Adenoviruses, Enteroviruses, Bocaviruses, and Metapneumoviruses, are detected at lower rates in pwCF and are sometimes found in co-infections with other viruses, complicating the determination of their individual clinical impact (Billard *et al.*, 2017). Respiratory viruses often coincide with bacterial infections, such as those involving *P. aeruginosa*, with the potential to increase morbidity (Jankauskaitė *et al.*, 2018). It has been suggested that these co-infections may be associated with acute pulmonary exacerbations (PEx) and reduced lung function, measured as forced expiratory volume in 1 second (FEV_1) (Billard *et al.*, 2017; Jankauskaitė *et al.*, 2018).

Beyond respiratory viruses, the virome of the CF lung includes bacteriophages, which form the majority of the virome and play a pivotal role in shaping microbial and immune dynamics. Bacteriophages, which specifically infect and replicate within bacterial hosts, influence the local microbial ecosystem in several ways: they can lyse their bacterial hosts, transfer antibiotic resistance genes, or facilitate bacterial adaptation to the unique environment of the CF lung (Jankauskaitė *et al.*, 2018; Ling *et al.*, 2023). These processes potentially contribute to the selection of bacterial strains and the evolution of multidrug-resistant pathogens. Diverse phages are associated with key bacterial pathogens in CF, including *P. aeruginosa*, *S. aureus*, and *Burkholderia cenocepacia* (Billard *et al.*, 2017; Jankauskaitė *et al.*, 2018). By modulating bacterial populations and interactions, bacteriophages contribute significantly to the adaptation and persistence of bacterial agents within the respiratory tract niche in pwCF.

The mycobiome often contains genera such as *Candida*, *Aspergillus*, or *Malassezia* (Willger *et al.*, 2014). However, their exact impact on disease progression remains unclear, compounded by the lack of distinction in diagnostics between airway colonisation and active infection. The prevalence of *Candida* spp. in pwCF ranges between 33.8% and 77.9%, with *C. albicans* being the most commonly detected species (Magee *et al.*, 2021 Micalo, & Chaudary, 2021). Studies have reported an association between *Candida* colonisation and a decline in FEV_1 (Chotirmall *et al.*, 2010). The prevalence of *Aspergillus fumigatus*-positive sputum cultures in pwCF ranges from 27% to 57%, and co-infection with *P. aeruginosa* has been linked to worse clinical outcomes (Burgel *et al.*, 2016). Strong evidence suggests that *A. fumigatus* contributes to the progression of structural lung damage in CF (Lv *et al.*, 2021). Therefore, the development of sensitive and specific image analysis methods for chest CT and MRI is essential to identify *A. fumigatus*-associated structural abnormalities and guide therapeutic decisions. In contrast, *Malassezia* prevalence in pwCF is significantly lower, detected in only a small percentage of patients (Abdillah & Ranque, 2021).

Some evidence indicates that archaea can also be found in the CF airways, although their presence seems to vary among patients, and their abundance is generally low (Koskinen *et al.*, 2017; Moran Losada *et al.*, 2016).

Long-term follow-up studies have highlighted the significance of microbial composition in the CF airway (Price *et al.*, 2013; Thornton *et al.*, 2022). These studies demonstrate that stable respiratory function is – somewhat counter-intuitively - closely associated with maintenance of a stable, but diverse microbial population. Generally, microbial diversity and lung function are greater in younger pwCF, although this decreases with age (Cox *et al.*, 2010; Klepac-Ceraj *et al.*, 2010). This decline often correlates with the rise of dominant populations of pathogens, especially *P. aeruginosa* (Coburn *et al.*, 2015; Frayman *et al.*, 2017; Jorth *et al.*, 2019; Zemanick *et al.*, 2017). Other potentially pathogenic bacteria, like *Staphylococcus* and *Burkholderia* sp., are also more common in the older CF population (Boutin *et al.*, 2015; Coburn *et al.*, 2015; Zemanick *et al.*, 2017).

Clinicians often use both empirical and targeted antibiotic therapies to prevent or control infections in pwCF. This frequent and prolonged administration of antibiotics has also been proposed to contribute to decreased microbial diversity (Li *et al.*, 2016; Patangia *et al.*, 2022). Additionally, colonizing microorganisms frequently develop unique “resistomes” (Li *et al.*,

2016; Patangia *et al.*, 2022). *P. aeruginosa* and *S. aureus* often exhibit such behaviour, making them responsible for the most challenging infections (Hatziagorou *et al.*, 2020; Jhun *et al.*, 2017). Further details of treating pseudomonal infections with antibiotics are described in *Section 1.3.2*.

Generally, the co-existence of bacteria, viruses, fungi, and archaea in the CF airways provides the possibility of inter-species as well as interkingdom interactions. Research has already demonstrated that the intricate interplay between species can affect patient outcomes, infections, and disease progression, as also discussed in *Section 1.5* (Delhaes *et al.*, 2012; Soret *et al.*, 2020; Willger *et al.*, 2014). Due to its clinical relevance and tendency to cause difficult infections, *P. aeruginosa* has been the focus of many studies on polymicrobial interactions. This is also the case for the present work and the next section of this chapter provides an overview of *P. aeruginosa*, highlighting its characteristics relevant to this study.

1.2. *Pseudomonas aeruginosa*

1.2.1. General characteristics

Since it was first described in the 19th century by the French pharmacist Carle Gessard (Diggle & Whiteley, 2020), our knowledge of *P. aeruginosa* has continuously expanded. It is a Gram-negative opportunistic pathogen known for its versatile nature, thriving in anthropic environments and the human body (Crone *et al.*, 2020; Hardalo & Edberg, 1997; Zannoni, 1989). In 2017, the World Health Organization (WHO) designated it as a "critical priority pathogen," and its relevance was renewed in 2024 as a "high priority pathogen" (WHO, 2017, 2024).

One of the most studied laboratory strains is PAO1 – which is also used in this work – originally isolated from a chronic wound in the 1950s (Askenasy *et al.*, 2024; Holloway, 1955). The PAO1 genome was first sequenced in 2000, uncovering 6.3 million base pairs and 5570 predicted open reading frames. This represented the largest bacterial genome sequenced up to that time (Diggle & Whiteley, 2020; Stover *et al.*, 2000). This extensive genome supports metabolic diversity, a wide array of virulence factors, and functional redundancy, enabling the bacterium to, for example, utilise various nutrients and achieve superior iron uptake. *P. aeruginosa* also possesses a wide range of antimicrobial weapons that can kill, inhibit growth, and restrict

critical cellular functions in other microbes (Filloux & Ramos, 2022). This study focuses on key aspects of microbial communication within *P. aeruginosa*, including quorum sensing (QS), secretion systems such as the Type VI Secretion System (T6SS), and briefly addresses iron homeostasis.

1.2.2. Quorum sensing

Like some other bacteria, *P. aeruginosa* cells communicate using chemical signals called QS molecules. Cells use these molecules to sense population density and coordinate the usage of multiple important traits. Such management is crucial since these traits only become profitable with accelerated production (Miranda *et al.*, 2022). This phenomenon of cell-to-cell signalling was first observed with luminescence in *Vibrio fischeri* and has been shown in other organisms since (Hastings & Nealson, 1977; Miranda *et al.*, 2022; Rutherford & Bassler, 2012).

In the last three decades, the QS system in *P. aeruginosa* has been widely and extensively studied. According to our current knowledge, the QS system in *P. aeruginosa* consists of three major circuits, which are arranged hierarchically, as detailed in *Figure 1.4*.

Two of the circuits employ *N*-acyl-homoserine lactones (AHL) as signalling molecules and consist of a signal receptor, its corresponding signal molecule, and the synthase of the latter. For the *las* system, these are LasR, *N*-(3-oxododecanoyl)-L-homoserine lactone (3-oxo-C12-HSL or OdDHL) and LasI, respectively. For the second, the *rhl* system, these are RhlR, *N*-butanoyl-L-homoserine lactone (C4-HSL or BHL), and RhlI, respectively (Gambello & Iglewski, 1991; Latifi *et al.*, 1995; Passador *et al.*, 1993). The third circuit, known as the *pqs* system, uses 4-hydroxy-2-alkylquinolines (HAQs) signalling molecules, which include 2-heptyl-3-hydroxy-4(1H)-quinolone (pseudomonas quinolone signal, PQS) and its biosynthetic precursor 2-heptyl-4-hydroxyquinoline (HHQ). PQS and HHQ bind to a receptor, PqsR (Calfee *et al.*, 2001; Heeb *et al.*, 2011; Wratten *et al.*, 1977).

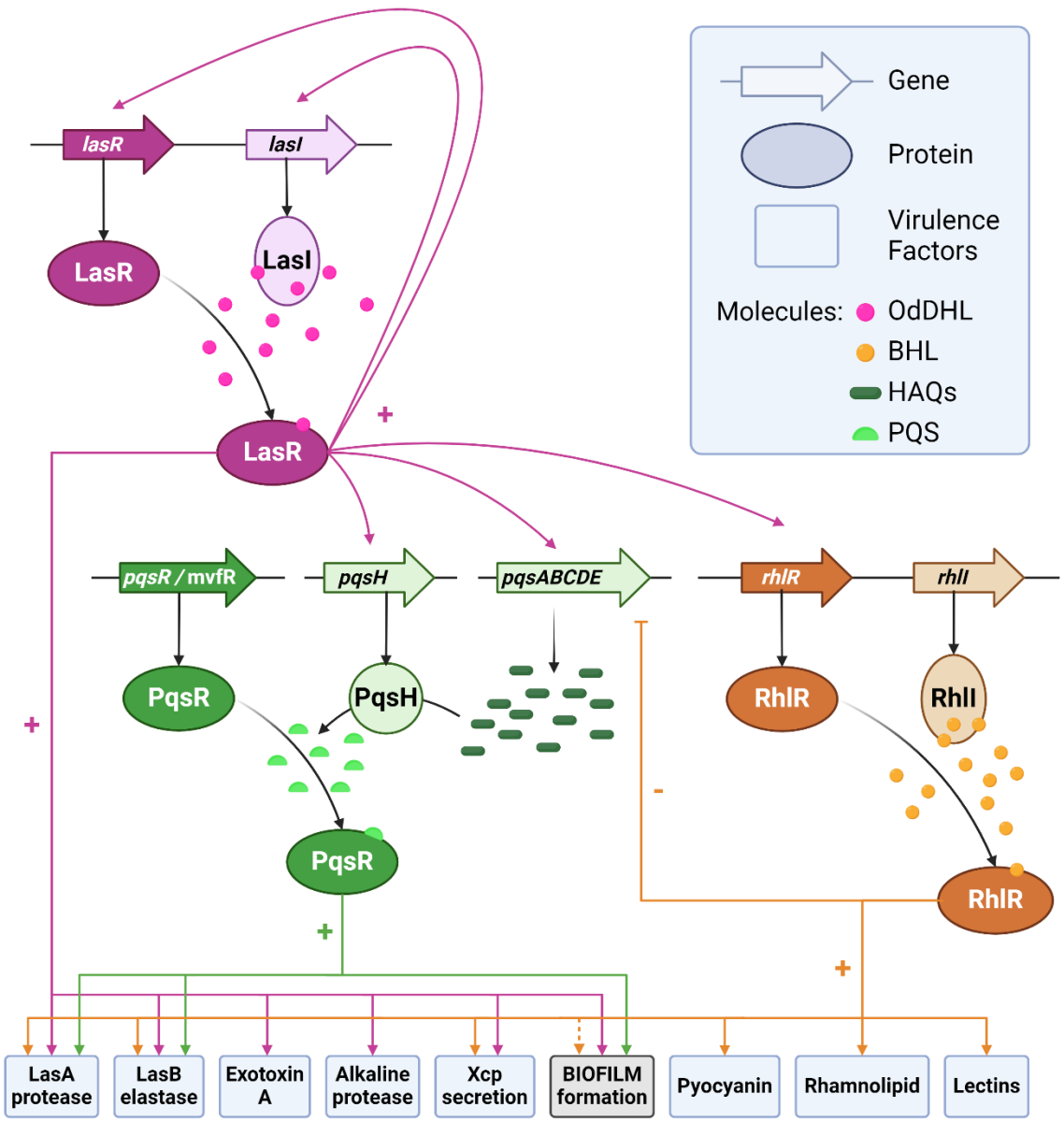

Figure 1.4 **Schematic illustration of the three quorum sensing systems in *Pseudomonas aeruginosa* and their effects**. The QS network of *P. aeruginosa* consists of three circuits: *las* (pink), *rhl* (orange), and *pqs* (green). Some regulated virulence factors, such as LasA, LasB, and biofilm formation, are controlled by multiple QS systems, while others, like rhamnolipids, are regulated by a single QS system. Coloured lines represent induction (arrows: →) and negative regulation (inhibitor signs: —|), corresponding to the colour of each circuit. The grey box provides information about the symbols. Abbreviations used: OdDHL, *N*-(3-oxododecanoyl)-L-homoserine lactone; BHL, *N*-butyryl-L-homoserine lactone; HAQs, 4-hydroxy-2-alkylquinolines; PQS, Pseudomonas quinolone signal. Created with *BioRender.com*.

The significance of the QS system is based on its association with various functions, including the regulation of biofilm formation and virulence factor production, such as elastase LasB, LasA, exotoxin A, pyocyanin, rhamnolipids, alkaline protease, and more (De Kievit, 2009; Miranda *et al.*, 2022; Rutherford & Bassler, 2012; Tang *et al.*, 1996). Importantly, the different circuits have been linked with polymicrobial interactions, as discussed in *Section 1.5* (Miranda *et al.*, 2022; Murray *et al.*, 2022).

Regarding the hierarchy, the *las* system is at the top of the signalling cascade because the OdDHL-bound-LasR complex serves as a transcriptional regulator and activates *lasR*, *lasI* as well as the other circuits (*Figure 1.4*) (Balasubramanian *et al.*, 2013; Pesci *et al.*, 1997). Notably, the whole *lasR* regulon consists of more than 300 genes, including transcriptional regulators, secreted factors, and secretion machinery (Gilbert *et al.*, 2009).

Remarkably, it has been discovered that there is plasticity in the hierarchy and function of QS-controlled genes. For example, certain genes depend only on LasR, and others depend solely on RhlR, whereas genes such as *lasB* have both LasR and RhlR binding sites in their promoter regions (Brint & Ohman, 1995; Gambello & Iglewski, 1991; Pesci *et al.*, 1997). Moreover, studies have shown that LasR is not always necessary for QS in *P. aeruginosa*, and RhlR can function in a LasR-independent manner. This can happen when there are simultaneous loss-of-function mutations both in *lasR* and *mexT*, for example (Chen *et al.*, 2019; Cruz *et al.*, 2020; Dekimpe & Déziel, 2009; Feltner *et al.*, 2016; Simanek *et al.*, 2023).

Moreover, although QS systems are found to be highly important in laboratory studies, a transcriptomic comparison of *in vitro* and human samples revealed they may have less relevance in infections. Cornforth (Cornforth *et al.*, 2018) showed that a core set of 42 genes within the *lasR* regulon has lower expression in human infections than in classic *in vitro* conditions, particularly in biofilm samples (Chugani *et al.*, 2012; Cornforth *et al.*, 2018).

Although extensive knowledge already exists about QS in *P. aeruginosa*, there are still gaps regarding its role(s) in polymicrobial infection scenarios. Specifically, I believe it is essential to study the role of *lasR*, especially given the clinical prevalence of loss-of-function *lasR* mutants in chronic infections, as discussed later in *Section 1.3.1*.

1.2.3. Type VI Secretions Systems

Besides contact-independent communication *via* QS, *P. aeruginosa* also employs various contact-dependent tools, primarily to defend itself against other species or distant relatives (Filloux, 2011). This competitive strategy is advantageous in mixed communities, where it helps the bacterium compete for limited resources and space. Generally, *P. aeruginosa* uses two types of molecules: effectors (toxins) and immunity proteins, often, but not exclusively, encoded in a tandem layout (Nolan & Allsopp, 2022). Effectors exhibit great diversity and typically target specific, critical functionalities in “prey” organisms (Allsopp *et al.*, 2020; Hernandez *et al.*, 2020; Nolan *et al.*, 2021). The immunity proteins can block the activity of their cognate effector proteins, usually through direct protein-protein interactions, thereby preventing self-toxicity and attacks from sister cells. Therefore, the selection of 'kin' is based on the presence of the relevant immunity protein (Allsopp *et al.*, 2020; Hernandez *et al.*, 2020). *P. aeruginosa* uses such mechanisms in various systems, including the type V secretion system and its subclass, the contact-dependent inhibition (CDI) system, as well as the T6SS. The current work focuses primarily on the T6SS.

The T6SS plays an important role in bacterial competition. Although the genes encoding T6SSs can be found in more than 25% of Gram-negative bacteria, its function was only demonstrated in 2010 (Allsopp *et al.*, 2020; Bingle *et al.*, 2008; Hernandez *et al.*, 2020; Hood *et al.*, 2010). The T6SS has apparent structural homology with bacteriophage T4 but with the twist of “firing outwards”, rather than projecting inwards (as is the case with a phage injectisome) (Wang *et al.*, 2019). *Figure 1.5* shows a schematic model of the T6SS apparatus during assembly, firing, and disassembly.

The apparatus has three main structural parts (the membrane complex, the baseplate complex, and the tube-sheath/tail complex) alongside the changing spike complex. The assembly starts by anchoring the baseplate to the inner membrane to serve as the foundation for the entire T6SS apparatus. Then, the inner tube and contractile sheath are formed. The inner tube, composed of stacked rings of the Hcp protein, forms a channel for the effector proteins. Surrounding the inner tube, the contractile sheath forms a helical structure. The spike complex, which includes VgrG proteins and often a PAAR-repeat protein, attaches to the distal end of the inner tube. This complex is critical for piercing the target cell membrane.

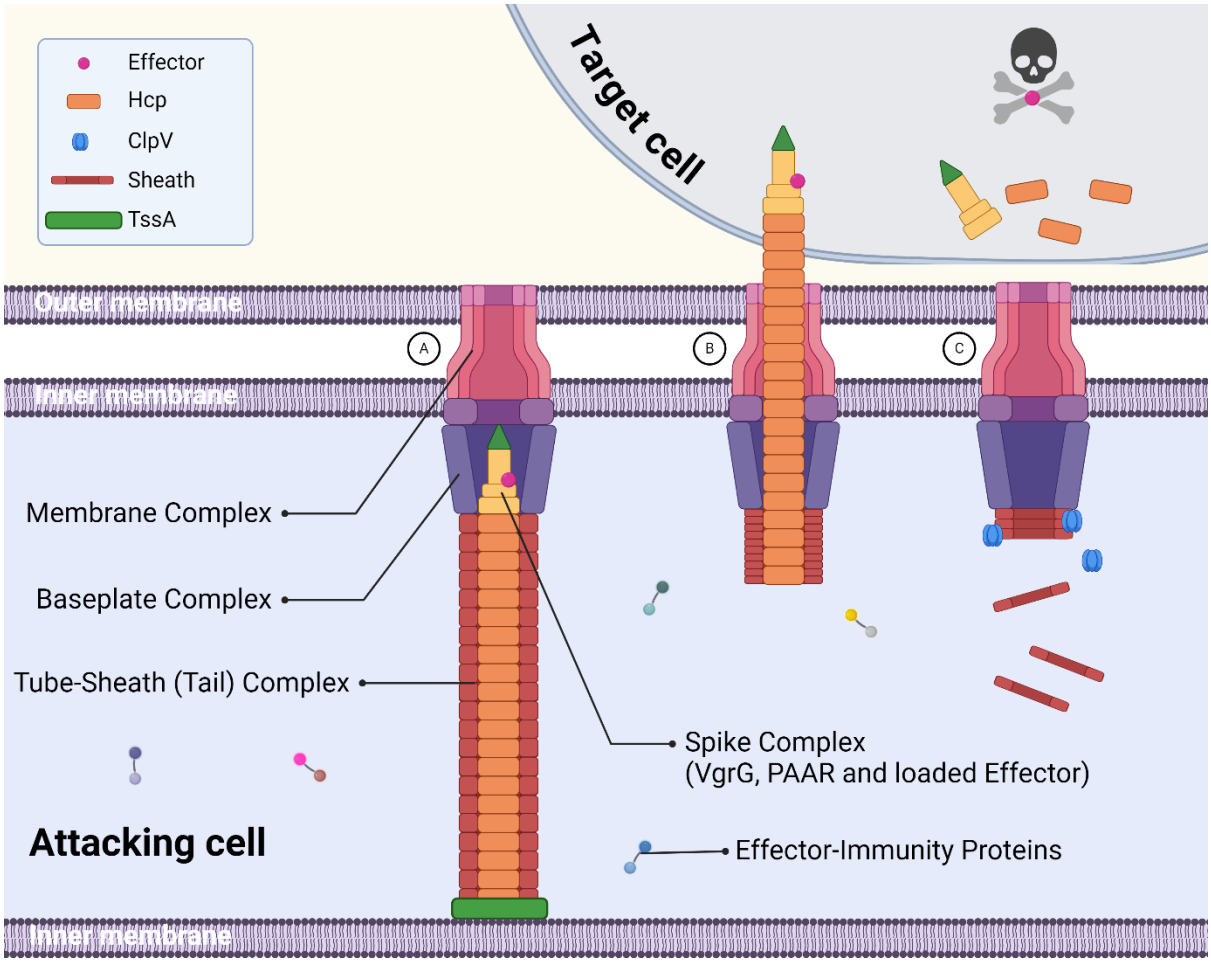

Figure 1.5. **Visualisation of the T6SS apparatus injecting an effector protein into a target cell.** The T6SS plays a crucial role in bacterial competition and pathogenesis. Its mechanism of action involves three stages: Assembly (A), Firing (B), and Disassembly (C). The apparatus, which includes the baseplate, membrane, tail, and spike complex, is formed during assembly. Upon receiving the firing signal, the sheath contracts, propelling the inner tube and delivering effectors into the target cell (or the extracellular medium). After contraction, the ATPase ClpV disassembles the sheath, recycling the components for future use. The grey box provides information about the symbols used in the visualisation. Created with *BioRender.com*.

The fully assembled structure is then secured to the bacterial cell membrane by a membrane complex, ensuring stability and proper orientation for the subsequent firing. Then, effector proteins are loaded onto the inner tube. Upon receiving a firing signal, the sheath undergoes a rapid contraction, akin to a spring mechanism releasing stored energy. This contraction propels the inner tube outward, allowing the spike complex to breach the target cell's membrane (Chen *et al.*, 2015; Filloux, 2011; Zoued *et al.*, 2014). Given that the T6SS can extend up to half the width of the bacterial cell, it can reach neighbouring prey cells as far as 500 nm away (Ho *et al.*, 2014). As the needle penetrates the target cell, the effector proteins are injected into the cytoplasm of the target cell, causing cellular damage or death, unless immunity proteins are present. After the firing event, proteins such as ClpV disassemble the contracted sheath, recycling the components for future use (Basler *et al.*, 2013; Nolan & Allsopp, 2022; Taylor *et al.*, 2016).

Three T6SS have been identified in *P. aeruginosa*, namely the H1-, H2-, and H3-T6SS. Most isolates contain all three, highlighting their importance (Nolan & Allsopp, 2022). They are encoded within three large operons with additional gene islands (Allsopp *et al.*, 2017). The triggering mechanisms for firing and the specific effectors transported vary across the different subtypes and remain only partially understood (Allsopp & Bernal, 2023).

Generally, most of the effectors target other microbes. However, some other effectors are not directly involved in antimicrobial processes, and these include iron acquisition, molybdate transport, or Cu^{2+} scavenging (J. Lin *et al.*, 2021; Lin *et al.*, 2017; Wang *et al.*, 2021). Surprisingly, a hybrid class of T6SS toxins has also been described to act in a contact-independent manner, highlighting the potential for greater complexity in the T6SS than previously expected (L. Lin *et al.*, 2021).

Over the past few years, many effectors and immunity proteins have been identified in *P. aeruginosa*. However, while the roles and conditions for some effectors have been identified, a significant gap remains in understanding the exact functions of others.

1.2.4. Iron homeostasis

Iron is a vital micronutrient for microbes, including *P. aeruginosa*, as it is crucial for key cellular functions like respiration, DNA synthesis, and metabolism (Llamas & Sánchez-Jiménez, 2022). To meet its iron requirements, *P. aeruginosa* has developed advanced systems to acquire, regulate, and efficiently utilise iron in environments where its availability may be limited.

To acquire iron, *P. aeruginosa* produces siderophores – small, high-affinity iron-chelating compounds like pyoverdine and pyochelin – that scavenge ferric iron from the environment (Cornelis & Dingemans, 2013; Sánchez-Jiménez *et al.*, 2023). In polymicrobial communities, these siderophores not only help *P. aeruginosa* secure iron but also influence interactions with other microorganisms. Some neighbouring microbes may exploit these siderophores to access iron themselves, while others produce their own siderophores to compete for the limited iron supply that can be used by *P. aeruginosa* (Chan & Burrows, 2023; Sánchez-Jiménez *et al.*, 2023). In reducing environments, the soluble Fe^{2+} ion becomes the major source of iron, transported *via* the ferrous iron transport (Feo) system and stabilised upon uptake to prevent its oxidation to Fe^{3+} and to prevent its inherent toxicity (Lau *et al.*, 2016; Sánchez-Jiménez *et al.*, 2023). Additionally, in the host environment, *P. aeruginosa* utilises host iron carriers, such as heme, and also expresses receptors capable of extracting iron directly from host proteins (Llamas & Sánchez-Jiménez, 2022). Moreover, PQS has been shown to chelate Fe^{3+} ions at physiological pH, and uptake of the PQS-Fe^{3+} complex is facilitated by a T6SS effector, TseF (Bredenbruch *et al.*, 2006; Diggle *et al.*, 2007; Lin *et al.*, 2017).

To regulate these processes and control the expression of genes involved in iron uptake and storage based on iron availability, *P. aeruginosa* uses a ferric uptake regulator (Fur) and small RNAs (Sánchez-Jiménez *et al.*, 2023). It also utilises ferritins and efflux systems for iron withdrawal to avoid excess and prevent toxicity (Llamas & Sánchez-Jiménez, 2022). Together, these ensure optimal function and can directly influence the virulence of *P. aeruginosa* based on iron availability, especially amidst the complexities of a mixed-species environment (Reinhart & Oglesby-Sherrouse, 2016). Iron also affects biofilm formation, as reported in several studies (Banin *et al.*, 2005; Kaneko *et al.*, 2007; Patriquin *et al.*, 2008).

1.3. Clinical relevance of *Pseudomonas aeruginosa* in cystic fibrosis

P. aeruginosa is present in the majority of adults with CF (McGarry & McColley, 2021). It is often acquired from the environment but can also be transmitted directly from patient-to-patient, particularly during outbreaks of highly transmissible strains, such as the Liverpool Epidemic Strain (Moore *et al.*, 2021). Regardless of its origin, *P. aeruginosa* typically progresses through the same stages in CF airways, from initial colonisation to chronic infection, as shown in *Figure 1.6*. Colonisation is classified as chronic based on the Leeds criteria, when more than half of samples from a patient test positive for *P. aeruginosa* (Lee *et al.*, 2003). The stages are associated with somewhat distinct metabolic features and varying levels of virulence, with the emergence and disappearance of various phenotypes and genetic variants (Ding *et al.*, 2018; Moradali *et al.*, 2017).

1.3.1. Common mutant derivates in clinical samples

Advancements in 'omics approaches' and longitudinal studies have not only enhanced our understanding of the microbiome but also of the common mutant derivatives of different species (Jorth *et al.*, 2015; Marvig *et al.*, 2015; Nguyen & Singh, 2006). As more information is gathered about these intra-species genetic variants, their relationships to infection stages and severity are becoming more apparent.

Initial isolates of *P. aeruginosa* mainly prefer to grow in the planktonic state, display high motility using pili and flagella, and produce damaging pro-inflammatory toxins such as elastase, pyocyanin, and pyoverdine (King *et al.*, 2022). During early phase colonisation, the production of virulence factors is primarily coordinated by QS, and isolates are generally more virulent (Ding *et al.*, 2018; Moradali *et al.*, 2017).

As the infection progresses (*Figure 1.6*), *P. aeruginosa* adapts through mutation. Several recurring differences between early and late isolates have been reported. Based on multiple studies, Camus identified 48 coding regions of *P. aeruginosa* that frequently exhibit non-synonymous mutations in CF isolates (Camus *et al.*, 2021). These include several global regulators such as *lasR*, *mucA*, *algU*, and *rpoN*; type III secretion-related genes such as *retS* and *exsA*; and antibiotic resistance-related genes such as *nfxB* and *mexZ*.

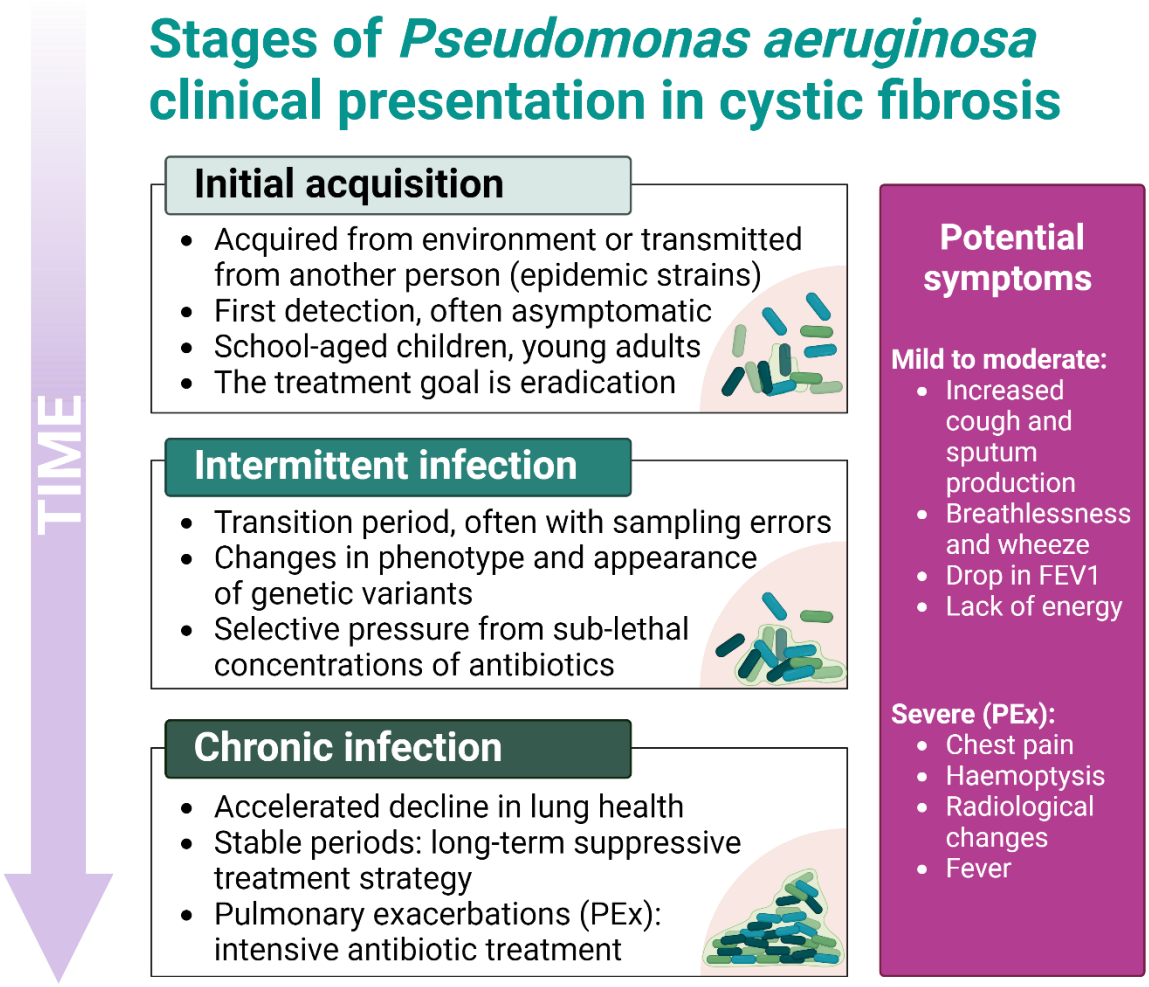

Figure 1.6. **Stages of *Pseudomonas aeruginosa* clinical presentation in cystic fibrosis.** *P. aeruginosa* exhibits different characteristics and results in various symptoms, from its initial acquisition to chronic infection. The presence of different phenotypes and genotypes, as illustrated in the corners, leads to varying clinical responses. Despite treatment efforts, the progression often trends toward long-term colonisation. However, symptoms can range from mild to severe throughout the timeline, depending on individual characteristics. Created with *BioRender.com*.

The most common of these mutations in clinical isolates is the loss-of-function mutation in the master QS regulator, *lasR* (Chen *et al.*, 2019; Cruz *et al.*, 2020; Feltner *et al.*, 2016; Kostylev *et al.*, 2019; Marvig *et al.*, 2015; Smith *et al.*, 2006; Zhao *et al.*, 2023). These *lasR* mutants are often linked with the progression of the infection and worse outcomes (Hoffman *et al.*, 2009; LaFayette *et al.*, 2015). *LasR* mutants are thought by some to be "social cheaters" because they do not participate in producing public goods but benefit from those made by cooperators (Chen *et al.*, 2019). On the one hand, cooperators try to suppress the appearance of cheaters through various mechanisms. For example, it has been suggested that cyanide or pyocyanin may be involved in this “policing” (Castañeda-Tamez *et al.*, 2018; Wang *et al.*, 2015). It is expected that the policing mechanisms are an integral part of the *lasR* regulon, and they appear to be mechanistically multifactorial. On the other hand, if cheaters are successful, such behaviour provides a potential fitness advantage for them. This can potentially lead to a shortage of public goods and the "tragedy of the commons" (Axelrod & Hamilton, 1981). However, such population collapse is rarely detected in host environments (Dandekar *et al.*, 2012).

Some findings suggest that *lasR* mutants are better adapted to the polymicrobial lung environment (Harrison *et al.*, 2014). Moreover, a polymorphic population of cooperators and cheaters seems to have survival advantages in animal models (Zhao *et al.*, 2023). Notably, studying clinical samples, several groups have observed partially restored QS activity even in the absence of a functioning *lasR* gene (Chen *et al.*, 2019; Cruz *et al.*, 2020; Feltner *et al.*, 2016; Kostylev *et al.*, 2019; Wang *et al.*, 2018). As mentioned previously, this phenomenon is often linked to simultaneous mutations in *mexT*, resulting in *lasR*-independent activation of the *rhl* system, highlighting the importance of the *rhl* system in chronic infections (Simanek *et al.*, 2023). Overall, while *lasR* mutants are clinically significant, their function and consequences in polymicrobial contexts are not yet fully understood.

Besides changes in the QS system, in the early stages of colonisation, *P. aeruginosa* also reduces its motility by losing its pili and flagella, making it less susceptible to phagocytosis. Additionally, environmental conditions stimulate the overproduction of alginate and exopolysaccharides, resulting in the mucoid phenotype also commonly observed in chronic *P. aeruginosa* populations (Behrends *et al.*, 2010; Worlitzsch *et al.*, 2002). This form can better

shield the cells from antibiotic treatments and host defence mechanisms, enhancing their survival.

Hypermutability also occurs relatively frequently, with approximately 28% of pwCF having at least one such hypermutator isolate, based on multiple studies (Auerbach *et al.*, 2015; Camus *et al.*, 2021; Hall & Henderson-Begg, 2006; Oliver & Mena, 2010; Rees *et al.*, 2019). However, hypermutable lineages quickly decline or disappear, indicating that they likely confer a fitness advantage only at specific stages of *P. aeruginosa* population evolution (Camus *et al.*, 2021; Mehta *et al.*, 2019).

Furthermore, various triggers, such as inadequate nutrition and sublethal concentrations of antibiotics also lead to the development of distinct genetic lines, resulting in heterogeneous populations (Camus *et al.*, 2021).

Overall, even clonally-derived *P. aeruginosa* exists in diverse populations characterised by a wide array of mutational variants, particularly during intermittent and chronic infections (Camus *et al.*, 2021; Zhao *et al.*, 2023). This diversity enables the bacterium to adapt to the harsh lung environment and endure challenging conditions, such as antimicrobial treatments (Camus *et al.*, 2021).

1.3.2. Anti-pseudomonal treatment

P. aeruginosa is challenging to treat with antibiotics due to its susceptibility to only a limited number of molecules and its increasing resistance to current treatments. Clinically problematic resistant variants evolve through the mutational activation of intrinsic resistance mechanisms, horizontal acquisition of antibiotic resistance genes, transient “phenotypic” resistance (“tolerance”), and persistence (King *et al.*, 2022). Generally, resistance leads to high mortality rates in both people with- and without-CF.

For pwCF, the choice of treatment targeting *P. aeruginosa* somewhat depends on the stage of the infection, as shown in *Figure 1.7*. Following the initial detection, the goal is to eliminate *P. aeruginosa* as soon as possible (Langton Hewer & Smyth, 2017). There are two main approaches: inhaled tobramycin (European and US guidelines) or oral ciprofloxacin and nebulised colistin (UK guidelines) (Hewer *et al.*, 2020; King *et al.*, 2022). Initial eradication attempts succeed in about 80% of cases, but this treatment outcome is only temporary.

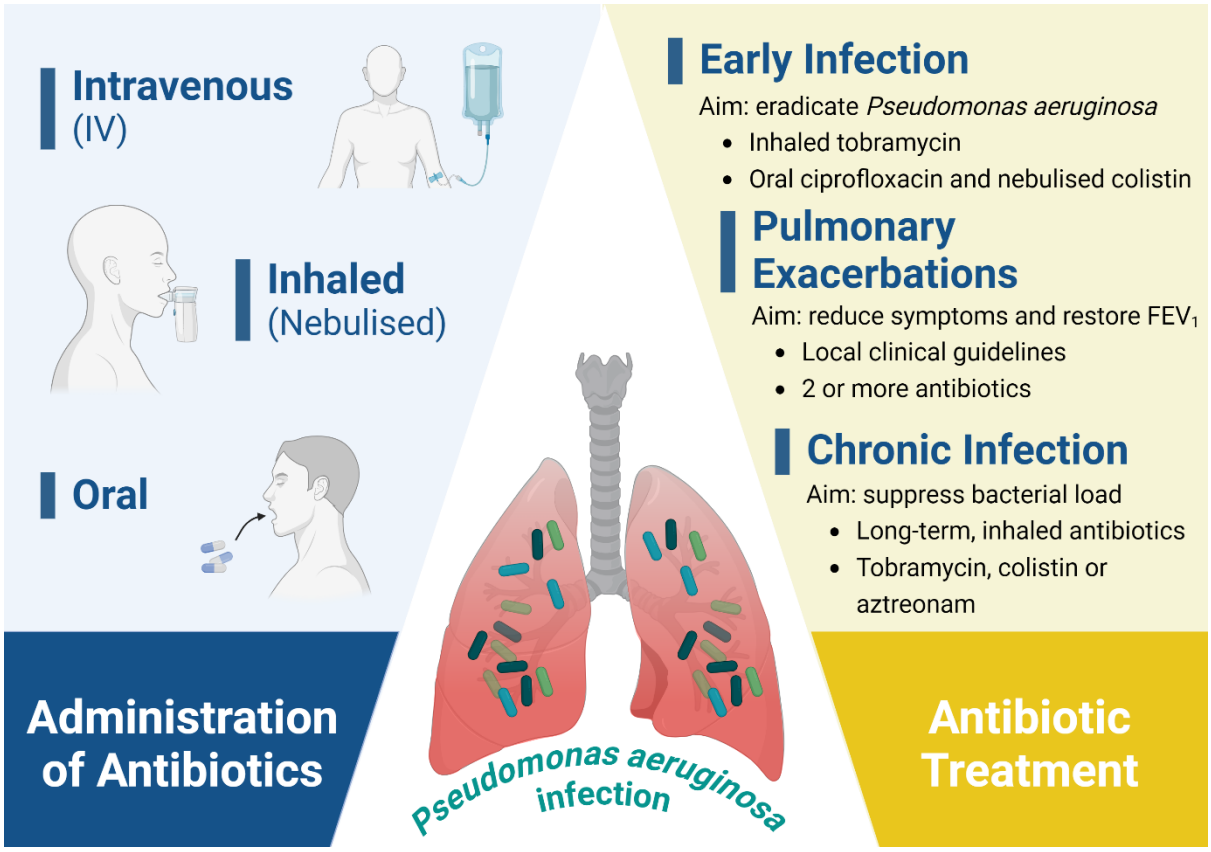

Figure 1.7. **Overview of anti-pseudomonal treatments.** Various administration options (blue background) and antibiotic choices (yellow background) are available for targeting P. aeruginosa infections in CF airways. Treatment strategies depend on the stage and severity of the infection and often involve a combination of drugs. Notably, deviations from the guidelines may occur based on individual patient needs. This work specifically focuses on two of the commonly used drugs: colistin and ciprofloxacin. Created with *BioRender.com*.

Eventually, approximately 60-70% of adults develop chronic infections due to the remarkable persistence of *P. aeruginosa* (Langton Hewer & Smyth, 2017).

As the infection progresses from the initial to the intermittent and chronic stages (*Figure 1.6*), the treatment goals shift to treating acute exacerbations and managing chronic infections (*Figure 1.7*) (Taccetti *et al.*, 2021). Notably, initial *P. aeruginosa* infection can be detected during a pulmonary exacerbation episode; however, pulmonary exacerbation more commonly occurs in chronically infected individuals. Treating acute episodes in individuals with chronic colonisation primarily relies on local clinical guidelines involving inhaled or intravenous (IV) antibiotics. It is recommended to use two anti-pseudomonal agents with different mechanisms of action to limit the development of resistance. During stable periods, the aim is to minimise the chances of sudden worsening. Although it is unclear what exactly triggers exacerbations, most guidelines recommend long-term, inhaled antibiotics, such as tobramycin, colistin, and aztreonam, to suppress bacterial load and inflammatory damage (Taccetti *et al.*, 2021).

Besides current options, there is an active pipeline of new approaches ranging from preclinical to mid-clinical phases (*CFF Pipeline*, 2024). Examples include the administration of gallium to limit iron accessibility in the IGNITE study, which the FDA has approved in Phase 2 for IV use in people and is being studied for its effectiveness in CF. Inhaled nitric oxide (LungFit™ GO) is being tested against non-tuberculous mycobacteria due to its ability to disrupt biofilms. Bacteriophage therapies by Armata Pharmaceuticals and BiomX are also showing promising results in clinical phases *(Armata Pharmaceuticals,* 2024*; BiomX Phage therapy*, 2024).

Overcoming increasing resistance remains the most significant challenge, particularly since clinical responses often do not align with laboratory antimicrobial susceptibility results (Little *et al.*, 2021; Syal *et al.*, 2017). Several factors contribute to this discrepancy, including the importance of the growth mode during testing, potential drug-drug interactions and inhibition from mucus components, poor penetration of antibiotics through biofilms, and the modifying effects of co-existing pathogens. The latter is particularly interesting, as inter-species interactions have already been associated with increased resistance; however, this area has historically been understudied due to technical difficulties (Beaudoin *et al.*, 2017; Dehbashi *et al.*, 2020; DeLeon *et al.*, 2014; Hoffman *et al.*, 2006; Lebrun *et al.*, 1978; O'Brien *et al.*, 2022; Orazi & O'Toole, 2017). Additionally, the genetic variations of pathogens, such as *P.*

aeruginosa, have the potential to complicate antibiotic treatments further (Madden *et al.*, 2024). Building a more detailed understanding of polymicrobial and polyclonal scenarios holds great potential for developing more effective treatment protocols using existing or new antimicrobial agents.

1.4. Investigating polymicrobial infection scenarios

Despite extensive research shedding light on various aspects of its metabolism, virulence mechanisms, and characteristics, our understanding of *P. aeruginosa* within polymicrobial communities has only recently begun to expand.

1.4.1. Considerations and challenges in research design

Over the last few decades, several infection-related concepts have been revised, such as the association of many chronic infections with only a single species (the "pathogen"). Nowadays, it is widely acknowledged that most infection scenarios involve a plethora of additional species, which may or may not contribute to the pathology of the disease. Interestingly, Pasteur already observed the polymicrobial nature of microbial communities in the nineteenth century. However, culture-independent techniques emerged only in the twenty-first century, revealing the intricacies of "microbial dark matter" (Bényei *et al.*, 2024; Lloyd *et al.*, 2018; Pasteur & Joubert, 1877). These groundbreaking techniques have revealed that an estimated 85–99% of species, members of different kingdoms, have been uncharacterised or understudied due to their unculturable nature (Bényei *et al.*, 2024; Lok, 2015; Rinke *et al.*, 2013).

Despite our understanding of the diverse nature of infection scenarios, technical challenges have complicated the investigation of details, especially under *in vitro* conditions. Unfortunately, simply inoculating a flask or microplate with a mixture of microbes does not adequately capture the true stability and diversity associated with chronic infections. These co-cultures exhibit significant dynamic changes (within days or even hours), leading to exaggerated conclusions regarding the importance of inter-microbial competition and dominance. Considering their significant advantages, being cost-effective and suitable for high throughput measurements, it is understandable that many research teams continue to utilise them (Bernardy *et al.*, 2022; Filkins *et al.*, 2015; Kvich *et al.*, 2022; Luján *et al.*, 2022; Magalhães *et al.*, 2019; Mitchell *et al.*, 2010; Pajon *et al.*, 2023; Price *et al.*, 2020; Tognon *et*

al., 2017; Vasiljevs *et al.*, 2023). On the other hand, novel and improved models that capture long-term polymicrobial stability and infection-associated characteristics have made successful debuts. However, these models often have higher financial costs and reduced data collection.

Recently, O'Toole and colleagues proposed a set of guidelines to enhance comparability and reproducibility across methods (O'Toole *et al.*, 2021). They emphasise that "all models are wrong, but some can be useful." This showcases the risk of relying solely on a single model system, possibly leading to questionable conclusions due to characteristics specific to that experimental system. In a recent review, we supported the notion that although simple *in vitro* and *ex vivo* systems offer greater manipulability and are conducive to hypothesis-driven research, they are the most accurate when interpreted alongside more complex and representative *in vivo* studies (although we also note that *in vivo* polymicrobial disease models are still in the early stages of development) (Bényei *et al.*, 2024). The desired combination of approaches is illustrated in *Figure 1.8*.

In research design, it is essential not only to select an appropriate model but also to choose an appropriate medium, if required, as it can greatly influence the results. For CF studies, Artificial Sputum Media (ASM) or Synthetic Cystic Fibrosis Sputum (SCFM) is favoured for the accurate representation of CF patient sputum composition (Aiyer & Manos, 2022; Kirchner *et al.*, 2012). This is evidenced by the gene expression patterns of *P. aeruginosa* in SCFM2, which are nearly identical to those in human sputum (Cornforth *et al.*, 2020; On *et al.*, 2023; Palmer *et al.*, 2007; Turner *et al.*, 2015). However, Neve (Neve *et al.*, 2021) have found that the variable formulation of ASM, primarily due to complex components like mucin, can affect bacterial behaviour and virulence, challenging the consistency of results. Additionally, while ASM/SCFM is tailored for *P. aeruginosa* in a CF lung environment, it was never formulated to enable cultivation of all CF-related pathogens, as some do not thrive in ASM. Therefore, the choice of model and medium should be carefully considered in research design.

Figure 1.8. **Illustration of model categories for studying polymicrobial scenarios**. In the diverse landscape of polymicrobial research, significant advancements are being made in both our understanding and the methodologies used. However, a gap remains in integrating these advances across different experimental approaches. This illustration is meant to emphasise the importance of connecting findings from *in vitro* (red background), *ex vivo* (yellow background), *in vivo* (green background), and *in silico* (blue background) studies to develop a more comprehensive understanding of polymicrobial scenarios (purple background). Created with *BioRender.com*.

1.4.2. Models of CF lung microbiology

In polymicrobial studies, models can be classified effectively by utilising the traditional framework of *in vitro*, *ex vivo*, *in vivo*, and *in silico* methodologies (*Figure 1.8*).

In vitro models

The *in vitro* method is highly favoured in laboratory settings because of its well-defined parameters, ease of monitoring, and adaptability to simulate environmental changes by adjusting pH, temperature, or microbial composition. However, it has well-known shortcomings in mimicking the complexity of natural environments and representing host factors.

In their study, Quinn and colleagues (Quinn *et al.*, 2015) introduce an *in vitro* Winogradsky-based culture model to investigate the impact of CF lung physiology on PEx (Quinn *et al.*, 2015). To create the model, they constructed Winogradsky columns using narrow-gauge capillary tubes filled with ASM. These columns were designed to mimic the physicochemical gradients found in CF bronchioles. They inoculated the columns with sputum samples obtained from pwCF during PEx. Their observations include changes in pH, gas production, and community composition, assessed with 16S rDNA analyses. The authors conclude that fluctuations in fermentative anaerobes likely contribute to PEx, and that anaerobic conditions may occur in CF lung because of the thick mucus.

To investigate the interactions between CF-relevant microbes, O'Brien and Welch – in the host laboratory of this work – developed an *in vitro* continuous-flow system using ASM (O'Brien & Welch, 2019). Following inoculation with a CF-associated Gram-negative species, *P. aeruginosa*, a Gram-positive CF species, *S. aureus*, and a fungal CF species, *Candida albicans*, the system consistently reached a steady state within 24 hours. Remarkably, the same steady state titres were achieved independent of the inoculation ratio of these microbes. This observation suggests a 'hardwired' ecological relationship among the species. This microbial population is maintained in slow exponential growth, just as in the CF airways (Bartell *et al.*, 2019; La Rosa *et al.*, 2021; O'Brien *et al.*, 2022; Yang *et al.*, 2008). Details of this system are discussed in *Chapter 3*.

Tolker-Nielsen and Sternberg, as well as Yang and colleagues, have used a similar flow-chamber system for co-culturing biofilms of *S. aureus* and *P. aeruginosa* (Tolker-Nielsen & Sternberg, 2011; Yang *et al.*, 2011).

Researchers have also developed *in vitro* models to capture the spatial and metabolic heterogeneity of CF lungs. For example, Lopes and colleagues explored how polymicrobial biofilm formation is influenced by oxygen availability (Lopes *et al.*, 2017). More recently, Kasetty and colleagues used microfluidics to assess the relationship between flow and biomass production in *P. aeruginosa* and *C. albicans* biofilms (Kasetty *et al.*, 2021). These approaches underscore the need for increasing complexity to be applied to study CF-related polymicrobial cultures *in vitro*.

Innovative models merging *in vitro* and *in vivo* characteristics have been established to address the gap caused by the absence of host cells and the immune system (López-Jiménez & Mostowy, 2021). Human cell culture and cellular microbiology infection models, such as chips, organ-on-chips, and organoids, hold promising potential. These models allow exploring interactions between microbes and human bronchial epithelial cells, especially those carrying the ΔF508 CFTR mutation (Filkins & O'Toole, 2015).

Currently, the number of co-cultured species within *in vitro* models typically ranges from two to four, and investigations involving more than five species are notably rare because of technical difficulties. From a research standpoint, the primary objective is to develop reliable models for exploring the complexities of polymicrobial communities. Meanwhile, from a practical perspective, a significant breakthrough would enable "personalised infection models". Such models, inoculated with sputum samples direct from the patient, would ideally capture not only the species present - preferably in the same ratios as found in the airways - but also the specific *lineages* of each species present in a given patient. Such a setup would enable ethical testing of antibiotic combinations on patient-derived microbiota. However, there is still a long way to go before such "bedside" applications become feasible, both technically and in interpreting polymicrobial scenarios.

Ex vivo models

Ex vivo models, particularly those employing porcine tissue, have gained prestige, primarily in mono-species experiments, for example, studying different mutant derivatives of *P.*

aeruginosa (Harrison *et al.*, 2014). In the context of polymicrobial infections and CF, a porcine lung model has also been developed to investigate the growth, virulence, and signalling mechanisms of *P. aeruginosa* and *S. aureus* (Harrison *et al.*, 2021; Sweeney *et al.*, 2021; Sweeney *et al.*, 2019). However, I note that although utilisation of lung tissue aligns with the context of these experiments, it is still not clear whether any cut of meat would suffice here, since lung tissue is the only substrate that has been tested in this model (Bényei *et al.*, 2024). Nevertheless, and overall, there is good potential for adapting *ex vivo* models to explore the polymicrobial communities associated with CF.

In vivo models

In vivo models play a crucial role in understanding infections because they allow the study of host and microbial interactions in dynamic environments. However, these models are typically more expensive and often necessitate specific training and licensing. They are also limited in replicating chronic infections involving multiple bacteria, as variations in inoculation methods can impact the outcomes and reproducibility (Rolain *et al.*, 2015). Despite these challenges, and rightly or wrongly, *in vivo* models remain a "gold standard" cornerstone for studying inter-species interactions.

In vivo models can be classified as either invertebrate or vertebrate.

A widely used invertebrate laboratory organism, *Caenorhabditis elegans* has been developed as a model to study *P. aeruginosa, C. albicans*, and *Staphylococcus epidermidis*, inoculated individually or in combination (Holt *et al.*, 2017; Powell & Ausubel, 2008). *Drosophila melanogaster* is another promising invertebrate model in polymicrobial infection research. Its advantages are based on the wide range of genetic tools available for creating disease-mimicking mutations. Additionally, the physiology and cell biology similarities between *Drosophila* and humans enhance its value (Apidianakis & Rahme, 2009; O'Brien & Welch, 2019). Notably, successful co-infection of *S. aureus* and *P. aeruginosa* in *Drosophila* has revealed some details of inter-species interactions (Korgaonkar *et al.*, 2013; Lee *et al.*, 2020).

Vertebrate models are also important in studying CF-related airway infections. They are primarily used for investigating lung colonisation and infection, typically inoculated through intratracheal or IV routes (Lebeaux *et al.*, 2013). While mouse models are popular, they have major limitations (although these have not stopped the mouse from being used as a gold

standard in the field). For instance, mice carrying CFTR mutations do not exhibit a lung phenotype (McCarron *et al.*, 2021). An alternative approach can be using β-ENaC mice, which have deficient epithelial sodium channels and manifest a CF-like lung phenotype (McCarron *et al.*, 2021). Besides mice, various animal models, including CF ferrets, rabbits, pigs, sheep, and rats, are available. These can offer pulmonary phenotypes that are more comparable to humans (Birket *et al.*, 2018; Cho *et al.*, 2018; Fan *et al.*, 2018; Stoltz *et al.*, 2015; Sun *et al.*, 2014). However, there remains a critical obstacle as animal microbiomes naturally differ from those of humans, implying that the lung environment in these models is inherently distinct. Humanised pig models, which closely mimic human characteristics, could be a valuable option for research (Lu & Kolls, 2021). However, they require specialised veterinary expertise and come with a high cost, even when used in small numbers. Humanised microbiome mouse models hold promise in bridging this gap, although their utility in CF research has yet to be explored (Fiorotto *et al.*, 2019).

In silico models

Experimental approaches have always been the gold standard in investigating the mechanistic basis of inter-species interactions. However, with the rapid advancement of computational capacity and models, using *in silico* methods has become essential for truly understanding diverse ecosystems and their complex properties. For example, such approaches are well-suited for analysing how polymicrobial interactions within one organ can influence other systems in the body, as illustrated by the gut-lung axis (O'Toole *et al.*, 2021). In the context of CF, Ho and colleagues applied computational methods to dissect the impact of key medications on the ecology of the airway microbiota (Ho *et al.*, 2023). Similarly, McKay and colleagues utilised computational approaches to differentiate the microbiota associated with pwCF and healthy individuals (McKay *et al.*, 2023). Both studies leveraged real-world clinical data, revealing tangible patterns and generating experimentally testable hypotheses. Technical obstacles arise from the somewhat gap-ridden nature of currently available databases and the difficulties in interpreting calculation results. However, the field is evolving, and these modelling approaches are continuously improving. The availability of metagenomic data is also accelerating progress, leading to the expectation that such modelling will become routine, or even essential, in future analyses. Additionally, artificial intelligence tools are set to open new perspectives in this field.

1.5. Polymicrobial interactions in the cystic fibrosis lung

The coexistence of microorganisms in various environments presents numerous opportunities for interactions. These interactions are complex and can simultaneously have conflicting effects, with the potential to both benefit and harm the microbes involved (Gomes-Fernandes *et al.*, 2022; Pallett *et al.*, 2019). Microbes in the human body, especially in the CF lung, face significant challenges posed by the host immune system and antibiotic treatments. Thus, they may co-evolve to cooperate during challenging times yet may attempt to gain an advantage whenever a suitable opportunity arises. Studying these interactions has become a primary focus in microbiology, particularly thanks to the aforementioned advancements and ongoing development of experimental models. However, a comprehensive picture of how microbes interact with each other has yet to be assembled.

1.5.1. Examples of bacterial interactions

Undoubtedly, the most studied microorganisms are bacteria, especially in the context of CF related scenarios. Within this group, most polymicrobial studies focus on the interactions of two pathogens: *P. aeruginosa* and *S. aureus*. These microbes commonly coexist in the CF airways and exhibit a complex spectrum of interactions, ranging from cooperation to competition. These interactions are also influenced by factors such as population diversity, clinical conditions, and environmental challenges (Briaud *et al.*, 2019; Ecfs, 2022; Limoli *et al.*, 2017).

Like other Gram-positive bacteria, *S. aureus* up-regulates virulence factor production in *P. aeruginosa* (Korgaonkar *et al.*, 2013; Rickard *et al.*, 2006). *P. aeruginosa* detects *N*-acetyl glucosamine (GlcNAc), derived from the peptidoglycan cell walls of *S. aureus*. This detection triggers the production of the PQS. PQS controls virulence factors, including pyocyanin, elastase, and 2-heptyl-4-hydroxyquinoline *N*-oxide (HQNO) (Korgaonkar *et al.*, 2013). Interestingly, *P. aeruginosa* variants lacking the peptidoglycan-sensing gene, *agtR*, are less successful in outcompeting *S. aureus*. This observation is a great example showing that ecological interactions are subject to the genetic variants present (Korgaonkar *et al.*, 2013).

HQNO negatively affects the biofilm development, spatial ordering, and biofilm growth of *S. aureus* (Barraza & Whiteley, 2021; Gomes-Fernandes *et al.*, 2022; Ibberson & Whiteley, 2020; Oluyombo *et al.*, 2019; Orazi & O'Toole, 2017). It also promotes the formation of small-colony

variants (SCVs), the most commonly found form of *S. aureus* in clinical samples (Hoffman *et al.*, 2006; Mitchell *et al.*, 2010). These variants exhibit defects in their electron transport systems. They are associated with a more effective survival strategy due to being less susceptible to *P. aeruginosa*-mediated killing than their non-SCV counterparts during co-habitation and increased antimicrobial resistance (Filkins *et al.*, 2015). Other studies have reported enhanced phenotypic resistance of SCVs to antibiotics (Biswas & Götz, 2022; Hammer *et al.*, 2014; Kahl *et al.*, 2016; Loss *et al.*, 2019; Melter & Radojevič, 2010). Notably, it has been found that *mucA* and *rpoN* mutants of *P. aeruginosa*, which are common in chronic infections, do not exhibit this microcolony formation effect (Camus *et al.*, 2021; Liang Yang *et al.*, 2011). Furthermore, HQNO secreted by *P. aeruginosa* also confers an advantage upon *S. aureus* by enhancing its resistance to tobramycin (by inhibiting the uptake of the antibiotic) (DeLeon *et al.*, 2014; Hoffman *et al.*, 2006; O'Brien *et al.*, 2022; Radlinski *et al.*, 2017).

Moreover, *S. aureus* has been shown to act as an iron donor to *P. aeruginosa*, down-regulating iron expression during co-culturing (Mashburn *et al.*, 2005). Similarly, Bisht and colleagues demonstrated that *P. aeruginosa* up-regulates quinolone production under iron deficiency conditions, causing the lysis of *S. aureus* and the subsequent release of iron for utilisation (Bisht *et al.*, 2020).

Conversely, *S. aureus* secretes compounds like acetoin, acetic acid, and possibly small peptides when glucose is present. These can effectively eliminate *P. aeruginosa,* in a dose-dependent manner (Kvich *et al.*, 2022; Vasiljevs *et al.*, 2023). Another study has demonstrated that *S. aureus* can make *P. aeruginosa* more susceptible to ciprofloxacin and aminoglycosides (Trizna *et al.*, 2020). These strategies may serve as a protective mechanism for the *S. aureus* population.

Showcasing a more collaborative approach, *P. aeruginosa* produces alginate that promotes the survival of *S. aureus,* suggesting that mucoid *P. aeruginosa* is more tempered in its engagements with its neighbour (Limoli *et al.*, 2017; Price *et al.*, 2020). Interestingly, the two microbes seem to coevolve within the CF lung, supported by a finding suggesting that *S. aureus* isolates have greater in-host survival when *P. aeruginosa* is present (Bernardy *et al.*, 2022).

It is worth noting that *P. aeruginosa* can impact *S. aureus* indirectly, by modulating the human immune response and stimulating production of a phospholipase, sPLA2-IIA, by bronchial

epithelial cells (Pernet *et al.*, 2014). This phospholipase kills *S. aureus*. Remarkably, the T6SS has been also shown to give *P. aeruginosa* a competitive edge over *S. aureus*, with the potential to inadvertently harm the host during co-infection (Wang *et al.*, 2023).

Additionally, environmental factors, such as oxygen gradients, nutrient availability, and pH levels, potentially affect polymicrobial interactions. For example, the thickness of a mucus or biofilm layer can change the local environment by creating oxygen gradients. This, in turn, can influence metabolic activity and alter microbial dynamics (Worlitzsch *et al.*, 2002). A notable example is the previously mentioned HQNO, which is produced exclusively under aerobic conditions. Consequently, in low-oxygen environments, HQNO plays little role in interactions between *P. aeruginosa* and *S. aureus* (Landa *et al.*, 2024). Low iron levels can also influence inter-species interactions, as both species rely heavily on iron for survival and growth, as discussed in *Chapter 1.2.4* (Reinhart & Oglesby-Sherrouse, 2016). Clinical factors, such as antibiotic exposure, can further modulate these dynamics by promoting biofilm formation or altering the expression of virulence factors (Nolan & Behrends, 2021).

This dissertation only focuses on the interactions between *P. aeruginosa* and *S. aureus*, which are highlighted as examples. Interactions between other bacterial pairs, both aerobes and anaerobes, have also been studied in the literature with fascinating findings (Aranda-Díaz *et al.*, 2020; Baishya *et al.*, 2021; Nair & Andersson, 2023). However, these interactions are not closely related to the focus of this work and thus are not discussed further here.

Overall, bacterial interactions are highly dynamic and shaped by a combination of intraspecies diversity, the microbes involved, as well as environmental and clinical factors (Bernardy *et al.*, 2022; Ibberson & Whiteley, 2020). This complexity underscores the need for further research to thoroughly understand these multifaceted interactions in detail.

1.5.2. Examples of interkingdom interactions: bacteria and fungi

Our understanding of fungal species present in CF-related chronic lung infections has been expanding, particularly concerning *C. albicans* and *A. fumigatus*. Increasing evidence demonstrates that fungi can exhibit contact-dependent communication and extracellular signalling, as well as profoundly influencing biofilm architecture. Consequently, this can affect virulence and antibiotic resistance (Du *et al.*, 2022; Rapala-Kozik *et al.*, 2023).

In this dissertation, I focus on the interactions between *C. albicans* and *P. aeruginosa* as well as *C. albicans* and *S. aureus*. Interactions between other pairings of bacteria and fungi have been studied in the literature, however, these are not discussed in this section (Bényei *et al.*, 2024; Keown *et al.*, 2020).

Regarding *C. albicans* and *P. aeruginosa*, both synergistic and antagonistic effects have been reported. On the one hand, two-species biofilms containing *C. albicans* and *P. aeruginosa* are thicker and rich in alginate, making these structures more robust (Kasetty *et al.*, 2021; Phuengmaung *et al.*, 2020). Moreover, these biofilms have also been reported to exhibit modified expression of proteins associated with virulence, multidrug resistance, and stress responses (Trejo-Hernández *et al.*, 2014). On the other hand, *C. albicans* and *P. aeruginosa* can also negatively influence each other. *P. aeruginosa* produces PQS and its precursor, HHQ, which suppresses biofilm formation by *C. albicans*. Specifically, PQS triggers phenazine release, promoting the formation of reactive oxygen species (ROS), thus disrupting fungal biofilm integrity and hyphal development (Kaleli *et al.*, 2007; Phelan *et al.*, 2014; Reen *et al.*, 2011). Notably, phenazines also enhance the activity of some antifungal agents (Nishanth Kumar *et al.*, 2014). *C. albicans* can also affect the growth and biofilm formation of *P. aeruginosa* by secreting farnesol, tyrosol, and eicosanoids. Farnesol not only inhibits pyocyanin production and rhamnolipid-mediated swarming of *P. aeruginosa* but also significantly impairs its virulence (Cugini *et al.*, 2007; Hassan Abdel-Rhman *et al.*, 2015; McAlester *et al.*, 2008). Likewise, tyrosol decreases the secretion of haemolysin and protease(s) (Hassan Abdel-Rhman *et al.*, 2015). Eicosanoids, including prostaglandin E2, may act as immunomodulatory agents in bacterial-fungal interactions.

Interestingly, *P. aeruginosa* may also influence the transition between yeast and hyphal forms of *C. albicans*. The hyphal form is more invasive than the yeast form, providing tissue adhesion and invasion capacity (Berman & Sudbery, 2002; Maza *et al.*, 2017). Hogan and Kolter observed that *P. aeruginosa* targets and eliminates the hyphal cells of *C. albicans* but not the yeast form in co-culture (Hogan & Kolter, 2002). This process involves several molecular signals, including OdDHL, which inhibits *C. albicans* filamentation without impacting fungal growth (Hogan *et al.*, 2004; Ovchinnikova *et al.*, 2012). Conversely, secreted pseudomonal proteases, such as LasB, stimulate fungal virulence (Peleg *et al.*, 2010).

The interplay between *S. aureus* and *C. albicans* shows a more synergistic relationship (Durand *et al.*, 2022; Short *et al.*, 2023). In a two-species biofilm, *S. aureus* adheres onto *C. albicans* hyphae *via* the fungal adhesin Als3p and uses fungal structures as a scaffold for growth and deeper tissue invasion (Kean *et al.*, 2017; Peters *et al.*, 2012; Peters *et al.*, 2013). This symbiosis increases not only the biofilm biomass but also enhances antimicrobial tolerance, perhaps due to the thicker extracellular matrix (Harriott & Noverr, 2011; Kean *et al.*, 2017; Pammi *et al.*, 2013; Peters *et al.*, 2019; Vila *et al.*, 2021). Moreover, *C. albicans* stimulates the *S. aureus agr* QS system, which supports toxin production and increases virulence (Todd *et al.*, 2019). However, the interactions between these species can also have adverse effects; for example, *C. albicans* can produce farnesol to disrupt *S. aureus* biofilm development (Jabra-Rizk *et al.*, 2006).

These findings demonstrate that bacteria and fungi can engage in both cooperative and antagonistic interactions. Notably, there are some discrepancies in reported outcomes, which are likely due to variations in experimental models and conditions, such as temperature and media composition, as highlighted in recent meta-analyses (Grainha *et al.*, 2020; Kahl *et al.*, 2023; Santos-Fernandez *et al.*, 2023).

Despite our expanding knowledge and new approaches, many aspects of inter-species interactions remain elusive. For example, much of the existing research has focused on dual-species cultures, yet real-world microbial communities are far more diverse, consisting of numerous species. To address this, it is essential to progressively shift towards more complex systems. Incorporating three, four, or even more species into experimental setups will provide deeper insights into how microbial behaviour and biological processes change in increasingly complex (and more realistic) environments. Moreover, it is important to recognise that microbial populations are not homogenous; multiple genetic variants of the same species can coexist within the same niche (Chung *et al.*, 2012). This intra-species heterogeneity plays a crucial role in shaping microbial dynamics and must be considered to fully understand how different – often clinically relevant – mutations influence these communities. For instance, there is a notable gap in our understanding of how the loss of LasR function impacts polymicrobial communities in the CF lung. Furthermore, inter-species interactions have been shown to influence the progression and outcomes of infections (Fourie *et al.*, 2017; Fourie *et al.*, 2016). Notably, polymicrobial environments can alter antimicrobial susceptibility, which

could have profound implications for infection treatment (O'Brien *et al.*, 2022). This underscores the urgency for deepening our understanding of these interactions, not only to advance scientific knowledge but also to improve antibiotic therapies at a time when antimicrobial resistance represents a critical challenge for modern medicine.

Chapter 2

Thesis

P. aeruginosa, a common inhabitant of the lungs of pwCF, often coexists with other microbes, leading to complex, polymicrobial infections. Factors like intra-species genetic variation and environmental challenges, such as antibiotic treatment, further complicate the situation. Understanding the biology underpinning microbial responses in such complex environments is not just of scientific interest; it also offers potential insights into improving clinical interventions.

In this project, I examine how a loss-of-function mutation in *lasR* (the master regulator of quorum-sensing, and a gene that is commonly mutated in clinical isolates of *P. aeruginosa* in the lungs of pwCF) impacts on inter-species interactions and dynamics in a polymicrobial model.

Specifically, it is my thesis that loss of LasR function reshapes inter-species interactions in a polymicrobial cystic fibrosis airway model, especially following antibiotic challenge.

The CF airway model utilised in this project enables the stable co-culture in ASM of *P. aeruginosa*, *S. aureus* and *C. albicans*.

My work initially aimed to test three hypotheses (1, 3, and 4), although as the investigations progressed, two additional ones (2 and 5) emerged and were studied.

My five hypotheses are:

1. That a loss-of-function mutation in *lasR* will significantly impact the interaction between *P. aeruginosa* and other species in the culture.
2. That in mixed populations of a PAO1 progenitor and an isogenic *lasR* mutant, the PAO1 will utilise a LasR-regulated T6SS effector (TseT) to constrain *lasR* mutant titres.
3. That *P. aeruginosa* will exhibit reduced susceptibility to ciprofloxacin in the presence of co-habiting species.

4. That antibiotics will differentially impact cultures containing *P. aeruginosa* PAO1 compared with cultures containing a *lasR* variant of the organism.

5. That antibacterial agents may also influence fungal dynamics, and that this influence may also involve proteins encoded by the *P. aeruginosa tseT* operon.

Chapter 3

Materials and methods

3.1. Microbial strains and routine culture conditions

The microbial strains used in this study were sourced from the Welch Laboratory collection and are detailed in *Table 3.1*. All *P. aeruginosa* variants were derived from PAO1. The 'wild type' ('WT') was designated as $PAO1_{MW}$ (Askenasy *et al.*, 2024), and the mutants are logically named based on their specific genetic modifications.

For routine overnight cultures, a single colony from Luria-Bertani (Lennox formulation LB, Formedium) agar plate was inoculated into 10 mL of LB and incubated at 37°C for 16-18 hours on a rotary drum cycling at 120 rpm. Microbial strains were kept at -80°C as glycerol stocks for long-term storage. For antibiotic selection, the agar plates and growth media were supplemented with antibiotics at the following final concentrations: 50 µg mL^{-1} tetracycline for the Δ*lasR* mutant, 30 µg mL^{-1} gentamicin for the chromosomally complemented Δ*lasR* mutants (Δ*lasR*+PA3904-08 and Δ*lasR*+Empty), 50 µg mL^{-1} ampicillin for maintaining pSB536 in the BHL biosensor strain, 10 µg mL^{-1} tetracycline for maintaining pSB1057 in the OdDHL biosensor strain, and 15 µg mL^{-1} fluconazole to inhibit *C. albicans* growth.

3.2. Growth media and solutions

Table 3.2 lists all growth media and solutions used in this study. Phosphate-buffered saline (PBS) was utilised for serial dilution and washing steps. In mixed-species experiments, selective agars were used to isolate *P. aeruginosa*, *C. albicans*, and *S. aureus*. QS molecule stock solutions were prepared to establish the standard curves for QS measurements. Isopropyl β-D-1-thiogalactopyranoside (IPTG) was used to induce the inserted genes in the complemented Δ*lasR* mutants (Δ*lasR*+PA3904-08 and Δ*lasR*+Empty).

Most ingredients or solutions requiring sterilisation were autoclaved at 121°C for 15 minutes. Exceptions included QS molecules, IPTG, and antibiotic stock solutions, which were sterilised by filtration through a 0.22 µm pore size filter units: Stericup Quick Release Vacuum Filtration System (Millipore) or Millex-GP Filter Unit (Millipore), based on the volume.

Table 3.1. **Microbial strains used in this study.** All were sourced from the Welch Laboratory collection. The ΔPA3904-08 mutant and the complemented Δ*lasR* mutants (Δ*lasR*+PA3904-08 mutant and Δ*lasR*+Empty mutant) were made for this study by Rahan Nazeer.

Name	Description	Reference
P. aeruginosa $PAO1_{MW}$	*P. aeruginosa* PAO1, a spontaneous chloramphenicol-resistant derivative that is used worldwide as a laboratory reference strain. First isolated Melbourne, Australia (1954).	Nguyen, 2011
C. albicans	*C. albicans* SC5314, a clinical isolate that is commonly used as a laboratory reference strain. First isolated in New York, USA (1980s).	Gillum, 1984
S. aureus	*S. aureus* Rosenbach (ATCC 25923), a methicillin sensitive clinical isolate lacking *mecA* and recombinases, that is commonly used as a laboratory reference strain. First isolated in Seattle, USA (1945).	Treangen, 2014
P. aeruginosa PQS biosensor	*P. aeruginosa* Δ*pqsA pqsA*::*luxCDABE*. Luciferase-based PQS biosensor is integrated at a neutral site in the genome.	Fletcher, 2007
E. coli BHL biosensor	*E. coli* JM109 pSB536. Luciferase-based BHL biosensor containing an *ahyR*+*PahyI*::*luxCDABE* fusion. Ampicillin resistant.	Swift, 1997
E. coli OdDHL biosensor	*E. coli* JM109 pSB1075. Luciferase-based OdDHL biosensor containing a *lasR*+*PlasI'*::*luxCDABE* fusion. Tetracycline resistant.	Winson, 1998
P. aeruginosa Δ*lasR* mutant	*P. aeruginosa* $PAO1_{BI}$ derivative, Δ*lasR*::Tc^R cassette, also referred to as PAO-R1. Tetracycline resistant.	Gambello & Iglewski, 1991
P. aeruginosa ΔPA3904-08 mutant	*P. aeruginosa* $PAO1_{MW}$ derivative, ΔPA3904-08. Deletion of PA3904 (PAAR4)-*tecT*-PA3906 (co-*tecT*)-*tseT*-*tsiT*.	Welch Laboratory
P. aeruginosa Δ*lasR*+PA3904-08 mutant	*P. aeruginosa* Δ*lasR*::Tc^R derivative with P*lac*-PA3904-3908-Gm^R::*att* Tn7 insertion. The promoter is IPTG-inducible. Tetracycline and gentamicin resistant.	Welch Laboratory

P. aeruginosa Δ*lasR*+Empty mutant	*P. aeruginosa* Δ*lasR*::Tc^R derivative with P*lac*-Gm^R::*att* Tn7 insertion. The promoter is IPTG-inducible. Tetracycline and gentamicin resistant.	Welch Laboratory

Table 3.2. **Growth media and solutions.** Composition of the growth media and solutions used in this study, with the exception of ASM, which is detailed in *Table 3.3*. Sterilisation methods included autoclaving at 121°C for 15 minutes or filtration, as indicated.

Media/ Solution	Composition
General	
LB	20 g L^{-1} LB-broth Lennox (Formedium) *Note*: sterilised by autoclaving
LB-agar	20 g L^{-1} LB-broth Lennox (Formedium) 15 g L^{-1} Agar Granulated, Bacteriological Grade (Formedium) *Note*: sterilised by autoclaving
Glycerol stocks	800 µL overnight culture or sample 800 µL 50% sterile glycerol (Fisher Scientific)
PBS	10 x Phosphate Buffered Saline tablets (Dulbecco A, Oxoid) for 1 L *Composition:* Sodium chloride 8.0 g L^{-1} Potassium chloride 0.2 g L^{-1} Disodium hydrogen phosphate 1.15 g L^{-1} Potassium dihydrogen phosphate 0.2 g L^{-1} *Note*: sterilised by autoclaving
IPTG	100mM IPTG (Melford) in dH_2O *Note*: made fresh before each experiment and filter sterilised.
Selective agars	
Pseudomonas Isolation Agar (PIA)	45.03 g L^{-1} Pseudomonas isolation agar powder (NutriSelect Plus, Millipore) 20 mL glycerol (Fisher Scientific) *Typical composition:* Magnesium chloride 1.4 g L^{-1} Peptic digest of animal tissue 20 g L^{-1} Potassium sulfate 10 g L^{-1} Triclosan (Irgasan) 0.025 g L^{-1} Agar 13.6 g L^{-1} *Note*: sterilised by autoclaving
Mannitol Salt Agar (MSA)	111 g L^{-1} Dehydrated mannitol salt agar powder (Oxoid) *Typical composition:* 'Lab-Lemco' powder 1.0 g L^{-1} Peptone 10.0 g L^{-1} Mannitol 10.0 g L^{-1}

	Sodium chloride 75.0 g L^{-1} Phenol red 0.025 g L^{-1} Agar 15.0 g L^{-1} *Note*: sterilised by autoclaving
BiGGY agar (Bismuth Glycine Glucose Yeast Agar; Nickerson Agar)	45 g L^{-1} Dehydrated BiGGY agar powder (NutriSelect® Plus, Millipore) *Typical composition:* Yeast extract 1.0 g L^{-1} Glycine 10.0 g L^{-1} Dextrose 10.0 g L^{-1} Bismuth ammonium citrate 5.0 g L^{-1} Sodium sulphite 3.0 g L^{-1} Agar 16.0 g L^{-1} *Note*: instead of autoclaving, the solution was boiled gently to dissolve the medium completely, as suggested by the manufacturer
QS solutions	
OdDHL stock solution	5mM OdDHL (Sigma-Aldrich) in dimethyl sulfoxide (DMSO) *Note*: filter sterilised and stored at -20° C
BHL stock solution	10 mM BHL (Sigma-Aldrich) in DMSO *Note*: filter sterilised and stored at -20° C
PQS stock solution	5 mM PQS (2-heptyl-3-hydroxy-4(1H)-quinolone) (Sigma-Aldrich) in methanol *Note*: filter sterilised and stored at -20° C
Antibiotics	
Colistin stock solution	20 mg mL^{-1} Colistin sulfate salt (Sigma) in dH_2O *Note*: made fresh prior to each experiment.
Ciprofloxacin stock solution	5 mg mL^{-1} Ciprofloxacin (Sigma) in 1% AcOH *Note*: made fresh prior to each experiment.
Tetracycline stock solution	25 mg mL^{-1} Tetracycline (Sigma) in 70% ethanol *Note*: filter sterilised and stored at -20° C
Gentamicin stock solution	25 mg mL^{-1} Gentamicin (Sigma) in dH_2O *Note*: filter sterilised and stored at -20° C
Ampicillin stock solution	100 mg mL^{-1} Ampicillin sodium salt (Sigma) in dH_2O *Note*: filter sterilised and stored at -20° C
Fluconazole stock solution	15 mg mL^{-1} Fluconazole (Sigma) in 95% ethanol *Note*: made fresh prior to each experiment.

ASM was prepared using a combination of SCFM2 formulations from Palmer (Palmer *et al.*, 2007), Kirchner (Kirchner *et al.*, 2012), and Turner (Turner *et al.*, 2015). The same formulation was utilised for previous projects in the host laboratory (O'Brien, 2021; O'Brien & Welch, 2019). *Table 3.3* provides the detailed composition of ASM and *Figure 3.1* illustrates the preparation process used in this study.

As illustrated in *Figure 3.1*, ASM preparation began with the creation of mucin-DNA and stock solutions. For the mucin-DNA solution, 5 g of mucin from porcine stomach (Type-II, Sigma-Aldrich) was added to 250 mL of sterile PBS and stirred overnight at 4°C. Simultaneously, 4 g of fish sperm DNA (Sigma-Aldrich) was dissolved in 250 mL of sterile demineralised water (dH_2O) in a shaking water bath set to 35°C at 180 rpm. The next day, the two solutions were combined, and any undissolved particles were removed by centrifugation at 4000 × *g* for 30 minutes at 4°C. The supernatant was then filter-sterilised using a 0.22 µm Stericup Quick Release Vacuum Filtration System (Millipore) with a vacuum pump (Charles Austen DA7C or Vacuubrand MZ 2C Diaphragm Vacuum Pump). This process – hereafter referred to as 'Stericup filter-sterilisation' – took 1-3 days, with the filter changed as needed. The sterile mucin-DNA solution was either used immediately or stored at room temperature in the dark until required.

Stock solutions were prepared in 50 mL using Falcon tubes (Corning) by adding the quantities specified in *Table 3.3* and diluting with dH_2O, unless otherwise noted. These stocks were stored at 4°C for up to a month, except for certain components listed in *Table 3.3*, which were freshly prepared on the day of use.

During mixing, solids were first added to a beaker containing 150 mL of dH_2O, followed by the appropriate volumes of amino acid stocks, buffered base stocks, and the mucin-DNA solution. The pH was adjusted to 6.8 using 5M NaOH. The mixing was completed by adding the nutrient stocks and egg yolk, with the final volume adjusted to 1 L using dH_2O. The ASM was then Stericup filter-sterilised and stored at 4°C for up to a month. It was pre-warmed before use.

Table 3.3. **List of components used for preparing 1 litre of ASM.** Additional notes provide clarification on specific preparation steps where applicable.

Name	Molecular weight *g mol^{-1}*	Mass for 50 mL stock solution *g*	Volume of stock to add for a litre *mL*	Final concentration *mM*
Mucin-DNA solution				
Mucin from porcine stomach [g]	*NA*	5	250	1.25
Fish sperm DNA [g]	*NA*	4	250	1
Amino acid stocks				
Ser	105.09	0.525	14.46	1.446
Glu·HCl	183.59	0.918	15.492	1.549
Pro	115.13	0.576	16.612	1.661
Gly	75.07	0.375	12.032	1.203
Ala	89.09	0.445	17.8	1.78
Val	117.15	0.586	11.172	1.117
Met	149.21	0.746	6.332	0.633
Ile	131.17	0.656	11.212	1.121
Leu	131.17	0.656	16.092	1.609
Orn·HCl	168.62	0.843	6.76	0.676
Lys·HCl	182.6	0.913	21.28	2.128
Arg·HCl	210.7	1.054	3.06	0.306
Trp [a]	204.23	1.021	0.132	0.013
Asp [b]	133.1	0.666	8.272	0.827
Tyr [cd]	181.19	0.906	8.02	0.802
Thr [d]	119.12	0.596	10.72	1.072
Cys·HCl [d]	157.6	0.788	1.6	0.16
Phe [d]	165.19	0.826	5.3	0.53
His·HCl·H_2O [d]	209.6	1.048	5.192	0.519
Buffered base stocks				
NaH_2PO_4	137.99	1.38	8.125	1.3
Na_2HPO_4	141.96	1.42	6.252	1.25
KNO_3	101.103	5.056	0.348	0.348
K_2SO_4	174.259	2.178	1.084	0.271
Solids [e]				
NH_4Cl	53.491	0.124	*NA*	2.2808

KCl	74.5513	1.116	*NA*	14.943
NaCl	58.44	3.032	*NA*	51.848
MOPS	209.2633	2.092	*NA*	10
Nutrient stocks				
Dextrose (D-glucose)	180.16	9.008	1.2	3
Lithium L-lactate [f]	96.01	4.801	9.3	9.3
$CaCl_2 \cdot 2H_2O$	147.014	7.3507	1.754	1.754
$MgCl_2 \cdot 6H_2O$	203.31	10.1655	0.606	0.606
$FeSO_4 \cdot 7H_2O$[d]	278.05	0.05	1	0.0036
N-acetylglucosamine	221.21	2.766	1.2	0.3
Egg yolk emulsion [g]	NA	NA	5	

[a] Prepared in 0.2 M NaOH [b] Prepared in 0.5 M NaOH [c] Prepared in 1 M NaOH

[d] Made fresh on the day of preparation [e] Added directly to the mixing beaker

[f] Adjusted to pH 7.0 with NaOH [g] Sigma-Aldrich

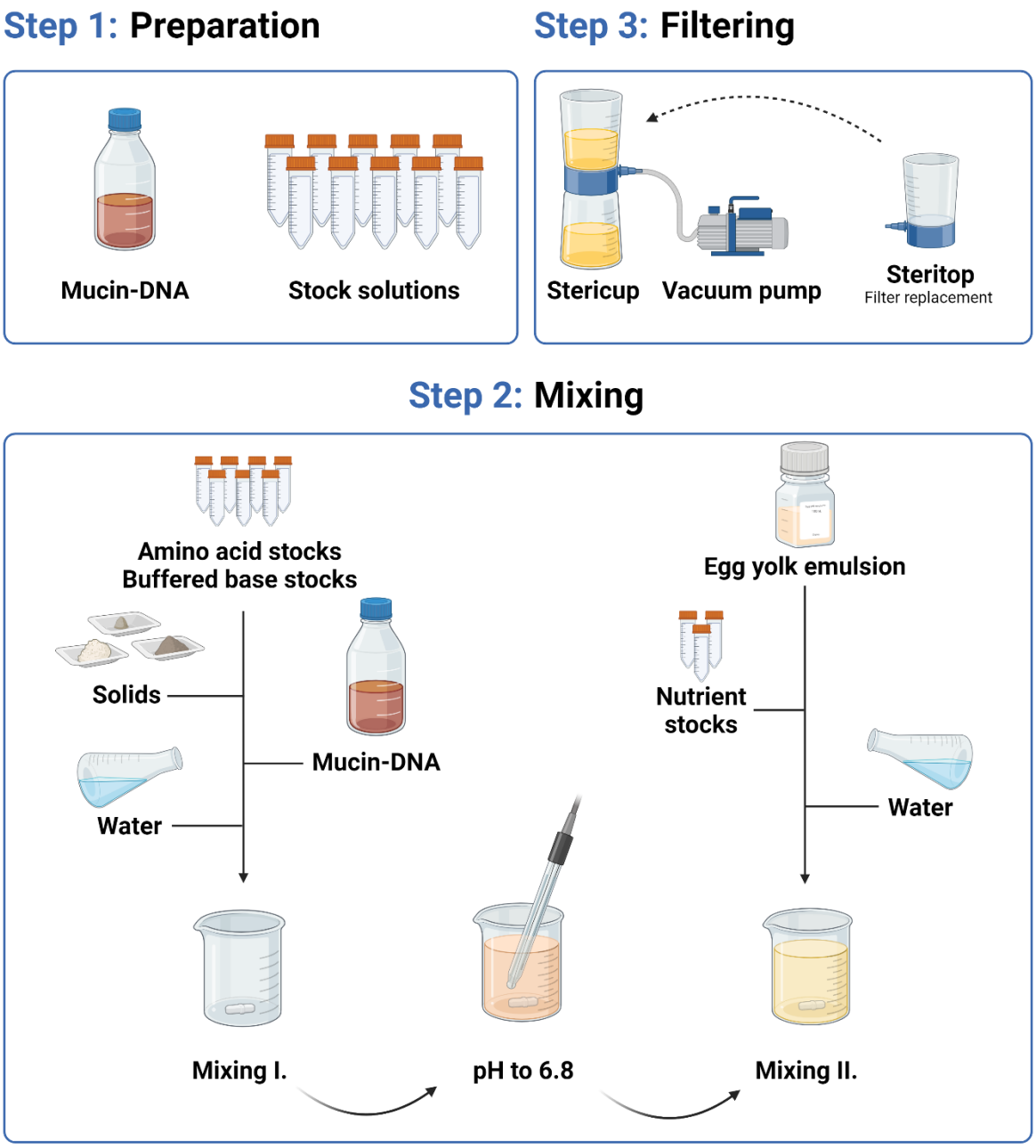

Figure 3.1. **Workflow for preparing artificial sputum media for this study.** The mucin-DNA solution and long-term stock solutions (stored for up to a month) were prepared in advance (Step 1). Fresh stock solutions were made on the day of preparation, solids were measured, and all components were mixed, with pH measured and set midway (Step 2). The final ASM mixture was filter-sterilised, with the filter replaced as necessary (Step 3). Created with *BioRender.com*.

3.3. Whole genome sequencing

Whole genome sequencing (WGS) was conducted on *P. aeruginosa* $PAO1_{MW}$ and Δ*lasR* mutant to identify the full spectrum of differences between these strains. MicrobesNG (Birmingham, UK) carried out the sequencing, following its established protocols (MicrobesNG *Methods*, 2024).

Sample preparation began with routine overnight cultures. The following day, 100 µL of each culture was transferred into 50 mL of fresh LB broth and incubated at 37°C with shaking at 100 rpm until mid-log phase was reached, as determined by optical density at 600 nm (OD_{600}). Cells were harvested, resuspended in DNA/RNA Shield (Zymo Research, USA), and sent to MicrobesNG for sequencing.

Genomic DNA libraries were prepared using the Nextera XT Library Prep Kit (Illumina, San Diego, USA), and sequencing was performed on an Illumina NovaSeq 6000 platform with a 250 bp paired-end protocol. Sequencing reads were adapter-trimmed using Trimmomatic (v0.30) with a sliding window quality cutoff of Q15 (Bolger *et al.*, 2014). De novo assembly was completed using SPAdes (v3.7), and the resulting contigs were annotated with Prokka (v1.11) (Bankevich *et al.*, 2012; Seemann, 2014). Reads were aligned to the reference genome (GCF_000006765.1) using BWA mem (v0.7.17), and SAMtools (v1.9) was used for processing (Stover *et al.*, 2000). Variants were called with VarScan (v2.4.0), using thresholds of 90% for sensitive and 10% for specific allele frequencies. Variant effects were predicted and annotated using SnpEff (v4.3). The Δ*lasR* mutant was compared with $PAO1_{MW}$ to identify genetic differences.

3.4. Growth in the continuous-flow culture model

Most experiments in this project were conducted using an *in vitro* continuous-flow system with ASM as the growth medium. Developed in the host laboratory by Dr Thomas O'Brien and adapted for this study, this model ensured a controlled environment for consistent microbial growth (O'Brien, 2021). The experimental setup, inoculation method, and growth conditions were standardised across all experiments, unless otherwise indicated.

3.4.1. Setup

The continuous-flow culture system, illustrated in *Figure 3.2*, was centred around a 100 mL Duran flask used as the culture vessel. This and the media reservoir were fitted with assembled 4-port HPLC GL80 screw caps (Duran). Sterile ASM was delivered from a 1 L media reservoir to the culture vessel via 1.5 mm bore Sterilin silicone tubing (Fisher Scientific), with flow precisely controlled by a 24-channel IPC ISM934C standard-speed digital peristaltic pump (Ismatec). Another channel on the pump simultaneously removed used media from the culture vessel into a waste bottle, ensuring a balanced system and constant culture volume.

Continuous stirring within the vessel was maintained at 100 rpm to ensure homogeneity, using a MULTISTIRRER6 multi-position magnetic stirrer (Velp Scientifica) placed beneath the culture vessels. The entire system was housed at 37°C in a temperature-controlled environment, providing optimal conditions for microbial growth.

The components of the continuous-flow system, excluding the media reservoir and waste bottle, were assembled and sterilised by autoclaving prior to inoculation.

3.4.2. Inoculation and growth

Typically, six experimental setups were assembled simultaneously in a biological safety cabinet (NU-437-400E, Nuaire) to ensure a sterile environment. This process involved filling the culture vessels with pre-warmed ASM and connecting the sterilised systems to their respective media reservoirs. For inoculation, routine overnight cultures were prepared and washed three times in PBS. Each microbe was introduced into the culture vessels at OD_{600} of 0.05.

The setups were transferred to a warm room set to 37°C, where they were incubated with continuous stirring for three hours before initiating the media flow. Once initiated, the media flow remained constant at 145 µL min^{-1} for all experiments, with brief interruptions only for sampling or the addition of antibiotics or IPTG.

Microbial cultures were sustained and followed for a total of 96 hours, after which the experiments were stopped, and all components of the system were thoroughly cleaned with Virkon (Rely+On).

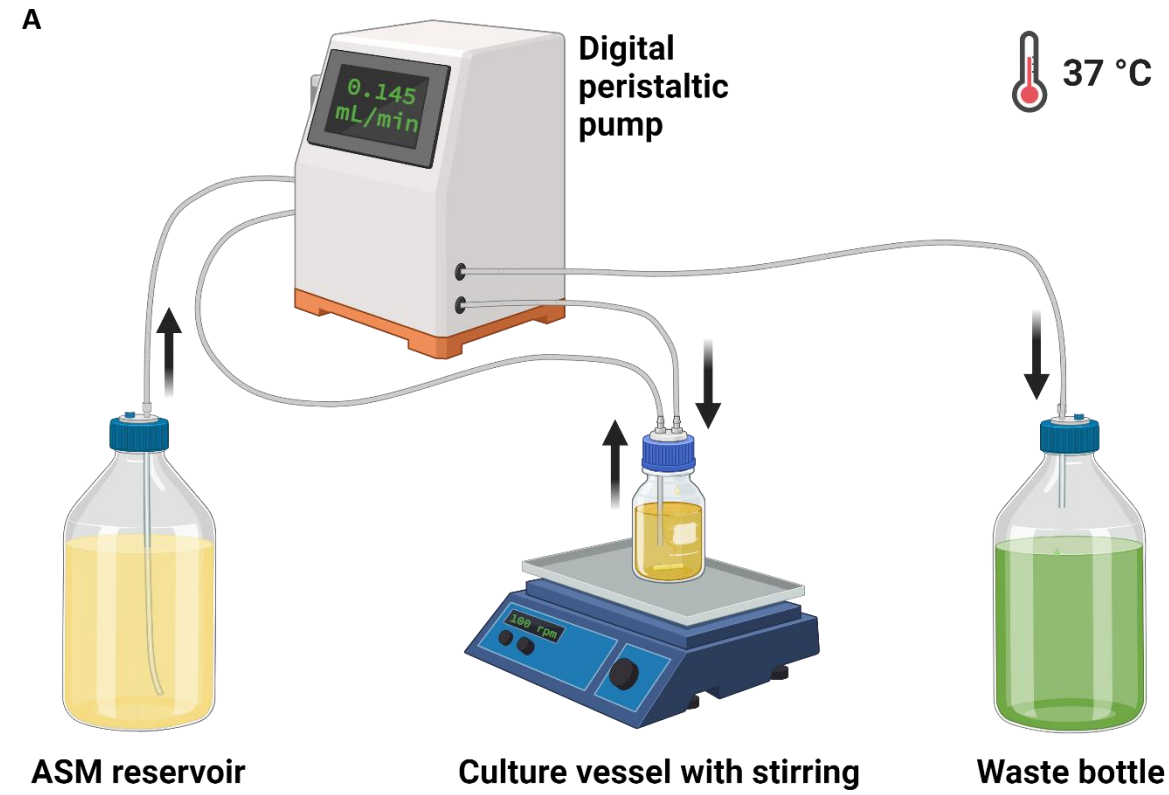

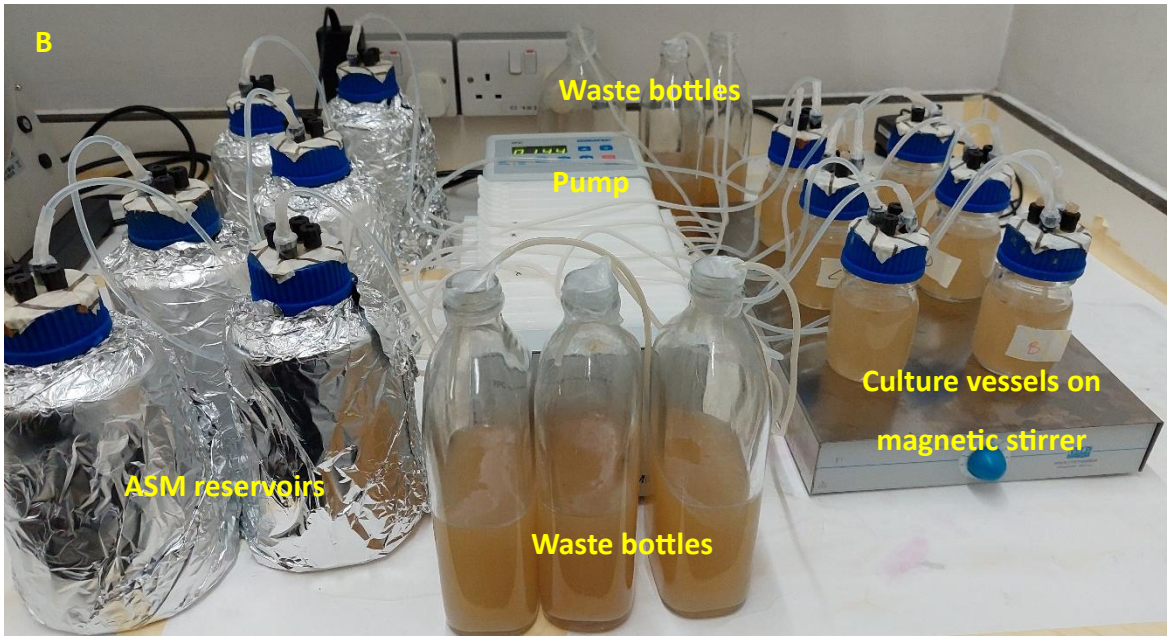

Figure 3.2. **Illustration of the continuous-flow system.** (A) The schematic image demonstrates a single setup with the direction of the flow. Created with *BioRender.com*. (B) The photo shows six setups running in parallel. Key components of the system are labelled.

3.5. Sample collection and processing

Two main sampling methods were utilised, differing in the volume collected and subsequent processing steps. A smaller volume of 1-2 mL was collected when samples were intended for downstream applications such as colony-forming unit (CFU) enumeration or imaging. In contrast, a larger volume of 6 mL was used for CFU enumeration, imaging, and additional processing steps.

Figure 3.3 illustrates the sampling and downstream processing protocols. *Figure 3.4* outlines the sampling regimes applied for different experiments within the continuous-flow system.

Samples were collected under sterile conditions using a portable Bunsen burner to maintain sterility during the procedure. Each culture was accessed directly by unscrewing the cap, and a sample was collected using a 5 mL serological pipette (Costar) with an electric pipette controller (ErgoOne FAST, Starlab). After collection, all samples were thoroughly mixed with a Vortex mixer (Scientific Industries) to ensure homogeneity.

3.5.1. Colony-forming unit enumeration

After thorough mixing, tenfold serial dilutions of sample aliquots were prepared with PBS. Using the single plate-serial dilution spotting method, 20 µL of each dilution was spotted onto selective agar plates, as described by Thomas and colleagues (Thomas *et al.*, 2015). Pseudomonas Isolation Agar (PIA, Millipore) was used to select for *P. aeruginosa*, Mannitol Salt Agar (MSA, Oxoid) for S. aureus, and BiGGY Agar (Bismuth Glycine Glucose Yeast agar, Millipore) for *C. albicans*. Plates were incubated at 37°C. Colonies of *P. aeruginosa* and *S. aureus* were typically counted after 16-18 hours of growth, but plates were re-incubated for up to 72 hours in cases of no or weak initial growth. This ensured that SCVs were also captured. *C. albicans* colonies were counted after 24 hours. CFU counts were determined as the average of at least two technical replicates for each biological replicate.

3.5.2. Processing and storage

Samples were processed for downstream measurements in three parallel ways to prepare glycerol stocks, sterile supernatant aliquots, and cell pellets.

Glycerol stocks were prepared by mixing 800 µL of each sample with 800 µL of sterile 50% glycerol. These aliquots were stored in cryotubes at -80°C until further use.

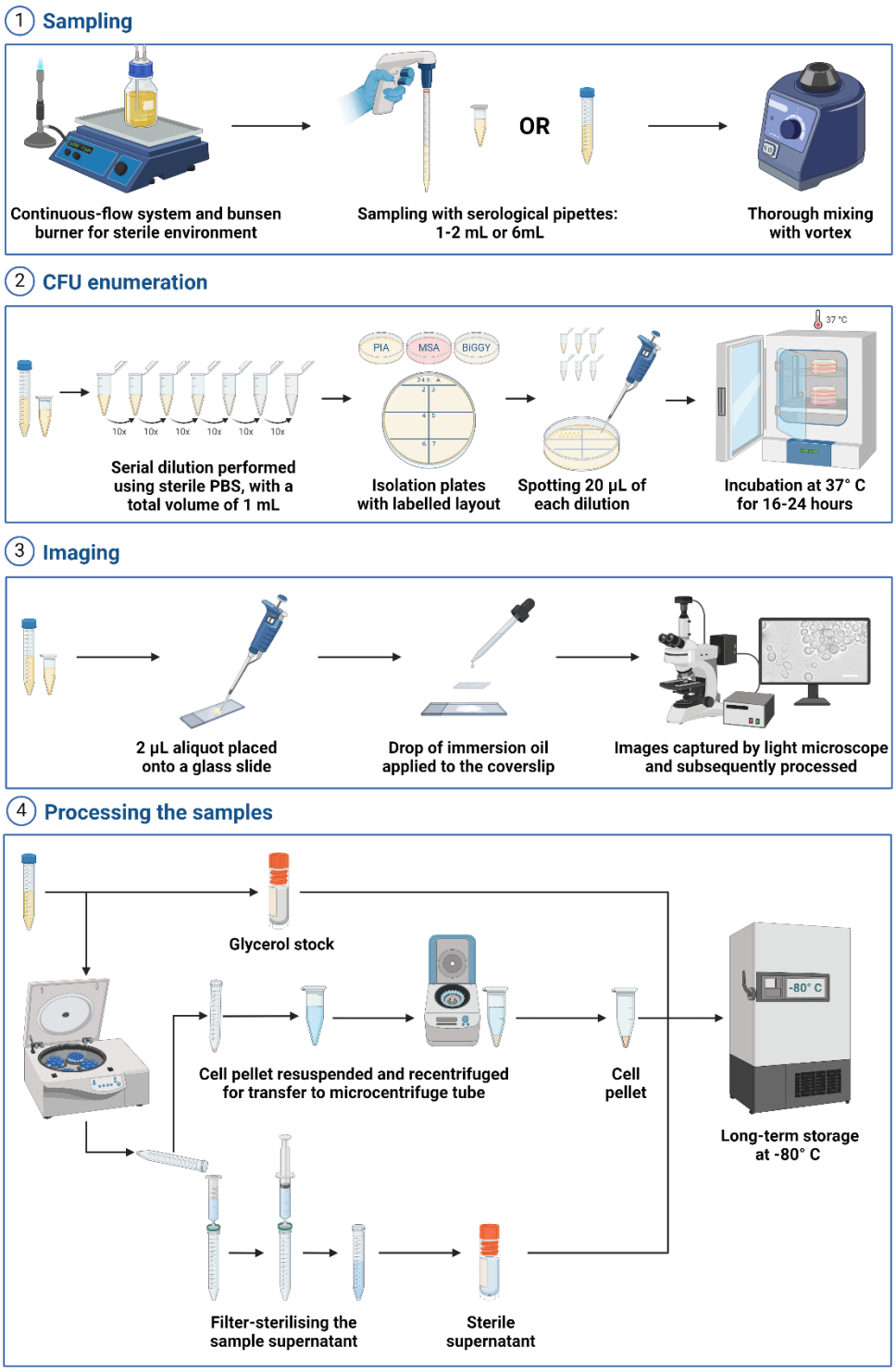

Figure 3.3. **Workflow for sampling and sample processing.** Sampling (1) was performed under sterile conditions, with samples rigorously vortexed to disrupt any aggregates. Microcentrifuge tubes represent 1–2 mL samples used for CFU enumeration (2) and potential imaging (3). Falcon tubes represent 6 mL samples, which were used for CFU enumeration (2), imaging (3), and additional processing (4) to prepare glycerol stocks, sterile supernatants, and cell pellets. Created with *BioRender.com*.

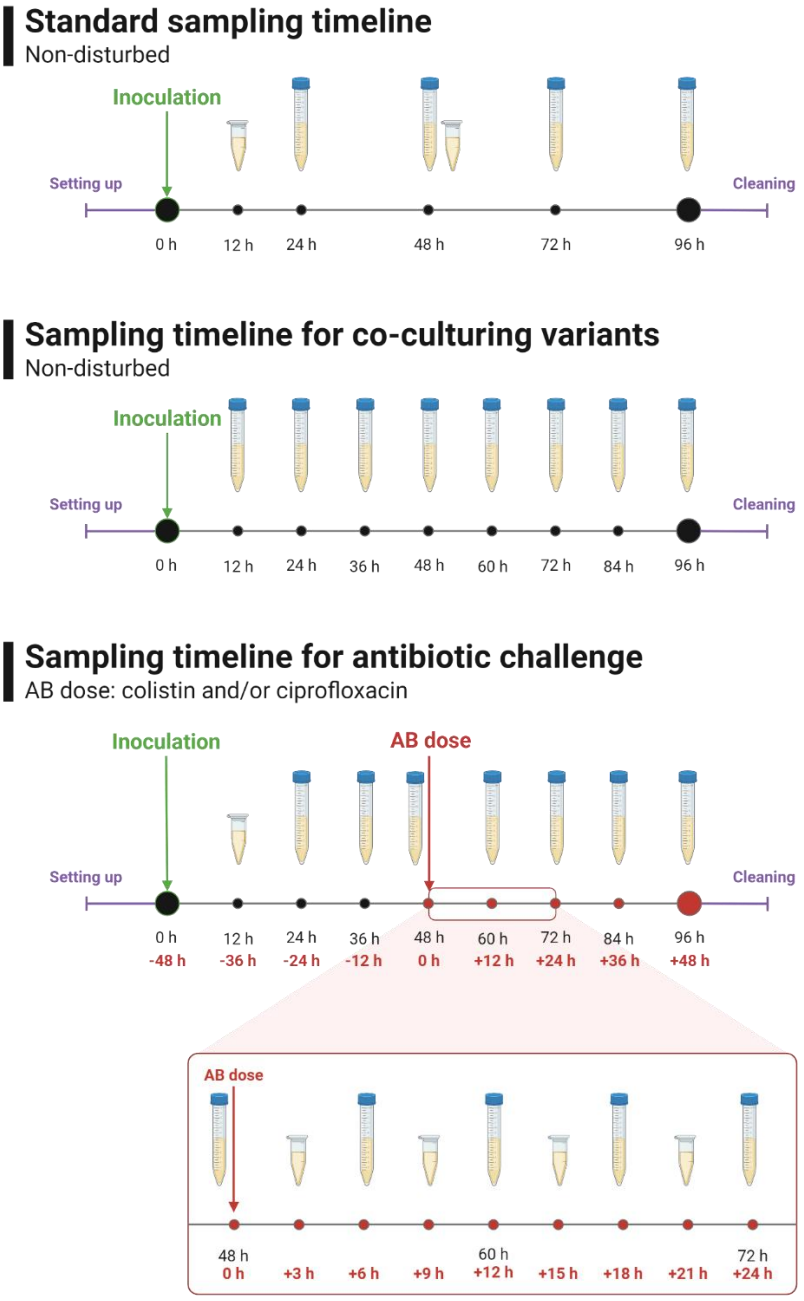

Figure 3.4. **Illustration of the different sampling regimes from the continuous-flow system.** The standard sampling timeline involved collecting samples every 24 hours post-inoculation, up to 96 hours. When co-culturing different genetic variants of *P. aeruginosa* in both monospecies and polymicrobial cultures, samples were collected every 12 hours. For antibiotic challenge experiments, samples were taken every 12 hours, with more frequent sampling during the 24-hour period following the addition of antibiotics, which occurred 48 hours post-inoculation. Red-marked timings represent the timeline centred around the addition of antibiotics (T=0), as used in the graphs presented in *Chapter 6*. Created with *BioRender.com*.

Sterile supernatant was obtained by pelleting cells from 5 mL of each sample via centrifugation at 4000 × *g* for 10 minutes at 4°C. The supernatant was poured into a syringe and filter-sterilised using 0.22 µm pore size syringe filters. The filtered supernatant was mixed, and 2 mL aliquots were stored in cryotubes at -80°C until further use.

For the cell pellets, the pelleted cells were resuspended in 900 µL PBS and transferred to 2 mL microcentrifuge tubes. After another centrifugation at 15,000 × *g* for 5 minutes at 4°C, the supernatant was removed, and the cell pellets were stored at -80°C until further use.

3.5.3. Imaging

For imaging, 2 µL aliquots were taken from thoroughly vortexed, well-mixed samples and placed on a glass slide, which was then covered with a coverslip. A drop of immersion oil was applied to the coverslip. An Olympus BX51 phase contrast microscope equipped with a 100X achromatic oil-immersion objective lens, and QICAM Fast 1394 camera was used for visualisation. The images were processed using Fiji ImageJ (v2.15.1).

3.6. Transcriptomic analysis

Samples for bulk RNA sequencing were collected at the 48-hour timepoint directly from the culture vessel of the continuous-flow system and lysed enzymatically. RNA extraction was performed using the Monarch Total RNA Miniprep Kit (T2010, NEB), following the "Total RNA Purification from Tough-to-Lyse Samples" protocol provided by the manufacturer. The extracted RNA samples were sent to the Nucleic Acid Sequencing Facility (Department of Biochemistry) for library preparation and sequencing. The output reads were returned and analysed using a custom pipeline developed in collaboration with a colleague, Anastasios Galanis. The data analysis was performed by myself. The main steps of the process are illustrated in *Figure 3.5*.

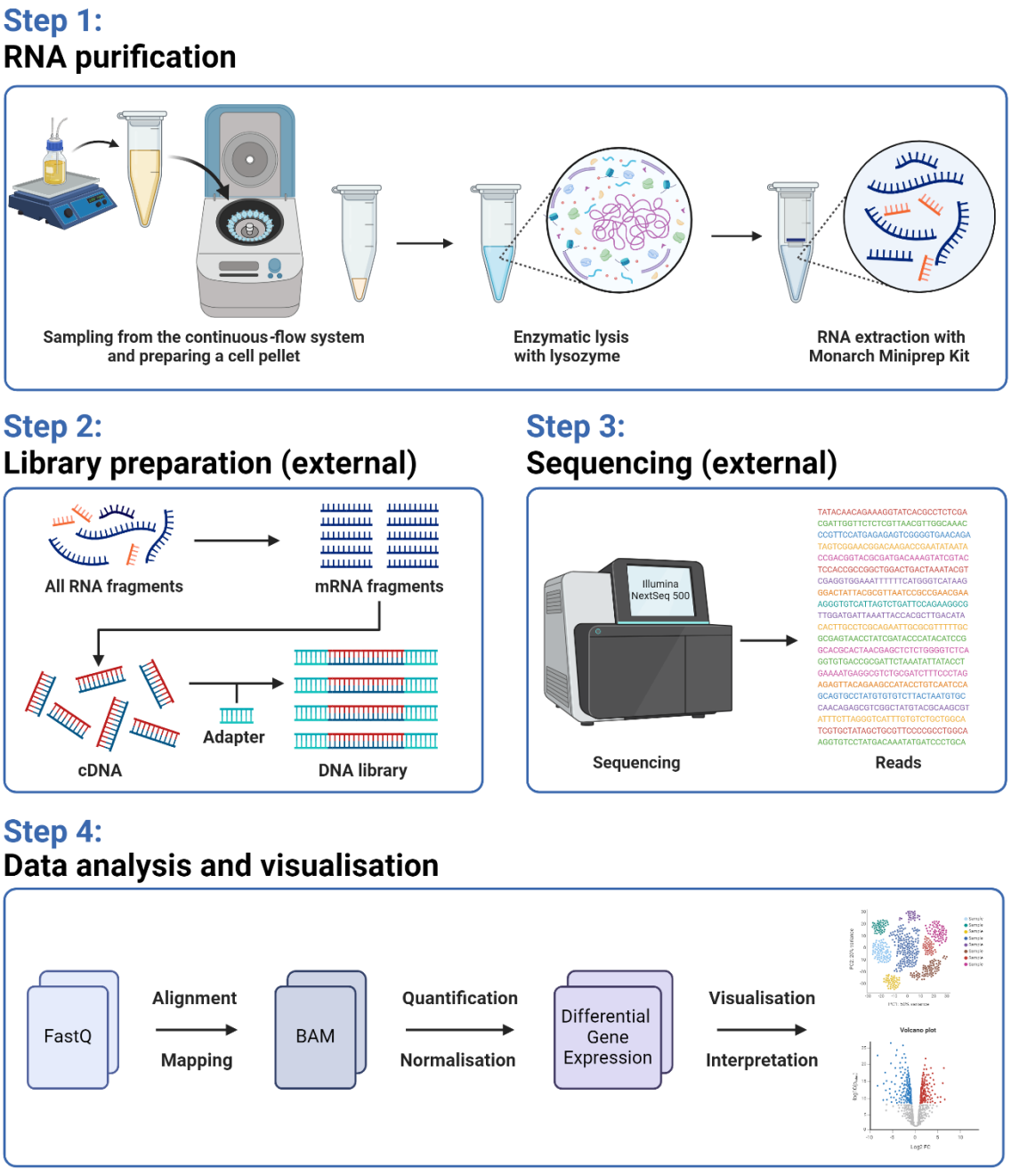

Figure 3.5. **Workflow for RNA sequencing and transcriptomics data analysis.** After collecting 2 mL sample aliquots from the continuous-flow system, RNA was purified using the Monarch Total RNA Miniprep Kit (NEB) following the manufacturer's instructions optimised for 'Tough-to-Lyse Samples' (Step 1). The samples were further processed by the Nucleic Acid Sequencing Facility (Department of Biochemistry), where mRNA fragments were purified, converted to cDNA, and the library was prepared (Step 2). Sequencing was performed using the Illumina NextSeq 500 platform (Step 3). The raw reads were then returned and analysed using a custom pipeline (Step 4). Created with *BioRender.com*.

3.6.1. RNA extraction

After collection, each 2 mL sample was pelleted by centrifugation at 15,000 x *g* for 5 minutes at 4°C, and the supernatant was discarded. Enzymatic lysis of the cells was performed at room temperature using 300 µL of 3 mg mL^{-1} lysozyme (Sigma) for 10 minutes. Then, 600 µL of RNA Lysis Buffer was added, and the mixture was vortexed vigorously for 10 seconds. The sample was then centrifuged at 15,000 × *g* for 2 minutes at room temperature to pellet cellular debris, after which the supernatant was transferred to an RNase-free microfuge tube.

RNA binding and elution were carried out according to the manufacturer's protocol for Monarch Total RNA Miniprep Kit (NEB). Briefly, the sample was passed through a gDNA removal column to eliminate genomic DNA, and the flowthrough was diluted with ethanol before being transferred to an RNA binding column. DNase treatment was applied to ensure complete removal of any residual gDNA. RNA Priming Buffer and Wash Buffer were used to eliminate contaminants, and RNA was eluted with nuclease-free water.

After elution, the RNA samples were centrifuged at 15,000 × *g* for 2 minutes, and RNA concentration, as well as $A_{260/280}$ and $A_{260/230}$ ratios, were measured from a 2 µL aliquot taken from the top of the sample using a NanoDrop (ND-1000, Thermo Scientific). Samples were labelled and stored at -80°C until further processed externally.

The protocols were explicitly tailored for *P. aeruginosa*, reflecting the primary focus of this research. The workstation was thoroughly cleaned with RNaseZap (Sigma) before starting and between steps.

3.6.2. Library preparation and sequencing

The Nucleic Acid Sequencing Facility (Department of Biochemistry) carried out the subsequent sample processing steps. First, RNA sample quality was assessed using an Agilent 2100 Bioanalyzer to confirm RNA integrity and provide RNA Integrity Number (RIN) values. Ribosomal RNA was depleted from bacterial RNA samples using the Ribo-Zero rRNA Removal Kit (Illumina) to enrich for mRNA selectively. The library was prepared using the TruSeq Stranded mRNA Library Prep Kit (Illumina).

Sequencing was conducted on an Illumina NextSeq 500 platform with a 150-cycle high-output run. Paired-end sequencing generated 75 bp reads in both directions, yielding approximately 400 million total reads, with an average of 22.5 million reads per sample.

The output FASTQ files were transferred back via the Illumina BaseSpace Sequence Hub and downloaded for data analysis.

3.6.3. Data analysis

As the first step of the data analysis, quality control (QC) of the raw reads was performed using FASTQC (v12.0) to assess base quality scores, GC content, and other metrics (Andrews, 2023).

For the first phase of the analysis, the reads were processed with high-performance computing (HPC) resources using a custom pipeline developed for this project. Miniconda3 (Conda v24.5.0) was used to manage the software environment and dependencies. Adapter sequences and low-quality bases were trimmed using Cutadapt (v4.9), and QC was repeated to confirm the integrity of the processed reads (Martin, 2011).

As the samples contained mixed reads from three microbial species – *P. aeruginosa*, *S. aureus* and *C. albicans* – a 'virtual' genome was created by combining the genomes of all microorganisms involved. The reads were aligned to this composite genome using Bowtie2 (v2.5.4), generating SAM files (Langmead & Salzberg, 2012). Samtools (v1.20) was used to filter out reads mapped to the *C. albicans* and *S. aureus* genomes, resulting in BAM files containing only reads mapped to the *P. aeruginosa* genome (Danecek *et al.*, 2021; Li *et al.*, 2009). FeatureCounts from the Subread package (v2.0.6) was used to count reads assigned to coding sequences (CDS) of the *P. aeruginosa* genome (Liao *et al.*, 2014). The results were exported as CSV files.

For the second phase of data analysis, R (v4.4.1) was used. DESeq2 package (v1.44.0) was utilised for normalisation and differential expression analysis (Love *et al.*, 2014). The analysis and visualisation pipeline were based on the "Analyzing RNA-seq data with DESeq2" protocol available on the Bioconductor website. Principal Component(s) Analysis (PCA) was generated to evaluate sample clustering using DESeq2 (v1.44.0) and ggplot2 (v3.5.1) packages (Love *et al.*, 2014).

EnhancedVolcano was employed to define and visualise differentially expressed genes (Blighe *et al.*, 2018). The significance thresholds were set at $|\log_2 FC| > 1.0$ and an adjusted p-value < 0.05. Functional and biological interactions between differentially expressed genes and related proteins were investigated using STRING (v12.0) (Szklarczyk *et al.*, 2023). Connections and interaction networks were visualised using the Markov Cluster Algorithm (MCL) with the inflation parameter set to 1.2, which allowed for less stringent clustering and the identification of broader interaction groups.

3.7. Quorum sensing molecule quantification

QS signal molecules – specifically PQS, OdDHL, and BHL – were quantified using reporter strains: *P. aeruginosa* PQS biosensor, *E. coli* OdDHL biosensors and *E. coli* BHL biosensor, as detailed in *Table 3.1*. Sterile culture supernatants were prepared according to the procedure described in *Section 3.5.2*. Samples were collected from -80°C storage and thawed on ice.

Measurements were carried out in 96-well plates with flat micro-clear bottom and black polystyrene wells (655090, Greiner). For sample wells, 60 µL of sterile culture supernatant was added. For controls and blanks, at least three wells contained 60 µL of sterile ASM and 120 µL of sterile ASM, respectively. Additionally, 12 wells were reserved for QS standards, containing 60 µL solutions of the relevant QS molecule in a 1:2 serial dilution, with a maximum concentration of 2000 nM. Stock solutions for these standards were prepared as shown in *Table 3.2* and freshly diluted to the required concentrations in sterile ASM.

Reporter strains were routinely grown as overnight cultures with the appropriate antibiotic, as described in *Section 3.1*. On the day of measurement, these cultures were sub-cultured and grown to OD_{600} of 1.0. Subsequently, 60 µL of the normalised culture was added to each well except the blanks.

Using the FLUOstar Omega microplate reader (BMG LABTECH), each 96-well plate was incubated for 3.5 hours with shaking at 500 rpm, during which OD_{600} and luminescence measurements were taken every 15 minutes. Growth was assessed based on OD measurements, and only data from plates with standard growth patterns and sterile blanks were processed further.

Standard curves were generated and based on these, molecule concentrations in the samples were determined where they were measurable. In cases where luminescence values exceeded the standard curve range, the experiment was repeated with diluted samples to ensure accuracy.

3.8. Co-culturing of *Pseudomonas aeruginosa* genetic variants in the continuous-flow system

The inoculation method followed the same procedure outlined in *Section 3.4.2*, with both *P. aeruginosa* genetic variants added simultaneously. Cultures containing two *P. aeruginosa* genetic variants are referred to as monospecies, whereas those also including *S. aureus* and *C. albicans* are classified as polymicrobial.

Samples were taken every 12 hours, as shown in *Figure 3.4*, and processed as described in *Section 3.5*. In all pairings of genetic variants, distinct antibiotic resistance was utilised to distinguish during CFU enumeration. When one *P. aeruginosa* variant possessed antibiotic resistance, and the other did not, samples were plated on two types of PIA plates: one set containing the relevant antibiotic and the other without antibiotics. At least two technical replicates were used for each type. The plates with antibiotics provided a direct count of the resistant variant, whereas those without antibiotics represented the total count of both strains combined. Subtraction of the antibiotic-resistant count from the total yielded the viable cell count of the non-resistant strain. In cases where both *P. aeruginosa* variants carried distinct antibiotic resistance cassettes, plates containing the relevant antibiotics were used to obtain direct counts for both.

3.9. Co-culturing of microbes in microtiter plate-based cultures

For microtiter plate-based cultures, each sample well contained ASM and two microbes: a genetic variant of *P. aeruginosa* paired with *S. aureus* or with *C. albicans*. Overnight cultures were prepared and washed three times in PBS before inoculation. Each species was added to the wells at OD_{600} of 0.05.

A total volume of 200 µL was used per well of clear-bottom 96-well plates (Nunc, Thermo Scientific). Cultures were incubated for 24 hours at 37°C with orbital shaking at 500 rpm using a FLUOstar Omega microplate reader (BMG LABTECH). Each plate included control wells with

monospecies cultures and blanks with only ASM. OD_{600} measurements were taken every 30 minutes to monitor growth. After 24 hours, the samples were processed for serial dilution and spotting, following the procedure outlined in *Section 3.5.1*. As before, selective agar plates were used to differentiate between the microbial species for CFU enumeration.

3.10. Antibiotic challenge

Antibiotic challenge was applied to assess the antimicrobial susceptibility of *P. aeruginosa* genetic variants in mono- and polymicrobial environments. Colistin and ciprofloxacin were selected for this project, as both are commonly used in clinical practice to treat *P. aeruginosa* lung infections. The combination of these two anti-pseudomonal drugs is frequently employed to eradicate *P. aeruginosa*, as discussed in *Section 1.3.2*.

3.10.1. Minimum inhibitory concentration

Initially, antimicrobial sensitivity was assessed using M.I.C.Evaluator Strips (Oxoid), where commercially prepared antibiotic-impregnated strips were placed on agar plates with microbial lawns. However, further usage of this method was discontinued due to the unavailability of the strips.

Subsequently, minimum inhibitory concentration (MIC) values for colistin and ciprofloxacin were determined using the broth microdilution method described by the Clinical and Laboratory Standards Institute (Clsi, 2021). Briefly, a 1:2 serial dilution of the antibiotics was prepared in ASM, with concentrations ranging from 0 µg mL^{-1} to 256 µg mL^{-1}. Routine overnight cultures were washed three times in sterile PBS, and the normalised cultures were inoculated into the wells at OD_{600} of 0.05, within a total volume of 150 µL per well. The plates were sealed with a gas-permeable membrane (4TITUDE) and incubated at 37°C for 16 hours with moderate shaking (50 rpm). The MIC was determined as the lowest antibiotic concentration at which no visible bacterial growth was detected.

3.10.2. Antimicrobial perturbation of steady-state cultures

Before adding antibiotics, each culture was grown for 48 hours to establish steady-state cultures. This timeline allowed to confirm that microbial populations had reached consistent levels before introducing the antibiotics. Fresh antibiotic stock solutions were prepared on the day of the experiment and diluted with ASM to 100 x final concentration. A 1 mL aliquot of

the relevant solution was added to each culture to achieve a final concentration of 5xMIC_{PA} for the corresponding *P. aeruginosa* genetic variant. As shown in *Figure 3.*4, antibiotics were introduced immediately after sampling at the 48-hour mark, designated as the T=0 hour timepoint on the graphs presented in *Chapter 6*. Following the addition of antibiotics, media flow was paused for one hour before being resumed. The calculated changes in antibiotic concentration over time, taking into account media flow and replacement rates, are illustrated in *Figure 3.6*.

3.10.3. Susceptibility of isolates from polymicrobial culture

To assess whether *P. aeruginosa* cells surviving antibiotic treatment exhibited resistance outside the polymicrobial experimental culture, samples were plated on PIA plates with the used anti-pseudomonal drugs. The steps of the process are illustrated in *Figure 3.7.*

PIA plates were prepared with colistin (20 µg mL^{-1}) or ciprofloxacin (5 µg mL^{-1}), alongside fluconazole (15 µg mL^{-1}) to inhibit fungal growth. Glycerol stocks, prepared as described in *Section 3.5.2*, were transferred from -80°C to dry ice to maintain their frozen state. Small aliquots from each stock were picked up with a pipette and carefully streaked onto the prepared plates. Samples from the following time points were tested: -24, 0, +6, +12, +18, and +24 hours. Plates were incubated at 37°C for 24 hours, after which bacterial growth was evaluated. Control PIA plates with fluconazole but without colistin or ciprofloxacin were used.

3.11. Statistical analysis

Unless otherwise stated, all data are reported as the median with a 95% confidence interval based on at least three independent biological replicates ($N \geq 3$). Statistical significance was defined as $p < 0.05$ for all analyses. Growth data from continuous-flow cultures were analysed using the Wilcoxon signed-rank test, conducted in either GraphPad Prism (v10.3.1) or R (v4.4.1). Competition assay results from microtiter plates were assessed using the Kruskal-Wallis test, conducted in GraphPad Prism (v10.3.1). The specifics of the RNA sequencing data analysis are outlined in *Section 3.6.3*.

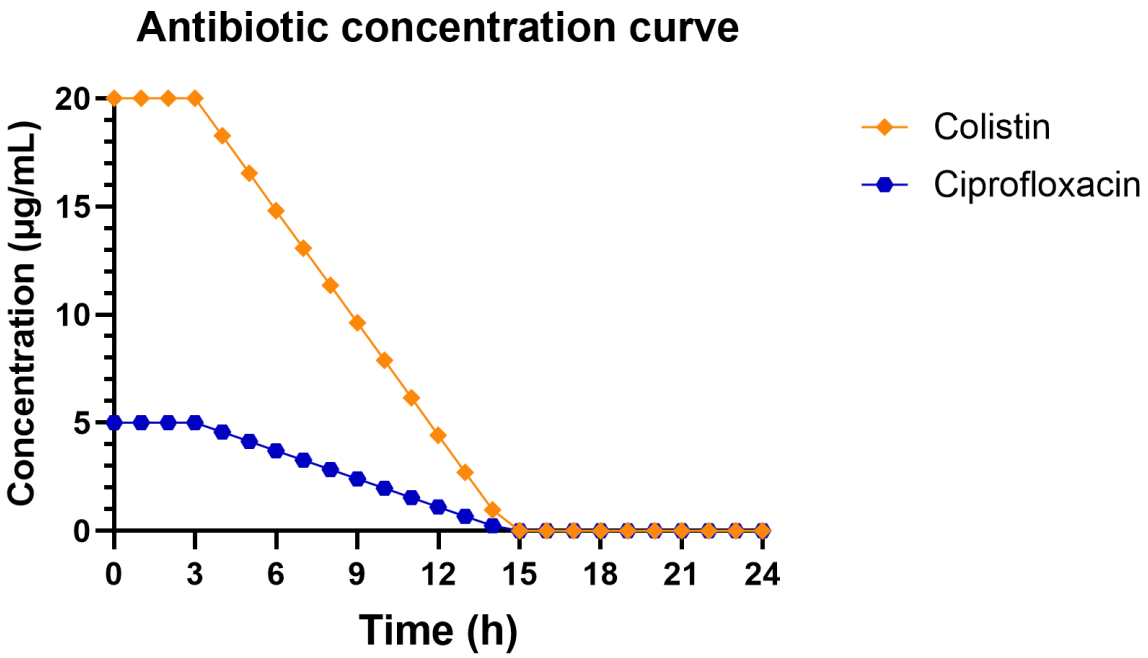

Figure 3.6. **Calculated antibiotic concentrations over time.** Colistin (orange rhombus) and ciprofloxacin (blue heptagons) were administered at 5x MIC_{PA} concentrations during the antibiotic challenge. The graph illustrates the calculated absolute concentrations of the antibiotics over a 24-hour period, starting from the time of administration. Concentrations drop below 1x MIC_{PA} approximately 12 hours after administration.

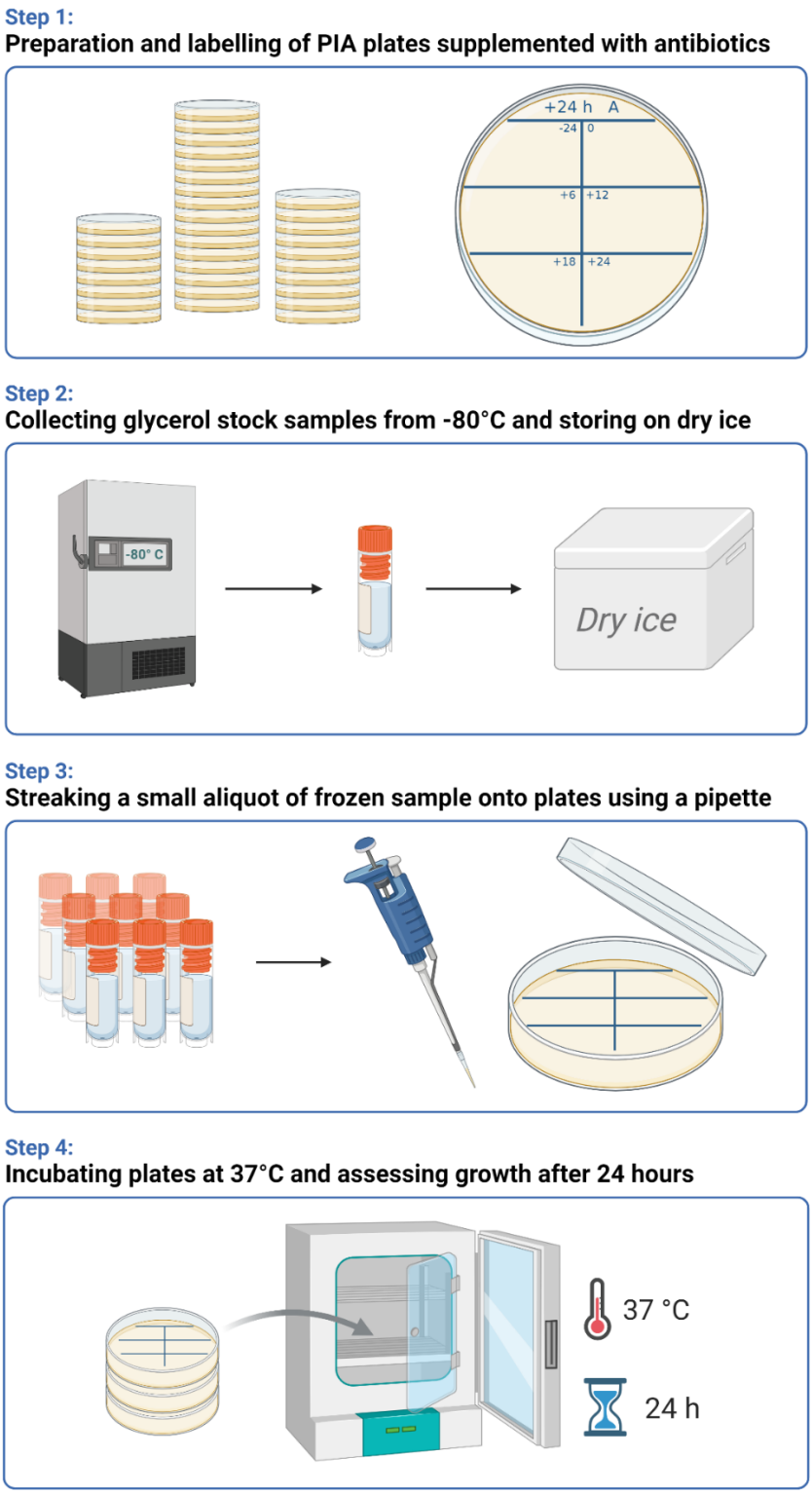

Figure 3.7. **Workflow for antimicrobial susceptibility testing of isolates from polymicrobial cultures.** PIA plates were supplemented with colistin or ciprofloxacin, along with fluconazole, and labelled using a matrix as shown (Step 1). Glycerol stock samples were transferred from -80°C to dry ice (Step 2), and small frozen aliquots were streaked onto the plates (Step 3). Plates were incubated at 37°C for 24 hours to assess bacterial growth (Step 4). Created with *BioRender.com*.

Chapter 4

Transcriptional profile of *Pseudomonas aeruginosa* genetic variants

4.1. Background and rationale

As discussed in *Section 1.1.2*, the CF lung environment hosts a diverse array of microbes, with *P. aeruginosa* typically being the most abundant when present. Furthermore, individuals colonised by *P. aeruginosa* often harbour multiple genetic variants of the bacterium (Kung *et al.*, 2010; Wolfgang *et al.*, 2003). This diversity typically arises from the genetic diversification of the infecting lineage within the airways, rather than co-colonisation by different strains (Chung *et al.*, 2012; Lei Yang *et al.*, 2011).

One of the most commonly found mutations in clinical isolates is in the master regulator of the QS system, *lasR* (D'Argenio *et al.*, 2007; Jayakumar *et al.*, 2022; Smith *et al.*, 2006). These *lasR* mutants are frequently associated with worsened disease prognosis (Hoffman *et al.*, 2009). However, little is known about how *P. aeruginosa* with such a loss-of-function mutation behaves within a polymicrobial community and what changes occur in its transcriptional profile.

The work presented in this chapter is about testing my first hypothesis that a loss-of-function mutation in *lasR* significantly impacts the interaction between *P. aeruginosa* and other species in the culture.

To address this hypothesis, the following objectives were established:

1. To evaluate the abundance of 'wild-type' $PAO1_{MW}$ and the loss-of-function *lasR* mutant (Δ*lasR* mutant) in both monospecies and polymicrobial cultures.
2. To analyse the cross-sectional transcriptional profiles at the 48-hour timepoint, when the cultures are in a steady state.
3. To measure the concentration of QS molecules in the *in vitro* continuous-flow system over time.

4.2. Non-disturbed polymicrobial cultures

As demonstrated previously, a recently developed continuous-flow model enables the stable maintenance of long-term *in vitro* co-cultures containing three distinct microbial species associated with CF airway infections: *P. aeruginosa*, *S. aureus,* and *C. albicans* (O'Brien, 2021). This setup offers a significant advantage over batch cultures, particularly for investigating steady-state scenarios. To address the first objective of this chapter – evaluating the abundance of different genetic variants of *P. aeruginosa* in both monospecies and polymicrobial cultures – this continuous-flow system was used. Initially, the reproducibility of results from prior studies with the $PAO1_{MW}$ was confirmed, both in mono- and poly-species cultures. Subsequently, the Δ*lasR* mutant was used to explore the behaviour of this common variant in mono- and polymicrobial cultures under non-disturbed conditions.

4.2.1. 'Wild-type' *Pseudomonas aeruginosa* $PAO1_{MW}$

To ensure research continuity, I first repeated previous experiments with *P. aeruginosa* $PAO1_{MW}$ in the continuous-flow system. My findings confirm that monospecies and triple-species co-cultures yield highly reproducible outcomes, with no significant differences between earlier results and my experimental repeats ($p > 0.5$). After approximately 24 hours, the single-species culture of *P. aeruginosa* stabilised at around 10^8 CFU mL^{-1} and this was maintained for the remainder of the 96-hour experiment. The polymicrobial culture also reached and sustained stable levels, as illustrated in *Figure 4.1*. Specifically, the titres of *P. aeruginosa* and *S. aureus* remained around 10^8 and 10^7 CFU mL^{-1}, respectively, while *C. albicans* was detected between 10^4 and 10^5 CFU mL^{-1} at Q = 145 µL min^{-1} flow, consistent with expectations.

To gain deeper insights into the initial 24-hour period following inoculation, I also conducted a sampling every three hours during the first 24 hours of a 48-hour experiment. During this settling-in period, the viable cell counts of *P. aeruginosa* and *S. aureus* fluctuated, potentially indicating a predominantly competitive dynamic between these species. Meanwhile, *C. albicans* rarely exceeded 10^5 CFU mL^{-1}, as shown in *Figure 4.2*. These findings provide valuable data for a computational ecology model developed by my bioinformatician colleague, Pok-Man Ho.

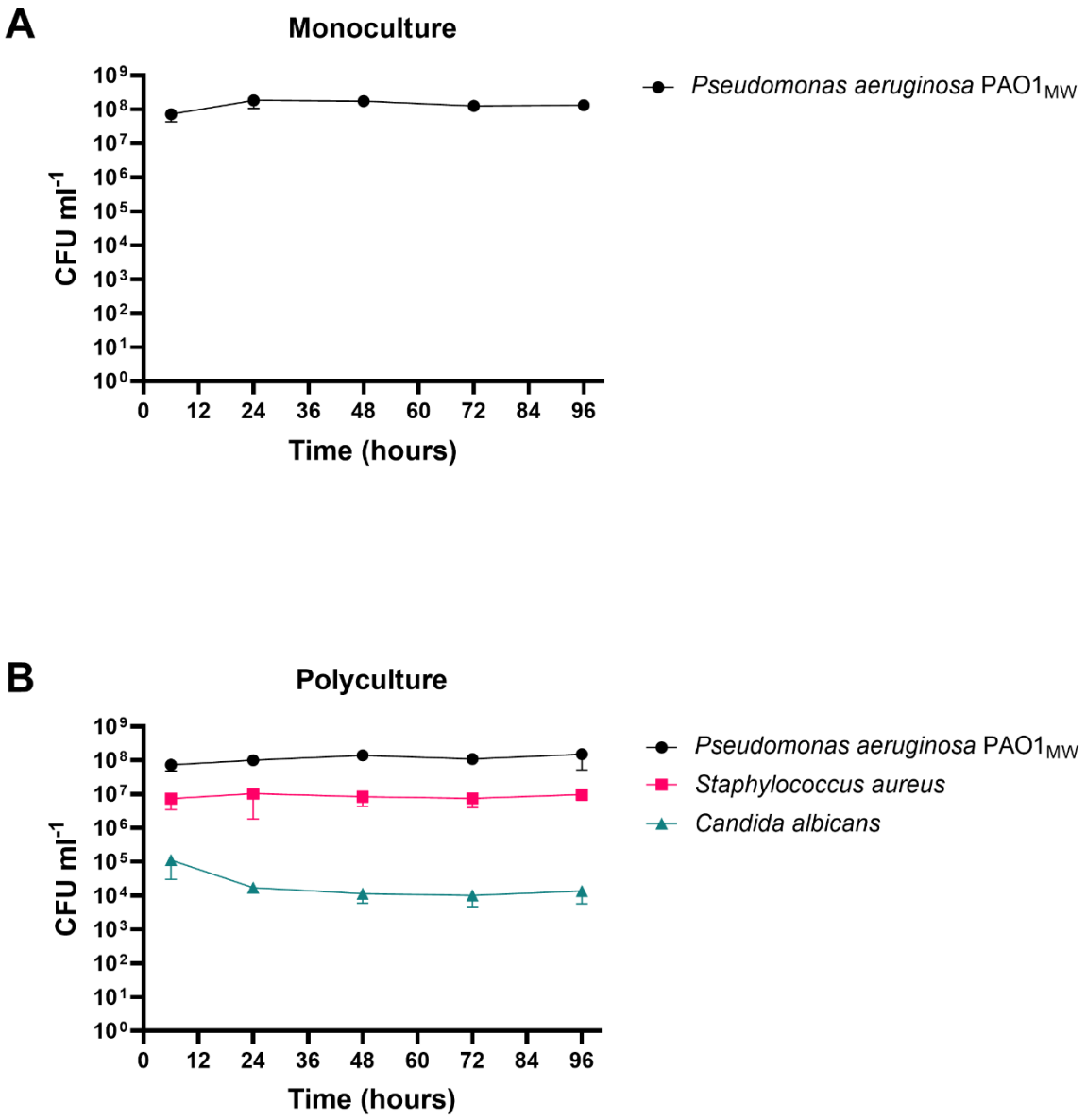

Figure 4.1. **Monoculture and polyculture with *Pseudomonas aeruginosa* PAO1$_{MW}$ in the continuous-flow system.** Viable cell counts of *P. aeruginosa PAO1$_{MW}$* (black circle), *S. aureus* (pink square), and *C. albicans* (turquoise triangle) in non-disturbed cultures within ASM at Q = 145 µL min^{-1} flow. CFU mL^{-1} values are plotted on a $\log_{10}$ scale. Data is represented as the median with a 95% confidence interval across six independent experiments (n=6). No significant differences were found in cell counts compared with the results at the 24-hour timepoint ($p > 0.2$).

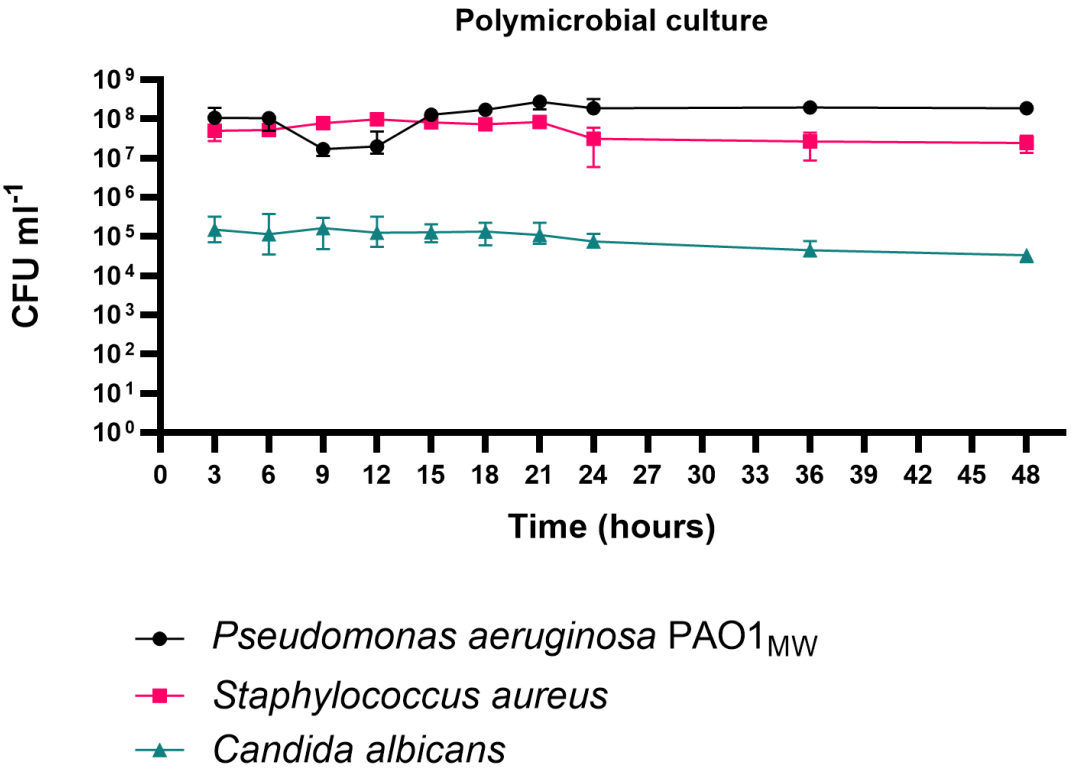

Figure 4.2. **Detailed sampling of the polyculture with *Pseudomonas aeruginosa* PAO1$_{MW}$ in the continuous-flow system.** Viable cell counts of *P. aeruginosa* PAO1$_{MW}$ (black circle), *S. aureus* (pink square), and *C. albicans* (turquoise triangle) in non-disturbed cultures within ASM at Q = 145 µL min^{-1} flow. CFU mL^{-1} values are plotted on a $\log_{10}$ scale. Data is represented as the median with a 95% confidence interval across three independent experiments (n=3).

4.2.2. Δ*lasR* mutant

Monospecies and polymicrobial cultures were made using the loss-of-function mutant of *P. aeruginosa* with an inserted tetracycline resistance cassette (Δ*lasR*::Tc^R, referred to as Δ*lasR* mutant hereafter), as shown in *Figure 4.3*. The monospecies culture of the Δ*lasR* mutant stabilised at approximately 10^8 CFU mL^{-1}, slightly but not significantly lower than the $PAO1_{MW}$ in *Figure 4.1*. In the triple-species culture, the steady-state levels were similar to those observed with the $PAO1_{MW}$ (*Figure 4.1*); however, *C. albicans* took longer to reach stable titres. This suggests that the absence of *lasR* function does potentially influence polymicrobial dynamics. However, it does not necessarily have a lasting impact on the long-term stability of the polymicrobial cultures under these experimental conditions, similar to previous findings (Cheng *et al.*, 2019).

4.3. Whole genome sequencing

Following best practices, WGS was performed on the strains used in this study, $PAO1_{MW}$ and Δ*lasR* mutant. This step was essential because the Δ*lasR* mutant had been generated externally, and although both strains were assumed to share the same PAO1 background, laboratory microevolution could have resulted in unexpected changes. (Askenasy *et al.*, 2024). Another key focus of this analysis was to determine whether any mutations existed in the *mexT* gene. This was important for two reasons: firstly, as discussed in *Section 1.3.1.*, a double *lasR* and *mexT* mutant can exhibit partial restoration of QS features. Secondly, as described by LoVullo and Schweizer, mutations in the *mexT* gene frequently occur in laboratory environments with the PAO1 strain (LoVullo & Schweizer, 2020). This is evident in the popular reference PAO1 genome used on *pseudomonas.com* (GCF_000006765.1), which contains an 8 bp insertion leading to premature termination, rendering MexT non-functional and unable to stimulate the expression of MexEF-OprN (Maseda *et al.*, 2000).

Based on the outcome of the WGS, both the $PAO1_{MW}$ and the Δ*lasR* mutant were found to possess an intact *mexT* gene in the strains used for this work. Aside from the expected difference, namely the *lasR* deletion, the additional mutations I identified are unlikely to have influenced the experimental outcomes. These mutations are detailed in *Table 4.1*.

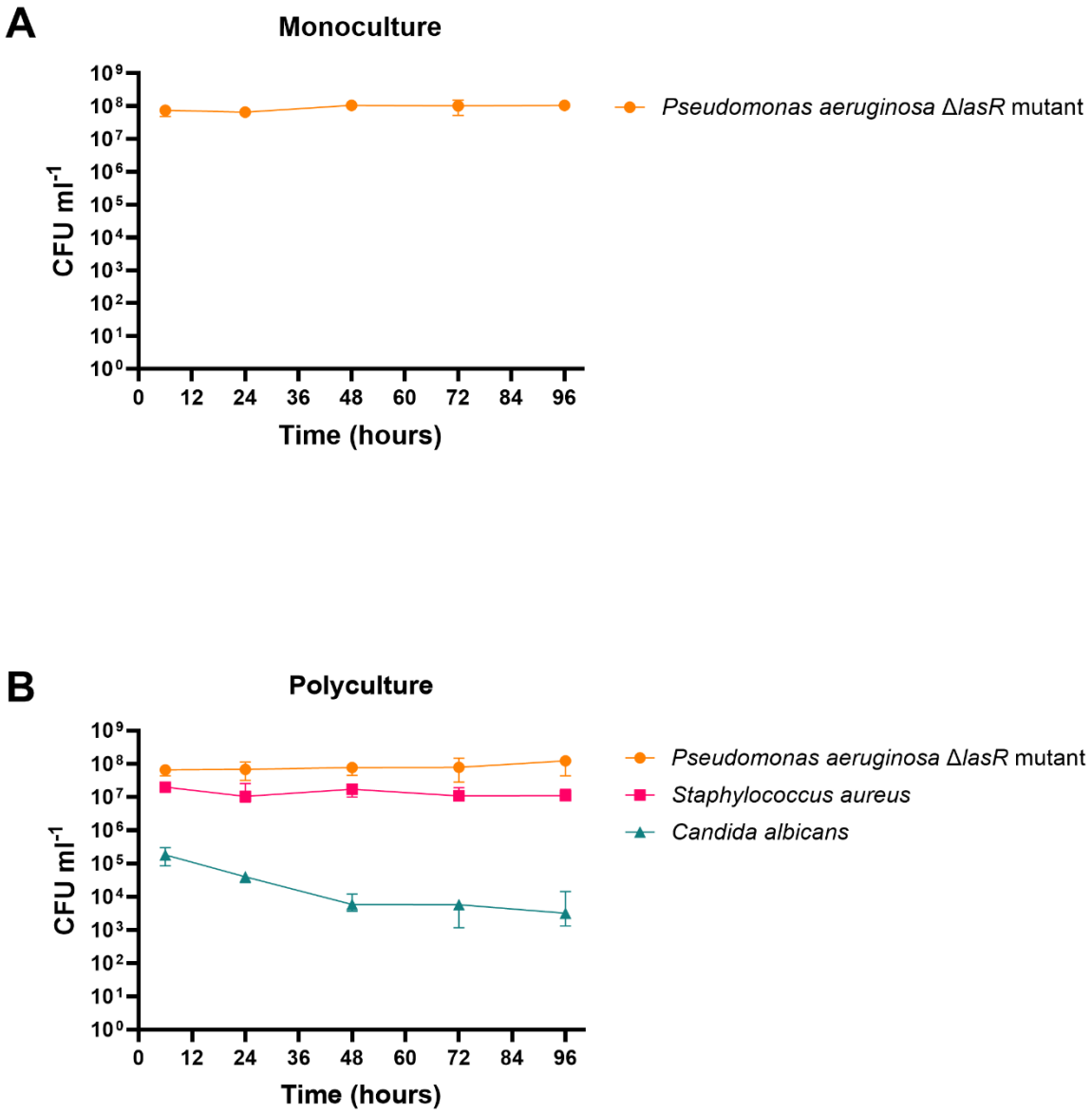

Figure 4.3. **Monoculture and polyculture with *Pseudomonas aeruginosa* Δ*lasR* mutant in the continuous-flow system.** Viable cell counts of *P. aeruginosa* Δ*lasR* mutant (orange circle), *S. aureus* (pink square), and *C. albicans* (turquoise triangle) in non-disturbed cultures within ASM at Q = 145 µL min^{-1} flow. CFU mL^{-1} values are plotted on a log_{10} scale. Data is represented as the median with a 95% confidence interval across four independent experiments (n=4). No significant differences were found in cell counts compared with the results at the 24-hour timepoint ($p > 0.2$).

Table 4.1. **Additional mutations in the *Pseudomonas aeruginosa* Δ*lasR* mutant compared with the PAO1$_{MW}$.**

Position	Locus	Product	Type	Mutation	Annotation
1,215,657	PA1122	Putative peptide deformylase	Frameshift mutation	A → AG	
4,212,201	PA3760	N-acetyl-D-glucosamine phosphotransferase system transporter	Missense mutation	A → G	H636R
4,771,865	PA4268	30S ribosomal protein S12	Missense mutation	T → C	K88R
5,655,220	PA5024	Conserved hypothetical protein	In-frame triplet deletion	C**CGG** → C	GW141W
5,676,046	PA5040	Type 4 fimbrial biogenesis outer membrane protein PilQ precursor	Missense mutation	G → T	P605T

4.4. Transcriptome profiling

To address the second objective of this chapter – analysing the cross-sectional transcriptional profiles at the 48-hour timepoint when the cultures had reached a steady state – samples were collected for bulk transcriptomic measurements as outlined in *Section 3.6*. The 48-hour timepoint was chosen because, by this stage, the population titres had stabilised.

The sequencing reads provided by the Nucleic Acid Sequencing Facility (Department of Biochemistry) were processed using HPC and bioinformatics tools, as described in *Section 3.6.3*. Briefly, the reads were first trimmed (using Cutadapt) and then aligned to a combined 'virtual' genome of the three species to filter out reads matching the *C. albicans* or *S. aureus* genomes (using Bowtie2 and Samtools). Feature counts were then generated from the reads that matched the *P. aeruginosa* PAO1 genome, with an additional quality filter applied (using FeatureCounts). The quality of the reads was continuously assessed throughout the process, yielding satisfactory results, as shown in *Table 4.2*. The analysis pipeline concluded with differential expression analysis (DESeq2), interpretation of the results, and visualisation.

PCA of the data revealed that the four sample groups clustered in a 2x2 pattern, as shown in *Figure 4.4*. The results indicate notable differences in gene expression between the culture types (mono- or poly-species) and between the strains ($PAO1_{MW}$ or Δ*lasR* mutant). Due to the nature of the analysis, pairwise comparisons were conducted between the samples to study transcriptional differences.

Table 4.2. **Quality control metrics and read counts across samples.** This table presents essential QC metrics for each sample, including RIN, GC content, and Base Quality Score (Phred Score), as well as read counts, such as the total number of reads, percentage of paired reads, overall alignment rate to the combined 'virtual' genome of three species, and percentage of reads mapped to the PAO1 genome.

Sample	RIN	GC content	Base Quality Scores	Total reads	Paired	Overall alignment rate	Mapped to PAO1
*lasR*_mono_A	9.9	57	30+	22,508,069	100%	97.63%	100%
*lasR*_mono_B	10	57	30+	20,945,546	100%	97.90%	99.99%
*lasR*_mono_C	10	57	30+	18,200,990	100%	97.67%	100%
WT_mono_A	9.7	56	30+	25,078,076	100%	98.70%	100%
WT_mono_B	9.8	57	30+	20,452,156	100%	98.51%	99.99%
WT_mono_C	8.8	58	30+	15,248,241	100%	97.61%	100%
*lasR*_poly_A	10	59	30+	15,062,703	100%	95.97%	98.98%
*lasR*_poly_B	9.7	59	30+	17,906,557	100%	87.01%	99.42%
*lasR*_poly_C	10	58	30+	15,566,407	100%	84.58%	98.42%
WT_poly_A	9.5	57	30+	21,406,291	100%	98.17%	99.95%
WT_poly_B	9.6	57	30+	24,394,084	100%	97.97%	99.89%
WT_poly_C	9.3	60	30+	19,977,580	100%	95.09%	99.84%

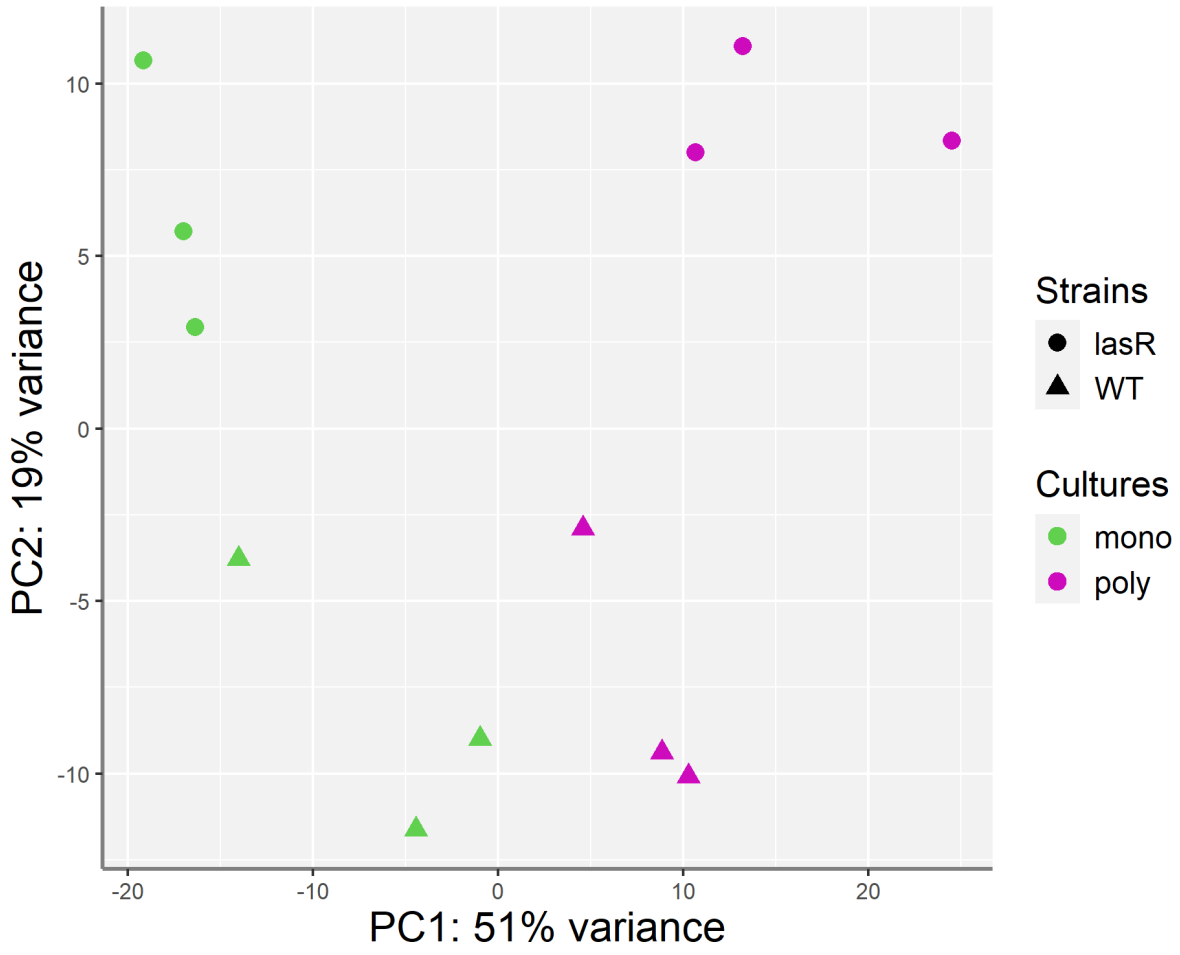

Figure 4.4. **Principal components analysis of the transcriptome profiling data.** This figure illustrates the variance among transcriptomes of *P. aeruginosa* from mono- and polymicrobial (green and magenta) cultures, including PAO1$_{MW}$ (WT; triangle) or Δ*lasR* mutant (lasR; circle) strains. The analysis was conducted on 2,606 genes with at least ten mapped reads across all samples. Each condition comprises three biological replicates (n=3).

4.4.1. Comparative analysis of $PAO1_{MW}$ mono- and polymicrobial culture samples

Firstly, the transcriptomic profiles of 'wild-type' *P. aeruginosa* $PAO1_{MW}$ (WT) in mono- and polymicrobial cultures were compared. A total of 5,574 genes were expressed in both conditions, each with more than ten reads across all samples. Among these, 12 genes showed significant up-regulation in the polymicrobial culture, and 61 genes were significantly down-regulated, as shown in *Figure 4.5*. Detailed list of transcripts with significant differences in abundance are provided in *Supplementary Table A*. As specified in *Section 3.6.3*, the significance thresholds for all comparisons were set at $|\log_2 FC| > 1.0$ and an adjusted p-value < 0.05.

Relatively few transcripts were affected by growth in a polymicrobial environment *cf*. a monomicrobial environment. The genes with significantly increased expression in the polymicrobial culture were grouped based on their functional roles, as illustrated in *Figure 4.6.*

Notably, a subset of up-regulated genes – *agtA, potB,* and *potC* – are involved in polyamine transport (*Figure 4.6*, Cluster 1). These genes are critical for regulating intracellular concentrations of polyamines and other essential molecules, which play a crucial role in survival and pathogenicity, particularly under stress (Long *et al.*, 2022). Another cluster includes genes associated with the cytochrome complexes (*Figure 4.6, Cluster 2*), which are key components of the electron transport chain and are vital for cellular respiration and bacterial adaptation to oxidative stress (Arai *et al.*, 2014). Additional clusters include amino acid biosynthesis, metabolism, and catabolism-related genes, such as *glyA2* and *gcvT2*, required for glycine and serine catabolism (*Figure 4.6*, Cluster 3) (Cianciulli Sesso *et al.*, 2021). These are essential processes for the growth and survival of *P. aeruginosa*. Genes coding hypothetical proteins linked to stress responses and resistance mechanisms, including chlorhexidine efflux, are also up-regulated (*Figure 4.6, Cluster 4*). Finally, another cluster of up-regulated genes includes PA4033 and *aqpZ*, which are related to cellular homeostasis, particularly in maintaining water balance and responding to osmotic stress (*Figure 4.6, Cluster 5*). Taken together, these data suggest that the presence of other microbes creates a more challenging environment, prompting *P. aeruginosa* to activate adaptive strategies.

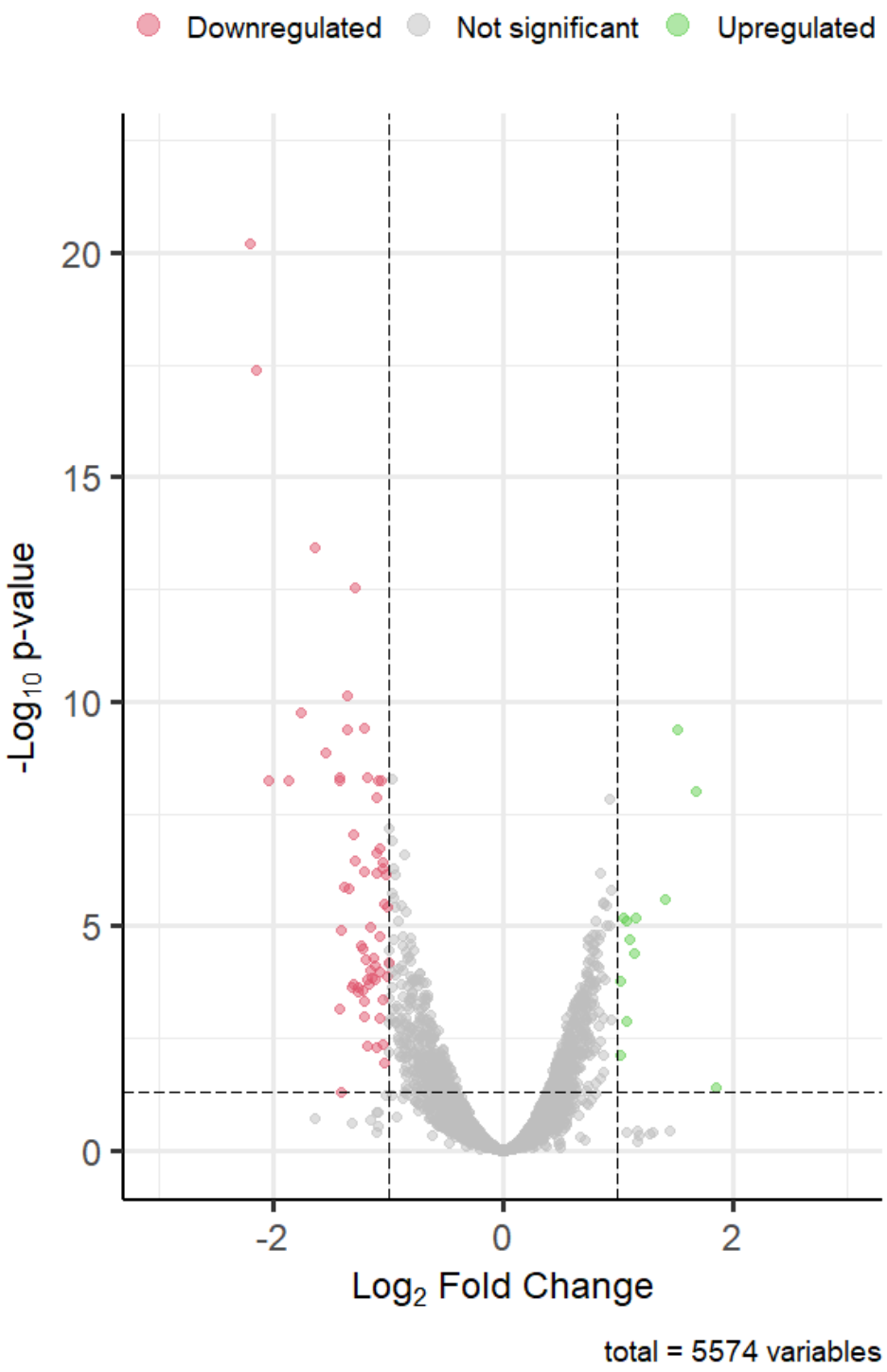

Figure 4.5. **Enhanced volcano plot illustrating the differentially expressed genes in polymicrobial *versus* monomicrobial cultures of *Pseudomonas aeruginosa* PAO1$_{MW}$.** Genes up-regulated in polymicrobial cultures are highlighted in green, whereas those down-regulated are shown in red. Thresholds for significant differential expression are set at $|\log_2 FC| > 1.0$ and an adjusted p-value < 0.05.

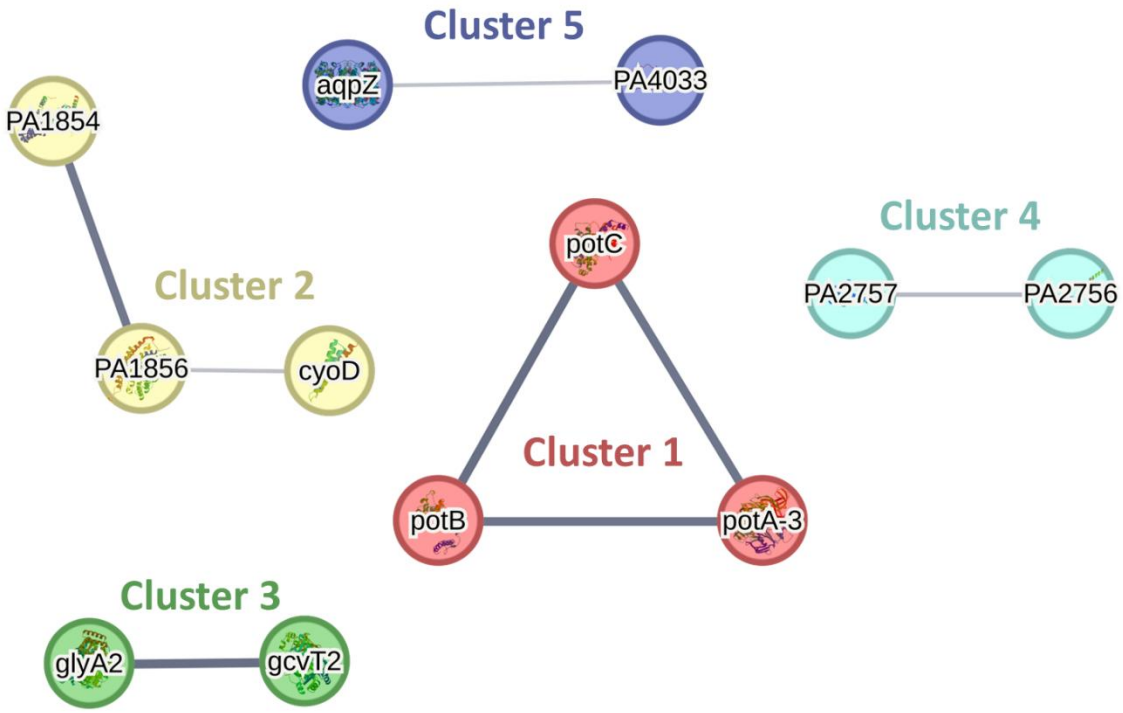

Cluster	Gene count	Description	Genes
Cluster 1	3	Polyamine transport, and MetI-like superfamily	*potA-3*, *potC*, *potB*
Cluster 2	3	Cytochrome complex	*cyoD*, PA1856, PA1854
Cluster 3	2	One carbon pool by folate Glycine catabolic process	*gcvT2*, *glyA2*
Cluster 4	2	Mixed, incl. Annealing activity, and Chlorhexidine efflux transporter	PA2756, PA2757
Cluster 5	2	-	PA4033, *aqpZ*

Figure 4.6. **Markov clustering of transcripts up-regulated in polymicrobial cultures with *Pseudomonas aeruginosa* PAO1$_{MW}$ compared with monospecies counterparts.** Clustering was performed using the STRING database, incorporating publicly available datasets. Genes are labelled with their corresponding locus or gene names.

By contrast, a larger number of transcripts showed decreased abundance in the polymicrobial cultures (*cf*. monomicrobial culture; *Figure 4.7*). Nearly half of the corresponding genes are involved in carbon compound catabolism as well as amino acid biosynthesis, metabolism, and transport of *P. aeruginosa* (*Figure 4.7, Clusters 1 and 4*). Examples include the *liu* operon encoding enzymes of the leucine utilisation pathway, *hut* genes related to histidine utilisation, *bkd-lpd* genes coding a branched-chain keto acid dehydrogenase, and the *hmgA-fahA-maiA* operon involved in tyrosine catabolism – a cluster that is often up-regulated during phage activity (Aguilar *et al.*, 2006; Blasdel *et al.*, 2017; Hester *et al.*, 2000; Zhang & Rainey, 2007).

Another set of genes plays a role in metabolic adaptability, particularly in nucleotide metabolism and nitrogen utilisation (*Figure 4.7, Cluster 2*). A smaller group of genes is involved in regulatory functions and fine-tuning metabolic pathways (*Figure 4.7, Cluster 5*). Regarding pathogenicity and survival, two distinct clusters can be formed. One group of genes is involved in secretion processes, potentially linked to biofilm formation or the T6SS (*Figure 4.7, Cluster 3*). The other set includes genes related to the chemotaxis system, enabling *P. aeruginosa* to navigate effectively (*Figure 4.7, Cluster 6*). The broader activation of metabolic pathways in monospecies cultures indicates greater metabolic flexibility in *P. aeruginosa* or a lack of cross-feeding of nutrients, such as amino acids, from other species.

Overall, the transcriptomic analysis comparing mono- and polymicrobial cultures of *P. aeruginosa* $PAO1_{MW}$ revealed only a moderate number of changes influenced by the presence of *S. aureus* and *C. albicans*. These findings suggest that under the studied non-disturbed, steady-state conditions, *P. aeruginosa* $PAO1_{MW}$ remains relatively unaffected by the presence of other species.

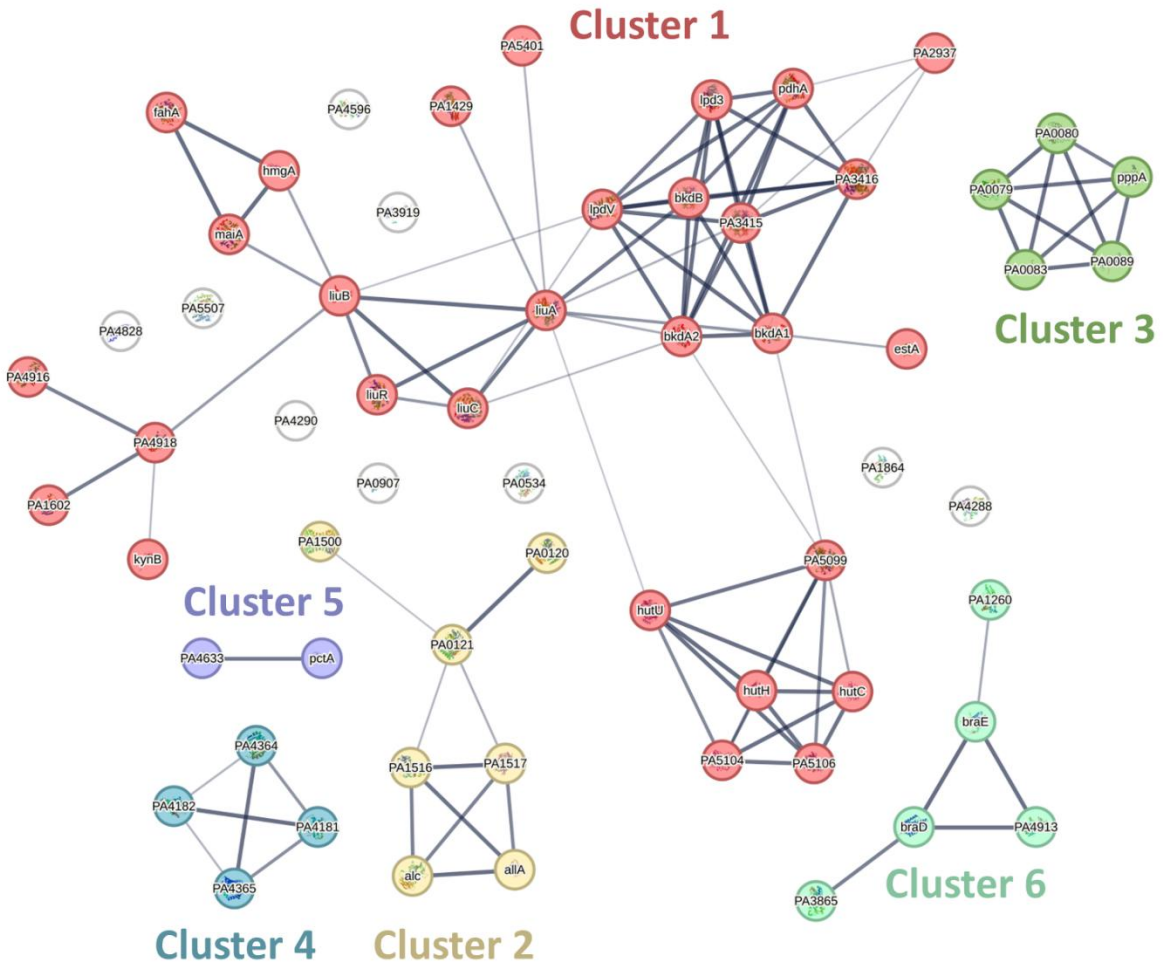

Cluster	Gene count	Description	Genes
Cluster 1	29	Oxidoreductase activity, acting on the aldehyde or oxo group of donors, disulfide as acceptor, and Fatty acid binding	PA1429, *liuA*, PA1602, PA4918, *maiA*, *liuB*, *fahA*, *hmgA*, *liuC*, *lpdV*, *bkdA2*, *liuR*, *hutU*, PA5401, PA3415, *bkdA1*, *bkdB*, *kynB*, PA5099, *estA*, *lpd3*, PA3416, *pdhA*, PA2937, PA4916, *hutH*, PA5104, PA5106, *hutC*
Cluster 2	7	Allantoin metabolic process Mixed, incl. Purine metabolism, and NodB homology domain	PA0120, PA0121, PA1500, PA1516, PA1517, *allA*, *alc*
Cluster 3	5	Biofilm formation - *P. aeruginosa* , and Tetratricopeptide repeat	*pppA*, PA0080, PA0089, PA0083, PA0079
Cluster 4	5	D-alanine transport Amino-acid transport	*braE*, PA1260, PA4913, *braD*, PA3865
Cluster 5	4	Mixed, incl. ACT domain , and B3/4 domain	PA4181, PA4364, PA4365, PA4182
Cluster 6	2	Transducer Methyl-accepting chemotaxis-like domains (chemotaxis sensory transducer) Cache domain, and Chemotaxis protein methyltransferase CheR	*pctA*, PA4633

Figure 4.7. **Markov clustering of transcripts down-regulated in polymicrobial versus monomicrobial cultures of *Pseudomonas aeruginosa* PAO1$_{MW}$.** Clustering was performed using the STRING database, incorporating publicly available datasets. Genes are labelled with their corresponding codes or gene names.

4.4.2. Comparative analysis of Δ*lasR* mutant mono- and polymicrobial culture

Following the analysis of the $PAO1_{MW}$, another comparison was performed for the transcriptional profiles of the Δ*lasR* mutant in mono- and polymicrobial cultures. A total of 5,560 genes were expressed in both growth conditions, each with more than ten reads across all samples. In the polymicrobial culture, 151 transcripts were significantly up-regulated, and 283 transcripts were down-regulated, as shown in *Figure 4.8*. Details of transcripts with significant differences in abundance are provided in *Supplementary Table B*. As specified in *Section 3.6.3*, the significance thresholds for all comparisons were set at $|\log_2 FC| > 1.0$ and an adjusted p-value < 0.05.

Among the transcripts up-regulated in the polymicrobial cultures of the Δ*lasR* mutant, the largest cluster, comprising 79 genes, is associated with oxidative phosphorylation and cytochrome c-type biogenesis – key components of aerobic respiration in *P. aeruginosa* (*Figure 4.9, Cluster 1*). This cluster includes transcripts derived from operons such as *ccm*, *cyo*, and *nuo*, as well as genes involved in transport mechanisms, siderophore synthesis, and iron chelation, including *pch* and *pvd* genes (Cornelis *et al.*, 2023; Ghssein & Ezzeddine, 2022; Kawakami *et al.*, 2010; Torres *et al.*, 2019). Notably, the up-regulation of cytochrome-related genes was also observed in $PAO1_{MW}$ polycultures. Another cluster of up-regulated genes in the polyculture, including the *cupA* gene cluster, facilitates biofilm formation and plays a role in cell adhesion (*Figure 4.9, Cluster 2*) (Deshamukhya *et al.*, 2022). Three smaller clusters of up-regulated genes related to environmental response and adaptation were identified. The first cluster includes six genes associated with defence mechanisms, such as efflux pumps, resistance factors, and membrane fusion proteins (*Figure 4.9, Cluster 3*). The second cluster involves genes related to extracellular polysaccharide biosynthesis, which is critical for biofilm formation and maintenance (*Figure 4.9, Cluster 4*). The third cluster contains genes involved in the urea catabolic process, suggesting an environment where nitrogen is limited or must be efficiently managed (*Figure 4.9, Cluster 6*). Other efflux transporter genes linked to chlorhexidine resistance were also up-regulated, mirroring the patterns observed in the $PAO1_{MW}$ polymicrobial culture (*Figure 4.9, Cluster 8*). This similarity is also noted with PA4033 and *aqpZ*. Further genes involved in metal ion homeostasis, particularly those regulating copper and iron, also showed increased expression (*Figure 4.9, Cluster 5*). Several up-regulated genes code for hypothetical proteins with yet-to-be-determined functions.

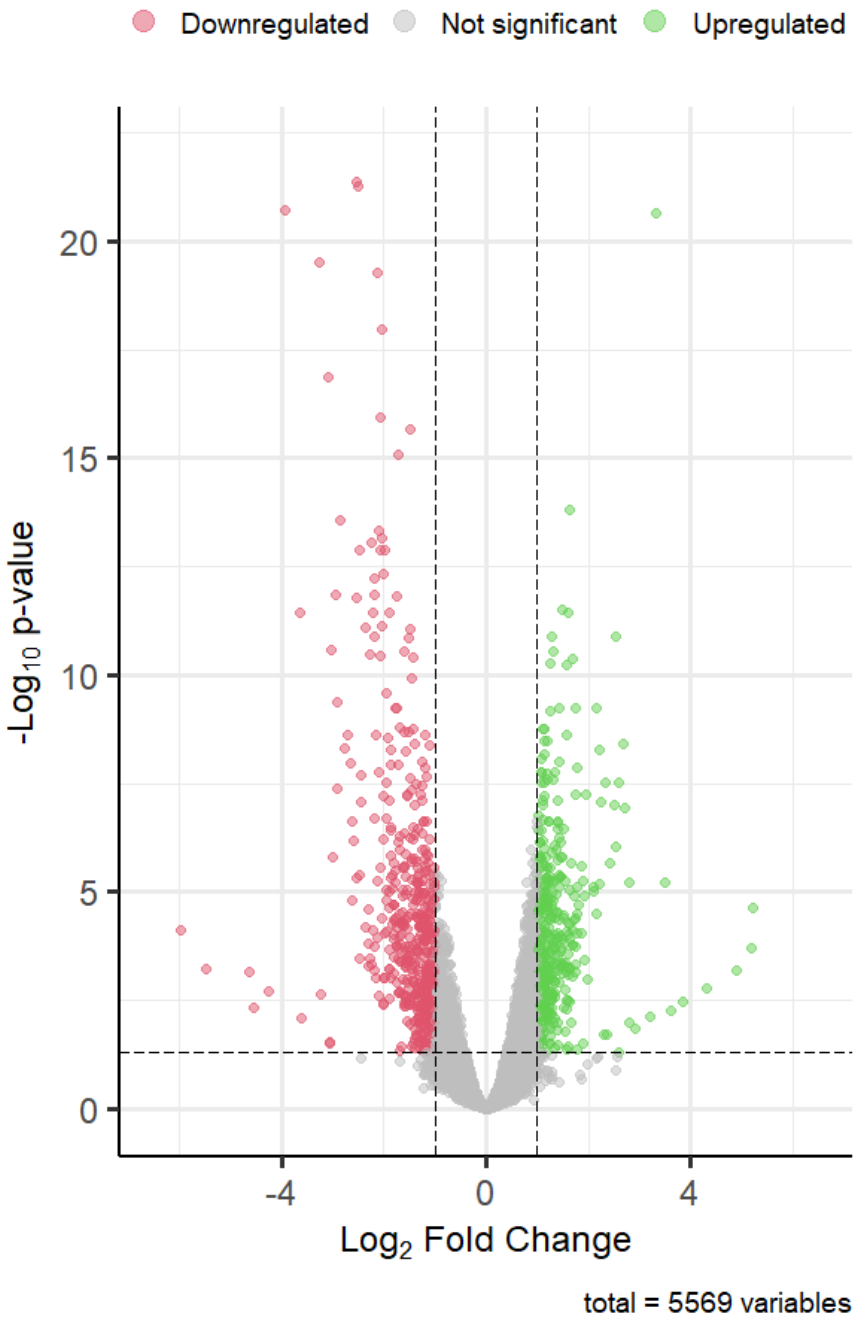

Figure 4.8. **Enhanced volcano plot illustrating the differentially expressed genes in polymicrobial *versus* monomicrobial cultures of the *Pseudomonas aeruginosa* Δ*lasR* mutant**. Genes up-regulated in polymicrobial cultures are highlighted in green, whereas those down-regulated are shown in red. Thresholds for significant differential expression are set at $|\log_2 FC| > 1.0$ and an adjusted p-value < 0.05.

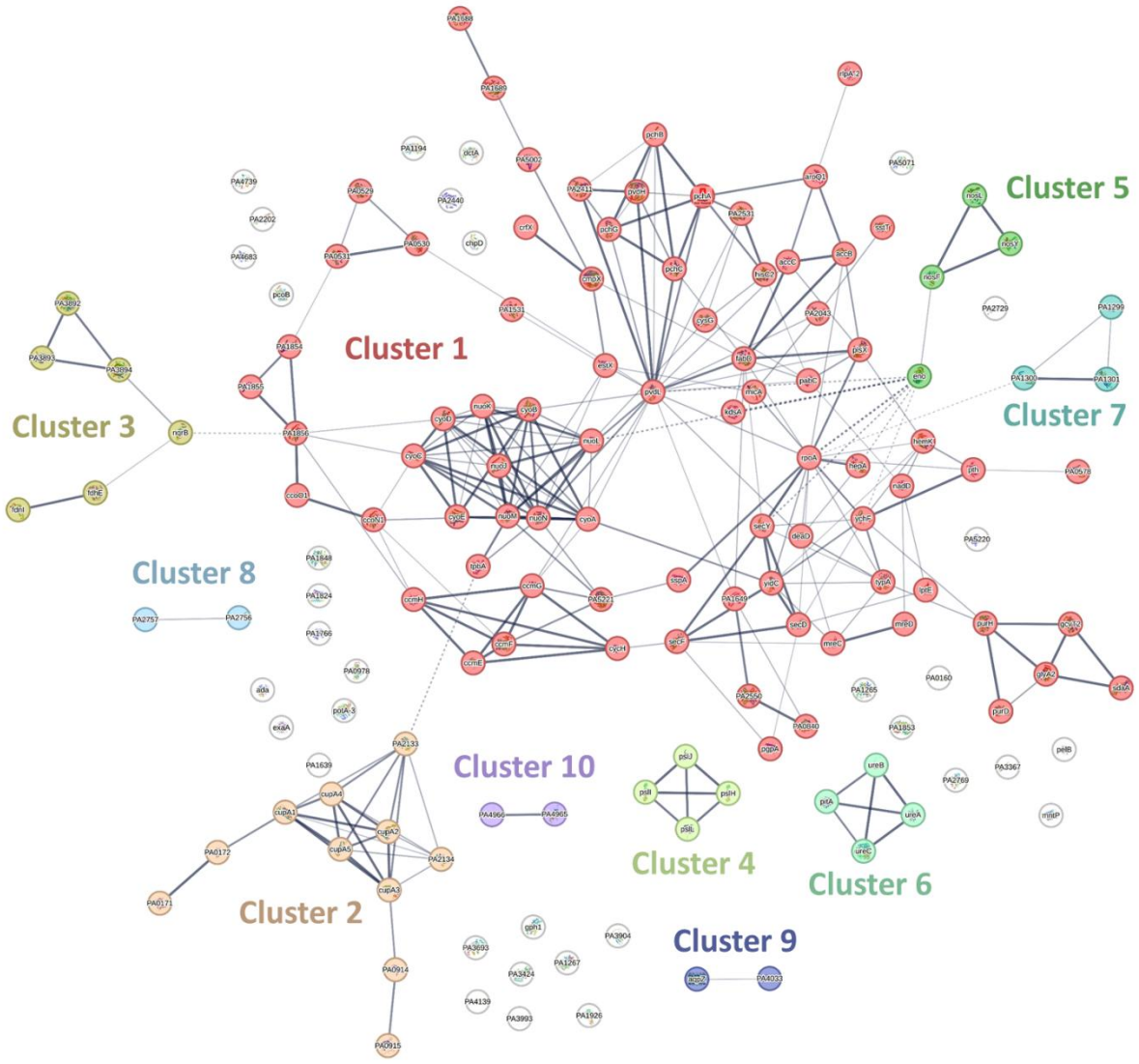

Cluster	Gene count	Description	Genes
Cluster 1	79	Mixed, incl. Oxidative phosphorylation, and Cytochrome c-type biogenesis	*micA*, *estX*, PA2043, *ychF*, PA0529, PA0531, PA0530, *pvdL*, PA1854, PA0578, *pth*, PA0840, PA1649, PA2550, *rpoA*, *cyoA*, *ccmG*, *nuoJ*, *nuoL*, *nuoK*, *yidC*, *nuoN*, *nuoM*, *cyoE*, *cyoB*, *cyoC*, *cyoD*, *ccoN1*, PA1856, *ccmE*, *cycH*, *ccmH*, *ccmF*, PA5221, *secF*, PA1531, *ccoO1*, *fabD*, PA1688, PA1689, PA5002, *cmpX*, *crfX*, PA1855, *sstT*, *tpbA*, PA2411, *pchB*, *pchG*, *pvdH*, *pchA*, *pchC*, *pabC*, *plsX*, PA2531, *accC*, *deaD*, *gcvT2*, *purH*, *sdaA*, *glyA2*, *purD*, *cysG*, *hisC2*, *mreC*, *hepA*, *typA*, *nadD*, *secY*, *kdsA*, *accB*, *hemK*, *pgpA*, *secD*, *lptE*, *mreD*, *aroQ1*, *sspA*, *rlpA-2*
Cluster 2	11	Cellular response to oxygen levels	PA0171, PA0172, *cupA1*, PA0914, *cupA3*, PA0915, PA2134, PA2133, *cupA4*, *cupA2*, *cupA5*
Cluster 3	6	Para-hydroxybenzoic acid efflux pump subunit AaeB/fusaric acid resistance protein, and Membrane fusion protein, biotin-lipoyl like domain	*nqrB*, *fdhE*, PA3894, PA3892, PA3893, *fdnI*

Cluster 4	4	Extracellular polysaccharide biosynthetic process	*pslH*, *pslL*, *pslJ*, *pslI*
Cluster 5	4	Mixed, incl. Copper centre Cu(A), and Parallel beta-helix repeat	*eno*, *nosF*, *nosL*, *nosY*
Cluster 6	4	Urea catabolic process	*ureA*, *pitA*, *ureB*, *ureC*
Cluster 7	3	-	PA1299, PA1301, PA1300
Cluster 8	2	Mixed, incl. Annealing activity, and Chlorhexidine efflux transporter	PA2756, PA2757
Cluster 9	2	-	PA4033, *aqpZ*
Cluster 10	2	DNA topoisomerase IV complex, and Retropepsin-like domain, bacterial	PA4965, PA4966

Figure 4.9. **Markov clustering of transcripts up-regulated in polymicrobial versus monomicrobial cultures of *Pseudomonas aeruginosa* Δ*lasR* mutant.** Clustering was performed using the STRING database, incorporating publicly available datasets. Genes are labelled with their corresponding locus codes or gene names.

In contrast, transcripts with reduced abundance in polymicrobial cultures – indicating greater abundance in monospecies cultures – highlight a broad range of functional responses, with a strong emphasis on general metabolic processes, environmental adaptation, and stress responses. Specifically, in the Δ*lasR* mutant monocultures, many genes associated with organic acid catabolic processes were up-regulated (*Figure 4.10, Cluster 1*). Genes related to stress responses and *Pf1* bacteriophage were also expressed at a significantly higher level in monocultures (*Figure 4.10, Clusters 2 and 6*), indicating that the *lasR* mutant might encounter or prepare for stressful conditions in ASM (Secor *et al.*, 2020). Transcriptional regulators, including those from the XRE and LysR families, were also affected. These regulators are known for controlling a wide range of metabolic processes, including amino acid synthesis, degradation pathways, and the regulation of virulence genes (*Figure 10.8, Clusters 3, 4, 8, and 12*). Interestingly, genes coding structural elements of T6SS and linked to biofilm formation were also up-regulated (*Figure 4.10, Cluster 7*).

Transcriptomic analysis reveals distinct gene expression patterns in the Δ*lasR* mutants between mono- and polymicrobial cultures. In polymicrobial settings, the Δ*lasR* mutant up-regulates pathways involved in oxidative phosphorylation, cytochrome biogenesis, iron chelation, and stress responses, suggesting an adaptive strategy for competition and survival. In contrast, monocultures show increased expression of genes related to nutrient acquisition, phage elements, different stress responses and biofilm formation, reflecting a focus on resource utilisation without competition being present.

The most striking finding from the transcriptomic analysis is the markedly higher number of changes in the Δ*lasR* mutant compared with the 'wild-type' $PAO1_{MW}$ when analysing differences between mono- and polymicrobial conditions. This indicates that the Δ*lasR* mutant undergoes more extensive transcriptional reprogramming to adapt to the polymicrobial environment. The larger number of differentially expressed genes suggests that the Δ*lasR* mutant requires a wider range of metabolic and regulatory adjustments to cope with the complexities of inter-species interactions, increased stress responses, and greater competition for resources than the $PAO1_{MW}$ does in similar conditions.

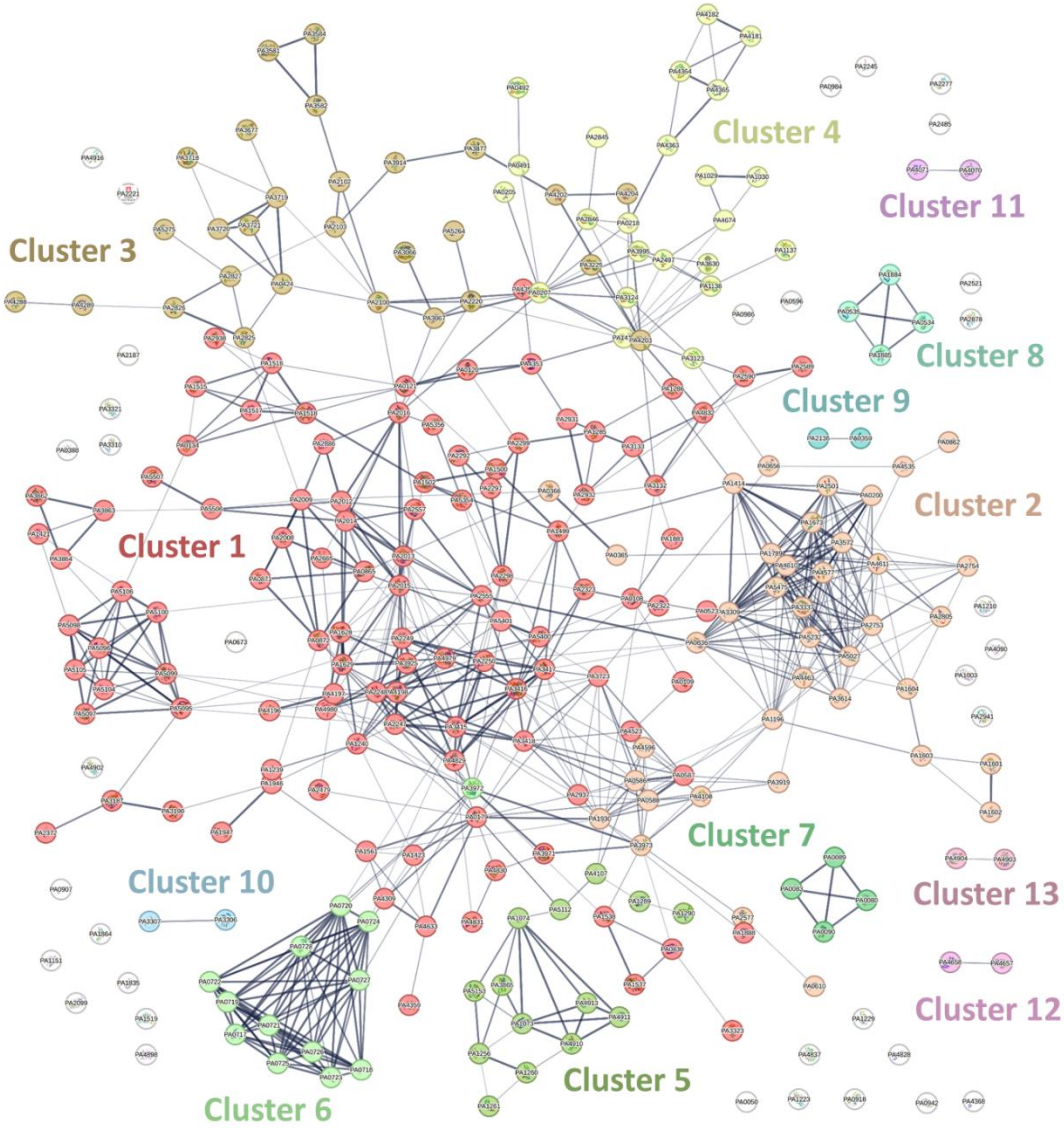

Cluster	Gene count	Description	Genes
Cluster 1	108	Organic acid catabolic process	PA0108, PA2298, PA5400, PA0109, PA3416, PA0523, PA1883, PA4523, PA0120, PA2299, PA4353, PA0121, PA1500, PA1516, PA1517, PA1518, PA0134, PA1515, PA5106, PA0179, PA4197, PA3418, PA2479, PA3723, PA4309, PA1423, PA1561, PA4633, PA2016, PA2009, PA0865, PA0587, PA3417, PA2937, PA3415, PA0830, PA3323, PA1538, PA1537, PA2250, PA2555, PA2012, PA2014, PA0871, PA2008, PA0872, PA2249, PA1946, PA2248, PA2247, PA1239, PA1240, PA2015, PA2013, PA4198, PA3925, PA4979, PA1628, PA1285, PA2931, PA1286, PA2932, PA3133, PA1499, PA1421, PA5100, PA5098, PA3863, PA1502, PA2323, PA5354, PA2938, PA5401, PA4980, PA1629, PA3132, PA1888, PA3190, PA1947, PA2886, PA5506, PA2557, PA2665, PA5356, PA5095, PA5099, PA4829, PA2292, PA2297, PA2322, PA2372, PA3187, PA2589, PA4832, PA2590, PA3862, PA3864, PA3971, PA4830, PA4196, PA4354, PA4359, PA4831, PA5104, PA5105, PA5097, PA5096, PA5507

Cluster 2	39	Mixed, incl. UspA, and Alcohol dehydrogenase, zinc-type, conserved site	PA0586, PA0588, PA1930, PA0200, PA1789, PA5232, PA2501, PA5027, PA4610, PA2753, PA3337, PA1673, PA3309, PA4577, PA3572, PA1414, PA5475, PA0365, PA0366, PA1196, PA3919, PA3973, PA4463, PA4596, PA4108, PA0610, PA2577, PA0656, PA4535, PA0836, PA1604, PA3614, PA0862, PA1603, PA4611, PA1601, PA1602, PA2754, PA2805
Cluster 3	28	LysR, substrate-binding, and HTH-type transcriptional regulator AraC-type, N-terminal	PA3225, PA2220, PA4203, PA2100, PA3067, PA0424, PA2825, PA3720, PA3721, PA3719, PA2103, PA2102, PA3582, PA2827, PA3914, PA5264, PA2826, PA4289, PA5275, PA3066, PA3581, PA3584, PA3677, PA3718, PA3877, PA4202, PA4204, PA4288
Cluster 4	23	LysR, substrate-binding, and HTH-type transcriptional regulator AraC-type, N-terminal	PA0205, PA0207, PA0491, PA0218, PA2846, PA1413, PA2497, PA3995, PA3124, PA4363, PA0492, PA3123, PA1029, PA4674, PA1030, PA1137, PA1138, PA3630, PA2845, PA4181, PA4364, PA4365, PA4182
Cluster 5	14	Branched-chain amino acid transport D-alanine transport, and Leucine-binding protein domain	PA5112, PA1073, PA1256, PA5153, PA3865, PA4911, PA4913, PA4910, PA1074, PA1261, PA1260, PA1289, PA4107, PA1290
Cluster 6	13	Mixed, incl. Virion	PA0717, PA0726, PA0727, PA0723, PA0728, PA0722, PA0721, PA0725, PA0720, PA0724, PA0718, PA0719, PA3972
Cluster 7	4	Biofilm formation - *P. aeruginosa* , and Tetratricopeptide repeat	PA0080, PA0090, PA0083, PA0089
Cluster 8	4	Mixed, incl. Helix-turn-helix XRE-family like proteins, and Bacterial extracellular solute-binding protein	PA0534, PA1884, PA1885, PA0535
Cluster 9	2	-	PA0359, PA2136
Cluster 10	2	Mixed, incl. 2-thiouracil desulfurase, and Oxoglutarate/iron-dependent dioxygenase	PA3306, PA3307
Cluster 11	2	-	PA4070, PA4071
Cluster 12	2	Mixed, incl. Helix_turn_helix, mercury resistance, and Chromophore	PA4657, PA4658
Cluster 13	2	-	PA4903, PA4904

Figure 4.10. **Markov clustering of transcripts down-regulated in *Pseudomonas aeruginosa* Δ*lasR* mutant polymicrobial versus monomicrobial cultures.** Clustering was performed using the STRING database, incorporating publicly available datasets. Genes are labelled with their corresponding locus codes or gene names. The inflation parameter was set at 1.2.

4.4.3. Comparative analysis of PAO1$_{MW}$ and Δ*lasR* mutant cultures

The PAO1$_{MW}$ and Δ*lasR* mutant transcriptomes were compared to identify the main differential gene expression patterns. In both mono- and polymicrobial cultures, 5,571 genes were consistently expressed in the two genetic variants, each with more than ten reads across all samples. Genes with significant differences in expression are detailed in *Supplementary Tables C* and *D*. As specified in *Section 3.6.3*, the significance thresholds for all comparisons were set at $|\log_2 FC| > 1.0$ and an adjusted p-value < 0.05.

When comparing mono-species cultures, only four transcripts displayed significant differences in abundance. These genes – *lasR*, *rasL*, *lasI*, and PA1433 – are all linked to the las regulatory system and had increased expression levels in the PAO1$_{MW}$, as anticipated. However, further differences were likely obscured due to variability within the PAO1$_{MW}$ samples themselves.

In contrast, the comparison of polymicrobial cultures revealed a more complex picture, with 112 genes significantly up-regulated in the PAO1$_{MW}$ and 96 genes significantly up-regulated in the Δ*lasR* mutant, as illustrated in *Figure 4.11*. As anticipated, several clusters of up-regulated genes in PAO1$_{MW}$ belong to the *lasR* regulon (*Figure 4.12. Clusters 3, 6, 11, and 13*) (Schuster *et al.*, 2003). For instance, the main genes of the *las* system – *lasR*, *rasL*, and *lasI* – as well as those they regulate, such as *rhlI*, *pqsH*, and *aprL*, were differentially expressed in the PAO1$_{MW}$ (*Figure 4.12, Cluster 3*). Additionally, the *ambBCDE* operon was up-regulated. Although several studies have suggested that the *ambBCDE* operon codes a fourth QS signal molecule, recent findings indicate it is not responsible for such biosynthesis (Cornelis, 2020; Rojas Murcia *et al.*, 2015). Many other up-regulated genes, partially or fully uncharacterised, are related to metabolic adaptation and regulatory changes (*Figure 4.12, Clusters 1, 2, 4, 5, 8, 11, and 12*). For example, genes in the *dauBAR* operon are associated with the racemisation and catabolism of D-arginine and D-lysine (*Figure 4.12, Cluster 12*). Other examples include genes encoding transcriptional regulators, such as *pcaR*, PA1884, and PA0535, featuring XRE-cupin architecture (Trouillon *et al.*, 2021). Defence and resistance mechanisms were also up-regulated in PAO1$_{MW}$, such as efflux systems and antibiotic resistance proteins (*Figure 4.12, Clusters 6, 7, and 9*). Notably, genes in the *tseT* operon, which encodes proteins associated with the H2-T6SS, showed up-regulated expression (*Figure 4.12, Cluster 13*). While this operon has been investigated, its specific target or function is yet to be determined (Burkinshaw *et al.*, 2018; Haas *et al.*, 2023).

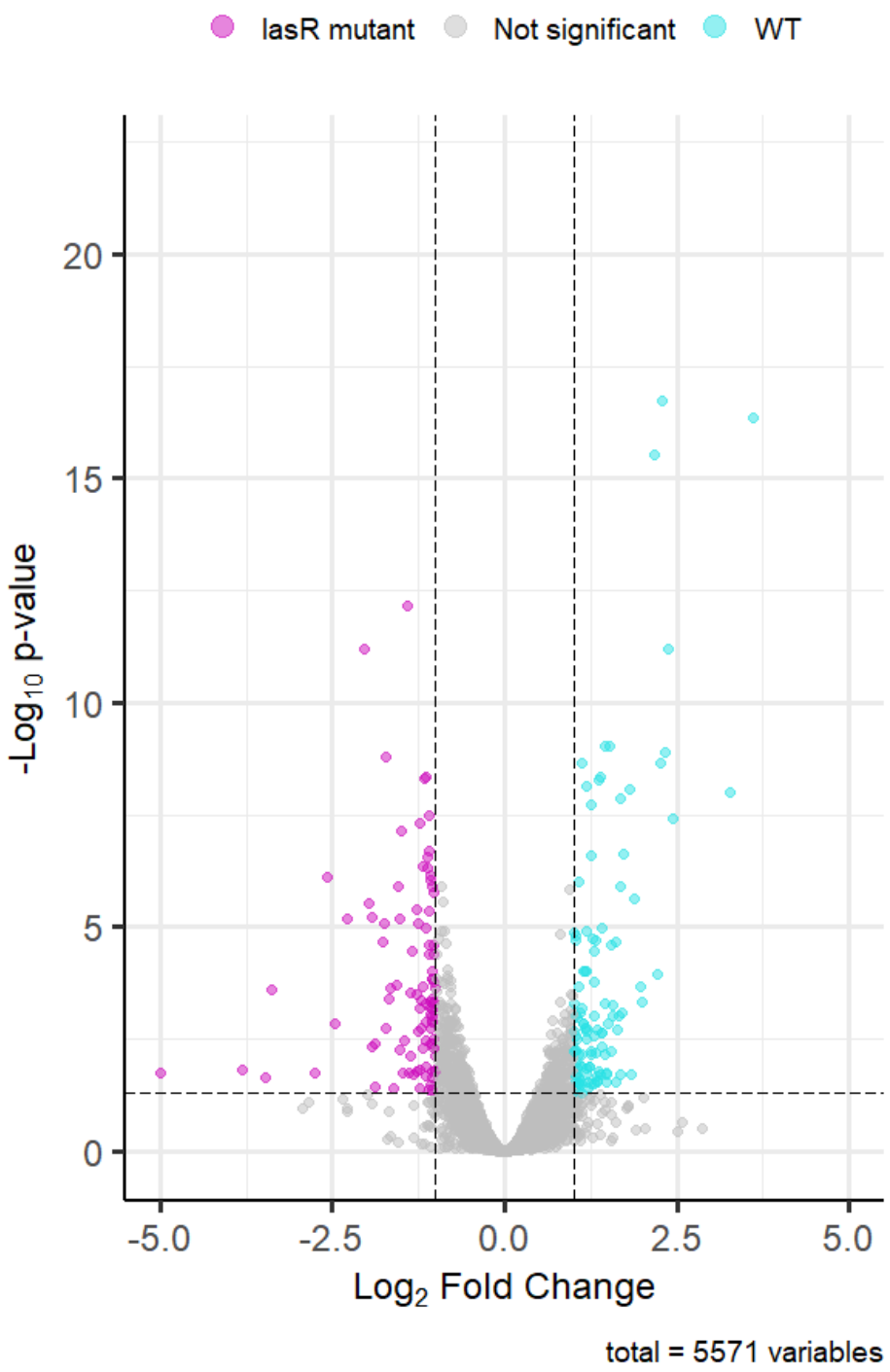

Figure 4.11. **Enhanced volcano plot illustrating the differentially expressed genes in polymicrobial $PAO1_{MW}$ cultures versus polymicrobial Δ*lasR* mutant cultures**. Genes up-regulated in $PAO1_{MW}$ cultures are highlighted in blue, whereas those in Δ*lasR* cultures are shown in magenta. Thresholds for significant differential expression are set at $|\log_2 FC| > 1.0$ and an adjusted p-value < 0.05.

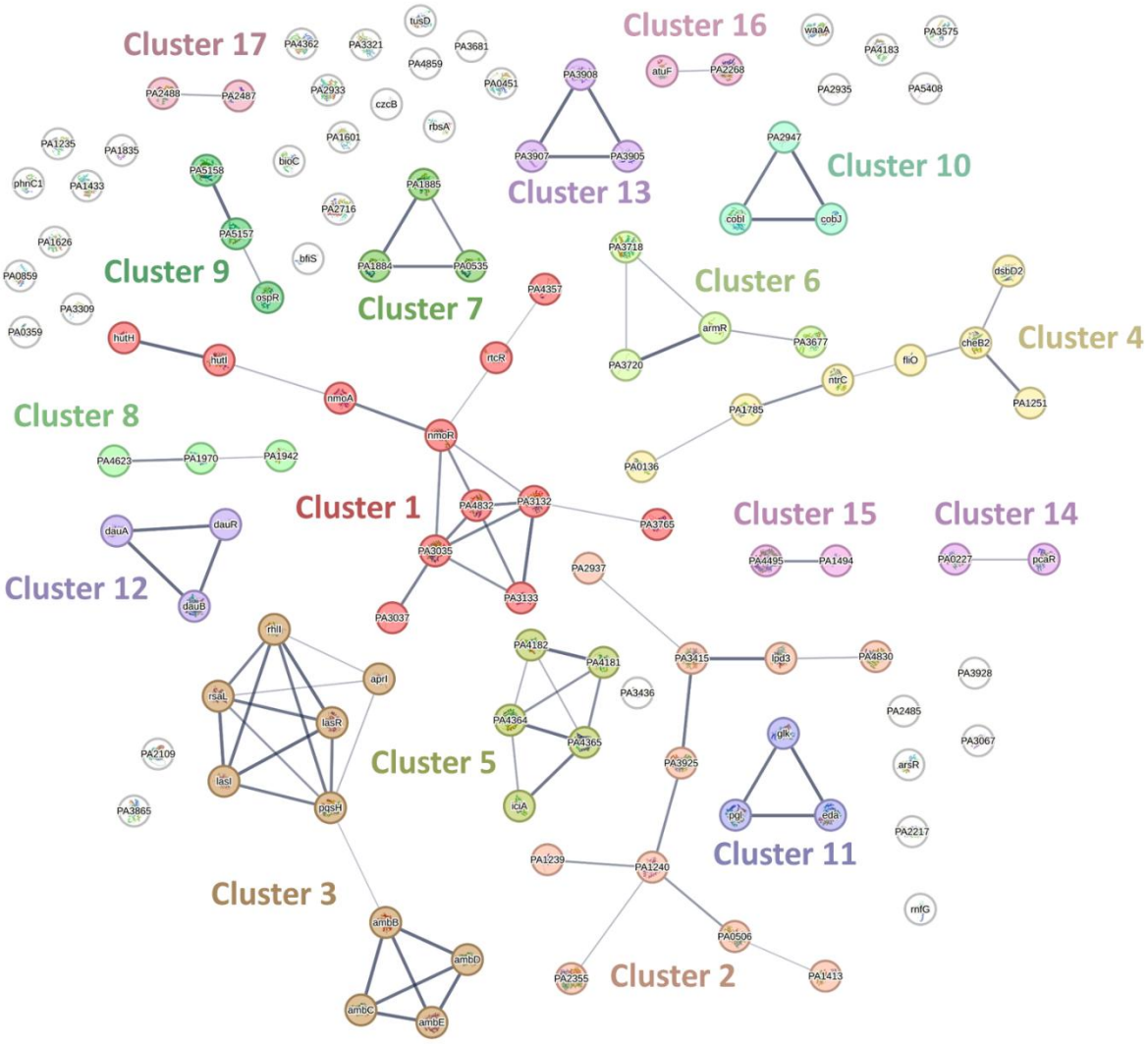

Cluster	Gene count	Description	Genes
Cluster 1	12	Mostly uncharacterized, incl. Nitrotoluene degradation, and Flavodoxin-like fold	PA3035, PA3133, *nmoR*, PA3132, PA4832, PA3037, PA3765, *nmoA*, *hutI*, *rtcR*, PA4357, *hutH*
Cluster 2	10	-	PA0506, PA1413, PA1240, PA1239, PA2355, PA3925, PA2937, PA3415, *lpd3*, PA4830
Cluster 3	10	QS Taurine catabolism dioxygenase TauD, TfdA family, and Cysteine transport	*aprI*, *rhlI*, *rsaL*, *pqsH*, *lasR*, *lasI*, *ambE*, *ambB*, *ambC*, *ambD*
Cluster 4	7	-	PA0136, PA1785, *cheB2*, *fliO*, *dsbD2*, PA1251, *ntrC*
Cluster 5	5	Mixed, incl. ACT domain , and B3/4 domain	PA4181, PA4364, PA4365, PA4182, *iciA*
Cluster 6	4	Mixed, incl. Efflux transmembrane transporter activity, and Acriflavin resistance protein	PA3677, *armR*, PA3718, PA3720
Cluster 7	3	Mixed, incl. Helix-turn-helix XRE-family like proteins, and Bacterial extracellular solute-binding protein	PA0535, PA1885, PA1884
Cluster 8	3	Protein of unknown function DUF2790, and Signal	PA1942, PA1970, PA4623
Cluster 9	3	Helix_turn_helix multiple antibiotic resistance protein Drug resistance transporter EmrB-like, and Cation efflux system protein CusB, domain 1	*ospR*, PA5157, PA5158

Cluster 10	3	Cobalamin biosynthetic process Porphyrin and chlorophyll metabolism	*cobJ*, PA2947, *cobI*
Cluster 11	3	Pentose-phosphate shunt, oxidative branch, and KDPG/KHG aldolase	*eda*, *pgl*, *glk*
Cluster 12	3	D-Arginine and D-ornithine metabolism Arginine biosynthetic process, and Arginine deiminase pathway	*dauB*, *dauR*, *dauA*
Cluster 13	3	Mixed, incl. Domain of unknown function DUF4123, and PAAR motif	PA3905, PA3907, PA3908
Cluster 14	2	Degradation of aromatic compounds, and Beta-ketoadipate pathway	*pcaR*, PA0227
Cluster 15	2	Mixed, incl. Integral component of external side of plasma membrane, and Negative regulation of DNA-templated transcription, initiation	PA1494, PA4495
Cluster 16	2	-	PA2268, *atuF*
Cluster 17	2	Mixed, incl. TOBE domain, and Serine/threonine-protein kinase	PA2487, PA2488

Figure 4.12. **Markov clustering of transcripts down-regulated in $PAO1_{MW}$ polymicrobial cultures compared with Δ*lasR* mutant polymicrobial cultures.** Clustering was performed using the STRING database, incorporating publicly available datasets. Genes are labelled with their corresponding locus codes or gene names. The inflation parameter was set at 1.2.

In contrast, in the Δ*lasR* mutant grown in polymicrobial culture, a third of the up-regulated genes are associated with siderophore biosynthesis and iron acquisition (*Figure 4.13*, Cluster 1). This includes genes from the *pvd* and *pch* operons, which are central to producing siderophores like pyoverdine and pyochelin, as well as the *cyo* operon encoding a bo_3-type oxidase, which is up-regulated during iron starvation (Arai *et al.*, 2014; Cornelis *et al.*, 2023; Ghssein & Ezzeddine, 2022; Kawakami *et al.*, 2010). The up-regulation of siderophore biosynthesis in the Δ*lasR* mutant suggests a compensatory mechanism for iron acquisition, potentially critical for survival in a competitive polymicrobial environment with *S. aureus* and *C. albicans* (Sánchez-Jiménez *et al.*, 2023). Other up-regulated genes in the Δ*lasR* mutant are associated with modifying surface structures and maintaining structural integrity. Specifically, *Cluster 2* is involved in defence mechanisms and surface modifications, *Cluster 3* contributes to membrane integrity and potentially novel stress responses, and *Cluster 4* supports nutrient acquisition and metabolic flexibility (*Figure 4.13*).

Further clusters are associated with the ability to compete, survive, and influence the microbial community. For instance, genes in the SiaABC threonine phosphorylation pathway control aggregate/biofilm formation in response to carbon availability (*Figure 4.13, Cluster 6*). Up-regulated transporters, such as *dctA* and *dctA1*, are linked to dicarboxylate transport (*Figure 4.13, Cluster 8*), whereas *opdC* and two neighbouring hypothetical proteins are associated with the transport of small molecules (*Figure 4.13, Cluster 5*). The high number of uncharacterised genes may represent novel roles in *P. aeruginosa* physiology or pathogenicity.

In summary, this comparative analysis underscores distinct differences in gene expression between the Δ*lasR* mutant and $PAO1_{MW}$ strains in polymicrobial environments. While many of the up-regulated genes in $PAO1_{MW}$ samples are part of the *lasR* regulon, others are not (yet) associated with *lasR*, suggesting areas for further investigation. Conversely, the increased siderophore production in the Δ*lasR* mutant indicates a possible compensatory mechanism, potentially influenced by interactions with other microbes.

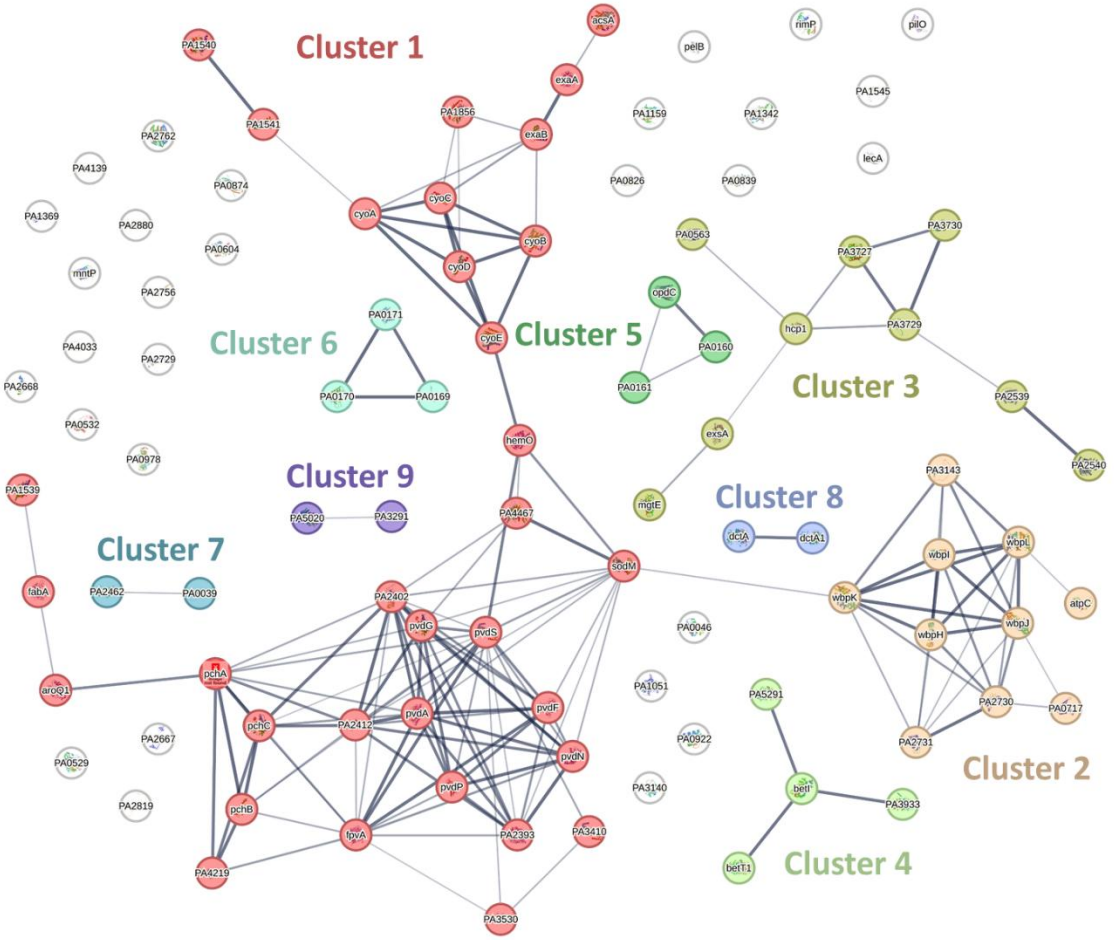

Cluster	Gene count	Description	Genes
Cluster 1	33	Siderophore biosynthetic process	*hemO*, PA4467, *sodM*, *pvdS*, *cyoE*, *acsA*, *exaA*, *cyoA*, PA1541, *exaB*, *cyoB*, *cyoC*, *cyoD*, PA1856, PA1539, *fabA*, PA1540, *aroQ1*, *pvdA*, *pchA*, *pchC*, PA2393, *pvdP*, *pvdG*, *pvdN*, PA2402, PA2412, *fpvA*, *pvdF*, PA3530, *pchB*, PA4219, PA3410
Cluster 2	10	O antigen metabolic process, and DNA modification	PA0717, *wbpJ*, PA2730, *wbpL*, *wbpK*, *wbpI*, *wbpH*, PA2731, PA3143, *atpC*
Cluster 3	9	Mostly uncharacterized, incl. Protein of unknown function (DUF805), and Acylglycerol O-acyltransferase activity	*hcp1*, *exsA*, PA0563, PA3727, PA3729, *mgtE*, PA2539, PA2540, PA3730
Cluster 4	4	Choline metabolic process Amine transmembrane transporter activity	PA3933, *betI*, PA5291, *betT1*
Cluster 5	3	Mixed, incl. Cytolysis, and SnoaL-like domain	PA0160, PA0161, *opdC*
Cluster 6	3	Mixed, incl. HD-GYP domain, and PPM-type phosphatase-like domain	PA0169, PA0171, PA0170
Cluster 7	2	-	PA0039, PA2462
Cluster 8	2	L-aspartate transmembrane transport Malate:proton symporter activity	*dctA1*, *dctA*
Cluster 9	2	-	PA3291, PA5020

Figure 4.13. **Markov clustering of transcripts down-regulated in Δ*lasR* mutant polymicrobial cultures compared with PAO1$_{MW}$ polymicrobial cultures.** Clustering was performed using the STRING database, incorporating publicly available datasets. Genes are labelled with their corresponding locus codes or gene names. The inflation parameter was set at 1.2.

4.4.4. Transcriptomic landscape in the literature

The findings of this study were compared with the relevant literature to further understand the characteristics of the continuous-flow system used. Unfortunately, direct comparisons were not always feasible; thus, normalised count values were used when needed for comparison.

The continuous-flow system can be positioned on the spectrum between traditional *in vitro* models and human samples based on a comparative framework suggested by Cornforth and colleagues (Cornforth *et al.*, 2020). They compared *P. aeruginosa* transcriptomes from human infections with those from laboratory conditions. They found lower expression of QS genes and higher expression of antibiotic tolerance determinants during human infection. They also identified a set of genes that can differentiate between human and *in vitro* samples. In my study using the continuous-flow system, approximately half of these distinguishing genes across all three categories showed expression patterns resembling those observed in human samples, setting them apart from in vitro samples. This indicates that the continuous-flow system may capture a broader spectrum of the *Pseudomonas* transcriptome compared to traditional in vitro methods, positioning it as an intermediary model between conventional *in vitro* setups and human samples. However, to quantify this distinction and assess how closely it reflects *in vivo* conditions, comparative transcriptomic analyses between traditional *in vitro* and continuous-flow system samples are essential, an aspect beyond the scope of this project.

Interestingly, based on their transcriptomic analysis of monospecies and polymicrobial cultures, Kesthely and colleagues reported that *P. aeruginosa* exhibits community agnosticism, showing no differential expression in response to the number of species or the genetic variants present (Kesthely *et al.*, 2023). Their study, which employed a four-species polymicrobial community including *P. aeruginosa*, *S. aureus*, *Streptococcus sanguinis*, and *Prevotella melaninogenica*, was conducted under anoxic conditions using a 96-well-plate-based biofilm model. They also used 'WT' and *lasR* mutant, but these were based on the PA14 background rather than PAO1. Interestingly, my findings somewhat differ from theirs. However, my significance thresholds were less conservative, and if the cutoff is increased, the $PAO1_{MW}$ in my experiments would also appear community agnostic. Although, the Δ*lasR* mutant would still show differential expression of most genes discussed above. This

discrepancy is likely due to differences in experimental setups, oxygen levels, and variations in microbial compositions, like the presence of fungi.

4.5. QS molecules

The concentration of the three key QS molecules produced by *P. aeruginosa* – OdDHL, BHL, and PQS – was measured in the culture supernatant from the *in vitro* continuous-flow system, as detailed in *Section 3.7*. This analysis aimed to track the variations in their concentrations over time, providing insights into the dynamics of QS during the experimental conditions.

The absolute concentrations of these molecules remained in the nanomolar range, not exceeding 500 nM, as shown in *Figure 4.14*. These results align with previous observations for *P. aeruginosa* $PAO1_{MW}$, indicating that QS may play a less significant role in populations maintained under continuous-flow conditions than in batch cultures (O'Brien, 2021).

Although the changes over time were not significantly different, some noteworthy biological trends can be observed. In $PAO1_{MW}$ monocultures, there was a decrease in OdDHL concentration with time, whereas BHL concentrations remained relatively constant, and PQS concentrations showed a slight increase. In $PAO1_{MW}$ polymicrobial cultures, OdDHL and BHL concentrations stayed consistently low, near the detection limit, whereas PQS levels were slightly elevated compared with monospecies cultures. As expected, in Δ*lasR* mutant monocultures, none of the three QS molecules were detectable. Interestingly, in Δ*lasR* mutant polymicrobial cultures, PQS concentration increased over time, surpassing the levels observed in $PAO1_{MW}$ cultures. OdDHL remained low, and BHL was essentially undetectable.

These findings suggest that QS molecule concentrations, particularly OdDHL and BHL, remain relatively low in the continuous-flow system used in this study, implying that they probably have only a limited impact on the observed microbial dynamics. However, the slightly (not significantly) elevated PQS concentration in polymicrobial cultures, especially in the Δ*lasR* mutant, hints at a potential – direct or indirect – contribution of PQS to inter-species interactions in this experimental setup. The expression of PQS in Δ*lasR* mutant may point to a bypass mechanism. The exact mechanism behind this requires further investigation to understand fully. However, this lies beyond the scope of the current work.

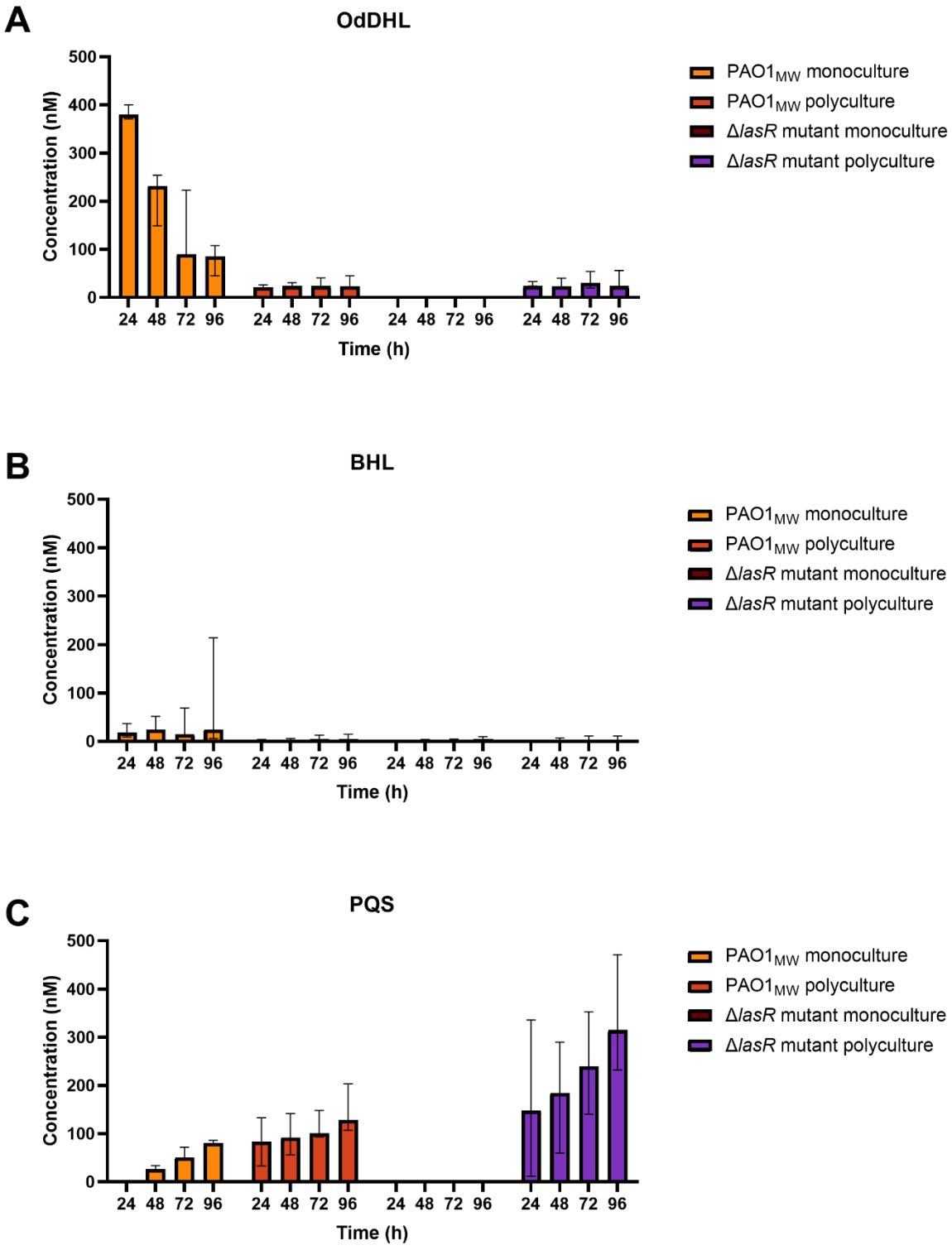

Figure 4.14. **Quantification of quorum sensing molecule concentrations in the continuous-flow system.** The concentration (nM) of the indicated QS molecules was measured in the supernatants of different culture conditions after 24, 48, 72, and 96 hours of incubation. (A) *N*-(3-oxododecanoyl)-L-homoserine lactone (OdDHL); (B) *N*-butanoyl-L-homoserine lactone (BHL); (C) Pseudomonas quinolone signal (PQS). Data are represented as median ± 95% confidence interval from three independent experiments.

4.6. Discussion

The results presented in this chapter focused on the influence of genetic variation on the polymicrobial ecosystem. The consistency of findings regarding 'wild-type' *P. aeruginosa* $PAO1_{MW}$ with previous measurements using the same experimental setup showcases the reproducibility and reliability of the system.

Comparisons between population dynamics within mono- and polymicrobial cultures revealed only slight differences between the presence of a functional or a non-functional LasR. The population abundance of *P. aeruginosa* remains consistent, regardless of whether the $PAO1_{MW}$ or Δ*lasR* mutant are present. In line with the findings by Cheng and colleagues, this reinforces the significance of LasR-independent mechanisms in maintaining population stability (Cheng *et al.*, 2019).

Cross-sectional bulk transcriptomic analyses at the 48-hour timepoint revealed the differences in gene expression under the studied conditions. In monocultures, both the $PAO1_{MW}$ and Δ*lasR* mutant exhibited increased metabolic activity, likely due to the absence of inter-species competition. This included increased expression of genes involved in carbon and organic acid metabolism, alongside elevated activity in biofilm formation and some stress response pathways compared with their polymicrobial counterparts. Similarly, other studies with various microbes have shown increased metabolic activity in monocultures (Mould *et al.*, 2024; Vandecandelaere *et al.*, 2017; Yasir *et al.*, 2024).

In the presence of neighbouring species, the $PAO1_{MW}$ and Δ*lasR* mutant exhibited up-regulation of genes associated with terminal oxidases, enhanced energy production and cellular respiration. This response may be driven by fluctuating oxygen concentrations or limitations in alternative electron acceptors (Arai *et al.*, 2014). Simultaneously, these cultures activated different stress responses and resistance mechanisms, improving their ability to withstand challenges such as osmotic stress and exposure to toxic or antimicrobial agents. These findings align with previous *ex vivo* transcriptomic studies, indicating that *P. aeruginosa* adapts its gene expression profile to maintain competitiveness and resilience in a polymicrobial environment (Thöming & Häussler, 2022).

Comparing the $PAO1_{MW}$ and Δ*lasR* mutant revealed several intriguing findings. Notably, the Δ*lasR* mutant exhibited a significant up-regulation of genes involved in siderophore

biosynthesis, highlighting increased competition for iron in polymicrobial cultures. Additionally, measurable levels of PQS were present in the Δ*lasR* mutant-containing polymicrobial culture. While these observations align with some studies in the literature, they contrast with others, highlighting that this remains an area of ongoing research with mixed and sometimes contradictory outcomes.

On the one hand, my results differed from the previously reported down-regulation of siderophore production in *lasR* mutants (Chadha *et al.*, 2021). Additionally, siderophore production has been shown to be down-regulated by both *S. aureus* and *C. albicans* in dual-species cultures (Chadha *et al.*, 2021; Cugini *et al.*, 2007; Lopez-Medina *et al.*, 2015).

On the other hand, it has also been demonstrated that *C. albicans*-produced farnesol can stimulate PQS production in LasR-defective *P. aeruginosa* strains (Cugini *et al.*, 2010; Tognon *et al.*, 2019). Cugini and colleagues proposed that ROS are responsible for activating downstream portions of this QS pathway, which aligns with the observed increase in PQS production in the continuous-flow system. Moreover, studies also showed that *lasR* mutants can produce low levels of PQS and accumulate high concentrations of HHQ due to low PqsH activity (Dekimpe & Déziel, 2009; Diggle *et al.*, 2003). Furthermore, a recent publication showed that *lasR* mutants increase pyoverdine production under certain conditions, especially in environments where QS-controlled traits are unnecessary (Figueiredo *et al.*, 2021). In line with these findings, my observations emphasise the increased need for iron chelation by the *lasR* mutant during polymicrobial growth.

The elevated siderophore production in Δ*lasR* mutant can be attributed to two potential explanations. Firstly, PQS has a high affinity for iron and can stimulate the expression of genes involved in siderophore biosynthesis, as suggested by several studies (Bredenbruch *et al.*, 2006; Diggle *et al.*, 2007). However, this link is not universally accepted and has been challenged in the literature (Rampioni *et al.*, 2010). Secondly, the increase may result from the loss of alternative iron acquisition strategies available to 'wild-type' *P. aeruginosa*. For example, *S. aureus* can serve as an iron source for *P. aeruginosa* in co-cultures due to lysis mediated by staphylolysin (LasA), which is regulated by the LasR system (Mashburn *et al.*, 2005). Additional, as yet unidentified, mechanisms may also play a role in this process.

I propose that LasR plays a significant role in enhancing survival and virulence in competitive environments. When *lasR* is defective, alternative strategies allow Δ*lasR* mutants to adapt and maintain similar abundance to 'wild-type' strains within polymicrobial cultures.

In the $PAO1_{MW}$ (WT) cultures, compared with their Δ*lasR* mutant counterparts, as expected, the most highly-up-regulated genes were central components of the QS system, regardless of the presence of other species. Activation of these QS systems in *P. aeruginosa* can lead to the production of several virulence factors that inhibit the growth of *S. aureus* and modulate interactions with *C. albicans*. For instance, QS molecules like OdDHL are involved in binding to *C. albicans* filaments and inhibiting its yeast-to-hyphae transition, while PQS and its precursor HHQ have been shown to repress *C. albicans* biofilm formation (Biswas & Götz, 2022; Hogan *et al.*, 2004; Kaleli *et al.*, 2007; Ovchinnikova *et al.*, 2012; Phelan *et al.*, 2014; Reen *et al.*, 2011). However, the actual concentrations of QS molecules in the cultures were relatively low, suggesting that their effects are likely localised rather than impacting the entire culture. Taken together, these results indicate that QS may play some role in shaping inter-species interactions but on a more confined, local scale.

Moreover, many other up-regulated genes in the $PAO1_{MW}$ (WT) strain remain partially or fully uncharacterised, indicating the potential for understanding unknown biological mechanisms. An intriguing example is the *tseT* operon, which was up-regulated in *P. aeruginosa* $PAO1_{MW}$ compared with Δ*lasR* mutants. This operon carries an upstream LasR binding site, indicating that LasR likely controls its expression and is part of the *lasR* regulon (Haas *et al.*, 2023). The *tseT* operon encodes proteins involved in the H2-T6SS that can be used as a contact-based weapon in microbial interactions (Filloux, 2024). Given that Δ*lasR* mutants – often referred to as 'social cheaters' – do not express this operon, it raises the possibility that the 'wild-type' *P. aeruginosa* $PAO1_{MW}$ may use the *tseT* operon to manage or suppress the growth of Δ*lasR* mutants in polymicrobial environments. This potential regulatory role could be key to the $PAO1_{MW}$ maintaining dominance and stability in mixed microbial communities. Consequently, the next chapter is dedicated to a detailed exploration of the *tseT* operon, aiming to uncover its specific functions and contributions to microbial interactions and community structure.

Several limitations of the experiments presented in this chapter should be acknowledged.

Firstly, bulk transcriptional profiles provide an aggregated view of gene expression, which may mask distinct transcriptional signatures of individual cells within the heterogeneous population. Future studies employing single-cell RNA sequencing could offer more detailed insights into these nuanced expression patterns.

Secondly, the limited sample size introduces constraints and potential biases, including batch effects, which could influence the results. Thirdly, the RNA purification methods were explicitly optimised for *P. aeruginosa*, restricting comprehensive gene expression analysis of other species in the polymicrobial community, particularly *C. albicans*.

The fourth limitation of this study is the selection of the significance threshold for $\log_2$ Fold Change (FC), which was set at one. This threshold was chosen to allow for a broader exploration of potential differences across various scenarios, facilitating the identification of patterns specific to the $PAO1_{MW}$ and Δ*lasR* mutant, as well as between mono- and polymicrobial cultures. While a more conservative threshold could theoretically increase statistical power, it would also limit the detection of more nuanced yet potentially biologically significant changes. By maintaining the threshold at one, this study aims to balance sensitivity and specificity, ensuring that a wide range of gene expression differences are captured for analysis without excessively narrowing the dataset.

Another limitation was that, despite thorough efforts to contextualise these findings within the existing literature, discrepancies in experimental approaches, microbial species, and strains posed challenges. Furthermore, the absence of directly comparable samples, such as human tissue or traditional batch cultures, limited the scope of comparative analysis and broader generalisations.

Lastly, a limitation is related to potential variations caused by using a semi-complex medium such as ASM. As previously noted, undefined components, such as commercial porcine gastric mucin or egg yolk, may lead to differences in microbial adaptation, behaviour, and transcriptional profile in the cultures (Neve *et al.*, 2021). Although an alternative approach like proteomics could have been considered, it was estimated to be more challenging given the complexity of ASM and the polymicrobial nature of the experiments.

Overall, the experiments presented in this chapter showed that the abundance of *P. aeruginosa* in polymicrobial cultures remains constant, regardless if $PAO1_{MW}$ or the Δ*lasR* mutant is present. This stability, however, is facilitated by distinct transcriptional profiles that adapt, as much as needed, to the inter-species interactions within the community. Thus, the findings support my hypothesis that a loss-of-function mutation in *lasR* significantly impacts the interactions between *P. aeruginosa* and other species by altering the transcriptional profile. The observed differences in gene expression have been comprehensively discussed, leading to the development of a novel hypothesis explored in detail in the next chapter.

Chapter 5

Polyclonal co-cultures of *Pseudomonas aeruginosa* strains

5.1. Background and rationale

In this chapter, co-cultures of different *P. aeruginosa* strains are studied to investigate a potential mechanism(s) responsible for constraining Δ*lasR* mutant titres or, in other words, 'policing cheaters'.

In microbial systems, 'cheating' refers to the behaviour of individuals that exploit a communal trait, such as public goods, while contributing less or not at all to the associated costs (Sandoz *et al.*, 2007; Özkaya *et al.*, 2018; Özkaya *et al.*, 2017). This can result in a fitness advantage for cheaters over cooperators, leading to an increased frequency of cheaters within the population. Over time, this imbalance can deplete public goods, potentially causing the collapse of the entire population (Özkaya *et al.*, 2018). Δ*lasR* mutants, common across different environments and associated with CF lung disease progression, are often considered cheaters (Hoffman *et al.*, 2009; O'Connor *et al.*, 2022; Smith *et al.*, 2006). Several studies have shown that they do not contribute to producing QS-regulated shared goods (D'Argenio *et al.*, 2007; Kostylev *et al.*, 2019; Wang *et al.*, 2018; Whiteley *et al.*, 2017).

'Policing' is a mechanism through which cooperators suppress the fitness of cheaters to maintain cooperation within a population. Such policing strategies ensure that cheaters do not dominate cooperators, preserving cooperative traits and preventing population collapse (Mould *et al.*, 2022). It has been demonstrated that this policing by *P. aeruginosa* can involve the production of toxic compounds such as hydrogen cyanide, rhamnolipids, or pyocyanin, which disproportionately affect cheaters (Castañeda-Tamez *et al.*, 2018; García-Contreras *et al.*, 2020). However, most of these studies have focused on single traits and specific, often resource-limited, environments. In contrast, natural environments are complex, presenting multiple constraints and allowing microbes to rely on various resources for survival. The CF lung is one such complex environment, and ASM was created to closely mimic the broad range of resources available to microbes (specifically, *P. aeruginosa*) in this setting (Fung *et al.*, 2010;

Palmer *et al.*, 2007). Moreover, clinical observations and laboratory experiments suggest that strains with intact and defective *lasR* can coexist stably, with the proportion of cheaters typically ranging between 10-40% (Asfahl *et al.*, 2015; Dandekar *et al.*, 2012; Robinson *et al.*, 2020; Sandoz *et al.*, 2007). This range suggests the presence of policing mechanisms to prevent the dominance of *lasR* mutants or, alternatively, indicates that cheating may not be necessary in a nutrient-rich environment (Luo *et al.*, 2024; Mould *et al.*, 2022).

Based on my RNA sequencing findings, I hypothesised that policing could involve the *tseT* operon (PA3904-08). This idea is based on the possibility that if Δ*lasR* mutants are indeed cheaters, they would be policed by a mechanism they cannot evade. The *tseT* operon comprises five genes preceded by an upstream LasR binding site. The operon encodes a PAAR4 protein, a chaperone and co-chaperone (TecT and co-TecT), a TOX-REase-5 domain-containing effector with nuclease activity (TseT), and an immunity protein (TsiT) (Burkinshaw *et al.*, 2018; Haas *et al.*, 2023; Wen *et al.*, 2021; Wood *et al.*, 2019). Due to the inability to produce the immunity protein, Δ*lasR* mutants would not be recognised as 'kin,' making them vulnerable to the nuclease effect of the TseT toxin. Moreover, the T6SS has previously been associated with policing mechanisms in *Burkholderia thailandensis* and *Yersinia pseudotuberculosis*, raising the potential for similar roles in other organisms as well (Filloux, 2024; Majerczyk *et al.*, 2016; Song *et al.*, 2024; Whiteley *et al.*, 2017)

I hypothesised that in polyclonal populations of *P. aeruginosa* 'wild-type' $PAO1_{MW}$ and Δ*lasR* mutant, the $PAO1_{MW}$ strain utilises the *tseT* operon, a component of the T6SS within the *lasR* regulon, to constrain the abundance of Δ*lasR* mutants.

To test this hypothesis, I pursued the following experimental objectives:

1. To co-culture $PAO1_{MW}$ and Δ*lasR* mutant strains in both mono- and polymicrobial environments to assess their relative abundances/behaviours.
2. To investigate co-cultures of $PAO1_{MW}$ and ΔPA3904-08 mutant as well as Δ*lasR* mutant and ΔPA3904-08 mutant in both mono- and polymicrobial environments to assess their relative abundances.
3. To evaluate the impact of complementing the *tseT* operon in a Δ*lasR* background (Δ*lasR*+PA3904-08 mutant).

5.2. Co-cultures of 'wild-type' PAO1$_{MW}$ and Δ*lasR* mutant

The continuous-flow system was extended to explore co-culturing not only different species but also two genetic variants of *P. aeruginosa*: the 'wild-type' PAO1$_{MW}$ and Δ*lasR* mutant strains. These experiments were designed to begin investigating the impact of intra-species diversity on microbial dynamics in mono- and polymicrobial environments.

In the monospecies setup, Δ*lasR* mutants constituted around 10% (8.9 ± 7.9%) of the *P. aeruginosa* population, as shown in *Figure 5.1.A-B*. This suggests that a mechanism for constraining Δ*lasR* mutants is present and independent of input from other species. When co-cultured with two additional species (*S. aureus* and *C. albicans*), the ratio of Δ*lasR* mutants in the *P. aeruginosa* population remained similar (7.4 ± 6.7%), as shown in *Figure 5.1.C-D*. These findings suggest that in an environment that chemically mimics the CF airways, Δ*lasR* mutant titres are constrained in both mono- and polymicrobial conditions. This observation aligns with clinical data from samples collected during the early and middle stages of chronic airway infection in individuals with CF (Asfahl *et al.*, 2015; Dandekar *et al.*, 2012; Robinson *et al.*, 2020; Sandoz *et al.*, 2007). Additionally, the overall *P. aeruginosa* titres remained consistent with those described in *Section 4.2*. Having established that co-cultures of different genetic variants can be effectively studied in the continuous-flow system, the next step was to investigate whether the *tseT* operon plays a role in regulating co-culture titres.

5.3. Role of the *tseT* operon in co-cultures

To test my hypothesis about the involvement of the *tseT* operon in policing, a mutant deleted for the entire *tseT* operon (referred to hereafter as ΔPA3904-08 mutant) was generated by my colleague, Rahan Nazeer. All five ORFs (PA3904 - PA3908) of the operon were deleted in this mutant. Initially, mono- and polymicrobial cultures containing only the ΔPA3904-08 mutant (no PAO1$_{MW}$ *P. aeruginosa*) were established to assess its baseline behaviour in the continuous-flow system. Subsequently, co-cultures were created by pairing the PAO1$_{MW}$ strain with the ΔPA3904-08 mutant, as well as the Δ*lasR* mutant with the ΔPA3904-08 mutant, to investigate how the absence of the *tseT* operon affects inter-species dynamics and to test for evidence of policing mechanisms.

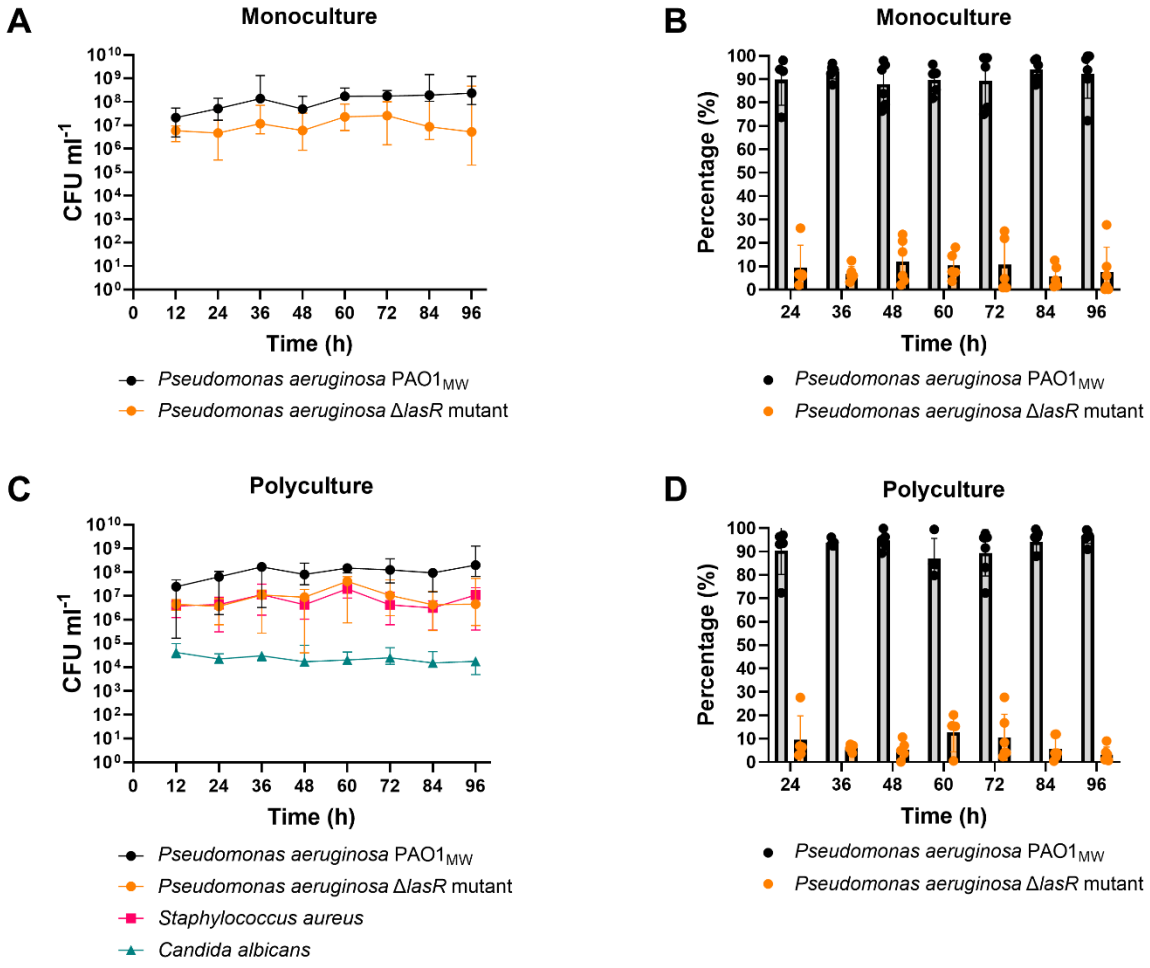

Figure 5.1. **Polyclonal cultures of *Pseudomonas aeruginosa* PAO1$_{MW}$ and Δ*lasR* mutant in monoculture and polyculture using the continuous-flow system.** ASM was continuously supplied at a flow rate of 145 µL min^{-1}. (A and C) The co-culturing results of PAO1$_{MW}$ (black circle) and Δ*lasR* mutant (orange circle) *P. aeruginosa*, showing consistent ratios of the variants in both monospecies and polymicrobial cultures. Data are presented as the median with 95% confidence intervals, based on six independent experiments. CFU mL^{-1} values are plotted on a log$_{10}$ scale. (B and D) Detailed ratios over time. In monospecies cultures, Δ*lasR* mutants constitute an average of 8.9% (± 7.9%) of the total *P. aeruginosa* population, while in polymicrobial cultures, they make up an average of 7.4% (± 6.7%).

The hypothesis is proven if the ΔPA3904-08 mutant mirrors the behaviour of the Δ*lasR* mutant in these co-culture experiments. Specifically, if the *tseT* operon is involved in policing, then in the co-culture with the 'wild-type' $PAO1_{MW}$, the ΔPA3904-08 mutant would be expected to constitute approximately 10% of the total *P. aeruginosa* population, similar to the proportion observed in co-cultures of the $PAO1_{MW}$ and Δ*lasR* mutant. However, in co-cultures of the ΔPA3904-08 mutant with the Δ*lasR* mutant, both strains would be expected to be present in roughly equal proportions, indicating no fitness advantage for either variant.

5.3.1. ΔPA3904-08 mutant

First, the behaviour of the ΔPA3904-08 mutant within the continuous-flow system was examined. In the monospecies cultures, the ΔPA3904-08 mutant reached the same titre as the $PAO1_{MW}$ or the Δ*lasR* mutant, as shown in *Figure 5.2.A*. This indicates that the ΔPA3904-08 mutant does not exhibit a fitness defect *per se*. In the poly-species culture, the ΔPA3904-08 mutant had the highest abundance among the species, reaching titres comparable to those of the Δ*lasR* mutant or $PAO1_{MW}$ (when grown in mono-culture). However, I noted that the dynamics of the other species present appeared to be moderately, although not significantly, shifted, as shown in *Figure 5.2.B*. *S. aureus* settled at around 10^6 CFU mL^{-1}, approximately 5-10-fold lower than that previously observed in the presence of 'wild-type' *P. aeruginosa*. Also, I noted that *C. albicans* initially maintained slightly higher titres, at around 10^5 CFU mL^{-1} (*cf.* in the presence of *P. aeruginosa* $PAO1_{MW}$, where titres reached 10^4 CFU mL^{-1}). However, these titres slowly declined over time below the steady-state levels seen with the $PAO1_{MW}$. A similar pattern for *C. albicans* was observed with the Δ*lasR* mutant in poly-species culture, as detailed in *Section 4.2.2*. Overall, I conclude that the ΔPA3904-08 mutant grows well in both mono- and polymicrobial cultures, and that it may moderately alter community dynamics.

5.3.2. Little role in policing mechanisms

After confirming the viability of the ΔPA3904-08 mutant in the continuous-flow system, it was co-cultured with $PAO1_{MW}$ *P. aeruginosa*. The ΔPA3904-08 mutant consistently maintained equal titres with the $PAO1_{MW}$ in both mono- and polymicrobial setups, with no statistically significant differences, as shown in *Figure 5.3 A-D*. In monospecies culture, the mean proportion of ΔPA3904-08 mutant *cf*. the $PAO1_{MW}$ was 49.1 ± 12.9%, whereas, in the polymicrobial environment, it was 44.6 ± 14.4%.

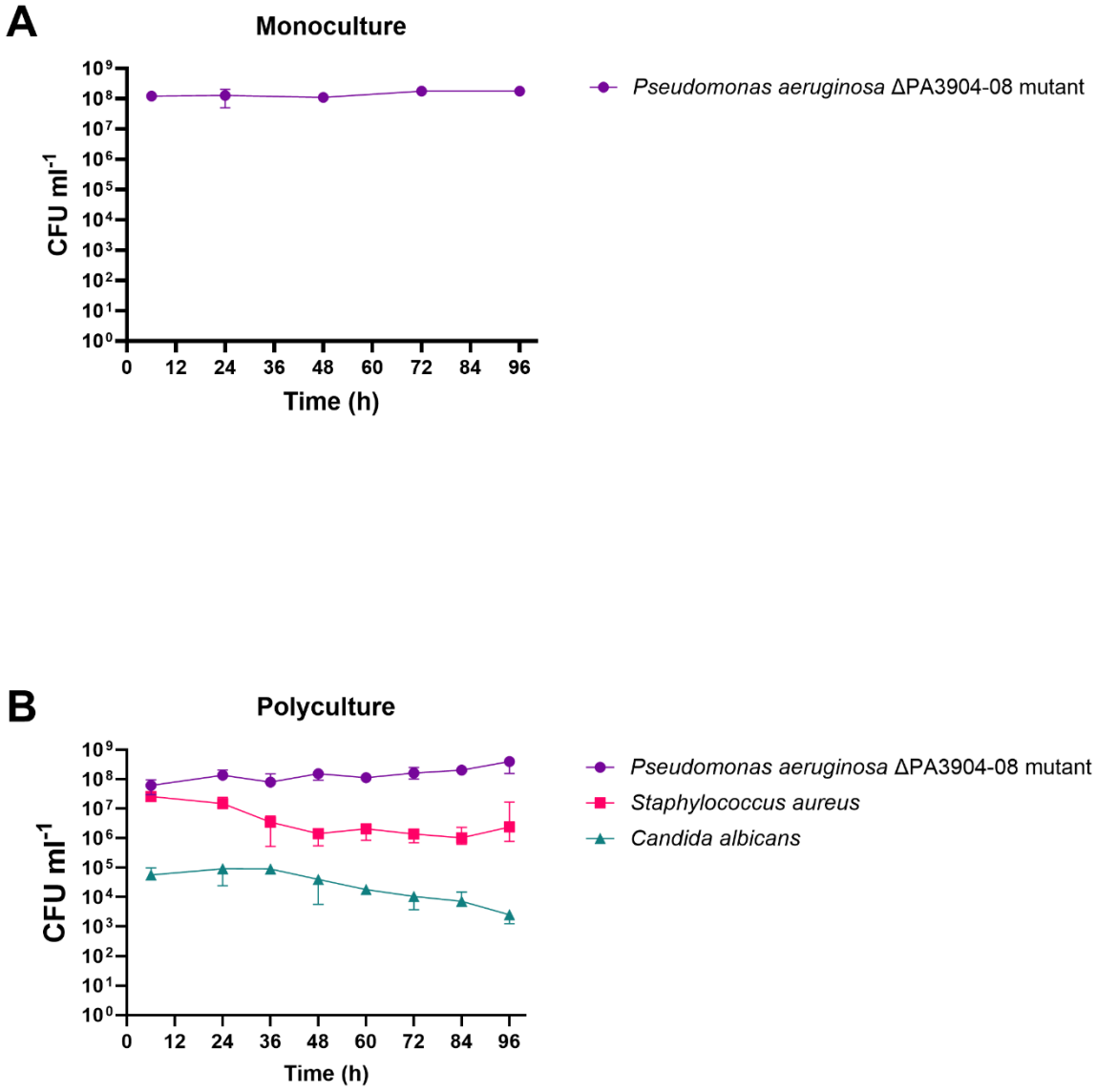

Figure 5.2. **Dynamics of the *Pseudomonas aeruginosa* ΔPA3904-08 mutant in monoculture and polyculture.** Viable cell counts of *P. aeruginosa* ΔPA3904-08 mutant (purple circle), *S. aureus* (pink square), and *C. albicans* (turquoise triangle) in non-disturbed cultures of ASM at Q = 145 µL min^{-1} flow. CFU mL^{-1} values are plotted on a log_{10} scale. Data is represented as the median with a 95% confidence interval across three independent experiments. No significant differences were found in cell counts compared with the results at the 24-hour timepoint ($p > 0.05$).

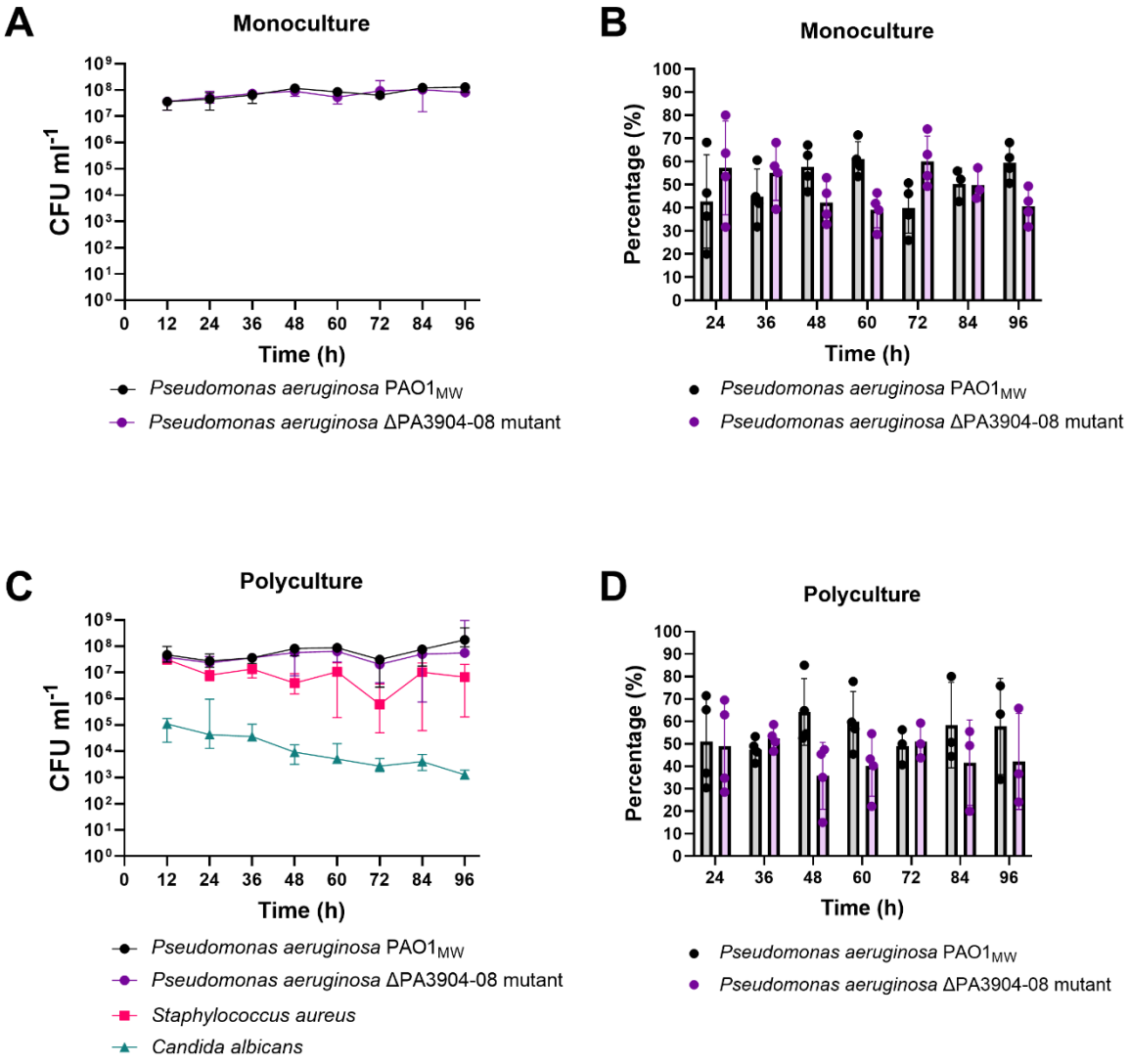

Figure 5.3. **Polyclonal cultures of *Pseudomonas aeruginosa* PAO1$_{MW}$ and Δ*lasR* mutant in monoculture and polyculture using the continuous-flow system.** ASM was continuously supplied at a flow rate of 145 µL min^{-1}. (A and C) The co-culturing results of PAO1$_{MW}$ with gentamicin resistance (black circle) and ΔPA3904-08 mutant (purple circle) *P. aeruginosa*, show consistent ratios of the variants in both monospecies and polymicrobial cultures. Data are presented as the median with 95% confidence intervals based on four independent experiments. CFU mL^{-1} values are plotted on a log$_{10}$ scale. (B and D) Detailed ratios over time. In monospecies cultures, ΔPA3904-08 mutants constitute an average of 49.1 ± 12.9% of the total *P. aeruginosa* population, while in polymicrobial cultures, they make up an average of 44.6 ± 14.4%.

Taken together, these results challenge my hypothesis that the *tseT* operon is involved in policing the appearance of *lasR* "cheats", since the ΔPA3904-08 mutant exhibited different behaviour compared with the Δ*lasR* mutant. However, and as previously noted, *S. aureus* and *C. albicans* population dynamics appeared different in these experiments compared with my previous findings with cultures containing only the $PAO1_{MW}$. Given the extremely reproducible nature of the experimental setup, these differences suggest that the presence of the ΔPA3904-08 mutant is associated with a less stable polymicrobial community.

Next, I co-cultured the ΔPA3904-08 mutant with the Δ*lasR* mutant. In monospecies cultures containing the ΔPA3904-08 mutant and the Δ*lasR* mutant together, Δ*lasR* mutant titres were again constrained to ca. 8.9 ± 5.8% of the population (*Figure 5.4.A-B*), similar to the dynamics seen when the Δ*lasR* mutant and $PAO1_{MW}$ were co-cultivated. These data collectively indicate that (i) the *tseT* operon is not involved in policing *per se*, or that (ii) additional policing mechanisms may be involved in suppressing the appearance of cheaters, even in the absence of the *tseT* operon. In the triple-species culture containing both the ΔPA3904-08 mutant and Δ*lasR* mutant, a similar pattern was observed, with the ΔPA3904-08 mutant behaving like the $PAO1_{MW}$ (*Figure 5.4.C-D*). Here, the mean titre of the Δ*lasR* mutant was 10.2 ± 7.3%. Furthermore, *S. aureus* and *C. albicans* exhibited population fluctuations similar to those seen when grown alongside the ΔPA3904-08 mutant alone (*Figure 5.2 B*). These findings collectively suggest that the *tseT* operon is not involved in Δ*lasR* mutant policing under the studied conditions but that it may play a role in inter-species interactions.

To confirm these results, another mutant was made to investigate the effects of restoring the *tseT* operon in the *lasR* background. Here, the *tseT* operon was inserted into a neutral site in the chromosome under the control of an IPTG inducible promoter (referred to as Δ*lasR*+PA3904-08 mutant). After verifying the fitness of this Δ*lasR*+PA3904-08 mutant in the continuous-flow system, it was co-cultured with 'wild-type' *P. aeruginosa*.

The results further challenged my hypothesis, as shown in *Figure 5.5*. Contrary to expectations, IPTG-induced expression of the *tseT* operon did not significantly increase the proportion of the mutant.

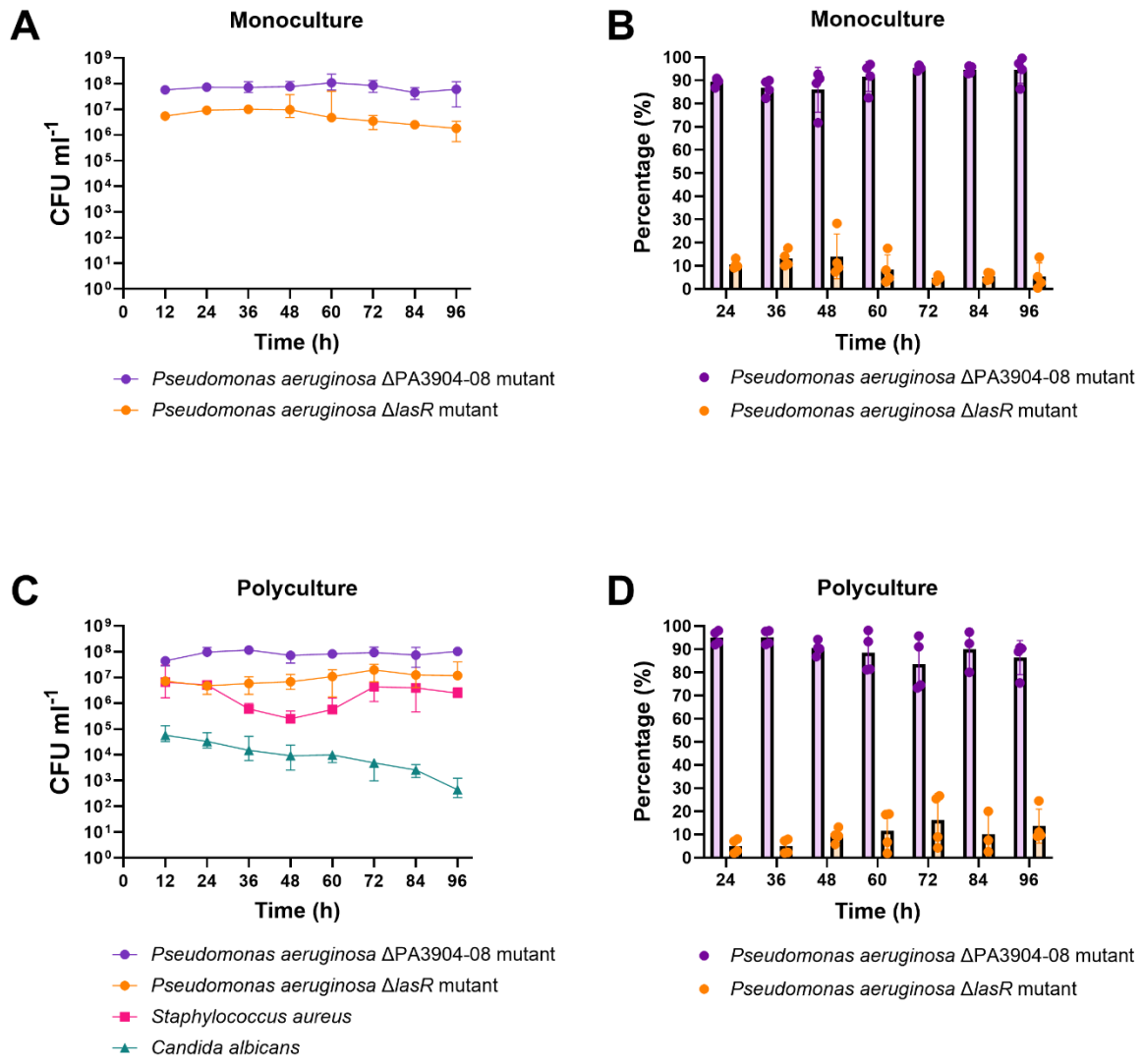

Figure 5.4. **Polyclonal cultures of *Pseudomonas aeruginosa* ΔPA3904-08 mutant and Δ*lasR* mutant in monoculture and polyculture using the continuous-flow system.** ASM was continuously supplied at a flow rate of 145 µL min^{-1}. (A and C) The co-culturing results of ΔPA3904-08 mutant (purple circle) and Δ*lasR* mutant (orange circle) *P. aeruginosa*, show consistent ratios of the variants in both monospecies and polymicrobial cultures. Data are presented as the median with 95% confidence intervals based on four independent experiments. CFU mL^{-1} values are plotted on a log_{10} scale. (B and D) Detailed ratios over time. In monospecies cultures, Δ*lasR* mutants constitute an average of 8.98 ± 5.77% of the total *P. aeruginosa* population, whereas in polymicrobial cultures, they make up an average of 10.15 ± 7.31%.

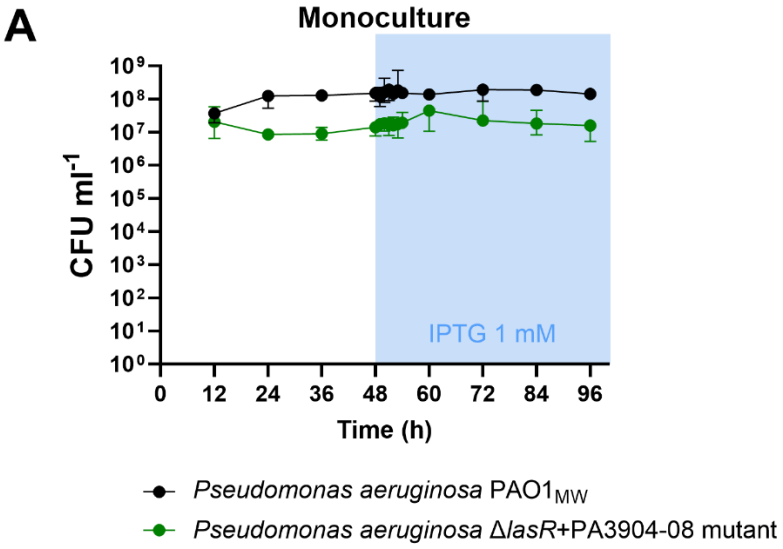

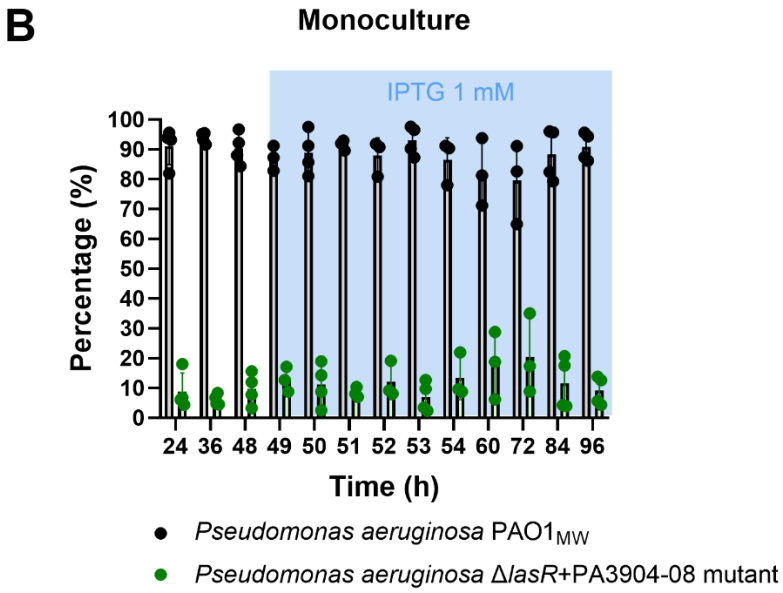

Figure 5.5. **Polyclonal cultures of *Pseudomonas aeruginosa* PAO1$_{MW}$ and Δ*lasR*+PA3904-08 mutant in monoculture using the continuous-flow system.** (A) Co-culturing results of PAO1$_{MW}$ (black circle) and Δ*lasR*+PA3904-08 mutant (green circle) *P. aeruginosa*. IPTG was supplied from 48 hours of co-culturing onwards at a final concentration of 1 mM. CFU mL^{-1} values are plotted on a $\log_{10}$ scale and data are presented as the median with 95% confidence intervals based on four independent experiments. ASM was continuously supplied at a flow rate of 145 µL min^{-1}. (B) Detailed ratios over time. The mean ratio of Δ*lasR*+PA3904-08 mutant was 8.22 ± 4.46% before the induction of the *tseT* operon and 12.00 ± 7.32% after induction, with no significant difference between the two datasets.

As shown in *Figure 5.5*, when I induced expression of the *tseT* operon (after 48 hours of co-culturing alongside the 'WT') with IPTG (itself, continuously added to the system *via* the medium feed), there was no significant effect on the titres of either the $PAO1_{MW}$ or Δ*lasR*+PA3904-08 mutant. The mean ratio of Δ*lasR*+PA3904-08 mutant was 8.22 ± 4.46% before switching on expression of the *tseT* operon and 12.00 ± 7.32% after, with no significant difference between the datasets ($p > 0.2$).

Overall, these results indicate that neither the absence of the *tseT* operon, nor its activation (*via* IPTG induction) had any significant influence on intra-species competition/dynamics. However, some of my observations did point toward a potential role for the *tseT* operon in dictating polymicrobial community dynamics.

5.4. *tseT* operon affecting polymicrobial dynamics

To further investigate the involvement of the *tseT* operon in polymicrobial interactions, the next step focused on examining its specific effects in greater detail. In the polymicrobial culture, *S. aureus* titres were notably lower when *tseT* was absent in a $PAO1_{MW}$ background, a phenomenon not observed in the Δ*lasR* background (where presumably, *tseT* function is also absent due to lack of LasR-induced *tseT* operon expression). However, in both the ΔPA3904-08 mutant and the Δ*lasR* mutant, *C. albicans* displayed altered behaviour compared with poly-species cultures containing $PAO1_{MW}$. These effects could result from direct dual-species interactions or arise indirectly from the more complex dynamics in the triple-species system.

To explore this, a further mutant was generated to assess the effects of restoring the *tseT* operon in the Δ*lasR* background. In addition to the previously introduced Δ*lasR*+PA3904-08 mutant, a control mutant (referred to as Δ*lasR*+Empty mutant) was generated by inserting an empty IPTG-inducible vector (without the cloned *tseT* operon) into a neutral site in the chromosome. Both mutants were co-cultured with the other species, with IPTG added 48-hours after inoculation and continuously supplied to observe the effects of activating the *tseT* operon in a Δ*lasR* mutant background. As shown in *Figure 5.6.A-B*, the most notable difference between these cultures was the behaviour of *C. albicans*. Following IPTG addition, the decline in *C. albicans* populations was halted and even moderately reversed in the culture with the restored *tseT* operon. While the values were not significantly different from the *C. albicans* titres when the Δ*lasR*+Empty mutant was present ($p=0.1$), they displayed a distinct trend.

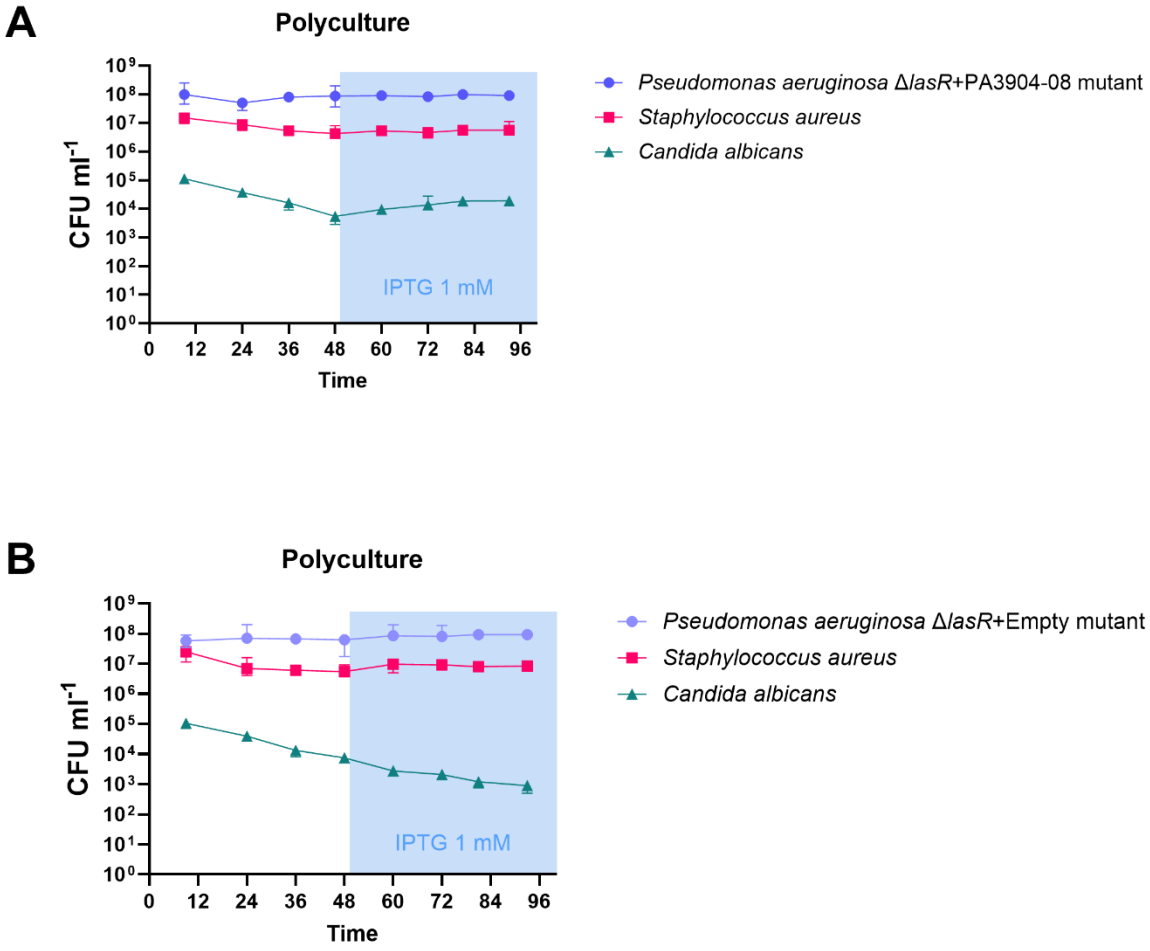

Figure 5.6. **Polymicrobial cultures of *Pseudomonas aeruginosa* Δ*lasR*+PA3904-08 and Δ*lasR*+Empty mutants in the continuous-flow system.** Viable cell counts of *P. aeruginosa* Δ*lasR*+PA3904-08 mutant (king blue circle), *P. aeruginosa* Δ*lasR*+Empty mutant (light purple circle), *S. aureus* (pink square), and *C. albicans* (turquoise triangles) are shown. CFU mL^{-1} values are plotted on a log_{10} scale, and data are presented as the median with 95% confidence intervals based on three independent experiments. IPTG was supplied from 48 hours of co-culturing onwards at a final concentration of 1 mM for both setups. ASM was continuously supplied at a flow rate of 145 µL min^{-1}. No significant differences were observed in *P. aeruginosa* or *S. aureus* cell counts compared with the values at the 24-hour timepoint ($p > 0.4$). (A) *C. albicans* cell counts within the Δ*lasR*+PA3904-08 culture were significantly different at the 48-hour and 60-hour timepoints compared with those at 24 hours ($p < 0.05$), but not at later timepoints ($p > 0.05$). (B) In the Δ*lasR*+Empty culture, *C. albicans* cell counts significantly differed from the 48-hour timepoint onwards compared with the 24-hour timepoint ($p < 0.05$).

The presence or absence of *tseT* operon in the Δ*lasR* background did not significantly affect the population size of *S. aureus*. This suggests that the *tseT* operon may influence interactions specifically with *C. albicans*, although this effect was only observed in the Δ*lasR* background.

[Due to technical challenges with cloning, it was not feasible to restore the *tseT* operon in the ΔPA3904-08 mutant within the scope of this project.]

Pairwise competition assays were conducted using a 96-well plate format to test for direct interactions, as outlined in *Section 3.9*. This approach aimed to determine whether the observed changes in the continuous-flow system were due to direct pairwise interactions between *P. aeruginosa* and *S. aureus* or *P. aeruginosa* and *C. albicans*, or if they arose only within the more complex triple-species community. Co-culturing lasted for 24 hours before processing the samples for CFU enumeration.

As shown in *Figure 5.7.A*, no significant differences were observed in the population sizes of the different *P. aeruginosa* genetic variants when cultured alone or in dual-species setups with other microbes ($p > 0.5$). However, in co-culture with *P. aeruginosa* $PAO1_{MW}$, the *S. aureus* population was significantly smaller compared with its growth in monoculture, in co-culture with *C. albicans*, or in co-cultures with *P. aeruginosa* variants carrying the Δ*lasR* mutation ($p < 0.01$) (*Figure 5.6.B*). These results are consistent with the expected role of QS mechanisms in mediating interactions between *P. aeruginosa* and *S. aureus* (Hotterbeekx *et al.*, 2017; Magalhães *et al.*, 2019). Interestingly, the ΔPA3904-08 mutant did not exhibit significant differences in *S. aureus* population size compared with other strains, suggesting it falls between the effects seen with the $PAO1_{MW}$ and genetic variants of Δ*lasR* background. This contrasts with the continuous-flow system results, where *S. aureus* titres notably declined in the presence of the ΔPA3904-08 mutant (*Figure 5.4C*), indicating that the *tseT* operon may manifest its function differently in more complex multi-species environments compared with simpler pairwise interactions. As for *C. albicans* (*Figure 5.7.C*), its population size was similarly affected by all *P. aeruginosa* genetic variants, with levels consistently lower than those observed in *C. albicans* monocultures ($p < 0.02$). These findings support the notion that interactions between *P. aeruginosa* and *C. albicans* are generally negative.

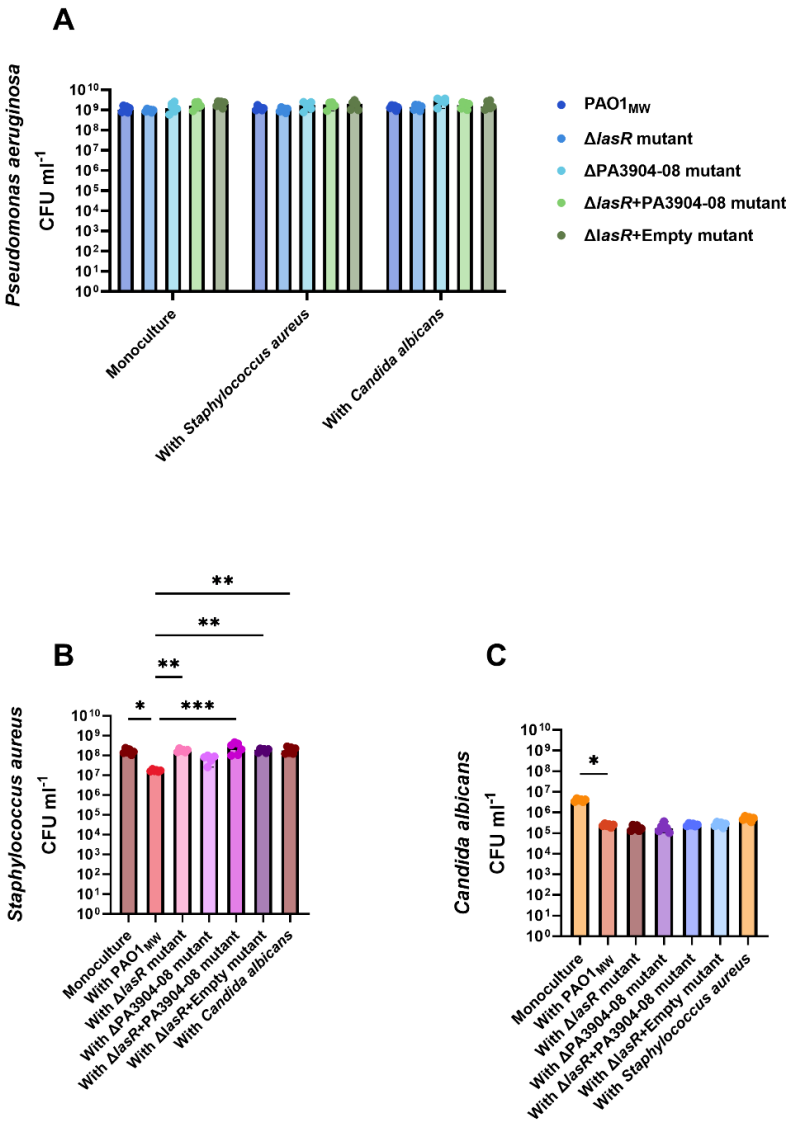

Figure 5.7. 96-well plate-based competition assay results evaluating dual-species cultures after 24 hours in ASM. CFU mL^{-1} values are plotted on a log_{10} scale, and data are presented as the median with 95% confidence intervals based on three independent experiments. IPTG was supplied for Δ*lasR*+PA3904-08 mutant and Δ*lasR*+Empty mutant cultures at a final concentration of 1 mM. ASM was continuously supplied at a flow rate of 145 µL min^{-1}. (A) Viable cell counts of different *P. aeruginosa* genetic variants in monoculture, and in co-culture with *S. aureus* or *C. albicans*. No significant differences were observed between the three culture conditions for the same genetic variant ($p > 0.5$). (B) Viable cell counts of *S. aureus* in monoculture and co-culture with different *P. aeruginosa* genetic variants or *C. albicans*. The co-culture with *P. aeruginosa* $PAO1_{MW}$ resulted in significantly lower *S. aureus* counts compared with monoculture, co-culture with *C. albicans*, or co-culture with any Δ*lasR* mutant variant ($p < 0.01$). (C) Viable cell counts of *C. albicans* in monoculture and co-culture with different *P. aeruginosa* genetic variants or *S. aureus*. Compared with co-culture with *P. aeruginosa* $PAO1_{MW}$, only the monoculture showed significant differences ($p < 0.02$).

Overall, the results indicate that the *tseT* operon plays some role in polymicrobial interactions in the continuous-flow system. For example, when the Δ*lasR* mutant background was complemented with the *tseT* operon (Δ*lasR*+PA3904-08 mutant) and induced by IPTG, it positively impacted *C. albicans* titres. However, these effects were not evident in dual-species cultures in 96-well plates. Potentially factors such as the constant media supply, extended time frames (96 hours *vs*. 24 hours), and the differences in spatial organisation of microbial sub-populations, such as aggregates commonly found in the continuous-flow system, likely contribute to these observed effects. These results highlight the increased complexity of microbial interactions in dynamic environments.

5.5. Discussion

In this chapter, I investigated my second hypothesis regarding the role of the *tseT* operon in intra-species interactions. The hypothesis arose from the RNA sequencing data discussed in *Chapter 4*, which indicated that 'wild-type' *P. aeruginosa* $PAO1_{MW}$ expresses the elements of the *tseT* operon in the continuous-flow system, compared with the transcriptome of a Δ*lasR* mutant. The *tseT* operon encodes a nuclease effector (TseT) and associated proteins (PAAR4, chaperone, co-chaperone, and immunity proteins) that are exported *via* the H2-T6SS. Since Δ*lasR* mutants cannot utilise the *tseT* operon due to its LasR-driven regulation, I hypothesised that this operon might play a role in constraining Δ*lasR* mutant titres within the *P. aeruginosa* population. However, my data do not support this conclusion. The ΔPA3904-08 mutant, in which the *tseT* operon was deleted in a $PAO1_{MW}$ background, behaved more like the $PAO1_{MW}$ than like a Δ*lasR* mutant in polyclonal culture. Specifically, in co-culture experiments, titres of the ΔPA3904-08 mutant and $PAO1_{MW}$ remained equal, whereas titres of the Δ*lasR* mutant with either the ΔPA3904-08 mutant or the $PAO1_{MW}$ were maintained at around 10% of that of the co-habiting strain.

Several theoretical explanations for these results can be drawn from the literature. First, the T6SS is a contact-dependent mechanism requiring close physical proximity between cells – typically less than 500 nm (Ho *et al.*, 2017). In the continuous-flow system, there is likely a mix of sessile and motile cells, with some forming visible aggregates observed under the microscope and occasionally with the naked eye. Combined with constant stirring, this variation could lead to greater distances and distinct subpopulations where contact-based

weaponry like T6SS becomes less effective. Unfortunately, the used experimental setup does not allow for the study of cellular spatial organisation, so it remains untested whether $PAO1_{MW}$ and Δ*lasR* mutant cells were sufficiently close to enable effective T6SS-mediated policing. A similar outcome has been described by Majerczyk and colleagues, who observed that *B. thailandensis* used a T6SS toxin activated by QS to constrain QS mutants, but only in agar plate colony co-cultures, not in broth (Majerczyk *et al.*, 2016).

Second, other limiting factors might prevent the *tseT* operon from being effectively transcribed or deployed. Haas and colleagues recently showed that low iron levels lead to reduced TseT production and prevent TseT-mediated competition (Haas *et al.*, 2023). They demonstrated that *P. aeruginosa* responds to increased iron levels, such as those occurring during viral infections and PEx, by up-regulating TseT expression to enhance competitiveness. However, the precise mechanism behind the effect of iron on TseT production remains unclear. In my study, the ASM used had lower iron concentrations (3.6 µM $FeSO_4$) compared with those used in the Haas study to induce TseT expression (25 µM FeCl3) (Haas *et al.*, 2023). Such elevated iron levels do not typically reflect the lung environment under normal conditions, though they may occur during exacerbations (Gifford *et al.*, 2012; Gifford *et al.*, 2021; Zhang *et al.*, 2019). This difference in iron availability could have prevented the full expression or function of the *tseT* operon in my system. Moreover, even when the *tseT* operon was artificially 'switched on' with IPTG induction, it is a formal possibility that the lower iron levels may have impaired necessary steps for effectively loading or firing it *via* H2-T6SS.

Third, Δ*lasR* mutants may have an immunity-independent protection mechanism that mitigates the effects of weaponry systems and toxins, such as T6SS and TseT. A comparable phenomenon has been demonstrated in *Escherichia coli* and *Vibrio cholerae*, where envelope stress responses provide defence against T6SS attacks without the need for immunity proteins (Hersch *et al.*, 2020). Theoretically, a similar mechanism could function in Δ*lasR* mutants, enabling them to survive T6SS-mediated attacks even without the TsiT immunity protein.

Although the *tseT* operon was hypothesised to constrain Δ*lasR* mutants, the results disproved this theory under the studied conditions.

Nevertheless, my experimental data do suggest that *tseT* plays a role in <u>*inter-species*</u> interactions. When the *tseT* operon was deleted in a $PAO1_{MW}$ background, *S. aureus* titres

were 5-10-fold lower compared with growth in the presence of *P. aeruginosa* $PAO1_{MW}$. Similarly, *C. albicans* titres in the ΔPA3904-08 mutant displayed a progressive instability, declining over time; a pattern also observed in the presence of the Δ*lasR* mutant. Although the 96-well plate-based competition assays did not verify these findings, this discrepancy can likely be explained by the differences between the 96-well plate setup (which favours interactions between sessile cells) and the continuous-flow system (which favours the planktonic lifestyle). For example, the continuous-flow system provides a constant supply of media, creating a more nutrient-rich environment that allows for long-term monitoring of population sizes – up to 96 hours in this project – with most changes appearing after 24 hours. The 96-well plates are limited to shorter time frames. After approximately 24 hours of co-culturing, fatal competition is manifested, with *P. aeruginosa* typically eliminating *S. aureus* or *C. albicans* from the dual-species cultures.

Based on my data, I speculated that the *tseT* operon plays a role in stabilising the triple-species culture. However, it remains unclear which species are affected and whether these interactions are direct or indirect. While my earlier results point to an interaction between *P. aeruginosa* and *C. albicans* mediated through LasR, this interaction may not be strictly routed through the *tseT* operon.

Several potential explanations can be drawn from the literature to better understand the direct or indirect involvement of TseT. Firstly, TseT is a nuclease that can kill target cells during competition. However, Basler and colleagues proposed that Tse effectors might be more crucial for lysing target species to release cytoplasmic contents, positioning T6SS effectors as nutrient scavengers rather than primarily mediators of lethality *per se* (Basler *et al.*, 2013). Based on this concept, it is theoretically possible that TseT could be deployed by *P. aeruginosa* when local nutrient availability is suboptimal, allowing the bacterium to access additional resources from lysed cells in its environment. Secondly, it is also worth considering whether the T6SS might benefit neighbouring microbes. While direct evidence supporting this hypothesis is currently lacking, it has been suggested in the literature that the T6SS could have a more intricate role in microbial communities than previously recognised (Chen *et al.*, 2015). Thirdly, an indirect effect is also plausible if TseT is not causing the observed modulation of inter-species dynamics, but rather, acts to limit the loading of other effectors into the H2-T6SS (a “molecular congestion” effect). Previous studies have reported competition between

effectors for loading into the T6SS machinery (Burkinshaw *et al.*, 2018). This means that the presence of TseT and its associated proteins may prevent the loading and firing of other molecules, such as PldA, PldB, Tle3, Tle4, and Tle1 proteins, all of which are transported via H2-T6SS (Wettstadt *et al.*, 2019). Notably, these are lipases that can target both eukaryotic and prokaryotic cells, which could contribute to the dynamics of a polymicrobial environment.

The work presented in this chapter has several limitations that impact the interpretation of the outcomes. One limitation is the small number of samples, ranging between 3-6 biological replicates. Despite efforts to conduct as many experiments as possible, a larger sample size would have improved the precision of the outcomes and potentially led to more robust interpretations. Additionally, a relevant mutant – the chromosomally-complemented version of the ΔPA3904-08 mutant – could not be produced due to time constraints and challenges with cloning. Including this mutant would have helped to confirm further the impact of the *tseT* operon deletion on inter-species dynamics. Another limitation stems from the nature of the sampling process, which represents overall population sizes but does not account for spatial organisation and differences between sub-communities. Moreover, previous studies have indicated that ASM can lead to metabolic and potentially genetic changes, which may introduce further variability (Neve *et al.*, 2021; Turner *et al.*, 2015). The method used to differentiate genetic variants in this study relies on the 'inbuilt' antibiotic resistance of the mutants. However, it has been demonstrated that spontaneous Δ*lasR* mutants can emerge during growth in rich media, like ASM, and these variants would not be accounted for using this approach (D'Argenio *et al.*, 2007). Importantly, a project is currently underway in the host laboratory that uses WGS to investigate mutations arising during microbial adaptation to ASM, both before and after cultivation in the experimental setup used in this study. Regarding comparisons with the literature, differences in species variants used across studies limit the ability to compare findings. Lastly, CFU measurements, while widely used, inherently carry a degree of error. In my experiments, this error typically averaged around 10%, adding an additional layer of uncertainty to the data. Although this level of variation is common in CFU assays, it must be considered when interpreting the results, particularly when differences between experimental groups are subtle.

Overall, I believe that I have eliminated the possibility that the *tseT* operon plays a key role in constraining the appearance/domination of Δ*lasR* mutants. However, the findings suggest

that the *tseT* operon does play a role in inter-species interactions, either directly or indirectly. Given the contact-dependent nature of T6SS, the *tseT* operon might be more relevant in scenarios where cell aggregation is enhanced, such as during antibiotic treatments. This potential role was explored further in the final part of this project, as detailed in the next chapter.

Chapter 6

Polymicrobial cultures and anti-pseudomonal challenge

6.1. Background and rationale

P. aeruginosa poses a significant challenge, particularly for individuals with CF, as it frequently causes chronic infections that are difficult to manage with antibiotics. These infections lead to a decline in lung function, increased morbidity, and a shortened life expectancy. A key issue in treatment failure is the discrepancy between *in vitro* antimicrobial susceptibility testing and the actual clinical response (Reece *et al.*, 2021). While this is partly due to the rapid development of antibiotic resistance, the polymicrobial nature of infections also plays a crucial role (Anju *et al.*, 2022; Filkins & O'Toole, 2015; Orazi & O'Toole, 2019). Increasing evidence shows that microorganisms within polymicrobial environments can interact synergistically, resulting in altered antimicrobial susceptibility through resistance and tolerance mechanisms (Little *et al.*, 2021). This is especially concerning as current clinical protocols for determining antimicrobial susceptibility focus exclusively on monospecies samples, despite evidence that mixed-species communities are generally more tolerant to antimicrobials than their monospecies counterparts (De Wit *et al.*, 2022; O'Brien *et al.*, 2022; Orazi & O'Toole, 2017).

In a previous project of the host laboratory, O'Brien and colleagues demonstrated in the continuous-flow system that growth within a polymicrobial environment protects *P. aeruginosa* from the effects of colistin (O'Brien *et al.*, 2022). Building on these findings, I developed two hypotheses. First, I speculated that this protective effect would extend beyond colistin to another commonly used antibiotic, ciprofloxacin. Second, I hypothesised that these protective mechanisms may be linked with QS, and therefore, loss of the master QS regulator, *lasR*, in *P. aeruginosa* would alter polymicrobial dynamics during antibiotic treatment.

While testing these two hypotheses, a third one emerged, prompted by the observed changes in *C. albicans* titres following antibiotic treatment with a combination of colistin and ciprofloxacin (referred to hereafter as combined treatment). Building on the results discussed

in the previous chapters, I speculated that this increase in *C. albicans* titres after antibiotic exposure may be linked to the activity of the *tseT* operon in *P. aeruginosa*.

To test these ideas, the following objectives were established:

1. To determine how ciprofloxacin affects 'wild-type' *P. aeruginosa* $PAO1_{MW}$ in monospecies and polymicrobial cultures.
2. To test if the presence of *S. aureus* and *C. albicans* also confers protection to a Δ*lasR* mutant of *P. aeruginosa* against colistin or ciprofloxacin.
3. To investigate whether the protective effect conferred by growth in a polymicrobial environment also extends to combinations of antibiotics, for both 'wild-type' $PAO1_{MW}$ and Δ*lasR* mutant *P. aeruginosa*.
4. To explore whether the observed fungal blooming is linked to expression or function of the ORFs encoded by the *tseT* operon.

6.2. Antibiotics and minimal inhibitory concentration

Colistin and ciprofloxacin were selected for three reasons. First, these antibiotics are frequently used in combination to target *P. aeruginosa*, particularly in early to mid-stage infections of pwCF. Second, colistin is considered a last-resort antibiotic, making it valuable to study its effectiveness in polymicrobial cultures. Third, this project aimed to build on previous colistin-related findings from the host laboratory, ensuring continuity in the research.

The minimal inhibitory concentration (MIC) of the two antimicrobials, colistin and ciprofloxacin, was determined separately in ASM for each species and/or genetic variant used in the experiments. MIC values were established using the broth microdilution method described in *Section 3.10.1*. The MIC was defined as the lowest antimicrobial concentration that inhibited visible microbial growth after overnight incubation. MIC measurements were repeated before each experiment for accuracy and reproducibility, with no changes observed. The results are summarised in *Table 6.1*. The MIC_{PA} of colistin for all genetic variants of *P. aeruginosa* was 4 μg mL^{-1}, whereas the MIC_{PA} for ciprofloxacin was 1 μg mL^{-1}. The MIC_{SA} of *S. aureus* for ciprofloxacin was 16 μg mL^{-1}. This means that the concentration used in this project ($5xMIC_{PA}$) was less than a third of the MIC_{SA}. As anticipated from previous studies, colistin did not affect *S. aureus* or *C. albicans*, and ciprofloxacin did not affect *C. albicans*.

Table 6.1. **Minimum inhibitory concentration of colistin and ciprofloxacin.** MIC values were determined using the broth microdilution method. *P. aeruginosa* genetic variants consistently showed susceptibility to colistin and ciprofloxacin, with MICs of 4 μg mL^{-1} and 1 μg mL^{-1}, respectively. As anticipated, *S. aureus* was not sensitive to colistin and had an MIC of 16 μg mL^{-1} for ciprofloxacin. *C. albicans* displayed no sensitivity to either antibiotic, as expected.

Species	**Strain**	**Minimum Inhibitory Concentration (μg mL^{-1})**	
		Colistin	**Ciprofloxacin**
P. aeruginosa	$PAO1_{MW}$	4	1
	Δ*lasR* mutant	4	1
	ΔPA3904-08 mutant	4	1
	Δ*lasR*+PA3904-08 mutant	4	1
S. aureus	ATCC 25923	>256	16
C. albicans	SC5314	>256	>256

6.3. Antibiotic monotherapy

Before working on the first objective of this part of the project, initial experiments on 'wild-type' $PAO1_{MW}$ cultures were conducted with colistin to replicate previous measurements. This ensured reproducibility and established a reliable benchmark for subsequent combination therapy experiments. Afterwards, ciprofloxacin was tested on $PAO1_{MW}$ cultures, followed by monotherapy with both antibiotics separately on Δ*lasR* mutant polymicrobial cultures.

Polymicrobial cultures were grown in ASM under continuous-flow conditions for 48 h prior to the addition of the antibiotic. The antibiotic treatment was applied as a pulse of 5xMIC for *P. aeruginosa* ($5xMIC_{PA}$). This timing enabled me to monitor population dynamics in the pre-established cultures to evaluate pre-treatment stability. The details of the antibiotic dosing are described in *Section 3.10.2*. The results are displayed with the addition of antibiotics indicated as T=0 hour, which occurred 48 hours after inoculation. Sampling at T=0 hour was performed immediately before the antibiotics were administered.

6.3.1. *Pseudomonas aeruginosa* $PAO1_{MW}$

Previously reported outcomes with colistin treatment on $PAO1_{MW}$ cultures were reproducible. There was no noticeable difference in CFU mL^{-1} counts during the stable, non-disturbed period, between the -24-hour and 0-hour timepoints ($p > 0.75$). Colistin had a pronounced effect on monospecies cultures, causing viable *P. aeruginosa* cells to become undetectable for several hours, as illustrated in *Figure 6.1.A*. This 8-log fold reduction was statistically significant comparing the stable titres before the antibiotic was added to the 1, 3, 5, and 8-hour timepoints post-treatment ($p < 0.04$). Interestingly, as reported previously, 48 hours after the addition of the antibiotics, there was an increase in population size compared with pre-antibiotic levels.

In contrast, the polymicrobial culture exhibited a smaller response to colistin, with a less than 2-log fold decrease in *P. aeruginosa* titres, as shown in *Figure 6.1.B*. This change was not significantly different from stable levels ($p > 0.3$). No significant change was observed in *S. aureus* or *C. albicans* titres throughout the sampling period ($p > 0.3$). To gain more insight, the 3-hour sampling routine was introduced for 24 hours following the antibiotic treatment to capture more detailed fluctuations in the polymicrobial response.

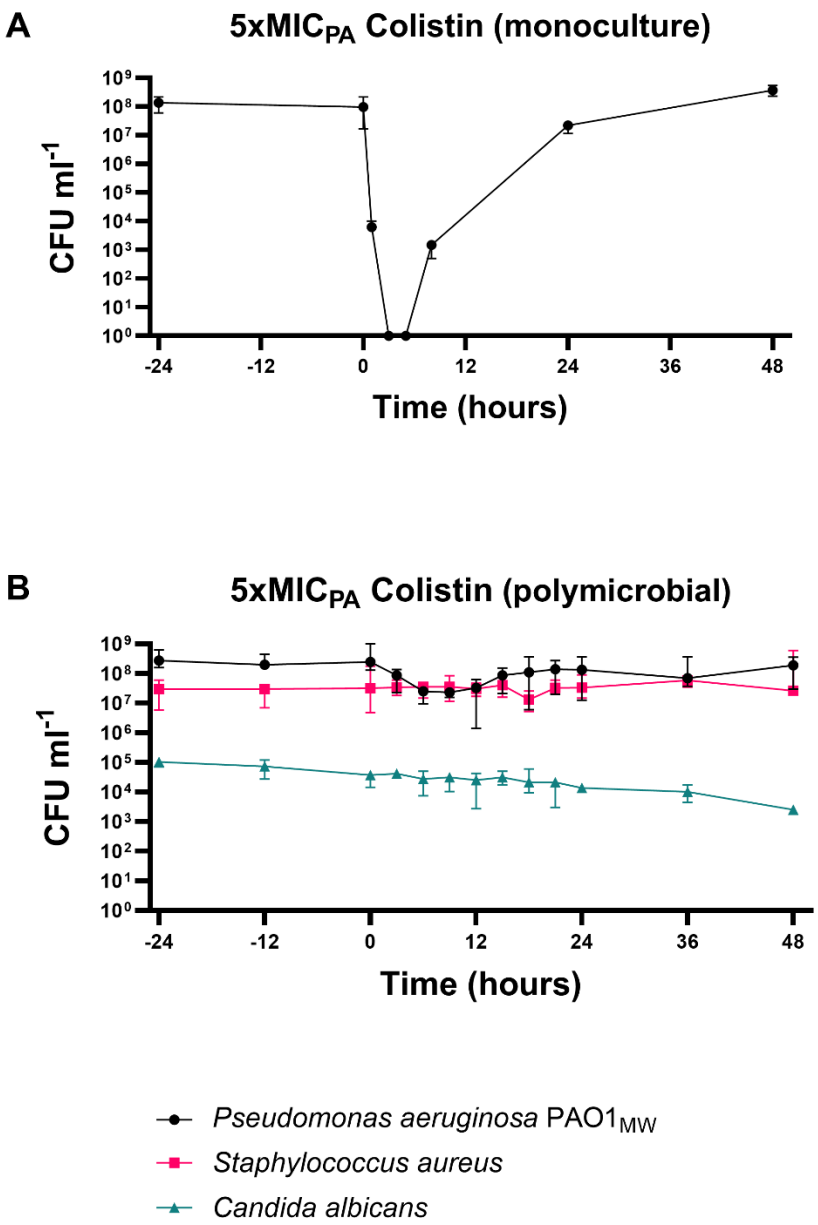

Figure 6.1. **Effect of 5xMIC$_{PA}$ colistin on *Pseudomonas aeruginosa* PAO1$_{MW}$ mono- and polycultures in the continuous-flow system.** CFU mL^{-1} values for *P. aeruginosa* PAO1$_{MW}$ (black circles), *S. aureus* (pink squares), and *C. albicans* (turquoise triangles) are plotted on a $\log_{10}$ scale. Data is presented as the median with a 95% confidence interval across six (A) and four (B) independent experiments. Cultures were grown in ASM with a continuous Q = 145 µL min^{-1} flow rate. Colistin was added at a final concentration of 5xMIC$_{PA}$ after 48 hours of co-culturing, which is indicated as T=0 hours on the graph. Before antibiotic addition, the cultures were stable, with no significant differences between timepoints in cell counts ($p > 0.75$). (A) Colistin significantly reduced the *P. aeruginosa* titre in the monospecies culture ($p < 0.04$). (B) In the polymicrobial environment, *P. aeruginosa* showed a more moderate response, with no significant change in population size ($p > 0.3$). No significant change in *S. aureus* or *C. albicans* titres was observed throughout the sampling period ($p > 0.3$).

The outcomes of the measurements with ciprofloxacin were similar. As before, there was no noticeable difference in CFU mL^{-1} counts during the stable, non-disturbed period, between the -24-hour and 0-hour timepoints ($p > 0.9$).

Ciprofloxacin had a robust impact in monospecies cultures, resulting in a significant 5-log fold decrease in *P. aeruginosa* titres compared with the stable levels before treatment ($p \leq 0.05$), as shown in *Figure 6.2.A*. In polymicrobial cultures, as shown in *Figure 6.2.B*, the community was stable prior to addition of the antibiotic, but upon treatment with ciprofloxacin, the *P. aeruginosa* levels declined slightly (less than 2-log fold), much like with colistin. This change was not statistically significant ($p > 0.15$). No significant changes were observed in *S. aureus* or *C. albicans* titres throughout the sampling period ($p > 0.25$).

To determine whether the observed resistance was phenotypic or genetic, samples were streaked on *P. aeruginosa* isolation plates containing either colistin or ciprofloxacin, as detailed in *Section 3.10.3*. No growth was observed, indicating that the resistance was situational rather than genetically inherited. While this does not rule out the possibility of genetic variations with resistance arising, such mutations did not dominate the population, as they would have been evident through growth on the antibiotic plates.

6.3.2. *Pseudomonas aeruginosa* Δ*lasR* mutant

The observed differences between $PAO1_{MW}$ mono- and polymicrobial cultures prompted me to investigate whether these effects are linked to the *lasR* regulon. I hypothesised that Δ*lasR* mutants may lack key traits needed to provide the same level of protection. Therefore, antibiotics would differentially impact cultures containing *P. aeruginosa* $PAO1_{MW}$ compared with those containing Δ*lasR* mutants. To test this hypothesis, I applied antimicrobial monotherapy to polymicrobial cultures containing the Δ*lasR* mutant.

The outcome was considerably different for *P. aeruginosa* when the polymicrobial culture containing the Δ*lasR* mutant was treated with colistin, as shown in *Figure 6.3.A*. While no noticeable difference in viable cell counts was observed before the antibiotic was added ($p > 0.25$), the *P. aeruginosa* titre rapidly dropped by 8-log fold upon colistin treatment. This decrease was significant up to the 36-hour timepoint compared with pre-antibiotic levels ($p < 0.05$). Although there was a slight increase in the population sizes of *S. aureus* and *C. albicans*, these changes were not statistically significant ($p \geq 0.1$).

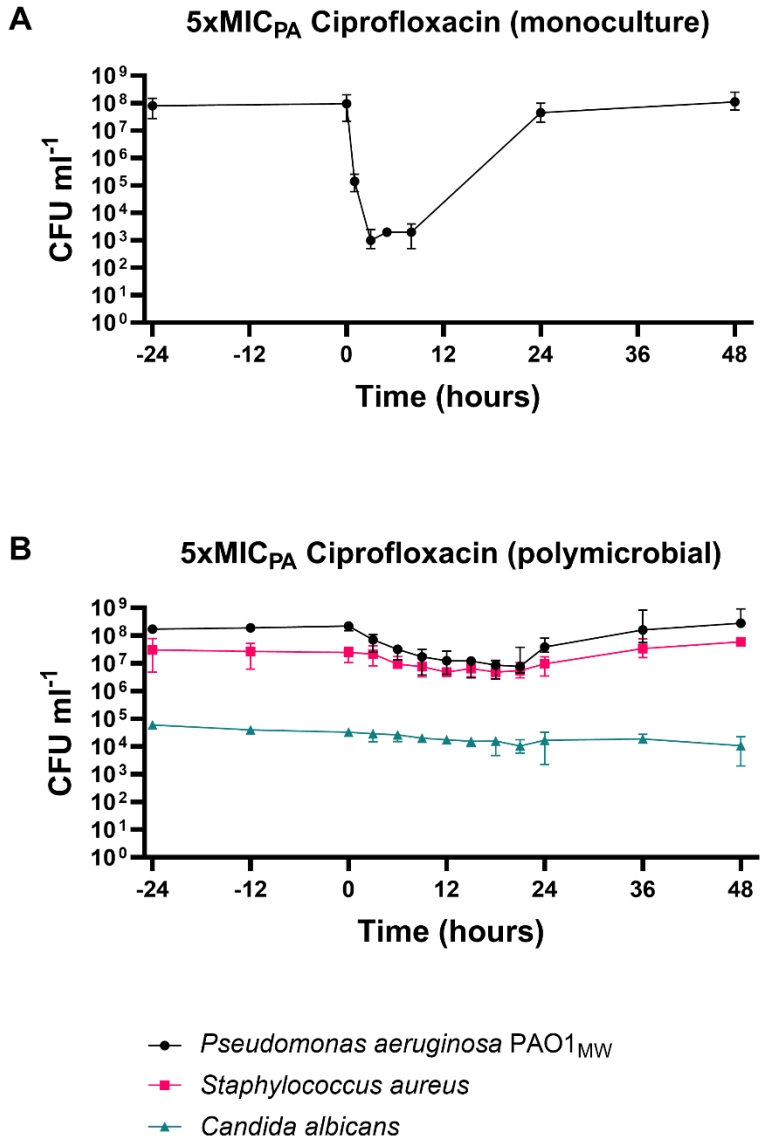

Figure 6.2. **Effect of 5xMIC$_{PA}$ ciprofloxacin on *Pseudomonas aeruginosa* PAO1$_{MW}$ mono- and polycultures in the continuous-flow system.** CFU mL^{-1} values for *P. aeruginosa* PAO1$_{MW}$ (black circles), *S. aureus* (pink squares), and *C. albicans* (turquoise triangles) are plotted on a $\log_{10}$ scale. Data is presented as the median with a 95% confidence interval across six (A) and four (B) independent experiments. Cultures were grown in ASM with a continuous Q = 145 µL min^{-1} flow rate. Ciprofloxacin was added at a final concentration of 5xMIC$_{PA}$ after 48 hours of co-culturing, which is indicated as T=0 hours on the graph. Before antibiotic addition, the cultures were stable, with no significant differences between timepoints in cell counts ($p > 0.9$). (A) Ciprofloxacin significantly reduced the *P. aeruginosa* titter in the monospecies culture ($p \leq 0.05$). (B) In the polymicrobial environment, *P. aeruginosa* showed a more moderate response, with no significant change in population size ($p > 0.15$). No significant change in *S. aureus* or *C. albicans* titres was observed throughout the sampling period ($p > 0.25$).

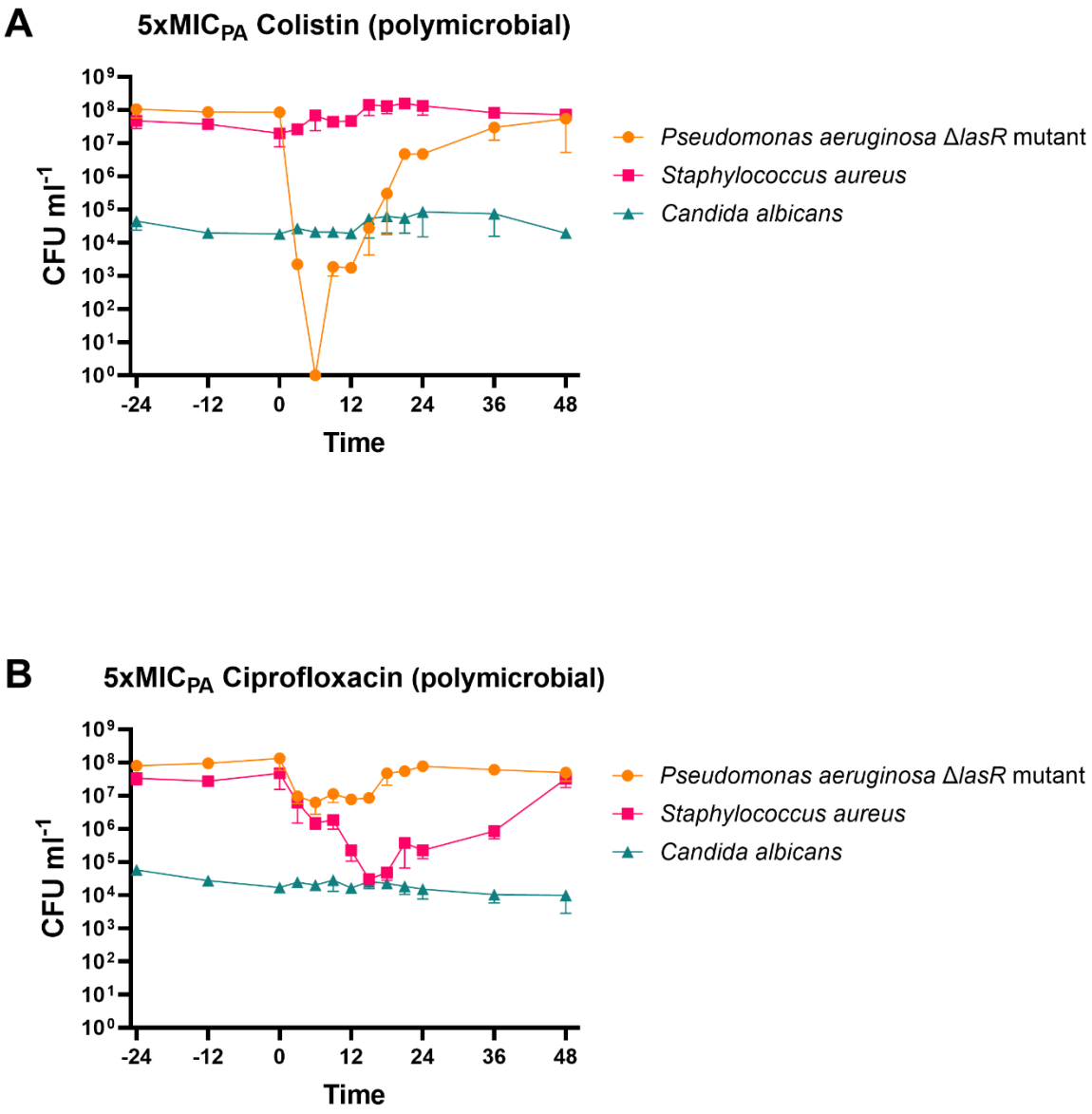

Figure 6.3. **Effect of 5xMIC$_{PA}$ colistin or ciprofloxacin on polycultures with *Pseudomonas aeruginosa* Δ*lasR* mutant in the continuous-flow system.** CFU mL^{-1} values for *P. aeruginosa* Δ*lasR* mutant (orange circles), *S. aureus* (pink squares), and *C. albicans* (turquoise triangles) are plotted on a $\log_{10}$ scale. Data is presented as the median with a 95% confidence interval across three independent experiments. Cultures were grown in ASM with a continuous flow rate of Q = 145 µL min^{-1}. Both antimicrobial compounds were added at a final concentration of 5xMIC$_{PA}$ after 48 hours of co-culturing, indicated as T=0 hours on the graph. Before antibiotic addition, cultures were stable with no significant differences in cell counts between timepoints ($p > 0.25$). (A) Colistin significantly reduced *P. aeruginosa* titres ($p < 0.05$), while *S. aureus* titres showed a slight, non-significant increase during treatment ($p \geq 0.1$). (B) Ciprofloxacin treatment resulted in a more moderate response in *P. aeruginosa*, with no significant change in population size ($p > 0.55$), while *S. aureus* titres exhibited a substantial reduction ($p < 0.04$). No significant changes in *C. albicans* titres were observed throughout the sampling period, though a slight increase was noted during colistin treatment ($p > 0.15$).

When the stable community was treated with ciprofloxacin, the *P. aeruginosa* Δ*lasR* mutant population responded similarly to the $PAO1_{MW}$, with a less than 2-log fold decrease, as shown in *Figure 6.3.B*. This change was moderate but not statistically significant ($p > 0.55$). Intriguingly, a substantial reduction in *S. aureus* titres was observed, significantly different from pre-antibiotics levels ($p < 0.04$). Given that MIC_{SA} measurements indicated a higher required concentration, as detailed in *Table 6.1*, these results suggest that *S. aureus* becomes more susceptible to ciprofloxacin in the presence of the Δ*lasR* mutant and *C. albicans*. No significant change was observed in the size of the *C. albicans* population ($p > 0.15$).

When samples were grown on *P. aeruginosa* isolation plates containing ciprofloxacin, no growth was observed, similar to the $PAO1_{MW}$. This suggests that the resistance is likely phenotypic rather than genetic.

6.4. Combined antibiotic therapy

As outlined in *Section 1.3.2*, combination antibiotic therapy is often preferred over monotherapy in clinical practice. This guided my approach in the continuous-flow system, where a combination of colistin and ciprofloxacin was applied to polymicrobial cultures containing either $PAO1_{MW}$ or Δ*lasR* mutant *P. aeruginosa*. For consistency, the concentrations of both antibiotics were maintained at $5xMIC_{PA}$ throughout the experiments.

6.4.1. Changing community dynamics

First, the combination of antibiotics was applied to polymicrobial cultures containing $PAO1_{MW}$ *P. aeruginosa*, as shown in *Figure 6.4*. The combined treatment had a greater effect on *P. aeruginosa*. It reduced *P. aeruginosa* titres by 4-log fold, with the change remaining statistically significant up to 15 hours post-treatment compared with pre-antibiotic levels ($p \leq 0.04$). *S. aureus* experienced a non-significant decline ($p > 0.07$). Remarkably, *C. albicans* titres began to increase a few hours after the treatment, in line with the recovery pattern of *P. aeruginosa*. The fungal population grew significantly larger than pre-treatment levels ($p < 0.05$). Given the physical size difference between *C. albicans* and the other two species, this increase also represented a substantial rise in biomass. This prompted me to observe the cultures under a microscope and visually compare the effects of monotherapy *versus* combined antibiotic treatment.

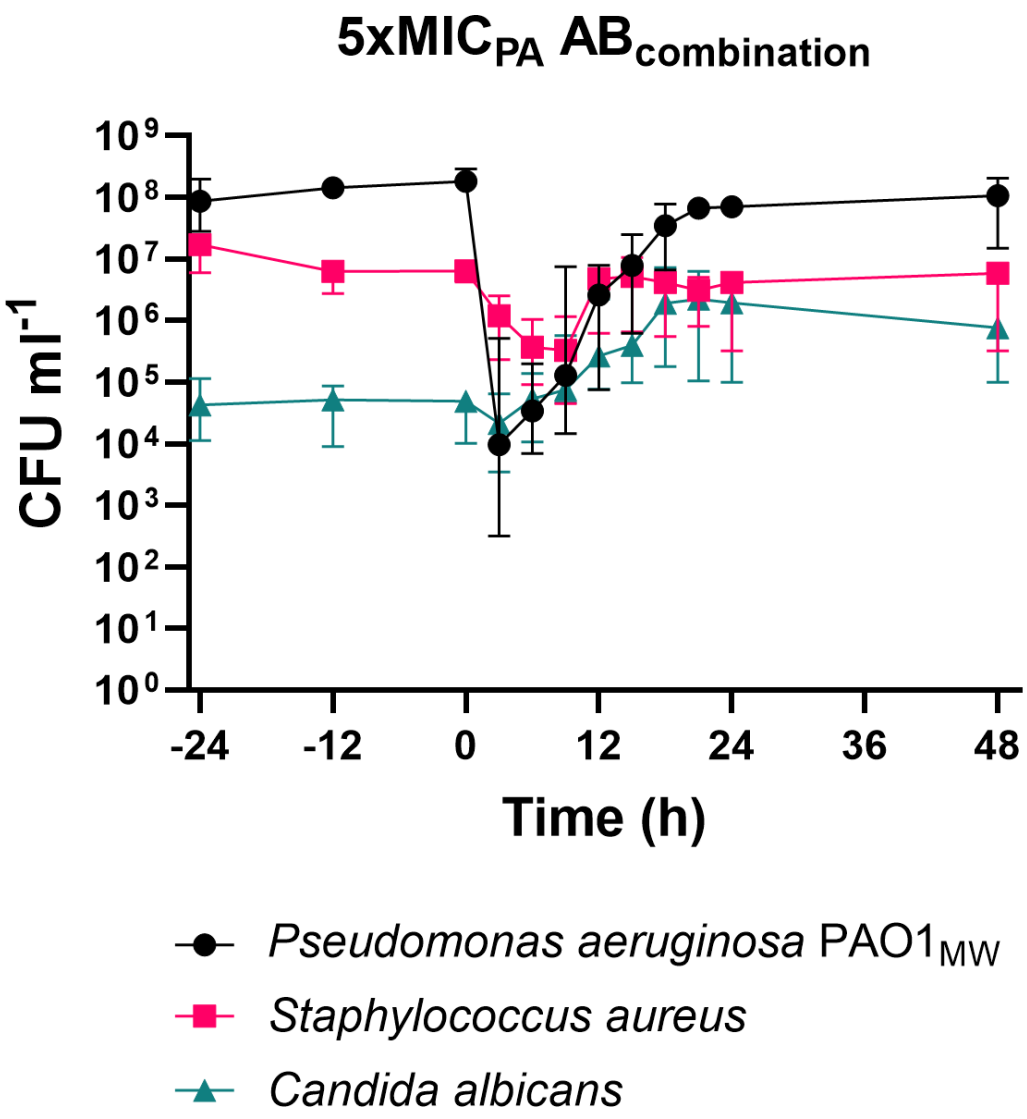

Figure 6.4. **Effect of 5xMIC$_{PA}$ combined antibiotic treatment on polycultures with *Pseudomonas aeruginosa* PAO1$_{MW}$ in the continuous-flow system.** CFU mL^{-1} values for *P. aeruginosa* PAO1$_{MW}$ (black circles), *S. aureus* (pink squares), and *C. albicans* (turquoise triangles) are plotted on a log$_{10}$ scale. Data is presented as the median with a 95% confidence interval across six independent experiments. Cultures were grown in ASM with a continuous flow rate of Q = 145 µL min^{-1}. Both antimicrobial compounds were added simultaneously at a final concentration of 5xMIC$_{PA}$ after 48 hours of co-culturing, indicated as T=0 hours on the graph. Before antibiotic addition, cultures were stable with no significant differences in cell counts between timepoints ($p > 0.2$). Following treatment, *P. aeruginosa* titres were significantly reduced ($p \leq 0.04$), while the *S. aureus* population showed a moderate decline ($p > 0.07$). In contrast, *C. albicans* titres increased substantially, with a statistically significant rise observed between 18- and 24-hours post-treatment compared with pre-treatment levels ($p < 0.05$).

6.4.2. Fungal bloom

C. albicans can transition between three biological forms: yeast, pseudohyphae, and hyphae. In LB overnight cultures, it predominantly appears in the yeast form, even at 37°C, as shown in *Figure 6.5.A*. However, in ASM, due to the presence of GlcNAc, *C. albicans* mainly shifts to the hyphal form, with a smaller proportion of cells in the yeast or pseudohyphae forms, as seen in *Figure 6.5.B*. *P. aeruginosa* in ASM maintains its well-known rod-shaped morphology, whereas spherical *S. aureus* cells form grape-like clusters, as shown in *Figure 6.5.C-D*.

In mixed cultures within the continuous-flow system, *P. aeruginosa* and *S. aureus* dominate in cell numbers, while *C. albicans* predominantly displays hyphal and pseudohyphal forms, as shown in *Figure 6.6*. Importantly, some cell aggregation was seen to occur in the non-perturbed cultures, with free-floating cells surrounding aggregated clusters of cells, as illustrated in *Figure 6.7 A-B*. Following antibiotic treatment, this aggregation was considerably enhanced, leaving few or no free-floating planktonic cells, as shown in *Figure 6.7 C-D*.

The observed increase in aggregation, and potentially in biofilm formation, creates a physical barrier that can hinder the penetration of antibiotics, contributing to the increased resistance observed (Lewis, 2008; Patel, 2005; Secor *et al.*, 2018). These aggregates are typically composed of a few hundred to a few thousand cells, making it challenging to differentiate between living and dead cells. Although LIVE/DEAD staining was attempted on the samples to gain more insight, the method proved ineffective for *P. aeruginosa* due to known staining difficulties, which I also experienced (Lewenza *et al.*, 2018; Stiefel *et al.*, 2015).

The primary finding from the microscopic examination was the notable change in the response of *C. albicans* following combined antimicrobial treatment, as illustrated in *Figure 6.8*. After monotherapy, aggregates mainly consisted of bacterial cells, with only occasional pseudo-hyphal or hyphal *C. albicans* present. Conversely, following combined treatment, hyphal cells became more prominent and present in most visual fields, which corresponded with a rise in CFU titres. Aggregates formed around these filamentous fungal cells, suggesting that they may play a central role in the structural organisation of the mixed-species communities under increased antibiotic stress. Notably, whereas the aggregates began to disassemble ca. 24 hours after monotherapies, those formed in the cultures treated with combined antibiotics remained intact for longer, indicating a more resilient structure.

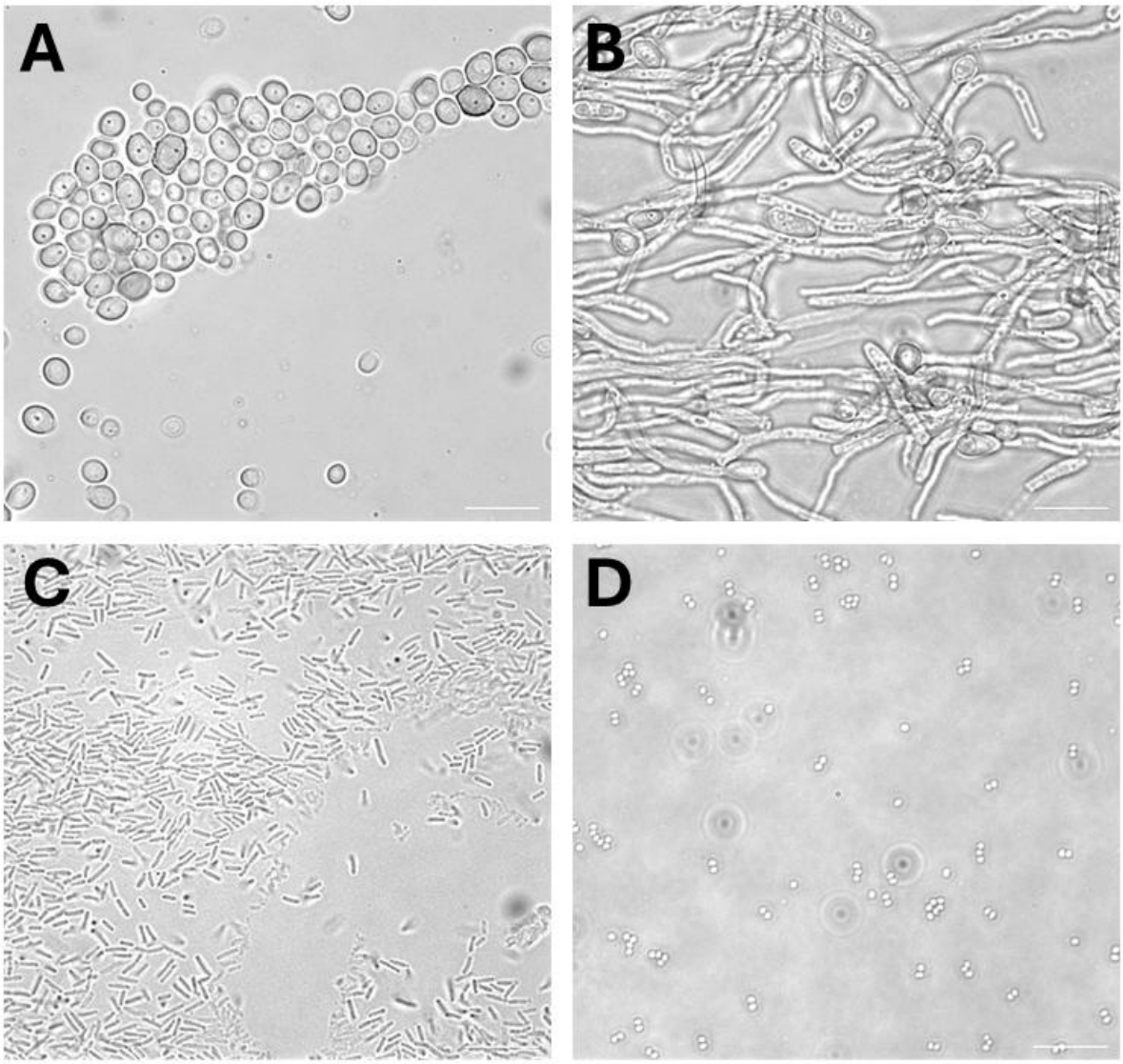

Figure 6.5. **Phase-contrast microscopy images of overnight cultures.** *C. albicans* predominantly exists in yeast form when grown in LB (A), whereas, in ASM, it primarily displays hyphal forms with some yeast cells present (B). *P. aeruginosa* has a rod-shaped morphology (C). *S. aureus* forms spherical cells that cluster in grape-like arrangements (D). Images were taken using an Olympus BX51 microscope equipped with a QICAM Fast 1394 camera. Scale bars represent 10 µm.

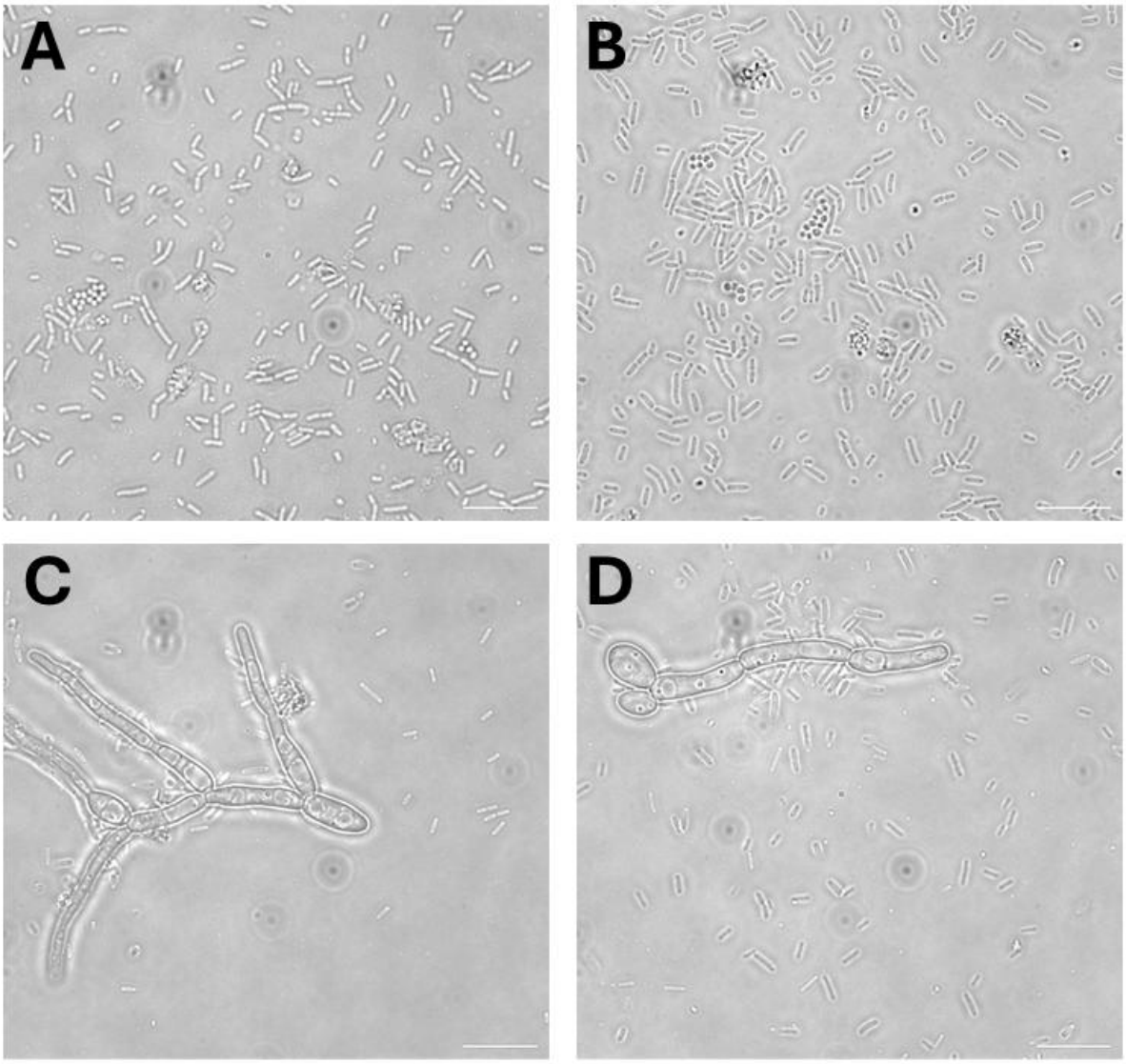

Figure 6.6. **Phase-contrast microscopy images of samples taken during steady-state growth in the *in vitro* continuous-flow system.** Planktonic *P. aeruginosa* and *S. aureus* dominate the cultures, consistent with the viable cell count results (A-B). *C. albicans* predominantly exists in hyphal or pseudohyphal forms (C-D). Images were taken using an Olympus BX51 microscope equipped with a QICAM Fast 1394 camera. Scale bars represent 10 µm.

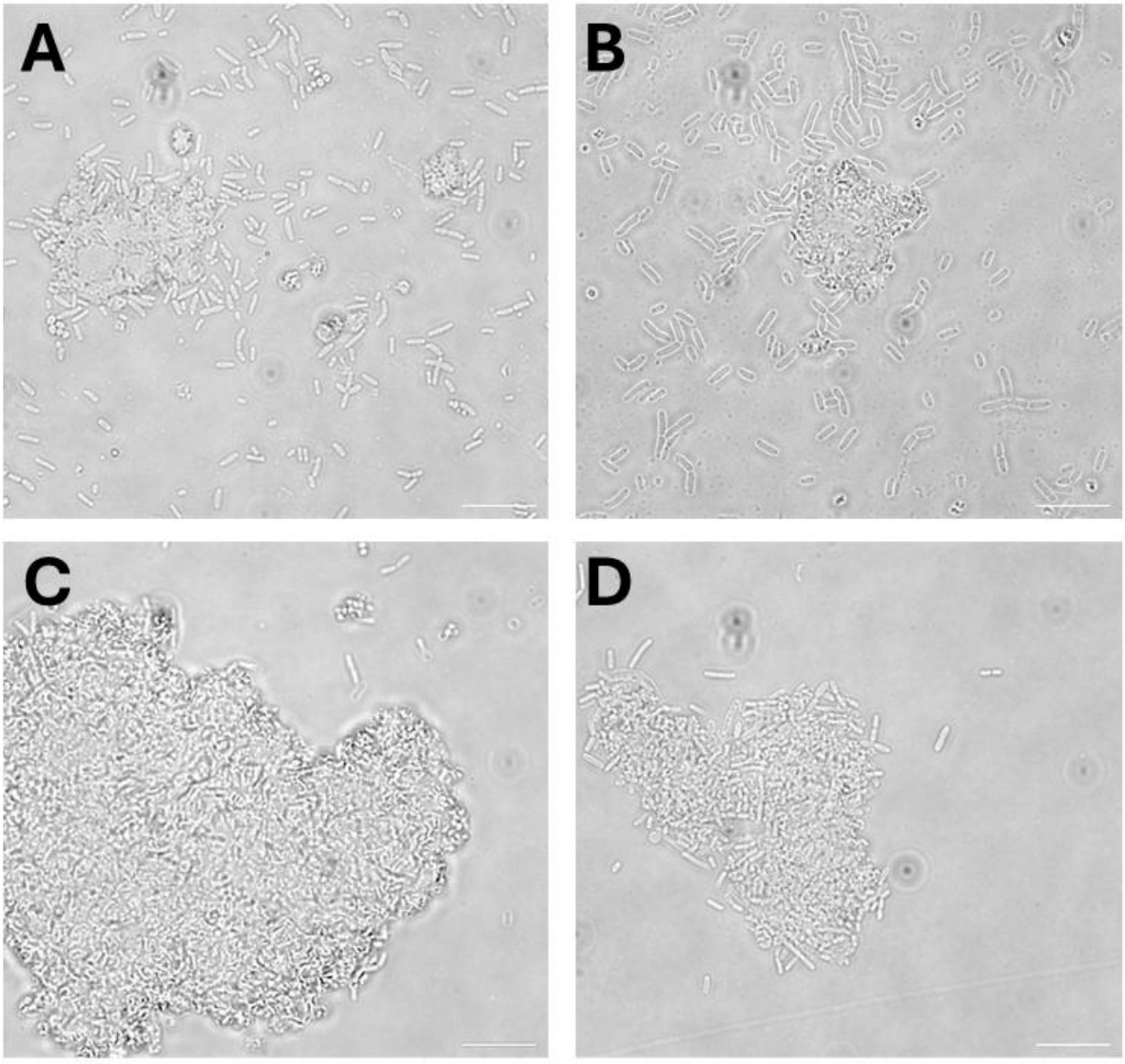

Figure 6.7. **Phase-contrast microscopy images of aggregates formed during steady-state growth in the *in vitro* continuous-flow system.** Aggregate formation was observed in non-antibiotic perturbed cultures, with free-living cells typically surrounding the structures (A-B). Following antibiotic treatment, this aggregation was visibly enhanced, leading to larger aggregates with fewer free-floating cells around them (C-D). Images were taken using an Olympus BX51 microscope equipped with a QICAM Fast 1394 camera. Scale bars represent 10 µm.

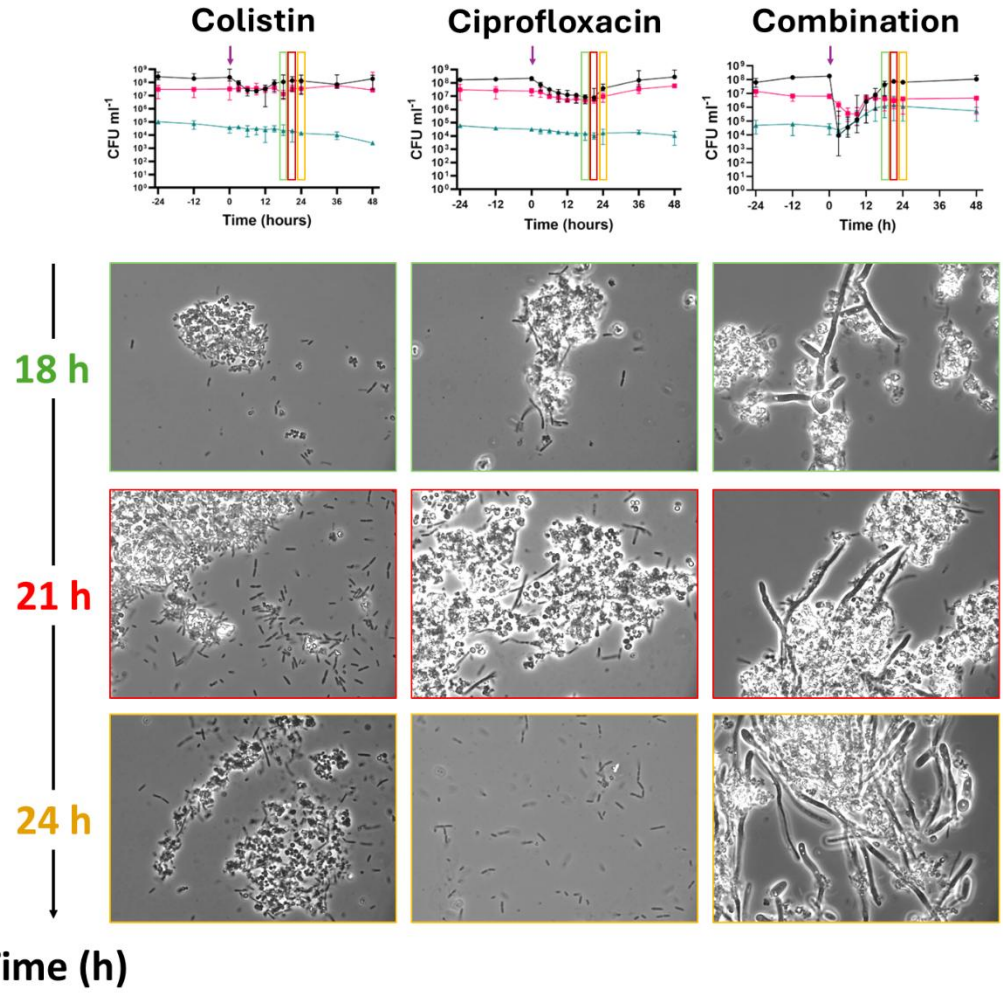

Figure 6.8. **Matrix of phase-contrast microscopy images of polymicrobial cultures following antibiotic treatment**. Images are organised into three columns according to the antibiotics used for treatment, as indicated for each column. The antibiotics were added as the dark pink arrows indicate (T=0). The rows represent different time points post-antibiotic addition, as marked on the graphs: 18 hours (green), 21 hours (red), and 24 hours (yellow), from top to bottom. Aggregation of cells is observed in all treatment scenarios; however, the combined antibiotic treatment induces visible fungal blooming, with hyphae providing additional surface area, as seen in the right column.

From this point forward, the phenomenon of increase in *C. albicans* titre will be referred to as "blooming" in accordance with the terminology used in the literature (Savage *et al.*, 2024).

Two additional cultures were treated with the combined antibiotics to understand the conditions necessary for fungal blooming better. First, a monospecies culture of *C. albicans* was tested to determine whether *C. albicans* alone reacted to the combined antibiotic treatment. Second, a dual-species culture of *P. aeruginosa* $PAO1_{MW}$ and *C. albicans* was used to assess if the blooming phenomenon results from interactions between the two species or if the presence of *S. aureus* is also required.

As shown in *Figure 6.9.A*, *C. albicans* monocultures do not react to antibiotic treatment, and the titres maintain a statistically stable level between 10^5-10^6 CFU mL^{-1} ($p > 0.45$). As noted earlier, these levels are higher than those in the polymicrobial cultures, suggesting that antagonistic mechanisms between the bacteria and fungi may constrain titres (O'Brien, 2021). Taken together, these data indicate that the observed blooming is not due to the fungi reacting to antibiotics; however, it has to be noted that the monoculture titres are the same as the highest levels achieved during fungal blooming in the polymicrobial cultures following combination treatment.

As shown in *Figure 6.9.B*, a more modest, not statistically significant increase of fungal titres was observed in the dual-species culture of *P. aeruginosa* $PAO1_{MW}$ and *C. albicans* from 15-hour timepoint onwards ($p \geq 0.1$). This smaller change may be partially attributable to the slightly higher pre-antibiotic titre for *C. albicans* in this setup. Taken together, these data indicate that the fungal bloom is likely driven by interactions between *P. aeruginosa* and *C. albicans*, but that the presence of *S. aureus* enhances its magnitude. Consequently, the triple-species polymicrobial culture was used for further investigation.

6.4.3. Impact of Δ*lasR* mutants

In previous experiments, *C. albicans* showed less stability when co-cultured with Δ*lasR* mutants compared with cultures involving $PAO1_{MW}$, and the Δ*lasR* mutants demonstrated a distinct response to colistin. Therefore, as the next step, I tested whether the extensive *lasR* regulon might play a role in causing the fungal bloom.

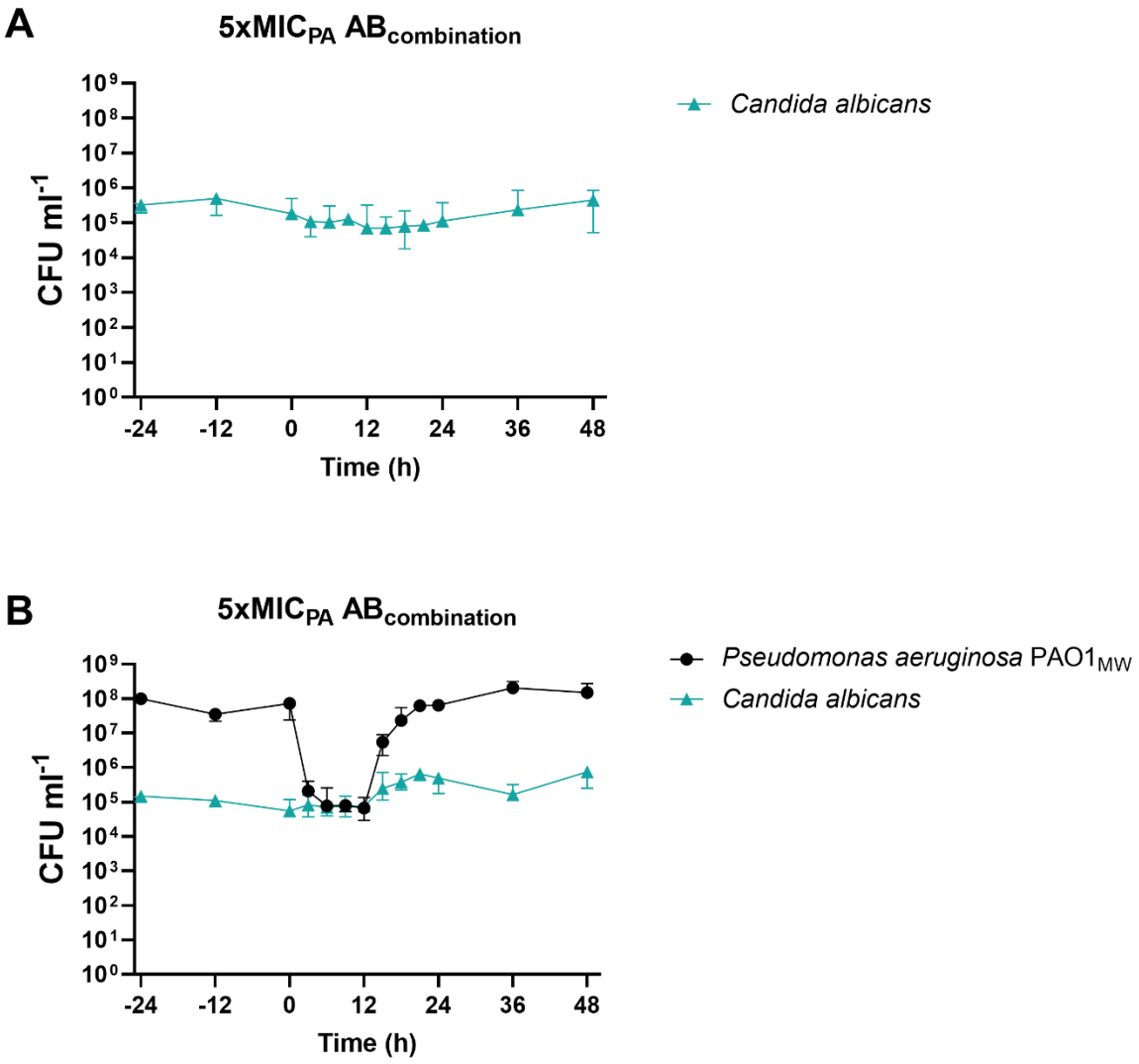

Figure 6.9. **Effect of 5xMIC$_{PA}$ combined antibiotic treatment on *C. albicans* monoculture and dual-species culture with *Pseudomonas aeruginosa* PAO1$_{MW}$ in the continuous-flow system.** CFU mL^{-1} values for *P. aeruginosa* PAO1$_{MW}$ (black circles) and *C. albicans* (turquoise triangles) are plotted on a $\log_{10}$ scale. Data is presented as the median with a 95% confidence interval across three independent experiments. Cultures were grown in ASM with a continuous flow rate of Q = 145 µL min^{-1}. Both antimicrobial compounds were added simultaneously at a final concentration of 5xMIC$_{PA}$ after 48 hours of co-culturing, indicated as T=0 hours on the graph. Before antibiotic treatment, cultures were stable with no significant differences in cell counts between timepoints ($p > 0.3$). (A) Post-treatment, the *C. albicans* population in monoculture remained relatively stable, showing no significant changes ($p > 0.45$). (B) In the co-culture, *P. aeruginosa* titres were significantly reduced, while *C. albicans* titres increased, although this increase was not statistically significant ($p \geq 0.1$).

As shown in *Figure 6.10*, the polymicrobial culture with *P. aeruginosa* Δ*lasR* mutant exhibited a somewhat different response to the combined antibiotic treatment compared with cultures containing the 'wild-type' $PAO1_{MW}$. The *P. aeruginosa* titres initially dropped from stable levels to ca. 10^4 CFU mL^{-1} and, up to 18 hours post-treatment, remained significantly low ($p < 0.05$), similar to what was observed in $PAO1_{MW}$ cultures. However, as titres gradually recovered as the antibiotic was diluted out due to the continuous flow, titres settled out at higher levels than in the pre-treatment condition.

The most notable difference between the polycultures containing the Δ*lasR* mutant compared with cultures containing the $PAO1_{MW}$ was that *S. aureus* titres declined sharply, consistent with the results from polymicrobial Δ*lasR* mutant cultures treated with ciprofloxacin alone ($p < 0.05$). This finding supports the notion that *S. aureus* is more susceptible to ciprofloxacin in the presence of the Δ*lasR* mutant. Notably, in samples taken from co-cultures with *P. aeruginosa* $PAO1_{MW}$, *S. aureus* colonies predominantly appeared as SCVs with extended growth time on isolation plates throughout the project. However, in the presence of the Δ*lasR* mutant, most *S. aureus* colonies were normal, in line with QS mechanisms inducing SCVs, as previously reported (Hotterbeekx *et al.*, 2017). The *C. albicans* titres remained stable throughout the experiment ($p > 0.05$), without the blooming phenomenon observed in the 'wild-type' $PAO1_{MW}$ co-cultures. These results suggest that the absence of *lasR* function alters the polymicrobial dynamics during antibiotic treatment.

6.5. Investigating the background of the blooming phenomenon

Based on the results just outlined, I speculated that a LasR-regulated mechanism might be responsible for the observed fungal bloom following combination antibiotic treatment. I further speculated that this mechanism might involve direct cell-cell contact, given my observations indicating that bacterial cells cluster around the fungal hyphae, allowing for potential contact-based communication. The link to *lasR* was assumed based on the findings in *Section 6.4*, showing intact *lasR* is necessary for this phenomenon to occur.

Given these observations, I hypothesised that the LasR-regulated *tseT* operon, which encodes a contact-dependent T6SS effector, may play a role in regulating the blooming phenomenon. To test this hypothesis, I examined the response of the ΔPA3904-08 mutant in polymicrobial culture to the combined treatment.

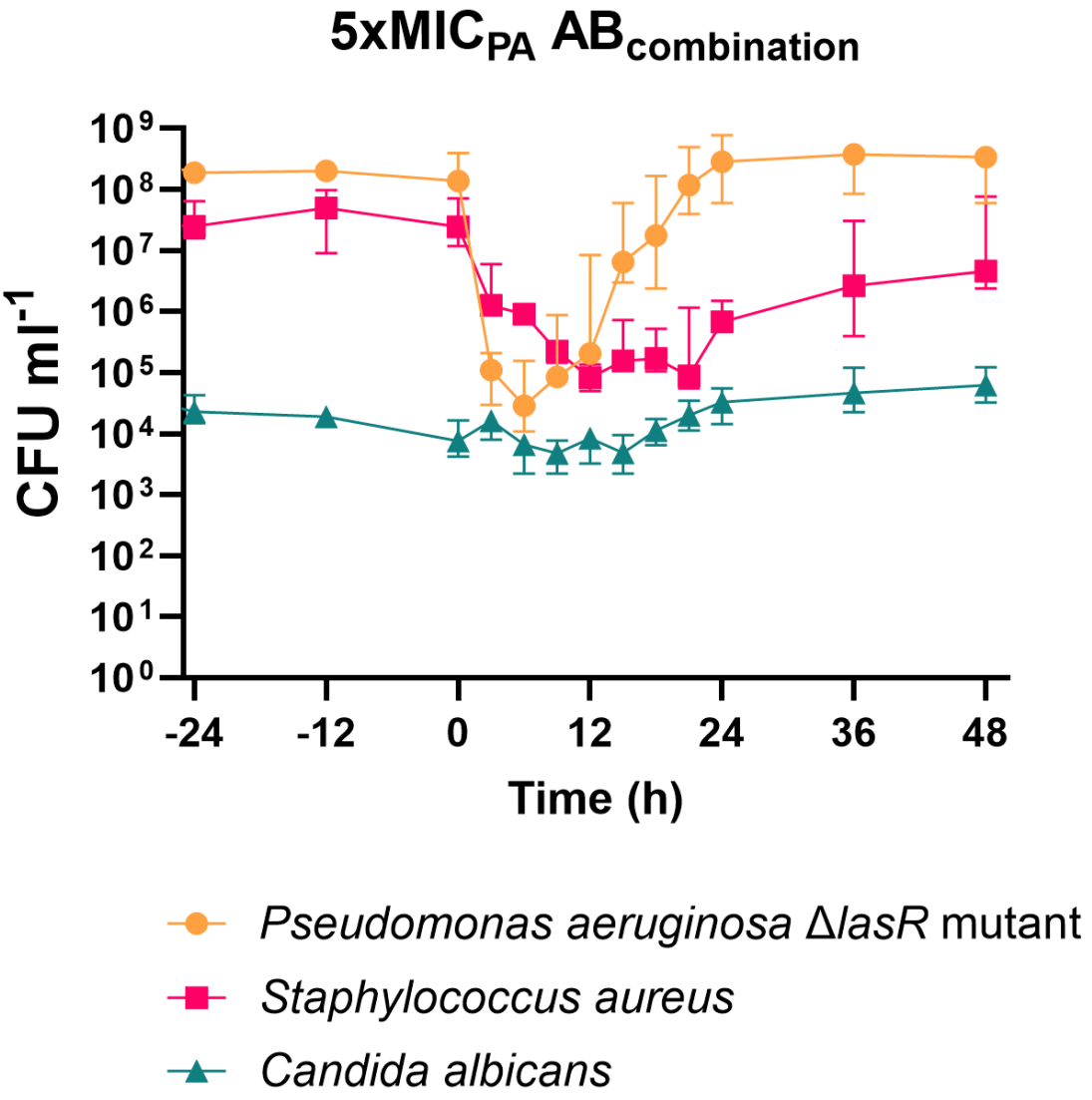

Figure 6.10. **Effect of 5xMIC$_{PA}$ combined antibiotic treatment on polycultures containing *Pseudomonas aeruginosa* Δ*lasR* mutant in the continuous-flow system.** CFU mL^{-1} values for *P. aeruginosa* Δ*lasR* mutant (orange circles), *S. aureus* (pink squares), and *C. albicans* (turquoise triangles) are plotted on a $\log_{10}$ scale. Data is presented as the median with a 95% confidence interval across six independent experiments. Cultures were grown in ASM with a continuous flow rate of Q = 145 µL min^{-1}. Both antimicrobial compounds were added simultaneously at a final concentration of 5xMIC$_{PA}$ after 48 hours of co-culturing, indicated as T=0 hours on the graph. Before antibiotic addition, cultures were stable with no significant differences in cell counts between timepoints ($p > 0.4$). Following treatment, *P. aeruginosa* titres showed a significant reduction ($p < 0.05$) but later recovered to levels higher than the pre-treatment titres. The *S. aureus* population also experienced a sharp decline, though its recovery was only partial ($p < 0.05$). Meanwhile, *C. albicans* titres remained relatively stable throughout the experiment, with no significant fluctuations observed ($p > 0.05$).

6.5.1. Absence of *tseT* operon prevents *Candida* blooming

When the polymicrobial culture containing the ΔPA3904-08 mutant was treated with colistin and ciprofloxacin, the *P. aeruginosa* population responded similarly to both the $PAO1_{MW}$ and Δ*lasR* mutant strains, as shown in *Figure 6.11*. The *P. aeruginosa* titre initially dropped to 10^4 CFU mL^{-1} but subsequently recovered ($p < 0.05$). The *S. aureus* population appeared less stable than when grown in the presence of *P. aeruginosa* $PAO1_{MW}$ even during the pre-antibiotic treatment regime and experienced a considerable decline following antibiotic treatment ($p > 0.05$). Meanwhile, the *C. albicans* titre exhibited minor fluctuations but no significant increase between pre- and post-antibiotic levels ($p > 0.5$). The absence of a fungal bloom in the ΔPA3904-08 mutant polycultures indicates that the *tseT* operon normally plays some functional role in stimulating the bloom.

6.5.2. Verification of results using Δ*lasR*+PA3904-08 mutant

To confirm the involvement of the *tseT* operon in the blooming phenomenon, the Δ*lasR*+PA3904-08 mutant was tested under the same conditions within the polymicrobial culture. As described earlier, this mutant carries the Δ*lasR*::Tc^R mutation and has the entire *tseT* operon inserted into a neutral site in the chromosome under IPTG-inducible regulation. The culture was treated with a pulse of combined antibiotics, and with IPTG continuously supplied at a concentration of 1 mM. I speculated that if the *tseT* operon is indeed responsible for the blooming phenomenon, restoring its expression, even in a *lasR* background, should provoke similar blooming.

As shown in *Figure 6.12*, *P. aeruginosa* exhibited the same significant decrease in titre, slightly below 10^4 CFU mL^{-1} ($p < 0.04$). However, its recovery was somewhat slower than other genetic variants, potentially due to the increased metabolic burden caused by IPTG-induced transcription of the *tseT* operon. There was greater variance between biological replicates during the recovery period. *S. aureus* levels showed a decline, consistent with previous observations in Δ*lasR* backgrounds ($p < 0.04$). Most notably, *C. albicans* titres increased significantly ($p \leq 0.04$), similar to what was observed with the 'wild-type' $PAO1_{MW}$ background, beginning at 15 hours post-treatment. This confirms the involvement of the *tseT* operon in the blooming phenomenon.

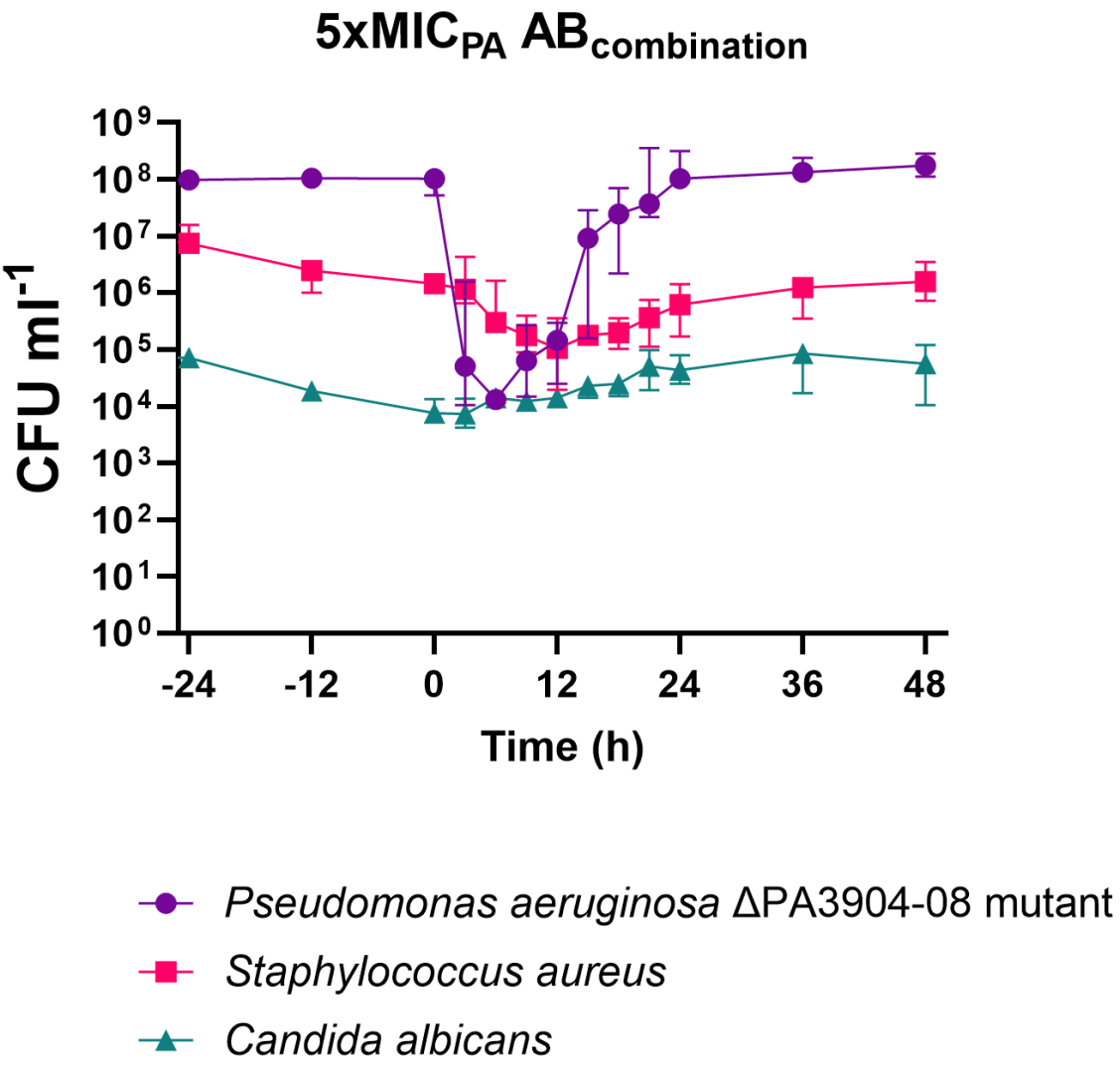

Figure 6.11. **Effect of 5xMIC$_{PA}$ combined antibiotic treatment on polycultures with *Pseudomonas aeruginosa* ΔPA3904-08 mutant in the continuous-flow system.** CFU mL^{-1} values for *P. aeruginosa* ΔPA3904-08 mutant (purple circles), *S. aureus* (pink squares), and *C. albicans* (turquoise triangles) are plotted on a $\log_{10}$ scale. Data is presented as the median with a 95% confidence interval across six independent experiments. Cultures were grown in ASM with a continuous flow rate of Q = 145 µL min^{-1}. Both antimicrobial compounds were added simultaneously at a final concentration of 5xMIC$_{PA}$ after 48 hours of co-culturing, indicated as T=0 hours on the graph. Prior to antibiotic addition, *P. aeruginosa* populations were stable with no significant differences in cell counts between timepoints ($p > 0.5$). Following treatment, *P. aeruginosa* titres were significantly reduced ($p < 0.05$) but later recovered to pre-treatment levels. The *S. aureus* and *C. albicans* titres showed a pre-treatment decline, and while they exhibited some fluctuation after antibiotics were added, these changes were not statistically significant ($p > 0.05$).

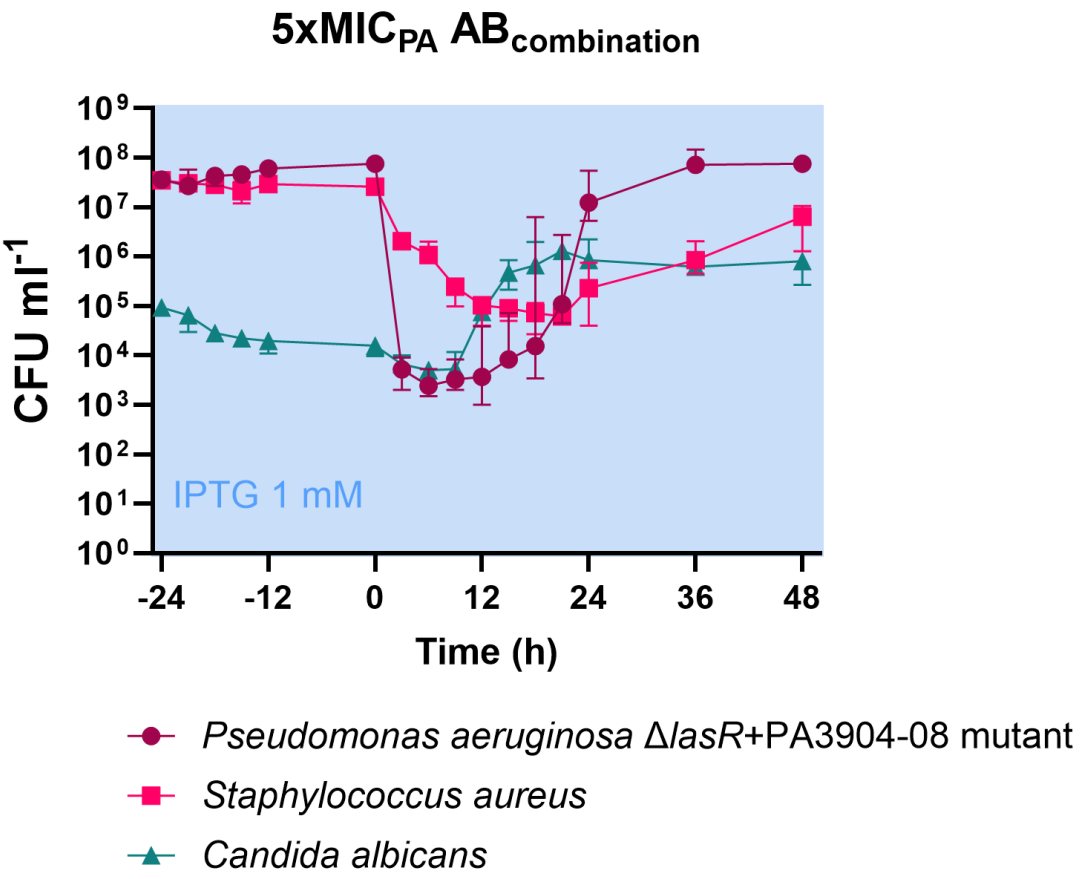

Figure 6.12. **Effect of 5xMIC$_{PA}$ combined antibiotic treatment on polycultures with *Pseudomonas aeruginosa* Δ*lasR*+PA3904-08 mutant in the continuous-flow system.** CFU mL^{-1} values for *P. aeruginosa* Δ*lasR*+PA3904-08 mutant (burgundy circles), *S. aureus* (pink squares), and *C. albicans* (turquoise triangles) are plotted on a $\log_{10}$ scale. Data is presented as the median with a 95% confidence interval across six independent experiments. Cultures were grown in ASM with a continuous flow rate of Q = 145 µL min^{-1}. IPTG was continuously supplied at a final concentration of 1 mM starting at 24 hours of co-culturing, indicated as T=-24 hours on the graph. Both antimicrobial compounds were added simultaneously at a final concentration of 5xMIC$_{PA}$ after 48 hours of co-culturing, indicated as T=0 hours on the graph. Before antibiotic addition, *P. aeruginosa* and *S. aureus* titres were stable, with no significant differences in cell counts between timepoints ($p > 0.1$). *C. albicans* titres fluctuated slightly after IPTG addition but stabilised 12 hours prior to antibiotic treatment ($p > 0.1$). Following treatment, *P. aeruginosa* titres were significantly reduced, with a slow but complete recovery ($p < 0.04$). *S. aureus* showed a sharp decline with only partial recovery ($p < 0.04$). *C. albicans* titres increased substantially, showing a statistically significant rise from 15 hours post-treatment onwards, compared with pre-treatment levels ($p \leq 0.04$).

6.6. Discussion

Alexander Fleming's discovery of penicillin and the subsequent introduction of antibiotics are among the most groundbreaking advancements in medical history. However, the growing prevalence of treatment failures is now a major concern in the fight against infections. Multiple factors contribute to this problem, including the rise of antibiotic resistance and uncertainty surrounding optimal treatment protocols. A crucial yet often overlooked factor of this is the presence of non-pathogenic microbes that, while not directly responsible for infections, can alter the efficacy of antibiotics. Investigating these complex microbial interactions has historically been challenging, but recent research is beginning to unravel how microbes influence one another during antibiotic treatments.

Many studies have reported that the presence of cohabiting microbial species can significantly alter antimicrobial susceptibility (Bottery *et al.*, 2022; Mitra *et al.*, 2022). For instance, *P. aeruginosa* and *S. aureus* co-cultures have shown increased tolerance to various antibiotics, including tobramycin, rifamycin, vancomycin, penicillin, cycloserine, gentamicin, and tetracycline (Beaudoin *et al.*, 2017; DeLeon *et al.*, 2014; Hoffman *et al.*, 2006; Lebrun *et al.*, 1978; Orazi & O'Toole, 2017). Conversely, *P. aeruginosa* has been reported to increase the sensitivity of *S. aureus* to antimicrobials, like chloroxylenol (Orazi *et al.*, 2019). In another pairing, *S. aureus* and *C. albicans* co-cultures have been associated with extended biofilm formation and exhibit increased tolerance to oxacillin, vancomycin, ciprofloxacin, delafloxacin, and rifampicin compared with *S. aureus* monocultures (Harriott & Noverr, 2009; Little *et al.*, 2021; Nabb *et al.*, 2019).

The aim of this part of my project was to deepen our understanding of polymicrobial behaviour in response to antibiotic treatment, explicitly focusing on the effects of genetic variation and combined antibiotic therapies. To the best of my knowledge, the latter aspect has not been previously explored, especially under continuous-flow conditions. Building on earlier work conducted in the host laboratory, the focus was on using colistin and ciprofloxacin on the triple-species model (O'Brien *et al.*, 2022).

The results of the experiments supported my third hypothesis, stating that *P. aeruginosa* will exhibit reduced susceptibility to ciprofloxacin in the presence of co-habiting species. I demonstrated that the triple-species polymicrobial culture provided protection for *P.*

aeruginosa against not only colistin but also ciprofloxacin. Interestingly, this protective effect extended to the Δ*lasR* mutant for ciprofloxacin but not for colistin. Given that the MICs were identical for both strains, this suggests that inter-species interactions influence antimicrobial susceptibility differently, depending on the genetic variants involved. It has been previously suggested that current MIC measurements may fall short in capturing the true antimicrobial susceptibility profile, partly because they do not account for the polymicrobial or polyclonal nature of infections (Little *et al.*, 2021; Syal *et al.*, 2017). My findings strongly support this view, as they underscore the complexity of microbial interactions in shaping antibiotic efficacy. However, developing and implementing a more accurate alternative poses significant challenges. Future research should aim to improve antimicrobial susceptibility testing by incorporating the effects of polymicrobial and polyclonal infections. This could involve adapting current MIC measurements or developing new models, such as continuous-flow systems, to reflect better the complex dynamics observed in clinical settings. Such advancements would provide a more realistic understanding of antimicrobial efficacy and resistance, leading to more effective and potentially personalised treatment strategies.

One phenomenon likely contributing to the observed resistance is the formation of microbial aggregates. Such formations, exhibiting diverse structures and sizes, have been shown to demonstrate enhanced resistance to antibiotics (Secor *et al.*, 2018). This effect is particularly significant when aggregation coincides with increased biofilm production (Lewis, 2008; Patel, 2005). Further testing of the project samples on antibiotic plates revealed that the observed resistance is phenotypic rather than genetic, strengthening the idea that aggregation and physical barriers play a critical role in antibiotic resistance. However, the differing outcomes between 'wild-type' $PAO1_{MW}$ and Δ*lasR* mutant strains suggest that these protective mechanisms may be activated through distinct pathways. The precise mechanisms driving the increased antimicrobial resistance in polymicrobial cultures remain unclear and warrant further investigation, which falls outside the scope of this project.

Another intriguing finding from my work was the observation that *S. aureus* became more sensitive to ciprofloxacin in the polymicrobial environment containing the Δ*lasR* mutant compared with polycultures containing the $PAO1_{MW}$ or monospecies cultures. Although I did not directly explore the molecular mechanism behind this, a plausible explanation can be drawn from existing literature. Several studies, along with my observations, have shown that

P. aeruginosa $PAO1_{MW}$ induces the formation of *S. aureus* SCVs, whereas Δ*lasR* mutants do not stimulate SCV formation (Hoffman *et al.*, 2006; Wolter *et al.*, 2013). SCVs are known to be more resistant to various stressors, including antibiotics (Loss *et al.*, 2019; Melter & Radojevič, 2010). I suggest that this resistance provided by the 'wild-type' $PAO1_{MW}$ extends to ciprofloxacin. Conversely, in co-cultures with Δ*lasR* mutants, where SCVs are either absent or present in only small proportions, *S. aureus* becomes more susceptible to ciprofloxacin. From an ecological perspective, it can be speculated that in situations when Δ*lasR* mutants potentially dominate the CF lung, *S. aureus* receives less protection, resulting in reduced microbial diversity following treatment with ciprofloxacin or other broad-spectrum antibiotics.

In line with clinical outcomes, the combined anti-pseudomonal treatment was significantly more effective against *P. aeruginosa*, even in polymicrobial cultures. However, the dynamics of the polymicrobial community shifted compared with monotherapy in the $PAO1_{MW}$. Intriguingly, a marked increase in *C. albicans* titres was observed. A similar phenomenon, often referred to as "fungal blooming," has been documented in clinical cases following antibiotic treatment (Sidransky & Pearl, 1961; Spatz *et al.*, 2023). Traditionally, this increase in fungal population has been attributed to the availability of space and resources following bacterial death. However, recent studies suggest that antibiotics can also impair the antifungal immune response, particularly in the gut, leading to fungal infections (Drummond *et al.*, 2022). Based on the findings of this study, I propose that there may also be direct microbial interactions contributing to the increase in fungal population size following antibiotic treatment. This conclusion is supported by further investigation into the mechanisms behind the blooming phenomenon.

It was hypothesised in this work that the loss of LasR function alters polymicrobial community dynamics. Evidence for that was demonstrated during combined antibiotic treatment, where *C. albicans* did not exhibit blooming in polymicrobial cultures containing the Δ*lasR* mutant, unlike in cultures containing the 'wild-type' $PAO1_{MW}$ progenitor. Based on these experimental outcomes, I propose that *lasR* is a keystone gene for *P. aeruginosa* in polymicrobial interactions.

It was further hypothesised that a contact-based mechanism drives this fungal blooming phenomenon, with the LasR-regulated *tseT* operon being a strong candidate for direct

mechanistic involvement. Moreover, it has been previously shown that *P. aeruginosa* expresses TseT in response to increased iron, which becomes available during the massive cell death of *P. aeruginosa* following combined antibiotic treatment (Ganne *et al.*, 2017; Haas *et al.*, 2023; Moreno-Fenoll *et al.*, 2024). The idea was tested using ΔPA3904-08 and Δ*lasR*+PA3904-08 mutants, and the results supported the hypothesis. Based on the outcomes, the *tseT* operon appears to drive *C. albicans* blooming in the triple-species culture of *P. aeruginosa*, *S. aureus*, and *C. albicans*. However, it is likely that additional mechanisms are also involved in this process.

Like other parts of this work, this segment has several limitations to consider when interpreting the outcomes. Firstly, the sample size was limited to 3 to 6 biological replicates per scenario. While these results provide valuable insights, additional repeats would enhance their statistical power. Secondly, the use of laboratory strains rather than clinical isolates may affect the clinical relevance of the results. Although these strains were selected for comparability with previous studies, further validation with clinical isolates is necessary to confirm the broader applicability of the outcomes. Another limitation lies in the duration of the experiments. Though 96 hours is a reasonable timeframe from a laboratory perspective, it may not fully capture the long-term effects seen in clinical infections. Alongside this, the labour-intensive nature of the 24-hour sampling schedule restricted the project to a single round of antibiotic treatment rather than allowing for a repeated regime that better reflects clinical practice. Finally, although IPTG should not theoretically affect any of the species used, its potential impact *per se* on the polymicrobial system cannot be entirely dismissed.

Overall, I believe this work provides valuable insights into polymicrobial interactions, particularly in the context of antibiotic treatment. Naturally, further research is needed to determine whether these findings extend to other isolates and antimicrobial compounds. Additionally, exploring repeated dosing regimens and alternative antibiotic combinations, such as incorporating antifungal treatments, could provide valuable insights into how polymicrobial systems respond to antimicrobial therapies. Furthermore, the role of the host environment in shaping these interactions remains a critical factor. Future investigations should focus on this aspect to better understand how complex microbial communities behave in real-world infection scenarios.

Chapter 7

Final conclusion

The microbial world is full of intricate interactions. In many ways, microbial communities mirror human societies, where communication and a spectrum of relationships – from cooperation to competition – govern dynamics (Al-Wrafy *et al.*, 2023). Much like human interactions, microbes can adapt their behaviour based on who else is present in the environment. A population may exhibit a particular pattern of behaviour when surrounded by 'kin', but that behaviour can shift significantly when other species or strains appear. This complexity adds layers to infection scenarios, especially those where multiple species coexist, influencing disease and treatment outcomes (Fourie *et al.*, 2017; Fourie *et al.*, 2016). Such dynamics are especially prominent in chronic CF lung infections, where a variety of microbial species co-habit in the same niche and interact with one another (Briaud *et al.*, 2019; Limoli *et al.*, 2017).

Techniques and approaches for studying polymicrobial scenarios are constantly advancing, expanding our understanding of these complex microbial communities (Bényei *et al.*, 2024). However, many mysteries remain, particularly regarding how microbes influence one another, how their biological processes differ in polymicrobial settings compared with monospecies scenarios, and how they respond to external challenges such as antimicrobial treatments. Additionally, adaptation to specific surroundings can result in widespread genomic diversity (Chung *et al.*, 2012; Lei Yang *et al.*, 2011). Thus, beyond the polymicrobial nature of infections, the polyclonal aspect also becomes crucial, adding another layer of complexity to understanding these environments.

7.1. *lasR* is a keystone gene for *P. aeruginosa*

Over the past three decades, research on *lasR* has significantly expanded our understanding of its role in *P. aeruginosa* biology. It is well-established as a master regulator of QS, and over 300 genes belong to the *lasR* regulon (Balasubramanian *et al.*, 2013; Gambello & Iglewski, 1991; Gilbert *et al.*, 2009; Pesci *et al.*, 1997). Interestingly, loss-of-function *lasR* mutations are frequently identified in clinical isolates, particularly in chronic infections of pwCF (Chen *et al.*, 2019; Cruz *et al.*, 2020; Feltner *et al.*, 2016; Kostylev *et al.*, 2019; Marvig *et al.*, 2015; Smith *et*

al., 2006; Zhao *et al.*, 2023). Several studies have shown that such mutations play a role in adaptation to the CF lung environment and are associated with worsened disease prognosis (Harrison *et al.*, 2014; Hoffman *et al.*, 2009; LaFayette *et al.*, 2015). However, despite this wealth of knowledge, significant gaps remain – for example in understanding how the loss of LasR function affects *P. aeruginosa* and other species in polymicrobial communities.

Much of the current work has centred around my thesis that the loss of LasR function reshapes inter-species interactions in a polymicrobial CF airway model, especially following antibiotic challenge. I investigated the behaviour of two genetic variants of *P. aeruginosa* – the 'wild-type' $PAO1_{MW}$ and a Δ*lasR* mutant – across various conditions, focusing on polymicrobial interactions, polyclonal dynamics, and the impact of antibiotic treatment.

In the first part of my study, I compared the population sizes and transcriptional profiles of *P. aeruginosa* $PAO1_{MW}$ and the Δ*lasR* mutant in both mono- and polymicrobial cultures. I observed that the overall population abundance of *P. aeruginosa* remained remarkably stable, irrespective of whether *lasR* was functional. However, the Δ*lasR* mutant displayed extensive transcriptional changes (presumably, in an effort to maintain this stability), whereas the 'wild-type' $PAO1_{MW}$ needed far fewer adjustments when transitioning from a monospecies to polymicrobial environment. These findings suggested that a functional LasR plays a crucial role in maintaining dominance in competitive environments. Without a functioning LasR protein, mutants must use alternative strategies to adapt and sustain their population levels similar to that of the 'WT' in polymicrobial cultures. Interestingly, several differentially regulated genes are currently uncharacterised, offering further avenues for exploring novel biological mechanisms.

In the second part of this project, I examined intra-species dynamics in both monospecies and polymicrobial cultures. I specifically investigated my hypothesis that in mixed populations of $PAO1_{MW}$ and a Δ*lasR* mutant, $PAO1_{MW}$ would use a LasR-regulated T6SS effector (TseT) to limit the growth of the Δ*lasR* mutant. Although the results ruled out a key role for the *tseT* operon in constraining Δ*lasR* mutants, several noteworthy findings emerged. First, $PAO1_{MW}$ does encode mechanisms that effectively restrict the Δ*lasR* mutant titres in the population, since these consistently remained around 10% (*cf*. the 'WT'), in spite of the nutrient-replete growth conditions. Second, my findings suggest that the *tseT* operon might still play a role in inter-species interactions, either directly or indirectly.

In the final part of this work, I focused on understanding how antibiotics impact monospecies and polymicrobial communities, where each culture contained either $PAO1_{MW}$ or a Δ*lasR* mutant of *P. aeruginosa*. Intriguingly, the presence of neighbouring species provided protection for $PAO1_{MW}$ against anti-pseudomonal drugs, colistin and ciprofloxacin. However, antibiotics had distinct effects on cultures containing the Δ*lasR* mutant, which benefited from protection only against ciprofloxacin but not colistin. Notably, *S. aureus* exhibited increased sensitivity to ciprofloxacin in polymicrobial cultures with the Δ*lasR* mutant, compared with polymicrobial cultures containing $PAO1_{MW}$ or with *S. aureus* monocultures. These findings suggest that the presence or absence of LasR function reshapes the effectiveness of antibiotics in polymicrobial cultures. The study was further extended to examine combined treatment with both antibiotics. This combined treatment was more effective against *P. aeruginosa* but unexpectedly, led to a bloom of *C. albicans* in polymicrobial cultures with $PAO1_{MW}$. However, this fungal bloom was not observed when the 'WT' was replaced with a Δ*lasR* mutant. Further investigation revealed that the fungal bloom was influenced by proteins encoded by the *P. aeruginosa tseT* operon, which is under LasR regulation.

Altogether, the results presented in this work support my thesis that the loss of LasR function reshapes inter-species interactions in a polymicrobial CF airway model, particularly following antibiotic challenge. This illustrates how a single gene can disproportionately influence polymicrobial interactions – it seems that *lasR* is indeed a "keystone gene." This notion originates from the ecological term "keystone species", which was first introduced in the late 1960s by zoologist Robert Paine. He described such species as pivotal in shaping their entire ecosystem and maintaining its structure (Paine, 1966; Paine, 1969). His work on the starfish *Pisaster ochraceus* demonstrated that "keystone species" play a crucial role in influencing the diversity and characteristics of species within their communities (Montefalcone *et al.*, 2011). Building on this idea, and more recently, Barbour and colleagues introduced the concept of a "keystone gene," where changes in just one gene of one species can significantly alter the dynamics of the broader ecosystem, as they showed in *Arabidopsis thaliana* (Barbour *et al.*, 2022).

In line with these concepts, I propose that *lasR* is an ecological "keystone gene" in cystic fibrosis-associated polymicrobial airway infections.

7.2. Limitations of the project

As with any scientific investigation, this project has several limitations to consider when interpreting the results. Given specific limitations for individual experiments were discussed in detail in *Chapters 4-6*, whereas this section addresses broader constraints and methodological decisions that have shaped the project.

As mentioned in *Chapter 1*, O'Toole and colleagues noted that "all models are wrong, but some can be useful" (O'Toole *et al.*, 2021). This statement holds particular relevance for the *in vitro* continuous-flow system used in this study (O'Brien & Welch, 2019). This model was chosen specifically for its remarkable reproducibility and its ability to maintain polymicrobial cultures in a steady state, making it well-suited for studying microbial interactions. However, it is essential to acknowledge that, as an *in vitro* system, it inherently lacks host factors that can significantly influence inter-species dynamics (Baishya *et al.*, 2021).

The growth medium used in this study, ASM, also posed several challenges. Firstly, preparing the large volumes required for the project was both time-consuming and labour-intensive. Secondly, variations in ASM formulations have been shown to cause significant differences in secondary metabolite production, which may influence experimental results (Neve *et al.*, 2021). Furthermore, the extended stability associated with the setup offers the possibility that spontaneous mutations might also arise during the course of the experiments, potentially affecting outcomes (D'Argenio *et al.*, 2007). These factors might introduce variability that could impact the interpretation of the findings.

This study used both monospecies and polymicrobial cultures, with the latter consisting of three species: *P. aeruginosa*, *S. aureus*, and *C. albicans*. Conducting triple-species experiments presented challenges, particularly due to the lack of optimised methods for processing such complex samples. Nonetheless, this experimental design served as a valuable foundation for exploring microbial interactions within a controlled environment. However, expanding the number of species in future experiments could provide a broader understanding of dynamics within the CF lung microbiome. Work towards this outcome is currently ongoing in the team.

Each microbe used in this study was a well-characterised, domesticated laboratory 'WT' or a genetic variant of such strains. This approach aligns with standard laboratory research practices and ensures better reproducibility as well as easier maintenance. However, clinical

isolates could reflect better the microbial behaviour of real-world infections. Therefore, further experiments involving clinical isolates will be necessary to assess whether the findings from this study are applicable to clinical contexts. Again, efforts in this regard are ongoing in the lab.

It is also important to recognise that the experimental setup and sampling methods did not capture the spatial organisation and unique characteristics of sub-populations within the cultures. Additionally, although sampling was carried out with reasonable frequency, interesting details could have been missed due to the limited temporal resolution of sampling.

Moreover, as with most experimental studies, the number of biological replicates was limited to just 3-6 per time point examined. Such constraints are typical due to finite time and resources but can potentially lead to biologically significant processes not reaching statistical significance. Therefore, careful consideration was given to balancing conservative statistical thresholds with biological relevance to ensure robust and meaningful insights.

7.3. Future directions

This study emphasised the importance of investigating polymicrobial and polyclonal scenarios, as they can alter antibiotic efficacy and reshape microbial behaviour. However, beyond this work, numerous interactions remain to be explored, and many questions are yet to be answered.

Future research using the *in vitro* continuous-flow system should expand beyond laboratory strains by incorporating clinical isolates, which may reveal additional interactions and novel mechanisms. Moreover, exploring a broader range of antibiotics could offer deeper insights into how neighbouring microbes confer protection. Repeated antibiotic dosing would be particularly valuable in assessing the durability of the observed protection and the impact of reshaped microbial dynamics. Such advancements could ultimately help refine antibiotic dosing strategies in clinical settings.

Additionally, introducing more microbial species into this or other experimental platforms is crucial for accurately representing the CF lung. However, a step-by-step approach is recommended to carefully delineate the specific outcomes of polymicrobial interactions and their impact on microbial dynamics. Methods such as microfluidics or single-cell approaches

could also further enhance our understanding by providing insights into microbial subpopulations, their spatial organisation, and the distinct lifestyles of planktonic and biofilm-associated cells within polymicrobial setups.

Further research into the influence of growth media and the impact of environmental changes on microbial behaviour is essential. Ongoing work in the host laboratory is exploring microbial evolution in ASM, focusing on mutations that arise in this nutrient-rich environment. Additionally, with the introduction of CFTR modulators, there may be a need for new ASM formulations that more accurately reflect the lung environment of CF patients receiving these treatments. Moreover, limited knowledge exists regarding the impact of other common clinical mutants, such as auxotrophs and hypermutators, as well as physiological factors like sex hormones. These are important areas for future exploration.

Computational modelling also offers a promising avenue for advancing our understanding of inter-species interactions. For instance, current research in the host laboratory employs Lokta-Volterra-based ecological models to analyse microbial behaviour, yielding valuable insights into microbial dynamics and relationships. Such models can complement experimental work by simulating complex interactions, predicting outcomes in different environmental conditions and guiding future experimental designs.

By integrating these efforts, we are advancing towards a more profound understanding of microbial behaviour in polymicrobial environments. In the future, along with enhanced sampling techniques and clinical advancements, such progress could lead to the development of "personalised infection models" using direct inoculation from sputum or BAL samples. Such models can potentially revolutionise the treatment of complex infections by enabling therapies tailored to the unique dynamics of the actual polymicrobial communities.

References

Abdillah, A., & Ranque, S. (2021). Chronic Diseases Associated with Malassezia Yeast. *Journal of Fungi*, *7*(10), 855. https://doi.org/10.3390/jof7100855

Aguilar, J. A., Zavala, A. N., Díaz-Pérez, C., Cervantes, C., Díaz-Pérez, A. L., & Campos-García, J. (2006). The atu and liu clusters are involved in the catabolic pathways for acyclic monoterpenes and leucine in *Pseudomonas aeruginosa*. *Applied and Environmental Microbiology*, *72*(3), 2070-2079. https://doi.org/10.1128/AEM.72.3.2070-2079.2006

Aiyer, A., & Manos, J. (2022). The Use of Artificial Sputum Media to Enhance Investigation and Subsequent Treatment of Cystic Fibrosis Bacterial Infections. *Microorganisms*, *10*(7), 1269. https://doi.org/10.3390/microorganisms10071269

Al-Wrafy, F. A., Alariqi, R., Noman, E. A., Al-Gheethi, A. A., & Mutahar, M. (2023). *Pseudomonas aeruginosa* behaviour in polymicrobial communities: The competitive and cooperative interactions conducting to the exacerbation of infections. *Microbiological Research*, *268*, 127298. https://doi.org/10.1016/j.micres.2022.127298

Allsopp, L. P., & Bernal, P. (2023). Killing in the name of: T6SS structure and effector diversity. *Microbiology*, *169*(7). https://doi.org/10.1099/mic.0.001367

Allsopp, L. P., Bernal, P., Nolan, L. M., & Filloux, A. (2020). Causalities of war: The connection between type VI secretion system and microbiota. *Cellular Microbiology*, *22*(3). https://doi.org/10.1111/cmi.13153

Allsopp, L. P., Wood, T. E., Howard, S. A., Maggiorelli, F., Nolan, L. M., Wettstadt, S., & Filloux, A. (2017). RsmA and AmrZ orchestrate the assembly of all three type VI secretion systems in *Pseudomonas aeruginosa*. *Proceedings of the National Academy of Sciences*, *114*(29), 7707-7712. https://doi.org/10.1073/pnas.1700286114

Andrews, S. (2023). FastQC A Quality Control tool for High Throughput Sequence Data. https://www.bioinformatics.babraham.ac.uk/projects/fastqc/

Anju, V. T., Busi, S., Imchen, M., Kumavath, R., Mohan, M. S., Salim, S. A.,…Dyavaiah, M. (2022). Polymicrobial Infections and Biofilms: Clinical Significance and Eradication Strategies. *Antibiotics*, *11*(12), 1731. https://doi.org/10.3390/antibiotics11121731

Apidianakis, Y., & Rahme, L. G. (2009). Drosophila melanogaster as a model host for studying *Pseudomonas aeruginosa* infection. *Nature Protocols*, *4*(9), 1285-1294. https://doi.org/10.1038/nprot.2009.124

Arai, H., Kawakami, T., Osamura, T., Hirai, T., Sakai, Y., & Ishii, M. (2014). Enzymatic Characterization and In Vivo Function of Five Terminal Oxidases in *Pseudomonas aeruginosa*. *Journal of Bacteriology*, *196*(24), 4206-4215. https://doi.org/10.1128/JB.02176-14

Aranda-Díaz, A., Obadia, B., Dodge, R., Thomsen, T., Hallberg, Z. F., Güvener, Z. T.,…Huang, K. C. (2020). Bacterial inter-species interactions modulate pH-mediated antibiotic tolerance. *eLife*, *9*, e51493. https://doi.org/10.7554/eLife.51493

Armata Pharmaceuticals. (2024). *Armata Pharmaceuticals*. https://www.armatapharma.com/

Asfahl, K. L., Walsh, J., Gilbert, K., & Schuster, M. (2015). Non-social adaptation defers a tragedy of the commons in *Pseudomonas aeruginosa* quorum sensing. *The ISME Journal*, *9*(8), 1734-1746. https://doi.org/10.1038/ismej.2014.259

Askenasy, I., Swain, J. E. V., Ho, P.-M., Nazeer, R. R., Welch, A., Bényei, É. B.,…Welch, M. (2024). 'Wild Type'. *Microbiology*, *170*(8), 001495. https://doi.org/10.1099/mic.0.001495

Auerbach, A., Kerem, E., Assous, M. V., Picard, E., & Bar-Meir, M. (2015). Is infection with hypermutable *Pseudomonas aeruginosa* clinically significant? *Journal of Cystic Fibrosis*, *14*(3), 347-352. https://doi.org/10.1016/j.jcf.2014.09.011

Axelrod, R., & Hamilton, W. D. (1981). The Evolution of Cooperation. *Science*, *211*(4489), 1390-1396. https://doi.org/10.1126/science.7466396

Baishya, J., Bisht, K., Rimbey, J. N., Yihunie, K. D., Islam, S., Al Mahmud, H.,…Wakeman, C. A. (2021). The Impact of Intraspecies and Inter-species Bacterial Interactions on Disease Outcome. *Pathogens*, *10*(2), 96. https://doi.org/10.3390/pathogens10020096

Balasubramanian, D., Schneper, L., Kumari, H., & Mathee, K. (2013). A dynamic and intricate regulatory network determines *Pseudomonas aeruginosa* virulence. *Nucleic Acids Research*, *41*(1), 1-20. https://doi.org/10.1093/nar/gks1039

Banin, E., Vasil, M. L., & Greenberg, E. P. (2005). Iron and *Pseudomonas aeruginosa* biofilm formation. *Proceedings of the National Academy of Sciences*, *102*(31), 11076-11081. https://doi.org/10.1073/pnas.0504266102

Bankevich, A., Nurk, S., Antipov, D., Gurevich, A. A., Dvorkin, M., Kulikov, A. S.,…Pevzner, P. A. (2012). SPAdes: A New Genome Assembly Algorithm and Its Applications to Single-Cell Sequencing. *Journal of Computational Biology*, *19*(5), 455-477. https://doi.org/10.1089/cmb.2012.0021

Barbour, M. A., Kliebenstein, D. J., & Bascompte, J. (2022). A keystone gene underlies the persistence of an experimental food web. *Science*, *376*(6588), 70-73. https://doi.org/10.1126/science.abf2232

Barraza, J. P., & Whiteley, M. (2021). A *Pseudomonas aeruginosa* Antimicrobial Affects the Biogeography but Not Fitness of *Staphylococcus aureus* during Coculture. *mBio*, *12*(2), e00047-00021. https://doi.org/10.1128/mBio.00047-21

Bartell, J. A., Sommer, L. M., Haagensen, J. A. J., Loch, A., Espinosa, R., Molin, S., & Johansen, H. K. (2019). Evolutionary highways to persistent bacterial infection. *Nature Communications*, *10*(1), 629. https://doi.org/10.1038/s41467-019-08504-7

Basler, M., Ho, Brian T., & Mekalanos, John J. (2013). Tit-for-Tat: Type VI Secretion System Counterattack during Bacterial Cell-Cell Interactions. *Cell*, *152*(4), 884-894. https://doi.org/10.1016/j.cell.2013.01.042

Bassis, C. M., Erb-Downward, J. R., Dickson, R. P., Freeman, C. M., Schmidt, T. M., Young, V. B.,…Huffnagle, G. B. (2015). Analysis of the Upper Respiratory Tract Microbiotas as the Source of the Lung and Gastric Microbiotas in Healthy Individuals. *mBio*, *6*(2), e00037-00015. https://doi.org/10.1128/mBio.00037-15

Beaudoin, T., Yau, Y. C. W., Stapleton, P. J., Gong, Y., Wang, P. W., Guttman, D. S., & Waters, V. (2017). *Staphylococcus aureus* interaction with *Pseudomonas aeruginosa* biofilm enhances tobramycin resistance. *npj Biofilms and Microbiomes*, *3*(1), 25. https://doi.org/10.1038/s41522-017-0035-0

Behrends, V., Ryall, B., Wang, X., Bundy, J. G., & Williams, H. D. (2010). Metabolic profiling of *Pseudomonas aeruginosa* demonstrates that the anti-sigma factor MucA modulates osmotic stress tolerance. *Molecular BioSystems*, *6*(3), 562. https://doi.org/10.1039/b918710c

Berman, J., & Sudbery, P. E. (2002). *Candida albicans*: A molecular revolution built on lessons from budding yeast. *Nature Reviews Genetics*, *3*(12), 918-931. https://doi.org/10.1038/nrg948

Bernardy, E. E., Raghuram, V., & Goldberg, J. B. (2022). *Staphylococcus aureus* and *Pseudomonas aeruginosa* Isolates from the Same Cystic Fibrosis Respiratory Sample Coexist in Coculture. *Microbiology Spectrum*, *10*(4), e00976-00922. https://doi.org/10.1128/spectrum.00976-22

Billard, L., Le Berre, R., Pilorgé, L., Payan, C., Héry-Arnaud, G., & Vallet, S. (2017). Viruses in cystic fibrosis patients' airways. *Critical Reviews in Microbiology*, *43*(6), 690-708. https://doi.org/10.1080/1040841X.2017.1297763

Bingle, L. E., Bailey, C. M., & Pallen, M. J. (2008). Type VI secretion: a beginner's guide. *Current Opinion in Microbiology*, *11*(1), 3-8. https://doi.org/10.1016/j.mib.2008.01.006

BiomX Phage therapy. (2024). *Biomx*. https://www.biomx.com/

Birket, S. E., Davis, J. M., Fernandez, C. M., Tuggle, K. L., Oden, A. M., Chu, K. K.,…Rowe, S. M. (2018). Development of an airway mucus defect in the cystic fibrosis rat. *JCI Insight*, *3*(1), e97199. https://doi.org/10.1172/jci.insight.97199

Bisht, K., Baishya, J., & Wakeman, C. A. (2020). *Pseudomonas aeruginosa* polymicrobial interactions during lung infection. *Current Opinion in Microbiology*, *53*, 1-8. https://doi.org/10.1016/j.mib.2020.01.014

Biswas, L., & Götz, F. (2022). Molecular Mechanisms of Staphylococcus and Pseudomonas Interactions in Cystic Fibrosis. *Frontiers in Cellular and Infection Microbiology*, *11*, 824042. https://doi.org/10.3389/fcimb.2021.824042

Bittinger, K., Charlson, E. S., Loy, E., Shirley, D. J., Haas, A. R., Laughlin, A.,…Bushman, F. D. (2014). Improved characterization of medically relevant fungi in the human respiratory tract using next-generation sequencing. *Genome Biology*, *15*(10), 487. https://doi.org/10.1186/s13059-014-0487-y

Blasdel, B. G., Chevallereau, A., Monot, M., Lavigne, R., & Debarbieux, L. (2017). Comparative transcriptomics analyses reveal the conservation of an ancestral infectious strategy in two bacteriophage genera. *The ISME journal*, *11*(9), 1988-1996. https://doi.org/10.1038/ismej.2017.63

Blighe, K., Rana, S., & Lewis, M. (2018). EnhancedVolcano: Publication-ready volcano plots with enhanced colouring and labeling. https://bioconductor.org/packages/devel/bioc/vignettes/EnhancedVolcano/inst/doc/EnhancedVolcano.html

Bolger, A. M., Lohse, M., & Usadel, B. (2014). Trimmomatic: a flexible trimmer for Illumina sequence data. *Bioinformatics*, *30*(15), 2114-2120. https://doi.org/10.1093/bioinformatics/btu170

Bottery, M. J., Matthews, J. L., Wood, A. J., Johansen, H. K., Pitchford, J. W., & Friman, V.-P. (2022). Inter-species interactions alter antibiotic efficacy in bacterial communities. *The ISME Journal*, *16*(3), 812-821. https://doi.org/10.1038/s41396-021-01130-6

Boutin, S., Graeber, S. Y., Weitnauer, M., Panitz, J., Stahl, M., Clausznitzer, D.,…Dalpke, A. H. (2015). Comparison of Microbiomes from Different Niches of Upper and Lower Airways in Children and Adolescents with Cystic Fibrosis. *PLOS ONE*, *10*(1), e0116029. https://doi.org/10.1371/journal.pone.0116029

Bredenbruch, F., Geffers, R., Nimtz, M., Buer, J., & Häussler, S. (2006). The *Pseudomonas aeruginosa* quinolone signal (PQS) has an iron-chelating activity. *Environmental Microbiology*, *8*(8), 1318-1329. https://doi.org/10.1111/j.1462-2920.2006.01025.x

Briaud, P., Camus, L., Bastien, S., Doléans-Jordheim, A., Vandenesch, F., & Moreau, K. (2019). Coexistence with *Pseudomonas aeruginosa* alters *Staphylococcus aureus* transcriptome, antibiotic resistance and internalization into epithelial cells. *Scientific Reports*, *9*(1), 16564. https://doi.org/10.1038/s41598-019-52975-z

Brint, J. M., & Ohman, D. E. (1995). Synthesis of multiple exoproducts in *Pseudomonas aeruginosa* is under the control of RhlR-RhlI, another set of regulators in strain PAO1 with homology to the autoinducer-responsive LuxR-LuxI family. *Journal of Bacteriology*, *177*(24), 7155-7163. https://doi.org/10.1128/jb.177.24.7155-7163.1995

Burgel, P.-R., Paugam, A., Hubert, D., & Martin, C. (2016). Aspergillus fumigatus in the cystic fibrosis lung: pros and cons of azole therapy. *Infection and Drug Resistance*, *9*, 229–238. https://doi.org/10.2147/IDR.S63621

Burkinshaw, B. J., Liang, X., Wong, M., Le, A. N. H., Lam, L., & Dong, T. G. (2018). A type VI secretion system effector delivery mechanism dependent on PAAR and a chaperone-

co-chaperone complex. *Nature Microbiology*, *3*(5), 632-640. https://doi.org/10.1038/s41564-018-0144-4

Bényei, É. B., Nazeer, R. R., Askenasy, I., Mancini, L., Ho, P.-M., Sivarajan, G. A. C.,…Welch, M. (2024). The past, present and future of polymicrobial infection research: Modelling, eavesdropping, terraforming and other stories. In *Advances in Microbial Physiology* (Vol. 85, pp. 259-323). Elsevier. https://doi.org/10.1016/bs.ampbs.2024.04.002

Calfee, M. W., Coleman, J. P., & Pesci, E. C. (2001). Interference with *Pseudomonas* quinolone signal synthesis inhibits virulence factor expression by *Pseudomonas aeruginosa*. *Proceedings of the National Academy of Sciences*, *98*(20), 11633-11637. https://doi.org/10.1073/pnas.201328498

Camus, L., Vandenesch, F., & Moreau, K. (2021). From genotype to phenotype: adaptations of *Pseudomonas aeruginosa* to the cystic fibrosis environment. *Microbial Genomics*, *7*(3). https://doi.org/10.1099/mgen.0.000513

Castañeda-Tamez, P., Ramírez-Peris, J., Pérez-Velázquez, J., Kuttler, C., Jalalimanesh, A., Saucedo-Mora, M. Á.,…García-Contreras, R. (2018). Pyocyanin Restricts Social Cheating in *Pseudomonas aeruginosa*. *Frontiers in Microbiology*, *9*, 1348. https://doi.org/10.3389/fmicb.2018.01348

Chadha, J., Harjai, K., & Chhibber, S. (2021). Revisiting the virulence hallmarks of *Pseudomonas aeruginosa*: a chronicle through the perspective of quorum sensing. *Environmental Microbiology*, *24*(6), 2630-2656. https://doi.org/10.1111/1462-2920.15784

Chan, D. C. K., & Burrows, L. L. (2023). *Pseudomonas aeruginosa* FpvB Is a High-Affinity Transporter for Xenosiderophores Ferrichrome and Ferrioxamine B. *mBio*, *14*(1), e03149-03122. https://doi.org/10.1128/mbio.03149-22

Charlson, E. S., Bittinger, K., Haas, A. R., Fitzgerald, A. S., Frank, I., Yadav, A.,…Collman, R. G. (2011). Topographical Continuity of Bacterial Populations in the Healthy Human

Respiratory Tract. *American Journal of Respiratory and Critical Care Medicine*, *184*(8), 957-963. https://doi.org/10.1164/rccm.201104-0655OC

Chen, L., Zou, Y., She, P., & Wu, Y. (2015). Composition, function, and regulation of T6SS in *Pseudomonas aeruginosa*. *Microbiological Research*, *172*, 19-25. https://doi.org/10.1016/j.micres.2015.01.004

Chen, R., Déziel, E., Groleau, M.-C., Schaefer, A. L., & Greenberg, E. P. (2019). Social cheating in a *Pseudomonas aeruginosa* quorum-sensing variant. *Proceedings of the National Academy of Sciences*, *116*(14), 7021-7026. https://doi.org/10.1073/pnas.1819801116

Cheng, Y., Yam, J. K. H., Cai, Z., Ding, Y., Zhang, L.-H., Deng, Y., & Yang, L. (2019). Population dynamics and transcriptomic responses of *Pseudomonas aeruginosa* in a complex laboratory microbial community. *NPJ Biofilms and Microbiomes*, *5*, 1. https://doi.org/10.1038/s41522-018-0076-z

Cho, D.-Y., Mackey, C., Van Der Pol, W. J., Skinner, D., Morrow, C. D., Schoeb, T. R.,…Woodworth, B. A. (2018). Sinus Microanatomy and Microbiota in a Rabbit Model of Rhinosinusitis. *Frontiers in Cellular and Infection Microbiology*, *7*, 540. https://doi.org/10.3389/fcimb.2017.00540

Chotirmall, S. H., O'Donoghue, E., Bennett, K., Gunaratnam, C., O'Neill, S. J., & McElvaney, N. G. (2010). Sputum Candida albicans Presages FEV 1 Decline and Hospital-Treated Exacerbations in Cystic Fibrosis. *Chest*, *138*(5), 1186–1195. https://doi.org/10.1378/chest.09-2996

Chugani, S., Kim, B. S., Phattarasukol, S., Brittnacher, M. J., Choi, S. H., Harwood, C. S., & Greenberg, E. P. (2012). Strain-dependent diversity in the *Pseudomonas aeruginosa* quorum-sensing regulon. *Proceedings of the National Academy of Sciences*, *109*(41). https://doi.org/10.1073/pnas.1214128109

Chung, J. C. S., Becq, J., Fraser, L., Schulz-Trieglaff, O., Bond, N. J., Foweraker, J.,…Welch, M. (2012). Genomic Variation among Contemporary *Pseudomonas aeruginosa* Isolates

from Chronically Infected Cystic Fibrosis Patients. *Journal of Bacteriology*, *194*(18), 4857-4866. https://doi.org/10.1128/JB.01050-12

Cianciulli Sesso, A., Lilić, B., Amman, F., Wolfinger, M. T., Sonnleitner, E., & Bläsi, U. (2021). Gene Expression Profiling of *Pseudomonas aeruginosa* Upon Exposure to Colistin and Tobramycin. *Frontiers in Microbiology*, *12*. https://doi.org/10.3389/fmicb.2021.626715

Clsi. (2021). M100 Performance standards for antimicrobial susceptibility testing. In: Clinical and Laboratory Standards Institute. https://www.nih.org.pk/wp-content/uploads/2021/02/CLSI-2020.pdf

Coburn, B., Wang, P. W., Diaz Caballero, J., Clark, S. T., Brahma, V., Donaldson, S.,…Guttman, D. S. (2015). Lung microbiota across age and disease stage in cystic fibrosis. *Scientific Reports*, *5*(1), 10241. https://doi.org/10.1038/srep10241

Cornelis, P. (2020). Putting an end to the *Pseudomonas aeruginosa* IQS controversy. *MicrobiologyOpen*, *9*(2), e962. https://doi.org/10.1002/mbo3.962

Cornelis, P., & Dingemans, J. (2013). *Pseudomonas aeruginosa* adapts its iron uptake strategies in function of the type of infections. *Frontiers in Cellular and Infection Microbiology*, *3*. https://doi.org/10.3389/fcimb.2013.00075

Cornelis, P., Tahrioui, A., Lesouhaitier, O., Bouffartigues, E., Feuilloley, M., Baysse, C., & Chevalier, S. (2023). High affinity iron uptake by pyoverdine in *Pseudomonas aeruginosa* involves multiple regulators besides Fur, PvdS, and FpvI. *BioMetals*, *36*(2), 255-261. https://doi.org/10.1007/s10534-022-00369-6

Cornforth, D. M., Dees, J. L., Ibberson, C. B., Huse, H. K., Mathiesen, I. H., Kirketerp-Møller, K.,…Whiteley, M. (2018). *Pseudomonas aeruginosa* transcriptome during human infection. *Proceedings of the National Academy of Sciences*, *115*(22). https://doi.org/10.1073/pnas.1717525115

Cornforth, D. M., Diggle, F. L., Melvin, J. A., Bomberger, J. M., & Whiteley, M. (2020). Quantitative Framework for Model Evaluation in Microbiology Research Using *Pseudomonas aeruginosa* and Cystic Fibrosis Infection as a Test Case. *mBio*, *11*(1), e03042-03019. https://doi.org/10.1128/mBio.03042-19

Cox, M. J., Allgaier, M., Taylor, B., Baek, M. S., Huang, Y. J., Daly, R. A.,…Lynch, S. V. (2010). Airway Microbiota and Pathogen Abundance in Age-Stratified Cystic Fibrosis Patients. *PLoS ONE*, *5*(6), e11044. https://doi.org/10.1371/journal.pone.0011044

Crone, S., Vives-Flórez, M., Kvich, L., Saunders, A. M., Malone, M., Nicolaisen, M. H.,…Bjarnsholt, T. (2020). The environmental occurrence of *Pseudomonas aeruginosa*. *APMIS: acta pathologica, microbiologica, et immunologica Scandinavica*, *128*(3), 220-231. https://doi.org/10.1111/apm.13010

Cruz, R. L., Asfahl, K. L., Van Den Bossche, S., Coenye, T., Crabbé, A., & Dandekar, A. A. (2020). RhlR-Regulated Acyl-Homoserine Lactone Quorum Sensing in a Cystic Fibrosis Isolate of *Pseudomonas aeruginosa*. *mBio*, *11*(2), e00532-00520. https://doi.org/10.1128/mBio.00532-20

Cugini, C., Calfee, M. W., Farrow, J. M., Morales, D. K., Pesci, E. C., & Hogan, D. A. (2007). Farnesol, a common sesquiterpene, inhibits PQS production in *Pseudomonas aeruginosa*. *Molecular Microbiology*, *65*(4), 896-906. https://doi.org/10.1111/j.1365-2958.2007.05840.x

Cugini, C., Morales, D. K., & Hogan, D. A. (2010). *Candida albicans*-produced farnesol stimulates Pseudomonas quinolone signal production in LasR-defective *Pseudomonas aeruginosa* strains. *Microbiology (Reading, England)*, *156*(Pt 10), 3096-3107. https://doi.org/10.1099/mic.0.037911-0

Cuthbertson, L., Rogers, G. B., Walker, A. W., Oliver, A., Green, L. E., Daniels, T. W. V.,…Van Der Gast, C. J. (2016). Respiratory microbiota resistance and resilience to pulmonary exacerbation and subsequent antimicrobial intervention. *The ISME Journal*, *10*(5), 1081-1091. https://doi.org/10.1038/ismej.2015.198

Cystic Fibrosis Foundation. (2024). About Cystic Fibrosis.*Cystic Fibrosis Foundation*. https://www.cff.org/intro-cf/about-cystic-fibrosis

Cystic Fibrosis Trust. (2024). The basics. *Cystic Fibrosis Trust*. https://www.cysticfibrosis.org.uk/what-is-cystic-fibrosis/faqs

D'Argenio, D. A., Wu, M., Hoffman, L. R., Kulasekara, H. D., Déziel, E., Smith, E. E.,…Miller, S. I. (2007). Growth phenotypes of *Pseudomonas aeruginosa* lasR mutants adapted to the airways of cystic fibrosis patients. *Molecular Microbiology*, *64*(2), 512-533. https://doi.org/10.1111/j.1365-2958.2007.05678.x

Dandekar, A. A., Chugani, S., & Greenberg, E. P. (2012). Bacterial Quorum Sensing and Metabolic Incentives to Cooperate. *Science*, *338*(6104), 264-266. https://doi.org/10.1126/science.1227289

Danecek, P., Bonfield, J. K., Liddle, J., Marshall, J., Ohan, V., Pollard, M. O.,…Li, H. (2021). Twelve years of SAMtools and BCFtools. *GigaScience*, *10*(2), giab008. https://doi.org/10.1093/gigascience/giab008

De Kievit, T. R. (2009). Quorum sensing in *Pseudomonas aeruginosa* biofilms. *Environmental Microbiology*, *11*(2), 279-288. https://doi.org/10.1111/j.1462-2920.2008.01792.x

De Wit, G., Svet, L., Lories, B., & Steenackers, H. P. (2022). Microbial Inter-species Interactions and Their Impact on the Emergence and Spread of Antimicrobial Resistance. *Annual Review of Microbiology*, *76*(1), 179-192. https://doi.org/10.1146/annurev-micro-041320-031627

Dehbashi, S., Pourmand, M. R., Alikhani, M. Y., Asl, S. S., & Arabestani, M. R. (2020). The effect of *Staphylococcus aureus* on the antibiotic resistance and pathogenicity of *Pseudomonas aeruginosa* based on crc gene as a metabolism regulator: An *in vitro* wound model study. *Infection, Genetics and Evolution*, *85*, 104509. https://doi.org/10.1016/j.meegid.2020.104509

Dekimpe, V., & Déziel, E. (2009). Revisiting the quorum-sensing hierarchy in *Pseudomonas aeruginosa*: the transcriptional regulator RhlR regulates LasR-specific factors. *Microbiology (Reading, England)*, *155*(Pt 3), 712-723. https://doi.org/10.1099/mic.0.022764-0

DeLeon, S., Clinton, A., Fowler, H., Everett, J., Horswill, A. R., & Rumbaugh, K. P. (2014). Synergistic Interactions of *Pseudomonas aeruginosa* and *Staphylococcus aureus* in an *In Vitro* Wound Model. *Infection and Immunity*, *82*(11), 4718-4728. https://doi.org/10.1128/IAI.02198-14

Delhaes, L., Monchy, S., Fréalle, E., Hubans, C., Salleron, J., Leroy, S.,…Viscogliosi, E. (2012). The Airway Microbiota in Cystic Fibrosis: A Complex Fungal and Bacterial Community—Implications for Therapeutic Management. *PLoS ONE*, *7*(4), e36313. https://doi.org/10.1371/journal.pone.0036313

Deshamukhya, C., Saikia, R., Das, B. J., Paul, D., Dhar, D., & Bhattacharjee, A. (2022). Expression of cupA gene cluster responsible for biofilm formation in *Pseudomonas aeruginosa* is enhanced against subinhibitory concentration of carbapenems. *Gene Reports*, *26*, 101427. https://doi.org/10.1016/j.genrep.2021.101427

Dickson, R. P., Erb-Downward, J. R., Freeman, C. M., McCloskey, L., Beck, J. M., Huffnagle, G. B., & Curtis, J. L. (2015). Spatial Variation in the Healthy Human Lung Microbiome and the Adapted Island Model of Lung Biogeography. *Annals of the American Thoracic Society*, *12*(6), 821-830. https://doi.org/10.1513/AnnalsATS.201501-029OC

Diggle, S. P., Matthijs, S., Wright, V. J., Fletcher, M. P., Chhabra, S. R., Lamont, I. L.,…Williams, P. (2007). The *Pseudomonas aeruginosa* 4-Quinolone Signal Molecules HHQ and PQS Play Multifunctional Roles in Quorum Sensing and Iron Entrapment. *Chemistry & Biology*, *14*(1), 87-96. https://doi.org/10.1016/j.chembiol.2006.11.014

Diggle, S. P., & Whiteley, M. (2020). Microbe Profile: *Pseudomonas aeruginosa*: opportunistic pathogen and lab rat: This article is part of the Microbe Profiles collection. *Microbiology*, *166*(1), 30-33. https://doi.org/10.1099/mic.0.000860

Diggle, S. P., Winzer, K., Chhabra, S. R., Worrall, K. E., Cámara, M., & Williams, P. (2003). The *Pseudomonas aeruginosa* quinolone signal molecule overcomes the cell density-dependency of the quorum sensing hierarchy, regulates rhl-dependent genes at the onset of stationary phase and can be produced in the absence of LasR. *Molecular Microbiology*, *50*(1), 29-43. https://doi.org/10.1046/j.1365-2958.2003.03672.x

Ding, F., Oinuma, K.-I., Smalley, N. E., Schaefer, A. L., Hamwy, O., Greenberg, E. P., & Dandekar, A. A. (2018). The *Pseudomonas aeruginosa* Orphan Quorum Sensing Signal Receptor QscR Regulates Global Quorum Sensing Gene Expression by Activating a Single Linked Operon. *mBio*, *9*(4), e01274-01218. https://doi.org/10.1128/mBio.01274-18

CFF Pipeline. (2024). *Drug Development Pipeline*. https://www.cff.org/Trials/Pipeline

Drummond, R. A., Desai, J. V., Ricotta, E. E., Swamydas, M., Deming, C., Conlan, S.,…Lionakis, M. S. (2022). Long-term antibiotic exposure promotes mortality after systemic fungal infection by driving lymphocyte dysfunction and systemic escape of commensal bacteria. *Cell Host & Microbe*, *30*(7), 1020-1033.e1026. https://doi.org/10.1016/j.chom.2022.04.013

Du, Q., Ren, B., Zhou, X., Zhang, L., & Xu, X. (2022). Cross-kingdom interaction between *Candida albicans* and oral bacteria. *Frontiers in Microbiology*, *13*, 911623. https://doi.org/10.3389/fmicb.2022.911623

Durand, B. A. R. N., Pouget, C., Magnan, C., Molle, V., Lavigne, J.-P., & Dunyach-Remy, C. (2022). Bacterial Interactions in the Context of Chronic Wound Biofilm: A Review. *Microorganisms*, *10*(8), 1500. https://doi.org/10.3390/microorganisms10081500

Ecfs. (2022). Annual Reports | European Cystic Fibrosis Society. https://www.ecfs.eu/projects/ecfs-patient-registry/annual-reports

Fan, Z., Perisse, I. V., Cotton, C. U., Regouski, M., Meng, Q., Domb, C.,…Polejaeva, I. A. (2018). A sheep model of cystic fibrosis generated by CRISPR/Cas9 disruption of the CFTR gene. *JCI Insight*, *3*(19), e123529. https://doi.org/10.1172/jci.insight.123529

Feltner, J. B., Wolter, D. J., Pope, C. E., Groleau, M.-C., Smalley, N. E., Greenberg, E. P.,…Dandekar, A. A. (2016). LasR Variant Cystic Fibrosis Isolates Reveal an Adaptable Quorum-Sensing Hierarchy in *Pseudomonas aeruginosa*. *mBio*, *7*(5), e01513-01516. https://doi.org/10.1128/mBio.01513-16

Figueiredo, A. R. T., Wagner, A., & Kümmerli, R. (2021). Ecology drives the evolution of diverse social strategies in *Pseudomonas aeruginosa*. *Molecular Ecology*, *30*(20), 5214-5228. https://doi.org/10.1111/mec.16119

Filkins, L. M., Graber, J. A., Olson, D. G., Dolben, E. L., Lynd, L. R., Bhuju, S., & O'Toole, G. A. (2015). Coculture of *Staphylococcus aureus* with *Pseudomonas aeruginosa* Drives S. aureus towards Fermentative Metabolism and Reduced Viability in a Cystic Fibrosis Model. *Journal of Bacteriology*, *197*(14), 2252-2264. https://doi.org/10.1128/JB.00059-15

Filkins, L. M., & O'Toole, G. A. (2015). Cystic Fibrosis Lung Infections: Polymicrobial, Complex, and Hard to Treat. *PLOS Pathogens*, *11*(12), e1005258. https://doi.org/10.1371/journal.ppat.1005258

Filloux, A. (2011). Protein Secretion Systems in *Pseudomonas aeruginosa*: An Essay on Diversity, Evolution, and Function. *Frontiers in Microbiology*, *2*. https://doi.org/10.3389/fmicb.2011.00155

Filloux, A. (2024). Bacterial type VI secretion system helps prevent cheating in microbial communities. *The ISME Journal*, *18*(1), wrae003. https://doi.org/10.1093/ismejo/wrae003

Filloux, A., & Ramos, J.-L. (2022). *Pseudomonas aeruginosa: Biology, Pathogenesis and Control Strategies* (A. Filloux & J.-L. Ramos, Eds. Vol. 1386). Springer International Publishing.

Fiorotto, R., Amenduni, M., Mariotti, V., Cadamuro, M., Fabris, L., Spirli, C., & Strazzabosco, M. (2019). Animal models for cystic fibrosis liver disease (CFLD). *Biochimica et Biophysica Acta (BBA) - Molecular Basis of Disease*, *1865*(5), 965-969. https://doi.org/10.1016/j.bbadis.2018.07.026

Fourie, R., Ells, R., Kemp, G., Sebolai, O. M., Albertyn, J., & Pohl, C. H. (2017). *Pseudomonas aeruginosa* produces aspirin insensitive eicosanoids and contributes to the eicosanoid profile of polymicrobial biofilms with *Candida albicans*. *Prostaglandins, Leukotrienes and Essential Fatty Acids*, *117*, 36-46. https://doi.org/10.1016/j.plefa.2017.01.008

Fourie, R., Ells, R., Swart, C. W., Sebolai, O. M., Albertyn, J., & Pohl, C. H. (2016). *Candida albicans* and *Pseudomonas aeruginosa* Interaction, with Focus on the Role of Eicosanoids. *Frontiers in Physiology*, *7*. https://doi.org/10.3389/fphys.2016.00064

Françoise, A., & Héry-Arnaud, G. (2020). The Microbiome in Cystic Fibrosis Pulmonary Disease. *Genes*, *11*(5), 536. https://doi.org/10.3390/genes11050536

Frayman, K. B., Armstrong, D. S., Carzino, R., Ferkol, T. W., Grimwood, K., Storch, G. A.,…Ranganathan, S. C. (2017). The lower airway microbiota in early cystic fibrosis lung disease: a longitudinal analysis. *Thorax*, *72*(12), 1104-1112. https://doi.org/10.1136/thoraxjnl-2016-209279

Fung, C., Naughton, S., Turnbull, L., Tingpej, P., Rose, B., Arthur, J.,…Manos, J. (2010). Gene expression of *Pseudomonas aeruginosa* in a mucin-containing synthetic growth medium mimicking cystic fibrosis lung sputum. *Journal of Medical Microbiology*, *59*(Pt 9), 1089-1100. https://doi.org/10.1099/jmm.0.019984-0

Gambello, M. J., & Iglewski, B. H. (1991). Cloning and characterization of the *Pseudomonas aeruginosa* lasR gene, a transcriptional activator of elastase expression. *Journal of Bacteriology*, *173*(9), 3000-3009. https://doi.org/10.1128/jb.173.9.3000-3009.1991

Ganne, G., Brillet, K., Basta, B., Roche, B., Hoegy, F., Gasser, V., & Schalk, I. J. (2017). Iron Release from the Siderophore Pyoverdine in *Pseudomonas aeruginosa* Involves Three New Actors: FpvC, FpvG, and FpvH. *ACS Chemical Biology*, *12*(4), 1056-1065. https://doi.org/10.1021/acschembio.6b01077

García-Contreras, R., Loarca, D., Pérez-González, C., Jiménez-Cortés, J. G., Gonzalez-Valdez, A., & Soberón-Chávez, G. (2020). Rhamnolipids stabilize quorum sensing mediated cooperation in *Pseudomonas aeruginosa*. *FEMS Microbiology Letters*, *367*(10), fnaa080. https://doi.org/10.1093/femsle/fnaa080

Ghssein, G., & Ezzeddine, Z. (2022). A Review of *Pseudomonas aeruginosa* Metallophores: Pyoverdine, Pyochelin and Pseudopaline. *Biology*, *11*(12), 1711. https://doi.org/10.3390/biology11121711

Gifford, A. H., Moulton, L. A., Dorman, D. B., Olbina, G., Westerman, M., Parker, H. W.,…O'Toole, G. A. (2012). Iron Homeostasis during Cystic Fibrosis Pulmonary Exacerbation. *Clinical and Translational Science*, *5*(4), 368-373. https://doi.org/10.1111/j.1752-8062.2012.00417.x

Gifford, A. H., Polineni, D., He, J., D'Amico, J. L., Dorman, D. B., Williams, M. A.,…Zuckerman, J. B. (2021). A pilot study of cystic fibrosis exacerbation response phenotypes reveals contrasting serum and sputum iron trends. *Scientific Reports*, *11*(1), 4897. https://doi.org/10.1038/s41598-021-84041-y

Gilbert, K. B., Kim, T. H., Gupta, R., Greenberg, E. P., & Schuster, M. (2009). Global position analysis of the *Pseudomonas aeruginosa* quorum-sensing transcription factor LasR. *Molecular Microbiology*, *73*(6), 1072-1085. https://doi.org/10.1111/j.1365-2958.2009.06832.x

Gomes-Fernandes, M., Gomez, A.-C., Bravo, M., Huedo, P., Coves, X., Prat-Aymerich, C.,…Yero, D. (2022). Strain-specific inter-species interactions between co-isolated pairs of *Staphylococcus aureus* and *Pseudomonas aeruginosa* from patients with tracheobronchitis or bronchial colonization. *Scientific Reports*, *12*(1), 3374. https://doi.org/10.1038/s41598-022-07018-5

Grainha, T., Jorge, P., Alves, D., Lopes, S. P., & Pereira, M. O. (2020). Unraveling *Pseudomonas aeruginosa* and *Candida albicans* Communication in Coinfection Scenarios: Insights Through Network Analysis. *Frontiers in Cellular and Infection Microbiology*, *10*, 550505. https://doi.org/10.3389/fcimb.2020.550505

Haas, A. L., Zemke, A. C., Melvin, J. A., Armbruster, C. R., Hendricks, M. R., Moore, J.,…Bomberger, J. M. (2023). Iron bioavailability regulates *Pseudomonas aeruginosa* inter-species interactions through type VI secretion expression. *Cell Reports*, *42*(3), 112270. https://doi.org/10.1016/j.celrep.2023.112270

Hall, L. M. C., & Henderson-Begg, S. K. (2006). Hypermutable bacteria isolated from humans – a critical analysis. *Microbiology*, *152*(9), 2505-2514. https://doi.org/10.1099/mic.0.29079-0

Hammer, Neal D., Cassat, James E., Noto, Michael J., Lojek, Lisa J., Chadha, Ashley D., Schmitz, Jonathan E.,…Skaar, Eric P. (2014). Inter- and Intraspecies Metabolite Exchange Promotes Virulence of Antibiotic-Resistant *Staphylococcus aureus*. *Cell Host & Microbe*, *16*(4), 531-537. https://doi.org/10.1016/j.chom.2014.09.002

Hardalo, C., & Edberg, S. C. (1997). *Pseudomonas aeruginosa*: Assessment of Risk from Drinking Water. *Critical Reviews in Microbiology*, *23*(1), 47-75. https://doi.org/10.3109/10408419709115130

Harriott, M. M., & Noverr, M. C. (2009). *Candida albicans* and *Staphylococcus aureus* Form Polymicrobial Biofilms: Effects on Antimicrobial Resistance. *Antimicrobial Agents and Chemotherapy*, *53*(9), 3914-3922. https://doi.org/10.1128/AAC.00657-09

Harriott, M. M., & Noverr, M. C. (2011). Importance of Candida–bacterial polymicrobial biofilms in disease. *Trends in Microbiology*, *19*(11), 557-563. https://doi.org/10.1016/j.tim.2011.07.004

Harrison, F., Muruli, A., Higgins, S., & Diggle, S. P. (2014). Development of an *Ex Vivo* Porcine Lung Model for Studying Growth, Virulence, and Signaling of *Pseudomonas aeruginosa*. *Infection and Immunity*, *82*(8), 3312-3323. https://doi.org/10.1128/IAI.01554-14

Harrison, P. W., Ahamed, A., Aslam, R., Alako, B. T. F., Burgin, J., Buso, N.,…Cochrane, G. (2021). The European Nucleotide Archive in 2020. *Nucleic Acids Research*, *49*(D1), D82-D85. https://doi.org/10.1093/nar/gkaa1028

Hassan Abdel-Rhman, S., Mostafa El-Mahdy, A., & El-Mowafy, M. (2015). Effect of Tyrosol and Farnesol on Virulence and Antibiotic Resistance of Clinical Isolates of *Pseudomonas aeruginosa*. *BioMed Research International*, *2015*, 1-7. https://doi.org/10.1155/2015/456463

Hastings, J. W., & Nealson, K. H. (1977). BACTERIAL BIOLUMINESCENCE. *Annual Review of Microbiology*, *31*(1), 549-595. https://doi.org/10.1146/annurev.mi.31.100177.003001

Hatziagorou, E., Orenti, A., Drevinek, P., Kashirskaya, N., Mei-Zahav, M., De Boeck, K.,…Zolin, A. (2020). Changing epidemiology of the respiratory bacteriology of patients with cystic fibrosis–data from the European cystic fibrosis society patient registry. *Journal of Cystic Fibrosis*, *19*(3), 376-383. https://doi.org/10.1016/j.jcf.2019.08.006

Heeb, S., Fletcher, M. P., Chhabra, S. R., Diggle, S. P., Williams, P., & Cámara, M. (2011). Quinolones: from antibiotics to autoinducers. *FEMS Microbiology Reviews*, *35*(2), 247-274. https://doi.org/10.1111/j.1574-6976.2010.00247.x

Hernandez, R. E., Gallegos-Monterrosa, R., & Coulthurst, S. J. (2020). Type VI secretion system effector proteins: Effective weapons for bacterial competitiveness. *Cellular Microbiology*, *22*(9). https://doi.org/10.1111/cmi.13241

Hersch, S. J., Watanabe, N., Stietz, M. S., Manera, K., Kamal, F., Burkinshaw, B.,…Dong, T. G. (2020). Envelope stress responses defend against type six secretion system attacks independently of immunity proteins. *Nature Microbiology*, *5*(5), 706-714. https://doi.org/10.1038/s41564-020-0672-6

Hester, K. L., Lehman, J., Najar, F., Song, L., Roe, B. A., MacGregor, C. H.,…Sokatch, J. R. (2000). Crc Is Involved in Catabolite Repression Control of the bkd Operons of Pseudomonas putida and *Pseudomonas aeruginosa*. *Journal of Bacteriology*, *182*(4), 1144-1149.

Hewer, S. C. L., Smyth, A. R., Brown, M., Jones, A. P., Hickey, H., Kenna, D.,…Williamson, P. R. (2020). Intravenous versus oral antibiotics for eradication of *Pseudomonas aeruginosa* in cystic fibrosis (TORPEDO-CF): a randomised controlled trial. *The Lancet Respiratory Medicine*, *8*(10), 975-986. https://doi.org/10.1016/S2213-2600(20)30331-3

Ho, Brian T., Dong, Tao G., & Mekalanos, John J. (2014). A View to a Kill: The Bacterial Type VI Secretion System. *Cell Host & Microbe*, *15*(1), 9-21. https://doi.org/10.1016/j.chom.2013.11.008

Ho, B. T., Fu, Y., Dong, T. G., & Mekalanos, J. J. (2017). *Vibrio cholerae* type 6 secretion system effector trafficking in target bacterial cells. *Proceedings of the National Academy of Sciences*, *114*(35), 9427-9432. https://doi.org/10.1073/pnas.1711219114

Ho, P.-M., Nazeer, R. R., & Welch, M. (2023). Therapeutic interventions alter ecological interactions among cystic fibrosis airway microbiota. *Frontiers in Microbiology*, *14*, 1178131. https://doi.org/10.3389/fmicb.2023.1178131

Hoffman, L. R., Déziel, E., D'Argenio, D. A., Lépine, F., Emerson, J., McNamara, S.,…Miller, S. I. (2006). Selection for *Staphylococcus aureus* small-colony variants due to growth in the presence of *Pseudomonas aeruginosa*. *Proceedings of the National Academy of Sciences*, *103*(52), 19890-19895. https://doi.org/10.1073/pnas.0606756104

Hoffman, L. R., Kulasekara, H. D., Emerson, J., Houston, L. S., Burns, J. L., Ramsey, B. W., & Miller, S. I. (2009). *Pseudomonas aeruginosa* lasR mutants are associated with cystic fibrosis lung disease progression. *Journal of Cystic Fibrosis*, *8*(1), 66-70. https://doi.org/10.1016/j.jcf.2008.09.006

Hogan, D. A., & Kolter, R. (2002). *Pseudomonas* - *Candida* Interactions: An Ecological Role for Virulence Factors. *Science*, *296*(5576), 2229-2232. https://doi.org/10.1126/science.1070784

Hogan, D. A., Vik, Å., & Kolter, R. (2004). A *Pseudomonas aeruginosa* quorum-sensing molecule influences *Candida albicans* morphology. *Molecular Microbiology*, *54*(5), 1212-1223. https://doi.org/10.1111/j.1365-2958.2004.04349.x

Holloway, B. W. (1955). Genetic Recombination in *Pseudomonas aeruginosa*. *Microbiology*, *13*(3), 572-581. https://doi.org/10.1099/00221287-13-3-572

Holt, J. E., Houston, A., Adams, C., Edwards, S., & Kjellerup, B. V. (2017). Role of extracellular polymeric substances in polymicrobial biofilm infections of Staphylococcus epidermidis and *Candida albicans* modelled in the nematode Caenorhabditis elegans. *Pathogens and Disease*, *75*(5). https://doi.org/10.1093/femspd/ftx052

Hood, R. D., Singh, P., Hsu, F., Güvener, T., Carl, M. A., Trinidad, R. R. S.,…Mougous, J. D. (2010). A Type VI Secretion System of *Pseudomonas aeruginosa* Targets a Toxin to Bacteria. *Cell Host & Microbe*, *7*(1), 25-37. https://doi.org/10.1016/j.chom.2009.12.007

Hotterbeekx, A., Kumar-Singh, S., Goossens, H., & Malhotra-Kumar, S. (2017). In vivo and In vitro Interactions between *Pseudomonas aeruginosa* and Staphylococcus spp. *Frontiers in Cellular and Infection Microbiology*, *7*. https://doi.org/10.3389/fcimb.2017.00106

Ibberson, C. B., & Whiteley, M. (2020). The social life of microbes in chronic infection. *Current Opinion in Microbiology*, *53*, 44-50. https://doi.org/10.1016/j.mib.2020.02.003

Jabra-Rizk, M. A., Meiller, T. F., James, C. E., & Shirtliff, M. E. (2006). Effect of Farnesol on *Staphylococcus aureus* Biofilm Formation and Antimicrobial Susceptibility. *Antimicrobial Agents and Chemotherapy*, *50*(4), 1463-1469. https://doi.org/10.1128/AAC.50.4.1463-1469.2006

Jankauskaitė, L., Misevičienė, V., Vaidelienė, L., & Kėvalas, R. (2018). Lower Airway Virology in Health and Disease—From Invaders to Symbionts. *Medicina*, *54*(5), 72. https://doi.org/10.3390/medicina54050072

Jayakumar, P., Figueiredo, A. R. T., & Kümmerli, R. (2022). Evolution of Quorum Sensing in *Pseudomonas aeruginosa* Can Occur via Loss of Function and Regulon Modulation. *mSystems*, *7*(5), e00354-00322. https://doi.org/10.1128/msystems.00354-22

Jhun, B. W., Jung, W. J., Hwang, N. Y., Park, H. Y., Jeon, K., Kang, E.-S., & Koh, W.-J. (2017). Risk factors for the development of chronic pulmonary aspergillosis in patients with nontuberculous mycobacterial lung disease. *PLOS ONE*, *12*(11), e0188716. https://doi.org/10.1371/journal.pone.0188716

Jorth, P., Ehsan, Z., Rezayat, A., Caldwell, E., Pope, C., Brewington, J. J.,…Singh, P. K. (2019). Direct Lung Sampling Indicates That Established Pathogens Dominate Early Infections in Children with Cystic Fibrosis. *Cell Reports*, *27*(4), 1190-1204.e1193. https://doi.org/10.1016/j.celrep.2019.03.086

Jorth, P., Staudinger, Benjamin J., Wu, X., Hisert, K. B., Hayden, H., Garudathri, J.,…Singh, Pradeep K. (2015). Regional Isolation Drives Bacterial Diversification within Cystic Fibrosis Lungs. *Cell Host & Microbe*, *18*(3), 307-319. https://doi.org/10.1016/j.chom.2015.07.006

Kahl, B. C., Becker, K., & Löffler, B. (2016). Clinical Significance and Pathogenesis of Staphylococcal Small Colony Variants in Persistent Infections. *Clinical Microbiology Reviews*, *29*(2), 401-427. https://doi.org/10.1128/CMR.00069-15

Kahl, L. J., Stremmel, N., Esparza-Mora, M. A., Wheatley, R. M., MacLean, R. C., & Ralser, M. (2023). Interkingdom interactions between *Pseudomonas aeruginosa* and *Candida albicans* affect clinical outcomes and antimicrobial responses. *Current Opinion in Microbiology*, *75*, 102368. https://doi.org/10.1016/j.mib.2023.102368

Kaleli, I., Cevahir, N., Demir, M., Yildirim, U., & Sahin, R. (2007). Anticandidal activity of *Pseudomonas aeruginosa* strains isolated from clinical specimens. *Mycoses*, *50*(1), 74-78. https://doi.org/10.1111/j.1439-0507.2006.01322.x

Kaneko, Y., Thoendel, M., Olakanmi, O., Britigan, B. E., & Singh, P. K. (2007). The transition metal gallium disrupts *Pseudomonas aeruginosa* iron metabolism and has antimicrobial and antibiofilm activity. *Journal of Clinical Investigation*, *117*(4), 877-888. https://doi.org/10.1172/JCI30783

Kasetty, S., Mould, D. L., Hogan, D. A., & Nadell, C. D. (2021). Both *Pseudomonas aeruginosa* and *Candida albicans* Accumulate Greater Biomass in Dual-Species Biofilms under Flow. *mSphere*, *6*(3), e00416-00421. https://doi.org/10.1128/mSphere.00416-21

Kawakami, T., Kuroki, M., Ishii, M., Igarashi, Y., & Arai, H. (2010). Differential expression of multiple terminal oxidases for aerobic respiration in *Pseudomonas aeruginosa*. *Environmental Microbiology*, *12*(6), 1399-1412. https://doi.org/10.1111/j.1462-2920.2009.02109.x

Kean, R., Rajendran, R., Haggarty, J., Townsend, E. M., Short, B., Burgess, K. E.,…Ramage, G. (2017). *Candida albicans* Mycofilms Support *Staphylococcus aureus* Colonization and Enhances Miconazole Resistance in Dual-Species Interactions. *Frontiers in Microbiology*, *8*. https://doi.org/10.3389/fmicb.2017.00258

Keown, K., Reid, A., Moore, J. E., Taggart, C. C., & Downey, D. G. (2020). Coinfection with *Pseudomonas aeruginosa* and *Aspergillus fumigatus* in cystic fibrosis. *European Respiratory Review*, *29*(158), 200011. https://doi.org/10.1183/16000617.0011-2020

Kesthely, C. A., Rogers, R. R., El Hafi, B., Jean-Pierre, F., & O'Toole, G. A. (2023). Transcriptional profiling and genetic analysis of a cystic fibrosis airway-relevant model shows asymmetric responses to growth in a polymicrobial community. *Microbiology Spectrum*, *11*(5), e02201-02223. https://doi.org/10.1128/spectrum.02201-23

King, J., Murphy, R., & Davies, J. C. (2022). *Pseudomonas aeruginosa* in the Cystic Fibrosis Lung. In A. Filloux & J.-L. Ramos (Eds.), *Pseudomonas aeruginosa* (Vol. 1386, pp. 347-369). Springer International Publishing.

Kirchner, S., Fothergill, J. L., Wright, E. A., James, C. E., Mowat, E., & Winstanley, C. (2012). Use of Artificial Sputum Medium to Test Antibiotic Efficacy Against *Pseudomonas aeruginosa* in Conditions More Relevant to the Cystic Fibrosis Lung. *Journal of Visualized Experiments*(64), 3857. https://doi.org/10.3791/3857

Klepac-Ceraj, V., Lemon, K. P., Martin, T. R., Allgaier, M., Kembel, S. W., Knapp, A. A.,…Kolter, R. (2010). Relationship between cystic fibrosis respiratory tract bacterial communities and age, genotype, antibiotics and *Pseudomonas aeruginosa*. *Environmental Microbiology*, *12*(5), 1293-1303. https://doi.org/10.1111/j.1462-2920.2010.02173.x

Korgaonkar, A., Trivedi, U., Rumbaugh, K. P., & Whiteley, M. (2013). Community surveillance enhances *Pseudomonas aeruginosa* virulence during polymicrobial infection. *Proceedings of the National Academy of Sciences*, *110*(3), 1059-1064. https://doi.org/10.1073/pnas.1214550110

Koskinen, K., Pausan, M. R., Perras, A. K., Beck, M., Bang, C., Mora, M.,…Moissl-Eichinger, C. (2017). First Insights into the Diverse Human Archaeome: Specific Detection of Archaea in the Gastrointestinal Tract, Lung, and Nose and on Skin. *mBio*, *8*(6), e00824-00817. https://doi.org/10.1128/mBio.00824-17

Kostylev, M., Kim, D. Y., Smalley, N. E., Salukhe, I., Greenberg, E. P., & Dandekar, A. A. (2019). Evolution of the *Pseudomonas aeruginosa* quorum-sensing hierarchy. *Proceedings of the National Academy of Sciences*, *116*(14), 7027-7032. https://doi.org/10.1073/pnas.1819796116

Kung, V. L., Ozer, E. A., & Hauser, A. R. (2010). The accessory genome of *Pseudomonas aeruginosa*. *Microbiology and molecular biology reviews: MMBR*, *74*(4), 621-641. https://doi.org/10.1128/MMBR.00027-10

Kvich, L., Crone, S., Christensen, M. H., Lima, R., Alhede, M., Alhede, M.,…Bjarnsholt, T. (2022). Investigation of the Mechanism and Chemistry Underlying *Staphylococcus aureus* ' Ability to Inhibit *Pseudomonas aeruginosa* Growth *In Vitro*. *Journal of Bacteriology*, *204*(11), e00174-00122. https://doi.org/10.1128/jb.00174-22

La Rosa, R., Rossi, E., Feist, A. M., Johansen, H. K., & Molin, S. (2021). Compensatory evolution of *Pseudomonas aeruginosa*'s slow growth phenotype suggests mechanisms of adaptation in cystic fibrosis. *Nature Communications*, *12*(1), 3186. https://doi.org/10.1038/s41467-021-23451-y

LaFayette, S. L., Houle, D., Beaudoin, T., Wojewodka, G., Radzioch, D., Hoffman, L. R.,…Nguyen, D. (2015). Cystic fibrosis–adapted *Pseudomonas aeruginosa* quorum sensing *lasR* mutants cause hyperinflammatory responses. *Science Advances*, *1*(6), e1500199. https://doi.org/10.1126/sciadv.1500199

Lamoureux, C., Guilloux, C.-A., Beauruelle, C., Gouriou, S., Ramel, S., Dirou, A.,…Héry-Arnaud, G. (2021). An observational study of anaerobic bacteria in cystic fibrosis lung using culture dependant and independent approaches. *Scientific Reports*, *11*(1), 6845. https://doi.org/10.1038/s41598-021-85592-w

Lamoureux, C., Guilloux, C.-A., Beauruelle, C., Jolivet-Gougeon, A., & Héry-Arnaud, G. (2019). Anaerobes in cystic fibrosis patients' airways. *Critical Reviews in Microbiology*, *45*(1), 103-117. https://doi.org/10.1080/1040841X.2018.1549019

Landa, G., Clarhaut, J., Buyck, J., Mendoza, G., Arruebo, M., & Tewes, F. (2024). Impact of mixed Staphylococcus aureus-Pseudomonas aeruginosa biofilm on susceptibility to antimicrobial treatments in a 3D in vitro model. *Scientific Reports*, *14*(1), 27877. https://doi.org/10.1038/s41598-024-79573-yLangmead, B., & Salzberg, S. L. (2012).

Fast gapped-read alignment with Bowtie 2. *Nature Methods*, *9*(4), 357-359. https://doi.org/10.1038/nmeth.1923

Langton Hewer, S. C., & Smyth, A. R. (2017). Antibiotic strategies for eradicating *Pseudomonas aeruginosa* in people with cystic fibrosis. *Cochrane Database of Systematic Reviews*, *2020*(2). https://doi.org/10.1002/14651858.CD004197.pub5

Latifi, A., Winson, M. K., Foglino, M., Bycroft, B. W., Stewart, G. S. A. B., Lazdunski, A., & Williams, P. (1995). Multiple homologues of LuxR and LuxI control expression of virulence determinants and secondary metabolites through quorum sensing in *Pseudomonas aeruginosa* PAO1. *Molecular Microbiology*, *17*(2), 333-343. https://doi.org/10.1111/j.1365-2958.1995.mmi_17020333.x

Lau, C. K. Y., Krewulak, K. D., & Vogel, H. J. (2016). Bacterial ferrous iron transport: the Feo system. *FEMS microbiology reviews*, *40*(2), 273-298. https://doi.org/10.1093/femsre/fuv049

Lebeaux, D., Chauhan, A., Rendueles, O., & Beloin, C. (2013). From *in vitro* to *in vivo* Models of Bacterial Biofilm-Related Infections. *Pathogens*, *2*(2), 288-356. https://doi.org/10.3390/pathogens2020288

Lebrun, M., Repentigny, J. D., & Mathieu, L. G. (1978). Diminution de l'activité antibactérienne d'antibiotiques dans des cultures et des infections expérimentales mixtes. *Canadian Journal of Microbiology*, *24*(2), 154-161. https://doi.org/10.1139/m78-028

Lee, C. Y., Cheu, R. K., Lemke, M. M., Gustin, A. T., France, M. T., Hampel, B.,…Arnold, K. B. (2020). Quantitative modeling predicts mechanistic links between pre-treatment microbiome composition and metronidazole efficacy in bacterial vaginosis. *Nature Communications*, *11*(1), 6147. https://doi.org/10.1038/s41467-020-19880-w

Lee, T. W. R., Brownlee, K. G., Conway, S. P., Denton, M., & Littlewood, J. M. (2003). Evaluation of a new definition for chronic *Pseudomonas aeruginosa* infection in cystic

fibrosis patients. *Journal of Cystic Fibrosis*, *2*(1), 29-34. https://doi.org/10.1016/S1569-1993(02)00141-8

Lewenza, S., Abboud, J., Poon, K., Kobryn, M., Humplik, I., Bell, J. R.,…Reckseidler-Zenteno, S. (2018). *Pseudomonas aeruginosa* displays a dormancy phenotype during long-term survival in water. *PLOS ONE*, *13*(9), e0198384. https://doi.org/10.1371/journal.pone.0198384

Lewis, K. (2008). Multidrug Tolerance of Biofilms and Persister Cells. In T. Romeo (Ed.), *Bacterial Biofilms* (pp. 107-131). Springer.

Li, H., Handsaker, B., Wysoker, A., Fennell, T., Ruan, J., Homer, N.,…Genome Project Data Processing, S. (2009). The Sequence Alignment/Map format and SAMtools. *Bioinformatics*, *25*(16), 2078-2079. https://doi.org/10.1093/bioinformatics/btp352

Li, J., Hao, C., Ren, L., Xiao, Y., Wang, J., & Qin, X. (2016). Data Mining of Lung Microbiota in Cystic Fibrosis Patients. *PLOS ONE*, *11*(10), e0164510. https://doi.org/10.1371/journal.pone.0164510

Liao, Y., Smyth, G. K., & Shi, W. (2014). featureCounts: an efficient general purpose program for assigning sequence reads to genomic features. *Bioinformatics*, *30*(7), 923-930. https://doi.org/10.1093/bioinformatics/btt656

Limoli, D. H., Whitfield, G. B., Kitao, T., Ivey, M. L., Davis, M. R., Grahl, N.,…Goldberg, J. B. (2017). *Pseudomonas aeruginosa* Alginate Overproduction Promotes Coexistence with *Staphylococcus aureus* in a Model of Cystic Fibrosis Respiratory Infection. *mBio*, *8*(2), e00186-00117. https://doi.org/10.1128/mBio.00186-17

Lin, J., Xu, L., Yang, J., Wang, Z., & Shen, X. (2021). Beyond dueling: roles of the type VI secretion system in microbiome modulation, pathogenesis and stress resistance. *Stress Biology*, *1*(1), 11. https://doi.org/10.1007/s44154-021-00008-z

Lin, J., Zhang, W., Cheng, J., Yang, X., Zhu, K., Wang, Y.,…Shen, X. (2017). A Pseudomonas T6SS effector recruits PQS-containing outer membrane vesicles for iron acquisition. *Nature Communications*, *8*(1), 14888. https://doi.org/10.1038/ncomms14888

Lin, L., Du, Y., Song, J., Wang, W., & Yang, C. (2021). Imaging Commensal Microbiota and Pathogenic Bacteria in the Gut. *Accounts of Chemical Research*, *54*(9), 2076-2087. https://doi.org/10.1021/acs.accounts.1c00068

Ling, K.-M., Stick, S. M., & Kicic, A. (2023). Pulmonary bacteriophage and cystic fibrosis airway mucus: friends or foes? *Frontiers in Medicine*, *10*, 1088494. https://doi.org/10.3389/fmed.2023.1088494Little, W., Black, C., & Smith, A. C. (2021). Clinical Implications of Polymicrobial Synergism Effects on Antimicrobial Susceptibility. *Pathogens*, *10*(2), 144. https://doi.org/10.3390/pathogens10020144

Llamas, M. A., & Sánchez-Jiménez, A. (2022). Iron Homeostasis in *Pseudomonas aeruginosa*: Targeting Iron Acquisition and Storage as an Antimicrobial Strategy. In A. Filloux & J.-L. Ramos (Eds.), *Pseudomonas aeruginosa* (Vol. 1386, pp. 29-68). Springer International Publishing.

Lloyd, K. G., Steen, A. D., Ladau, J., Yin, J., & Crosby, L. (2018). Phylogenetically Novel Uncultured Microbial Cells Dominate Earth Microbiomes. *mSystems*, *3*(5). https://doi.org/10.1128/mSystems.00055-18

Lok, C. (2015). Mining the microbial dark matter. *Nature*, *522*(7556), 270-273. https://doi.org/10.1038/522270a

Long, X., Wang, X., Mao, D., Wu, W., & Luo, Y. (2022). A Novel XRE-Type Regulator Mediates Phage Lytic Development and Multiple Host Metabolic Processes in *Pseudomonas aeruginosa*. *Microbiology Spectrum*, *10*(6), e03511-03522. https://doi.org/10.1128/spectrum.03511-22

Lopes, S. P., Azevedo, N. F., & Pereira, M. O. (2017). Developing a model for cystic fibrosis sociomicrobiology based on antibiotic and environmental stress. *International Journal of Medical Microbiology*, *307*(8), 460-470. https://doi.org/10.1016/j.ijmm.2017.09.018

Lopez-Medina, E., Fan, D., Coughlin, L. A., Ho, E. X., Lamont, I. L., Reimmann, C.,…Koh, A. Y. (2015). *Candida albicans* Inhibits *Pseudomonas aeruginosa* Virulence through Suppression of Pyochelin and Pyoverdine Biosynthesis. *PLOS Pathogens*, *11*(8), e1005129. https://doi.org/10.1371/journal.ppat.1005129

Loss, G., Simões, P. M., Valour, F., Cortês, M. F., Gonzaga, L., Bergot, M.,…Laurent, F. (2019). *Staphylococcus aureus* Small Colony Variants (SCVs): News From a Chronic Prosthetic Joint Infection. *Frontiers in Cellular and Infection Microbiology*, *9*, 363. https://doi.org/10.3389/fcimb.2019.00363

Love, M. I., Huber, W., & Anders, S. (2014). Moderated estimation of fold change and dispersion for RNA-seq data with DESeq2. *Genome Biology*, *15*(12), 550. https://doi.org/10.1186/s13059-014-0550-8

LoVullo, E. D., & Schweizer, H. P. (2020). *Pseudomonas aeruginosa* mexT is an indicator of PAO1 strain integrity. *Journal of Medical Microbiology*, *69*(1), 139-145. https://doi.org/10.1099/jmm.0.001128

Lu, S., & Kolls, J. K. (2021). Early Antibiotics in Cystic Fibrosis: Lessons from the Cystic Fibrosis Pig Model. *American Journal of Respiratory and Critical Care Medicine*, *204*(6), 626-627. https://doi.org/10.1164/rccm.202106-1383ED

Luján, A. M., Paterson, S., Hesse, E., Sommer, L. M., Marvig, R. L., Sharma, M. D.,…Buckling, A. (2022). Polymicrobial infections can select against *Pseudomonas aeruginosa* mutators because of quorum-sensing trade-offs. *Nature Ecology & Evolution*, *6*(7), 979-988. https://doi.org/10.1038/s41559-022-01768-1

Luo, N., Lu, J., Şimşek, E., Silver, A., Yao, Y., Ouyang, X.,…You, L. (2024). The collapse of cooperation during range expansion of *Pseudomonas aeruginosa*. *Nature Microbiology*, *9*(5), 1220-1230. https://doi.org/10.1038/s41564-024-01627-8

López-Jiménez, A. T., & Mostowy, S. (2021). Emerging technologies and infection models in cellular microbiology. *Nature Communications*, *12*(1), 6764. https://doi.org/10.1038/s41467-021-26641-w

Lv, Q., Elders, B. B. L. J., Warris, A., Caudri, D., Ciet, P., & Tiddens, H. A. W. M. (2021). *Aspergillus* -related lung disease in people with cystic fibrosis: can imaging help us to diagnose disease? *European Respiratory Review*, *30*(162), 210103. https://doi.org/10.1183/16000617.0103-2021

Madden, D. E., Baird, T., Bell, S. C., McCarthy, K. L., Price, E. P., & Sarovich, D. S. (2024). Keeping up with the pathogens: improved antimicrobial resistance detection and prediction from *Pseudomonas aeruginosa* genomes. *Genome Medicine*, *16*(1), 78. https://doi.org/10.1186/s13073-024-01346-z

Magalhães, A. P., Jorge, P., & Pereira, M. O. (2019). *Pseudomonas aeruginosa* and *Staphylococcus aureus* communication in biofilm infections: insights through network and database construction. *Critical Reviews in Microbiology*, *45*(5-6), 712-728. https://doi.org/10.1080/1040841X.2019.1700209

Magee, L. C., Louis, M., Khan, V., Micalo, L., & Chaudary, N. (2021). Managing Fungal Infections in Cystic Fibrosis Patients: Challenges in Clinical Practice. *Infection and Drug Resistance*, *14*, 1141-1153. https://doi.org/10.2147/IDR.S267219

Magurran, A. E., & Henderson, P. A. (2003). Explaining the excess of rare species in natural species abundance distributions. *Nature*, *422*(6933), 714-716. https://doi.org/10.1038/nature01547

Majerczyk, C., Schneider, E., & Greenberg, E. P. (2016). Quorum sensing control of Type VI secretion factors restricts the proliferation of quorum-sensing mutants. *eLife*, *5*, e14712. https://doi.org/10.7554/eLife.14712

Martin, M. (2011). Cutadapt removes adapter sequences from high-throughput sequencing reads. *EMBnet.journal*, *17*(1), 10. https://doi.org/10.14806/ej.17.1.200

Martinsen, E. M. H., Eagan, T. M. L., Leiten, E. O., Haaland, I., Husebø, G. R., Knudsen, K. S.,…Nielsen, R. (2021). The pulmonary mycobiome—A study of subjects with and without chronic obstructive pulmonary disease. *PLOS ONE*, *16*(4), e0248967. https://doi.org/10.1371/journal.pone.0248967

Marvig, R. L., Sommer, L. M., Molin, S., & Johansen, H. K. (2015). Convergent evolution and adaptation of *Pseudomonas aeruginosa* within patients with cystic fibrosis. *Nature Genetics*, *47*(1), 57-64. https://doi.org/10.1038/ng.3148

Maseda, H., Saito, K., Nakajima, A., & Nakae, T. (2000). Variation of the mexT gene, a regulator of the MexEF-oprN efflux pump expression in wild-type strains of *Pseudomonas aeruginosa*. *FEMS microbiology letters*, *192*(1), 107-112. https://doi.org/10.1111/j.1574-6968.2000.tb09367.x

Mashburn, L. M., Jett, A. M., Akins, D. R., & Whiteley, M. (2005). *Staphylococcus aureus* Serves as an Iron Source for *Pseudomonas aeruginosa* during In Vivo Coculture. *Journal of Bacteriology*, *187*(2), 554-566. https://doi.org/10.1128/JB.187.2.554-566.2005

Maza, P. K., Bonfim-Melo, A., Padovan, A. C. B., Mortara, R. A., Orikaza, C. M., Ramos, L. M. D.,…Bahia, D. (2017). *Candida albicans*: The Ability to Invade Epithelial Cells and Survive under Oxidative Stress Is Unlinked to Hyphal Length. *Frontiers in Microbiology*, *8*, 1235. https://doi.org/10.3389/fmicb.2017.01235

McAlester, G., O'Gara, F., & Morrissey, J. P. (2008). Signal-mediated interactions between *Pseudomonas aeruginosa* and *Candida albicans*. *Journal of Medical Microbiology*, *57*(5), 563-569. https://doi.org/10.1099/jmm.0.47705-0

McCarron, A., Parsons, D., & Donnelley, M. (2021). Animal and Cell Culture Models for Cystic Fibrosis: Which Model Is Right for Your Application? *The American Journal of Pathology*, *191*(2), 228-242. https://doi.org/10.1016/j.ajpath.2020.10.017

McGarry, M. E., & McColley, S. A. (2021). Cystic fibrosis patients of minority race and ethnicity less likely eligible for CFTR modulators based on *CFTR* genotype. *Pediatric Pulmonology*, *56*(6), 1496-1503. https://doi.org/10.1002/ppul.25285

McKay, I., Van Dorst, J., Katz, T., Doumit, M., Prentice, B., Owens, L.,…Ooi, C. Y. (2023). Diet and the gut-lung axis in cystic fibrosis – direct & indirect links. *Gut Microbes*, *15*(1), 2156254. https://doi.org/10.1080/19490976.2022.2156254

Mehta, H. H., Prater, A. G., Beabout, K., Elworth, R. A. L., Karavis, M., Gibbons, H. S., & Shamoo, Y. (2019). The Essential Role of Hypermutation in Rapid Adaptation to Antibiotic Stress. *Antimicrobial Agents and Chemotherapy*, *63*(7), e00744-00719. https://doi.org/10.1128/AAC.00744-19

Melter, O., & Radojevič, B. (2010). Small colony variants of *Staphylococcus aureus* — review. *Folia Microbiologica*, *55*(6), 548-558. https://doi.org/10.1007/s12223-010-0089-3

Mika, M., Korten, I., Qi, W., Regamey, N., Frey, U., Casaulta, C.,…Hilty, M. (2016). The nasal microbiota in infants with cystic fibrosis in the first year of life: a prospective cohort study. *The Lancet Respiratory Medicine*, *4*(8), 627-635. https://doi.org/10.1016/S2213-2600(16)30081-9

Miranda, S. W., Asfahl, K. L., Dandekar, A. A., & Greenberg, E. P. (2022). *Pseudomonas aeruginosa* Quorum Sensing. In A. Filloux & J.-L. Ramos (Eds.), *Pseudomonas aeruginosa: Biology, Pathogenesis and Control Strategies* (pp. 95-115). Springer International Publishing.

Mitchell, G., Séguin, D. L., Asselin, A.-E., Déziel, E., Cantin, A. M., Frost, E. H.,…Malouin, F. (2010). *Staphylococcus aureus* sigma B-dependent emergence of small-colony variants and biofilm production following exposure to *Pseudomonas aeruginosa* 4-hydroxy-2-

heptylquinoline-N- oxide. *BMC Microbiology*, *10*(1), 33. https://doi.org/10.1186/1471-2180-10-33

Mitra, S., Mallick, A., & Priyadarshini, S. (2022). Effect of Polymicrobial Interactions on Antimicrobial Resistance: An *in vitro* Analysis in Human Ocular Infections. *Future Microbiology*, *17*(7), 491-504. https://doi.org/10.2217/fmb-2021-0114

Moffatt, M. F., & Cookson, W. O. (2017). The lung microbiome in health and disease. *Clinical Medicine*, *17*(6), 525-529. https://doi.org/10.7861/clinmedicine.17-6-525

Montefalcone, M., Parravicini, V., & Bianchi, C. N. (2011). Quantification of Coastal Ecosystem Resilience. In *Treatise on Estuarine and Coastal Science* (pp. 49-70). Elsevier.

Moore, M. P., Lamont, I. L., Williams, D., Paterson, S., Kukavica-Ibrulj, I., Tucker, N. P.,…Winstanley, C. (2021). Transmission, adaptation and geographical spread of the *Pseudomonas aeruginosa* Liverpool epidemic strain. *Microbial Genomics*, *7*(3). https://doi.org/10.1099/mgen.0.000511

Moradali, M. F., Ghods, S., & Rehm, B. H. A. (2017). *Pseudomonas aeruginosa* Lifestyle: A Paradigm for Adaptation, Survival, and Persistence. *Frontiers in Cellular and Infection Microbiology*, *7*. https://doi.org/10.3389/fcimb.2017.00039

Moran Losada, P., Chouvarine, P., Dorda, M., Hedtfeld, S., Mielke, S., Schulz, A.,…Tümmler, B. (2016). The cystic fibrosis lower airways microbial metagenome. *ERJ Open Research*, *2*(2), 00096-02015. https://doi.org/10.1183/23120541.00096-2015

Moreno-Fenoll, C., Ardré, M., & Rainey, P. B. (2024). Polar accumulation of pyoverdin and exit from stationary phase. *microLife*, *5*, uqae001. https://doi.org/10.1093/femsml/uqae001

Mould, D. L., Finger, C. E., Conaway, A., Botelho, N., Stuut, S. E., & Hogan, D. A. (2024). Citrate cross-feeding by *Pseudomonas aeruginosa* supports lasR mutant fitness. *mBio*, *15*(2), e0127823. https://doi.org/10.1128/mbio.01278-23

Mould, D. L., Stevanovic, M., Ashare, A., Schultz, D., & Hogan, D. A. (2022). Metabolic basis for the evolution of a common pathogenic *Pseudomonas aeruginosa* variant. *eLife*, *11*, e76555. https://doi.org/10.7554/eLife.76555

Murray, E. J., Dubern, J.-F., Chan, W. C., Chhabra, S. R., & Williams, P. (2022). A *Pseudomonas aeruginosa* PQS quorum-sensing system inhibitor with anti-staphylococcal activity sensitizes polymicrobial biofilms to tobramycin. *Cell Chemical Biology*, *29*(7), 1187-1199.e1186. https://doi.org/10.1016/j.chembiol.2022.02.007

Nabb, D. L., Song, S., Kluthe, K. E., Daubert, T. A., Luedtke, B. E., & Nuxoll, A. S. (2019). Polymicrobial Interactions Induce Multidrug Tolerance in *Staphylococcus aureus* Through Energy Depletion. *Frontiers in Microbiology*, *10*. https://doi.org/10.3389/fmicb.2019.02803

Nair, R. R., & Andersson, D. I. (2023). Inter-species interaction reduces selection for antibiotic resistance in Escherichia coli. *Communications Biology*, *6*(1), 1-9. https://doi.org/10.1038/s42003-023-04716-2

Naito, Y., Charman, S., Duckers, J., Clarke, S., Hughes, S., Kisanga, M.,…Cystic Fibrosis, T. (2023). *UK Cystic Fibrosis Registry 2022 Annual Data Report*. https://www.cysticfibrosis.org.uk/sites/default/files/2023-10/CFT_2022_Annual_Data_Report_FINAL_v8.pdf

Neve, R. L., Carrillo, B. D., & Phelan, V. V. (2021). Impact of Artificial Sputum Medium Formulation on *Pseudomonas aeruginosa* Secondary Metabolite Production. *Journal of Bacteriology*, *203*(21), e00250-00221. https://doi.org/10.1128/JB.00250-21

Nguyen, D., & Singh, P. K. (2006). Evolving stealth: Genetic adaptation of *Pseudomonas aeruginosa* during cystic fibrosis infections. *Proceedings of the National Academy of Sciences*, *103*(22), 8305-8306. https://doi.org/10.1073/pnas.0602526103

Nishanth Kumar, S., Nisha, G. V., Sudaresan, A., Venugopal, V. V., Sree Kumar, M. M., Lankalapalli, R. S., & Dileep Kumar, B. S. (2014). Synergistic activity of phenazines

isolated from *Pseudomonas aeruginosa* in combination with azoles against Candida species. *Medical Mycology*, *52*(5), 482-490. https://doi.org/10.1093/mmy/myu012

Nolan, L. M., & Allsopp, L. P. (2022). Antimicrobial Weapons of *Pseudomonas aeruginosa*. In A. Filloux & J.-L. Ramos (Eds.), *Pseudomonas aeruginosa* (Vol. 1386, pp. 223-256). Springer International Publishing.

Nolan, C., & Behrends, V. (2021). Sub-Inhibitory Antibiotic Exposure and Virulence in Pseudomonas aeruginosa. *Antibiotics*, *10*(11), 1393. https://doi.org/10.3390/antibiotics10111393

Nolan, L. M., Cain, A. K., Clamens, T., Furniss, R. C. D., Manoli, E., Sainz-Polo, M. A.,…Filloux, A. (2021). Identification of Tse8 as a Type VI secretion system toxin from *Pseudomonas aeruginosa* that targets the bacterial transamidosome to inhibit protein synthesis in prey cells. *Nature Microbiology*, *6*(9), 1199-1210. https://doi.org/10.1038/s41564-021-00950-8

O'Brien, T. J. (2021). *In vitro Recapitulation of the Polymicrobial Communities Associated with Cystic Fibrosis Airway Infections* [dissertation]. https://www.repository.cam.ac.uk/handle/1810/323425

O'Brien, T. J., Figueroa, W., & Welch, M. (2022). Decreased efficacy of antimicrobial agents in a polymicrobial environment. *The ISME Journal*, *16*(7), 1694-1704. https://doi.org/10.1038/s41396-022-01218-7

O'Brien, T. J., & Welch, M. (2019). Recapitulation of polymicrobial communities associated with cystic fibrosis airway infections: a perspective. *Future Microbiology*, *14*(16), 1437-1450. https://doi.org/10.2217/fmb-2019-0200

Oliver, A., & Mena, A. (2010). Bacterial hypermutation in cystic fibrosis, not only for antibiotic resistance. *Clinical Microbiology and Infection*, *16*(7), 798-808. https://doi.org/10.1111/j.1469-0691.2010.03250.x

Oluyombo, O., Penfold, C. N., & Diggle, S. P. (2019). Competition in Biofilms between Cystic Fibrosis Isolates of *Pseudomonas aeruginosa* Is Shaped by R-Pyocins. *mBio*, *10*(1), e01828-01818. https://doi.org/10.1128/mBio.01828-18

On, Y. Y., Figueroa, W., Fan, C., Ho, P.-M., Bényei, É. B., Weimann, A.,…Welch, M. (2023). Impact of transient acquired hypermutability on the inter- and intra-species competitiveness of *Pseudomonas aeruginosa*. *The ISME Journal*, *17*(11), 1931-1939. https://doi.org/10.1038/s41396-023-01503-z

Orazi, G., & O'Toole, G. A. (2017). *Pseudomonas aeruginosa* Alters *Staphylococcus aureus* Sensitivity to Vancomycin in a Biofilm Model of Cystic Fibrosis Infection. *mBio*, *8*(4), e00873-00817. https://doi.org/10.1128/mBio.00873-17

Orazi, G., & O'Toole, G. A. (2019). "It Takes a Village": Mechanisms Underlying Antimicrobial Recalcitrance of Polymicrobial Biofilms. *Journal of Bacteriology*, *202*(1). https://doi.org/10.1128/JB.00530-19

Orazi, G., Ruoff, K. L., & O'Toole, G. A. (2019). *Pseudomonas aeruginosa* Increases the Sensitivity of Biofilm-Grown *Staphylococcus aureus* to Membrane-Targeting Antiseptics and Antibiotics. *mBio*, *10*(4), e01501-01519. https://doi.org/10.1128/mBio.01501-19

Ovchinnikova, E. S., Krom, B. P., Mei, H. C. v. d., & Busscher, H. J. (2012). Force microscopic and thermodynamic analysis of the adhesion between *Pseudomonas aeruginosa* and *Candida albicans*. *Soft Matter*, *8*(24), 6454-6461. https://doi.org/10.1039/C2SM25100K

O'Brien, T. J., & Welch, M. (2019). A Continuous-Flow Model for in vitro Cultivation of Mixed Microbial Populations Associated With Cystic Fibrosis Airway Infections. *Frontiers in Microbiology*, *10*, 2713. https://doi.org/10.3389/fmicb.2019.02713

O'Connor, K., Zhao, C. Y., Mei, M., & Diggle, S. P. (2022). Frequency of quorum-sensing mutations in *Pseudomonas aeruginosa* strains isolated from different environments. *Microbiology*, *168*(12), 001265. https://doi.org/10.1099/mic.0.001265

O'Toole, G. A., Crabbé, A., Kümmerli, R., LiPuma, J. J., Bomberger, J. M., Davies, J. C.,…Whiteson, K. (2021). Model Systems to Study the Chronic, Polymicrobial Infections in Cystic Fibrosis: Current Approaches and Exploring Future Directions. *mBio*, *12*(5), e01763-01721. https://doi.org/10.1128/mBio.01763-21

Özkaya, Ö., Balbontín, R., Gordo, I., & Xavier, K. B. (2018). Cheating on Cheaters Stabilizes Cooperation in *Pseudomonas aeruginosa*. *Current Biology*, *28*(13), 2070-2080.e2076. https://doi.org/10.1016/j.cub.2018.04.093

Özkaya, Ö., Xavier, K. B., Dionisio, F., & Balbontín, R. (2017). Maintenance of Microbial Cooperation Mediated by Public Goods in Single- and Multiple-Trait Scenarios. *Journal of Bacteriology*, *199*(22). https://doi.org/10.1128/JB.00297-17

Paine, R. T. (1966). Food Web Complexity and Species Diversity. *The American Naturalist*, *100*(910), 65-75.

Paine, R. T. (1969). A Note on Trophic Complexity and Community Stability. *The American Naturalist*, *103*(929), 91-93. https://doi.org/10.1086/282586

Pajon, C., Fortoul, M. C., Diaz-Tang, G., Marin Meneses, E., Kalifa, A. R., Sevy, E.,…Smith, R. P. (2023). Interactions between metabolism and growth can determine the co-existence of *Staphylococcus aureus* and *Pseudomonas aeruginosa*. *eLife*, *12*, e83664. https://doi.org/10.7554/eLife.83664

Pallett, R., Leslie, L. J., Lambert, P. A., Milic, I., Devitt, A., & Marshall, L. J. (2019). Anaerobiosis influences virulence properties of *Pseudomonas aeruginosa* cystic fibrosis isolates and the interaction with *Staphylococcus aureus*. *Scientific Reports*, *9*(1), 6748. https://doi.org/10.1038/s41598-019-42952-x

Palmer, K. L., Aye, L. M., & Whiteley, M. (2007). Nutritional Cues Control *Pseudomonas aeruginosa* Multicellular Behavior in Cystic Fibrosis Sputum. *Journal of Bacteriology*, *189*(22), 8079-8087. https://doi.org/10.1128/JB.01138-07

Pammi, M., Liang, R., Hicks, J., Mistretta, T.-A., & Versalovic, J. (2013). Biofilm extracellular DNA enhances mixed species biofilms of Staphylococcus epidermidis and *Candida albicans*. *BMC Microbiology*, *13*(1), 257. https://doi.org/10.1186/1471-2180-13-257

Passador, L., Cook, J. M., Gambello, M. J., Rust, L., & Iglewski, B. H. (1993). Expression of *Pseudomonas aeruginosa* Virulence Genes Requires Cell-to-Cell Communication. *Science*, *260*(5111), 1127-1130. https://doi.org/10.1126/science.8493556

Pasteur, L., & Joubert, J. (1877). *Charbon et septicémie*. Gauthier-Villars.

Patangia, D. V., Anthony Ryan, C., Dempsey, E., Paul Ross, R., & Stanton, C. (2022). Impact of antibiotics on the human microbiome and consequences for host health. *MicrobiologyOpen*, *11*(1), e1260. https://doi.org/10.1002/mbo3.1260

Patel, R. (2005). Biofilms and Antimicrobial Resistance. *Clinical Orthopaedics and Related Research*, *&NA;*(437), 41-47. https://doi.org/10.1097/01.blo.0000175714.68624.74

Patriquin, G. M., Banin, E., Gilmour, C., Tuchman, R., Greenberg, E. P., & Poole, K. (2008). Influence of Quorum Sensing and Iron on Twitching Motility and Biofilm Formation in *Pseudomonas aeruginosa*. *Journal of Bacteriology*, *190*(2), 662-671. https://doi.org/10.1128/JB.01473-07

Peleg, A. Y., Hogan, D. A., & Mylonakis, E. (2010). Medically important bacterial–fungal interactions. *Nature Reviews Microbiology*, *8*(5), 340-349. https://doi.org/10.1038/nrmicro2313

Pernet, E., Guillemot, L., Burgel, P.-R., Martin, C., Lambeau, G., Sermet-Gaudelus, I.,…Touqui, L. (2014). *Pseudomonas aeruginosa* eradicates *Staphylococcus aureus* by manipulating the host immunity. *Nature Communications*, *5*(1), 5105. https://doi.org/10.1038/ncomms6105

Pesci, E. C., Pearson, J. P., Seed, P. C., & Iglewski, B. H. (1997). Regulation of las and rhl quorum sensing in *Pseudomonas aeruginosa*. *Journal of Bacteriology*, *179*(10), 3127-3132. https://doi.org/10.1128/jb.179.10.3127-3132.1997

Peters, B. A., Hayes, R. B., Goparaju, C., Reid, C., Pass, H. I., & Ahn, J. (2019). The Microbiome in Lung Cancer Tissue and Recurrence-Free Survival. *Cancer Epidemiology, Biomarkers & Prevention*, *28*(4), 731-740. https://doi.org/10.1158/1055-9965.EPI-18-0966

Peters, B. M., Ovchinnikova, E. S., Krom, B. P., Schlecht, L. M., Zhou, H., Hoyer, L. L.,…Shirtliff, M. E. (2012). *Staphylococcus aureus* adherence to *Candida albicans* hyphae is mediated by the hyphal adhesin Als3p. *Microbiology*, *158*(12), 2975-2986. https://doi.org/10.1099/mic.0.062109-0

Peters, B. M., Ward, R. M., Rane, H. S., Lee, S. A., & Noverr, M. C. (2013). Efficacy of Ethanol against *Candida albicans* and *Staphylococcus aureus* Polymicrobial Biofilms. *Antimicrobial Agents and Chemotherapy*, *57*(1), 74-82. https://doi.org/10.1128/AAC.01599-12

Phelan, V. V., Moree, W. J., Aguilar, J., Cornett, D. S., Koumoutsi, A., Noble, S. M.,…Dorrestein, P. C. (2014). Impact of a Transposon Insertion in *phzF2* on the Specialized Metabolite Production and Interkingdom Interactions of *Pseudomonas aeruginosa*. *Journal of Bacteriology*, *196*(9), 1683-1693. https://doi.org/10.1128/JB.01258-13

Phuengmaung, P., Somparn, P., Panpetch, W., Singkham-In, U., Wannigama, D. L., Chatsuwan, T., & Leelahavanichkul, A. (2020). Coexistence of *Pseudomonas aeruginosa* With *Candida albicans* Enhances Biofilm Thickness Through Alginate-Related Extracellular Matrix but Is Attenuated by N-acetyl-l-cysteine. *Frontiers in Cellular and Infection Microbiology*, *10*, 594336. https://doi.org/10.3389/fcimb.2020.594336

Powell, J. R., & Ausubel, F. M. (2008). Models of Caenorhabditis elegans Infection by Bacterial and Fungal Pathogens. In J. Ewbank & E. Vivier (Eds.), *Innate Immunity* (pp. 403-427). Humana Press.

Price, C. E., Brown, D. G., Limoli, D. H., Phelan, V. V., & O'Toole, G. A. (2020). Exogenous Alginate Protects *Staphylococcus aureus* from Killing by *Pseudomonas aeruginosa*. *Journal of Bacteriology*, *202*(8). https://doi.org/10.1128/JB.00559-19

Price, K. E., Hampton, T. H., Gifford, A. H., Dolben, E. L., Hogan, D. A., Morrison, H. G.,…O'Toole, G. A. (2013). Unique microbial communities persist in individual cystic fibrosis patients throughout a clinical exacerbation. *Microbiome*, *1*(1), 27. https://doi.org/10.1186/2049-2618-1-27

Quinn, R. A., Whiteson, K., Lim, Y.-W., Salamon, P., Bailey, B., Mienardi, S.,…Rohwer, F. (2015). A Winogradsky-based culture system shows an association between microbial fermentation and cystic fibrosis exacerbation. *The ISME Journal*, *9*(4), 1024-1038. https://doi.org/10.1038/ismej.2014.234

Radlinski, L., Rowe, S. E., Kartchner, L. B., Maile, R., Cairns, B. A., Vitko, N. P.,…Conlon, B. P. (2017). *Pseudomonas aeruginosa* exoproducts determine antibiotic efficacy against *Staphylococcus aureus*. *PLOS Biology*, *15*(11), e2003981. https://doi.org/10.1371/journal.pbio.2003981

Rampioni, G., Pustelny, C., Fletcher, M. P., Wright, V. J., Bruce, M., Rumbaugh, K. P.,…Williams, P. (2010). Transcriptomic analysis reveals a global alkyl-quinolone-independent regulatory role for PqsE in facilitating the environmental adaptation of *Pseudomonas aeruginosa* to plant and animal hosts. *Environmental Microbiology*, *12*(6), 1659-1673. https://doi.org/10.1111/j.1462-2920.2010.02214.x

Rapala-Kozik, M., Surowiec, M., Juszczak, M., Wronowska, E., Kulig, K., Bednarek, A.,…Kozik, A. (2023). Living together: The role of *Candida albicans* in the formation of polymicrobial biofilms in the oral cavity. *Yeast*, *40*(8), 303-317. https://doi.org/10.1002/yea.3855

Reece, E., Bettio, P. H. D. A., & Renwick, J. (2021). Polymicrobial Interactions in the Cystic Fibrosis Airway Microbiome Impact the Antimicrobial Susceptibility of *Pseudomonas aeruginosa*. *Antibiotics*, *10*(7), 827. https://doi.org/10.3390/antibiotics10070827

Reen, F. J., Mooij, M. J., Holcombe, L. J., McSweeney, C. M., McGlacken, G. P., Morrissey, J. P., & O'Gara, F. (2011). The Pseudomonas quinolone signal (PQS), and its precursor HHQ, modulate inter-species and interkingdom behaviour. *FEMS microbiology ecology*, *77*(2), 413-428. https://doi.org/10.1111/j.1574-6941.2011.01121.x

Rees, V. E., Deveson Lucas, D. S., López-Causapé, C., Huang, Y., Kotsimbos, T., Bulitta, J. B.,…Landersdorfer, C. B. (2019). Characterization of Hypermutator *Pseudomonas aeruginosa* Isolates from Patients with Cystic Fibrosis in Australia. *Antimicrobial Agents and Chemotherapy*, *63*(4), e02538-02518. https://doi.org/10.1128/AAC.02538-18

Reinhart, A., & Oglesby-Sherrouse, A. (2016). Regulation of *Pseudomonas aeruginosa* Virulence by Distinct Iron Sources. *Genes*, *7*(12), 126. https://doi.org/10.3390/genes7120126

Rickard, A. H., Palmer, R. J., Blehert, D. S., Campagna, S. R., Semmelhack, M. F., Egland, P. G.,…Kolenbrander, P. E. (2006). Autoinducer 2: a concentration-dependent signal for mutualistic bacterial biofilm growth. *Molecular Microbiology*, *60*(6), 1446-1456. https://doi.org/10.1111/j.1365-2958.2006.05202.x

Rinke, C., Schwientek, P., Sczyrba, A., Ivanova, N. N., Anderson, I. J., Cheng, J.-F.,…Woyke, T. (2013). Insights into the phylogeny and coding potential of microbial dark matter. *Nature*, *499*(7459), 431-437. https://doi.org/10.1038/nature12352

Riordan, J. R., Rommens, J. M., Kerem, B.-S., Alon, N., Rozmahel, R., Grzelczak, Z.,…Tsui, L.-C. (1989). Identification of the Cystic Fibrosis Gene: Cloning and Characterization of Complementary DNA. *Science*, *245*(4922), 1066-1073. https://doi.org/10.1126/science.2475911

Robinson, T., Smith, P., Alberts, E. R., Colussi-Pelaez, M., & Schuster, M. (2020). Cooperation and Cheating through a Secreted Aminopeptidase in the *Pseudomonas aeruginosa* RpoS Response. *mBio*, *11*(2), e03090-03019. https://doi.org/10.1128/mBio.03090-19

Rojas Murcia, N., Lee, X., Waridel, P., Maspoli, A., Imker, H. J., Chai, T.,…Reimmann, C. (2015). The *Pseudomonas aeruginosa* antimetabolite L -2-amino-4-methoxy-trans-3-butenoic acid (AMB) is made from glutamate and two alanine residues via a thiotemplate-linked tripeptide precursor. *Frontiers in Microbiology*, *6*. https://doi.org/10.3389/fmicb.2015.00170

Rolain, J.-M., Hraiech, S., Papazian, L., & Bregeon, F. (2015). Animal models of polymicrobial pneumonia. *Drug Design, Development and Therapy*, 3279. https://doi.org/10.2147/DDDT.S70993

Rutherford, S. T., & Bassler, B. L. (2012). Bacterial Quorum Sensing: Its Role in Virulence and Possibilities for Its Control. *Cold Spring Harbor Perspectives in Medicine*, *2*(11), a012427-a012427. https://doi.org/10.1101/cshperspect.a012427

Saluzzo, F., Riberi, L., Messore, B., Loré, N. I., Esposito, I., Bignamini, E., & De Rose, V. (2022). CFTR Modulator Therapies: Potential Impact on Airway Infections in Cystic Fibrosis. *Cells*, *11*(7), 1243. https://doi.org/10.3390/cells11071243

Sandoz, K. M., Mitzimberg, S. M., & Schuster, M. (2007). Social cheating in *Pseudomonas aeruginosa* quorum sensing. *Proceedings of the National Academy of Sciences*, *104*(40), 15876-15881. https://doi.org/10.1073/pnas.0705653104

Santos-Fernandez, E., Martin-Souto, L., Antoran, A., Areitio, M., Aparicio-Fernandez, L., Bouchara, J.-P.,…Ramirez-Garcia, A. (2023). Microbiota and fungal-bacterial interactions in the cystic fibrosis lung. *FEMS Microbiology Reviews*, *47*(3), fuad029. https://doi.org/10.1093/femsre/fuad029

Savage, H. P., Bays, D. J., Tiffany, C. R., Gonzalez, M. A. F., Bejarano, E. J., Carvalho, T. P.,…Bäumler, A. J. (2024). Epithelial hypoxia maintains colonization resistance against *Candida albicans*. *Cell Host & Microbe*, *32*(7), 1103-1113.e1106. https://doi.org/10.1016/j.chom.2024.05.008

Schuster, M., Lostroh, C. P., Ogi, T., & Greenberg, E. P. (2003). Identification, Timing, and Signal Specificity of *Pseudomonas aeruginosa* Quorum-Controlled Genes: a Transcriptome Analysis. *Journal of Bacteriology*, *185*(7), 2066-2079. https://doi.org/10.1128/JB.185.7.2066-2079.2003

Secor, P. R., Burgener, E. B., Kinnersley, M., Jennings, L. K., Roman-Cruz, V., Popescu, M.,…Bollyky, P. L. (2020). Pf Bacteriophage and Their Impact on Pseudomonas Virulence, Mammalian Immunity, and Chronic Infections. *Frontiers in Immunology*, *11*, 244. https://doi.org/10.3389/fimmu.2020.00244

Secor, P. R., Michaels, L. A., Ratjen, A., Jennings, L. K., & Singh, P. K. (2018). Entropically driven aggregation of bacteria by host polymers promotes antibiotic tolerance in *Pseudomonas aeruginosa*. *Proceedings of the National Academy of Sciences of the United States of America*, *115*(42), 10780-10785. https://doi.org/10.1073/pnas.1806005115

Seemann, T. (2014). Prokka: rapid prokaryotic genome annotation. *Bioinformatics*, *30*(14), 2068-2069. https://doi.org/10.1093/bioinformatics/btu153

Short, B., Bakri, A., Baz, A., Williams, C., Brown, J., & Ramage, G. (2023). There Is More to Wounds than Bacteria: Fungal Biofilms in Chronic Wounds. *Current Clinical Microbiology Reports*, *10*(1), 9-16. https://doi.org/10.1007/s40588-022-00187-x

Shteinberg, M., Haq, I. J., Polineni, D., & Davies, J. C. (2021). Cystic fibrosis. *The Lancet*, *397*(10290), 2195-2211. https://doi.org/10.1016/S0140-6736(20)32542-3

Sidransky, H., & Pearl, M. A. (1961). Pulmonary Fungus Infections Associated with Steroid and Antibiotic Therapy. *Diseases of the Chest*, *39*(6), 630-642. https://doi.org/10.1378/chest.39.6.630

Simanek, K. A., Schumacher, M. L., Mallery, C. P., Shen, S., Li, L., & Paczkowski, J. E. (2023). Quorum-sensing synthase mutations re-calibrate autoinducer concentrations in clinical

isolates of *Pseudomonas aeruginosa* to enhance pathogenesis. *Nature Communications*, *14*(1), 7986. https://doi.org/10.1038/s41467-023-43702-4

Smith, E. E., Buckley, D. G., Wu, Z., Saenphimmachak, C., Hoffman, L. R., D'Argenio, D. A.,…Olson, M. V. (2006). Genetic adaptation by *Pseudomonas aeruginosa* to the airways of cystic fibrosis patients. *Proceedings of the National Academy of Sciences*, *103*(22), 8487-8492. https://doi.org/10.1073/pnas.0602138103

Song, L., Xu, L., Wu, T., Shi, Z., Kareem, H. A., Wang, Z.,…Shen, X. (2024). Trojan horselike T6SS effector TepC mediates both interference competition and exploitative competition. *The ISME Journal*, *18*(1), wrad028. https://doi.org/10.1093/ismejo/wrad028

Soret, P., Vandenborght, L.-E., Francis, F., Coron, N., Enaud, R., Avalos, M.,…Turck, D. (2020). Respiratory mycobiome and suggestion of inter-kingdom network during acute pulmonary exacerbation in cystic fibrosis. *Scientific Reports*, *10*(1), 3589. https://doi.org/10.1038/s41598-020-60015-4

Spatz, M., Da Costa, G., Ventin-Holmberg, R., Planchais, J., Michaudel, C., Wang, Y.,…Richard, M. L. (2023). Antibiotic treatment using amoxicillin-clavulanic acid impairs gut mycobiota development through modification of the bacterial ecosystem. *Microbiome*, *11*(1), 73. https://doi.org/10.1186/s40168-023-01516-y

Stiefel, P., Schmidt-Emrich, S., Maniura-Weber, K., & Ren, Q. (2015). Critical aspects of using bacterial cell viability assays with the fluorophores SYTO9 and propidium iodide. *BMC Microbiology*, *15*(1), 36. https://doi.org/10.1186/s12866-015-0376-x

Stoltz, D. A., Meyerholz, D. K., & Welsh, M. J. (2015). Origins of Cystic Fibrosis Lung Disease. *New England Journal of Medicine*, *372*(4), 351-362. https://doi.org/10.1056/NEJMra1300109

Stover, C. K., Pham, X.-Q. T., Erwin, A. L., Mizoguchi, S. D., Warrener, P., Hickey, M. J.,…Olson, M. V. (2000). Complete genome sequence of *Pseudomonas aeruginosa* PAO1, an

opportunistic pathogen. *Nature*, *406*(6799), 959-964. https://doi.org/10.1038/35023079

Sun, X., Olivier, A. K., Liang, B., Yi, Y., Sui, H., Evans, T. I. A.,…Engelhardt, J. F. (2014). Lung Phenotype of Juvenile and Adult Cystic Fibrosis Transmembrane Conductance Regulator–Knockout Ferrets. *American Journal of Respiratory Cell and Molecular Biology*, *50*(3), 502-512. https://doi.org/10.1165/rcmb.2013-0261OC

Surette, M. G. (2014). The Cystic Fibrosis Lung Microbiome. *Annals of the American Thoracic Society*, *11*(Supplement 1), S61-S65. https://doi.org/10.1513/AnnalsATS.201306-159MG

Sweeney, E., Harrington, N. E., Harley Henriques, A. G., Hassan, M. M., Crealock-Ashurst, B., Smyth, A. R.,…Harrison, F. (2021). An ex vivo cystic fibrosis model recapitulates key clinical aspects of chronic *Staphylococcus aureus* infection. *Microbiology*, *167*(1). https://doi.org/10.1099/mic.0.000987

Sweeney, E., Hassan, M. M., Harrington, N. E., Smyth, A. R., Hurley, M. N., Tormo-Mas, M. Á., & Harrison, F. (2019). *An ex vivo cystic fibrosis model recapitulates key clinical aspects of chronic Staphylococcus aureus infection* [preprint]. http://biorxiv.org/lookup/doi/10.1101/604363

Syal, K., Mo, M., Yu, H., Iriya, R., Jing, W., Guodong, S.,…Tao, N. (2017). Current and emerging techniques for antibiotic susceptibility tests. *Theranostics*, *7*(7), 1795-1805. https://doi.org/10.7150/thno.19217

Szklarczyk, D., Kirsch, R., Koutrouli, M., Nastou, K., Mehryary, F., Hachilif, R.,…von Mering, C. (2023). The STRING database in 2023: protein–protein association networks and functional enrichment analyses for any sequenced genome of interest. *Nucleic Acids Research*, *51*(D1), D638-D646. https://doi.org/10.1093/nar/gkac1000

Sánchez-Jiménez, A., Marcos-Torres, F. J., & Llamas, M. A. (2023). Mechanisms of iron homeostasis in *Pseudomonas aeruginosa* and emerging therapeutics directed to

disrupt this vital process. *Microbial Biotechnology*, *16*(7), 1475-1491. https://doi.org/10.1111/1751-7915.14241

Taccetti, G., Francalanci, M., Pizzamiglio, G., Messore, B., Carnovale, V., Cimino, G., & Cipolli, M. (2021). Cystic Fibrosis: Recent Insights into Inhaled Antibiotic Treatment and Future Perspectives. *Antibiotics*, *10*(3), 338. https://doi.org/10.3390/antibiotics10030338

Tang, H. B., DiMango, E., Bryan, R., Gambello, M., Iglewski, B. H., Goldberg, J. B., & Prince, A. (1996). Contribution of specific *Pseudomonas aeruginosa* virulence factors to pathogenesis of pneumonia in a neonatal mouse model of infection. *Infection and Immunity*, *64*(1), 37-43. https://doi.org/10.1128/iai.64.1.37-43.1996

Taylor, N. M. I., Prokhorov, N. S., Guerrero-Ferreira, R. C., Shneider, M. M., Browning, C., Goldie, K. N.,…Leiman, P. G. (2016). Structure of the T4 baseplate and its function in triggering sheath contraction. *Nature*, *533*(7603), 346-352. https://doi.org/10.1038/nature17971

CFTR2. (2023). *The Clinical and Functional TRanslation of CFTR*. https://cftr2.org/

Thomas, P., Sekhar, A. C., Upreti, R., Mujawar, M. M., & Pasha, S. S. (2015). Optimization of single plate-serial dilution spotting (SP-SDS) with sample anchoring as an assured method for bacterial and yeast cfu enumeration and single colony isolation from diverse samples. *Biotechnology Reports*, *8*, 45-55. https://doi.org/10.1016/j.btre.2015.08.003

Thornton, C. S., Acosta, N., Surette, M. G., & Parkins, M. D. (2022). Exploring the Cystic Fibrosis Lung Microbiome: Making the Most of a Sticky Situation. *Journal of the Pediatric Infectious Diseases Society*, *11*(Supplement_2), S13-S22. https://doi.org/10.1093/jpids/piac036

Thöming, J. G., & Häussler, S. (2022). Transcriptional Profiling of *Pseudomonas aeruginosa* Infections. In A. Filloux & J.-L. Ramos (Eds.), *Pseudomonas aeruginosa* (Vol. 1386, pp. 303-323). Springer International Publishing.

Todd, O. A., Fidel, P. L., Harro, J. M., Hilliard, J. J., Tkaczyk, C., Sellman, B. R.,…Peters, B. M. (2019). *Candida albicans* Augments *Staphylococcus aureus* Virulence by Engaging the Staphylococcal *agr* Quorum Sensing System. *mBio*, *10*(3), e00910-00919. https://doi.org/10.1128/mBio.00910-19

Tognon, M., Köhler, T., Gdaniec, B. G., Hao, Y., Lam, J. S., Beaume, M.,…Van Delden, C. (2017). Co-evolution with *Staphylococcus aureus* leads to lipopolysaccharide alterations in *Pseudomonas aeruginosa*. *The ISME Journal*, *11*(10), 2233-2243. https://doi.org/10.1038/ismej.2017.83

Tognon, M., Köhler, T., Luscher, A., & van Delden, C. (2019). Transcriptional profiling of *Pseudomonas aeruginosa* and *Staphylococcus aureus* during in vitro co-culture. *BMC Genomics*, *20*(1), 30. https://doi.org/10.1186/s12864-018-5398-y

Tolker-Nielsen, T., & Sternberg, C. (2011). Growing and Analyzing Biofilms in Flow Chambers. *Current Protocols in Microbiology*, *21*(1). https://doi.org/10.1002/9780471729259.mc01b02s21

Torres, A., Kasturiarachi, N., DuPont, M., Cooper, V. S., Bomberger, J., & Zemke, A. (2019). NADH Dehydrogenases in *Pseudomonas aeruginosa* Growth and Virulence. *Frontiers in Microbiology*, *10*, 75. https://doi.org/10.3389/fmicb.2019.00075

Trejo-Hernández, A., Andrade-Domínguez, A., Hernández, M., & Encarnación, S. (2014). Inter-species competition triggers virulence and mutability in *Candida albicans* – *Pseudomonas aeruginosa* mixed biofilms. *The ISME Journal*, *8*(10), 1974-1988. https://doi.org/10.1038/ismej.2014.53

Trizna, E. Y., Yarullina, M. N., Baidamshina, D. R., Mironova, A. V., Akhatova, F. S., Rozhina, E. V.,…Kayumov, A. R. (2020). Bidirectional alterations in antibiotics susceptibility in *Staphylococcus aureus—Pseudomonas aeruginosa* dual-species biofilm. *Scientific Reports*, *10*(1), 14849. https://doi.org/10.1038/s41598-020-71834-w

Trouillon, J., Ragno, M., Simon, V., Attrée, I., & Elsen, S. (2021). Transcription Inhibitors with XRE DNA-Binding and Cupin Signal-Sensing Domains Drive Metabolic Diversification in *Pseudomonas*. *mSystems*, *6*(1), e00753-00720. https://doi.org/10.1128/mSystems.00753-20

Turner, K. H., Wessel, A. K., Palmer, G. C., Murray, J. L., & Whiteley, M. (2015). Essential genome of *Pseudomonas aeruginosa* in cystic fibrosis sputum. *Proceedings of the National Academy of Sciences*, *112*(13), 4110-4115. https://doi.org/10.1073/pnas.1419677112

Van Der Gast, C. J., Walker, A. W., Stressmann, F. A., Rogers, G. B., Scott, P., Daniels, T. W.,…Bruce, K. D. (2011). Partitioning core and satellite taxa from within cystic fibrosis lung bacterial communities. *The ISME Journal*, *5*(5), 780-791. https://doi.org/10.1038/ismej.2010.175

Van Woerden, H. C., Gregory, C., Brown, R., Marchesi, J. R., Hoogendoorn, B., & Matthews, I. P. (2013). Differences in fungi present in induced sputum samples from asthma patients and non-atopic controls: a community based case control study. *BMC Infectious Diseases*, *13*(1), 69. https://doi.org/10.1186/1471-2334-13-69

Vandecandelaere, I., Nieuwerburgh, F. V., Deforce, D., & Coenye, T. (2017). Metabolic activity, urease production, antibiotic resistance and virulence in dual species biofilms of Staphylococcus epidermidis and *Staphylococcus aureus*. *PLOS ONE*, *12*(3), e0172700. https://doi.org/10.1371/journal.pone.0172700

Vasiljevs, S., Gupta, A., & Baines, D. (2023). Effect of glucose on growth and co-culture of *Staphylococcus aureus* and *Pseudomonas aeruginosa* in artificial sputum medium. *Heliyon*, *9*(11), e21469. https://doi.org/10.1016/j.heliyon.2023.e21469

Veit, G., Avramescu, R. G., Chiang, A. N., Houck, S. A., Cai, Z., Peters, K. W.,…Lukacs, G. L. (2016). From CFTR biology toward combinatorial pharmacotherapy: expanded classification of cystic fibrosis mutations. *Molecular Biology of the Cell*, *27*(3), 424-433. https://doi.org/10.1091/mbc.e14-04-0935

Vila, T., Kong, E. F., Montelongo-Jauregui, D., Van Dijck, P., Shetty, A. C., McCracken, C.,…Jabra-Rizk, M. A. (2021). Therapeutic implications of *C. albicans-S. aureus* mixed biofilm in a murine subcutaneous catheter model of polymicrobial infection. *Virulence*, *12*(1), 835-851. https://doi.org/10.1080/21505594.2021.1894834

Wang, G. Z., Warren, E. A., Haas, A. L., Peña, A. S., Kiedrowski, M. R., Lomenick, B.,…Limoli, D. H. (2023). *Staphylococcal secreted cytotoxins are competition sensing signals for Pseudomonas aeruginosa* [preprint]. http://biorxiv.org/lookup/doi/10.1101/2023.01.29.526047

Wang, J., Brodmann, M., & Basler, M. (2019). Assembly and Subcellular Localization of Bacterial Type VI Secretion Systems. *Annual Review of Microbiology*, *73*(1), 621-638. https://doi.org/10.1146/annurev-micro-020518-115420

Wang, M., Schaefer, A. L., Dandekar, A. A., & Greenberg, E. P. (2015). Quorum sensing and policing of *Pseudomonas aeruginosa* social cheaters. *Proceedings of the National Academy of Sciences*, *112*(7), 2187-2191. https://doi.org/10.1073/pnas.1500704112

Wang, Y., Gao, L., Rao, X., Wang, J., Yu, H., Jiang, J.,…Hua, Z. (2018). Characterization of lasR-deficient clinical isolates of *Pseudomonas aeruginosa*. *Scientific Reports*, *8*(1), 13344. https://doi.org/10.1038/s41598-018-30813-y

Wang, Y., Yu, Q., Zhou, R., Feng, T., Hilal, M. G., & Li, H. (2021). Nationality and body location alter human skin microbiome. *Applied Microbiology and Biotechnology*, *105*(12), 5241-5256. https://doi.org/10.1007/s00253-021-11387-8

Wen, H., Liu, G., Geng, Z., Zhang, H., Li, Y., She, Z., & Dong, Y. (2021). Structure and SAXS studies unveiled a novel inhibition mechanism of the *Pseudomonas aeruginosa* T6SS TseT-TsiT complex. *International Journal of Biological Macromolecules*, *188*, 450-459. https://doi.org/10.1016/j.ijbiomac.2021.08.029

Wettstadt, S., Wood, T. E., Fecht, S., & Filloux, A. (2019). Delivery of the *Pseudomonas aeruginosa* Phospholipase Effectors PldA and PldB in a VgrG- and H2-T6SS-Dependent

Manner. *Frontiers in Microbiology*, *10*, 1718. https://doi.org/10.3389/fmicb.2019.01718

Whiteley, M., Diggle, S. P., & Greenberg, E. P. (2017). Progress in and promise of bacterial quorum sensing research. *Nature*, *551*(7680), 313-320. https://doi.org/10.1038/nature24624

Willger, S. D., Grim, S. L., Dolben, E. L., Shipunova, A., Hampton, T. H., Morrison, H. G.,…Hogan, D. A. (2014). Characterization and quantification of the fungal microbiome in serial samples from individuals with cystic fibrosis. *Microbiome*, *2*(1), 40. https://doi.org/10.1186/2049-2618-2-40

Wolfgang, M. C., Kulasekara, B. R., Liang, X., Boyd, D., Wu, K., Yang, Q.,…Lory, S. (2003). Conservation of genome content and virulence determinants among clinical and environmental isolates of *Pseudomonas aeruginosa*. *Proceedings of the National Academy of Sciences of the United States of America*, *100*(14), 8484-8489. https://doi.org/10.1073/pnas.0832438100

Wolter, D. J., Emerson, J. C., McNamara, S., Buccat, A. M., Qin, X., Cochrane, E.,…Hoffman, L. R. (2013). *Staphylococcus aureus* Small-Colony Variants Are Independently Associated With Worse Lung Disease in Children With Cystic Fibrosis. *Clinical Infectious Diseases*, *57*(3), 384-391. https://doi.org/10.1093/cid/cit270

Wood, T. E., Howard, S. A., Förster, A., Nolan, L. M., Manoli, E., Bullen, N. P.,…Filloux, A. (2019). The *Pseudomonas aeruginosa* T6SS Delivers a Periplasmic Toxin that Disrupts Bacterial Cell Morphology. *Cell Reports*, *29*(1), 187-201.e187. https://doi.org/10.1016/j.celrep.2019.08.094

WHO. (2017). *Prioritization of pathogens to guide discovery, research and development of new antibiotics for drug-resistant bacterial infections, including tuberculosis* (WHO/EMP/IAU/2017.12).).

WHO. (2024). *WHO Bacterial Priority Pathogens List, 2024: bacterial pathogens of public health importance to guide research, development and strategies to prevent and control antimicrobial resistance* (978-92-4-009346-1). https://iris.who.int/bitstream/handle/10665/376776/9789240093461-eng.pdf?sequence=1

Worlitzsch, D., Tarran, R., Ulrich, M., Schwab, U., Cekici, A., Meyer, K. C.,…Döring, G. (2002). Effects of reduced mucus oxygen concentration in airway Pseudomonas infections of cystic fibrosis patients. *Journal of Clinical Investigation*, *109*(3), 317-325. https://doi.org/10.1172/JCI0213870

Wratten, S. J., Wolfe, M. S., Andersen, R. J., & Faulkner, D. J. (1977). Antibiotic Metabolites from a Marine Pseudomonad. *Antimicrobial Agents and Chemotherapy*, *11*(3), 411-414. https://doi.org/10.1128/AAC.11.3.411

Yang, L., Haagensen, J. A. J., Jelsbak, L., Johansen, H. K., Sternberg, C., Høiby, N., & Molin, S. (2008). In Situ Growth Rates and Biofilm Development of *Pseudomonas aeruginosa* Populations in Chronic Lung Infections. *Journal of Bacteriology*, *190*(8), 2767-2776. https://doi.org/10.1128/JB.01581-07

Yang, L., Jelsbak, L., Marvig, R. L., Damkiær, S., Workman, C. T., Rau, M. H.,…Molin, S. (2011). Evolutionary dynamics of bacteria in a human host environment. *Proceedings of the National Academy of Sciences of the United States of America*, *108*(18), 7481-7486. https://doi.org/10.1073/pnas.1018249108

Yang, L., Liu, Y., Markussen, T., Høiby, N., Tolker-Nielsen, T., & Molin, S. (2011). Pattern differentiation in co-culture biofilms formed by *Staphylococcus aureus* and *Pseudomonas aeruginosa*. *FEMS Immunology & Medical Microbiology*, *62*(3), 339-347. https://doi.org/10.1111/j.1574-695X.2011.00820.x

Yasir, M., Thomson, N. M., Turner, A. K., Webber, M. A., & Charles, I. G. (2024). Overflow metabolism provides a selective advantage to Escherichia coli in mixed cultures. *Annals of Microbiology*, *74*(1), 15. https://doi.org/10.1186/s13213-024-01760-z

Zannoni, D. (1989). The respiratory chains of pathogenic pseudomonads. *Biochimica et Biophysica Acta (BBA) - Bioenergetics*, *975*(3), 299-316. https://doi.org/10.1016/S0005-2728(89)80337-8

Zemanick, E. T., Wagner, B. D., Robertson, C. E., Ahrens, Richard C., Chmiel, J. F., Clancy, J. P.,…Harris, J. K. (2017). Airway microbiota across age and disease spectrum in cystic fibrosis. *European Respiratory Journal*, *50*(5), 1700832. https://doi.org/10.1183/13993003.00832-2017

Zhang, V., Nemeth, E., & Kim, A. (2019). Iron in Lung Pathology. *Pharmaceuticals*, *12*(1), 30. https://doi.org/10.3390/ph12010030

Zhang, X.-X., & Rainey, P. B. (2007). Genetic Analysis of the Histidine Utilization (hut) Genes in Pseudomonas fluorescens SBW25. *Genetics*, *176*(4), 2165-2176. https://doi.org/10.1534/genetics.107.075713

Zhao, K., Yang, X., Zeng, Q., Zhang, Y., Li, H., Yan, C.,…Zhou, X. (2023). Evolution of lasR mutants in polymorphic *Pseudomonas aeruginosa* populations facilitates chronic infection of the lung. *Nature Communications*, *14*(1), 5976. https://doi.org/10.1038/s41467-023-41704-w

Zoued, A., Brunet, Y. R., Durand, E., Aschtgen, M.-S., Logger, L., Douzi, B.,…Cascales, E. (2014). Architecture and assembly of the Type VI secretion system. *Biochimica et Biophysica Acta (BBA) - Molecular Cell Research*, *1843*(8), 1664-1673. https://doi.org/10.1016/j.bbamcr.2014.03.018

Appendix

Supplementary Table A.

Detailed list of PAO1$_{MW}$ transcripts with significant differences in abundance: polymicrobial cultures (+) versus monospecies conditions (-)

Gene	Name	Product	log_2 FC	Adjusted p-value
PA0075	*pppA*	PppA	-1.046	4.13E-03
PA0079	*tssK1*	TssK1	-1.120	7.48E-05
PA0080	*tssJ1*	TssJ1	-1.299	1.94E-04
PA0083	*tssB1*	TssB1	-1.284	3.58E-07
PA0089	*tssG1*	TssG1	-1.179	4.75E-03
PA0120	probable transcriptional regulator	NA	-1.189	1.60E-04
PA0121	hypothetical protein	NA	-1.213	6.16E-07
PA0534	*pauB1*	NA	-1.237	2.78E-05
PA0603	*agtA*	AgtA	1.523	4.19E-10
PA0907	*alpA*	NA	-1.038	3.32E-06
PA1072	*braE*	branched-chain amino acid transport protein BraE	-1.001	6.37E-05
PA1073	*braD*	branched-chain amino acid transport protein BraD	-1.080	1.74E-05
PA1260	*lhpP*	NA	-1.134	4.98E-05
PA1320	*cyoD*	cytochrome o ubiquinol oxidase subunit IV	1.024	7.26E-03
PA1429	probable cation-transporting P-type ATPase	NA	-1.072	1.78E-07
PA1500	probable oxidoreductase	probable oxidoreductase	-1.319	2.29E-04
PA1514	ureidoglycolate hydrolaseYbbT	ureidoglycolate hydrolaseYbbT	-1.053	3.64E-07
PA1515	*alc*	allantoicase	-1.351	4.19E-10
PA1516	hypothetical protein	NA	-1.207	3.82E-10
PA1517	conserved hypothetical protein	NA	-1.286	2.86E-13
PA1602	probable oxidoreductase	probable oxidoreductase	-1.009	3.77E-06

Gene	Name	Product	log_2 FC	Adjusted p-value
PA1854	conserved hypothetical protein	NA	1.675	9.82E-09
PA1856	probable cytochrome oxidase subunit	probable cytochrome oxidase subunit	1.854	4.03E-02
PA1864	probable transcriptional regulator	NA	-1.054	4.26E-04
PA2007	*maiA*	maleylacetoacetate isomerase	-1.421	7.13E-04
PA2008	*fahA*	fumarylacetoacetase	-1.413	1.22E-05
PA2009	*hmgA*	homogentisate 1	-1.415	4.87E-02
PA2013	*liuC*	putative 3-methylglutaconyl-CoA hydratase	-1.104	4.84E-03
PA2014	*liuB*	methylcrotonyl-CoA carboxylase	-1.384	1.38E-06
PA2015	*liuA*	putative isovaleryl-CoA dehydrogenase	-1.418	4.74E-09
PA2016	*liuR*	NA	-1.197	5.69E-05
PA2081	*kynB*	kynurenine formamidase	-1.146	1.39E-04
PA2247	*bkdA1*	2-oxoisovalerate dehydrogenase (alpha subunit)	-2.149	4.27E-18
PA2248	*bkdA2*	2-oxoisovalerate dehydrogenase (beta subunit)	-2.209	6.45E-21
PA2249	*bkdB*	branched-chain alpha-keto acid dehydrogenase (lipoamide component)	-1.763	1.75E-10
PA2250	*lpdV*	lipoamide dehydrogenase-Val	-1.547	1.36E-09
PA2442	*gcvT2*	glycine cleavage system protein T2	1.159	6.59E-06
PA2444	*glyA2*	serine hydroxymethyltransferase	1.069	1.26E-03
PA2756	hypothetical protein	NA	1.145	3.96E-05
PA2757	hypothetical protein	NA	1.405	2.53E-06

Gene	Name	Product	log_2 FC	Adjusted p-value
PA2937	hypothetical protein	NA	-1.003	1.32E-04
PA3415	probable dihydrolipoamide acetyltransferase	probable dihydrolipoamide acetyltransferase	-1.034	1.06E-02
PA3416	probable pyruvate dehydrogenase E1 component	probable pyruvate dehydrogenase E1 component	-1.212	1.01E-03
PA3417	probable pyruvate dehydrogenase E1 component	probable pyruvate dehydrogenase E1 component	-1.261	2.29E-04
PA3608	*potB*	polyamine transport protein PotB	1.015	1.66E-04
PA3609	*potC*	polyamine transport protein PotC	1.102	1.97E-05
PA3865	putative periplasmic lysine-	putative periplasmic lysine-	-1.106	1.40E-08
PA3919	conserved hypothetical protein	NA	-1.107	6.79E-07
PA4033	*mucE*	NA	1.079	7.83E-06
PA4034	*aqpZ*	NA	1.051	6.63E-06
PA4181	hypothetical protein	NA	-1.263	2.82E-04
PA4182	hypothetical protein	NA	-1.162	1.02E-05
PA4288	probable transcriptional regulator	NA	-1.363	7.37E-11
PA4290	probable chemotaxis transducer	probable chemotaxis transducer	-1.076	1.07E-03
PA4309	*pctA*	chemotactic transducer PctA	-1.104	2.30E-07
PA4364	hypothetical protein	NA	-2.044	5.48E-09
PA4365	*lysE*	NA	-1.861	5.48E-09
PA4596	*esrC*	NA	-1.225	2.76E-04
PA4633	probable chemotaxis transducer	probable chemotaxis transducer	-1.310	9.14E-08
PA4828	conserved hypothetical protein	NA	-1.163	2.02E-04

Gene	Name	Product	log_2 FC	Adjusted p-value
PA4829	*lpd3*	dihydrolipoamide dehydrogenase 3	-1.072	1.02E-04
PA4913	probable binding protein component of ABC transporter	probable binding protein component of ABC transporter	-1.049	5.31E-07
PA4916	*nrtR*	NA	-1.120	1.51E-04
PA4918	*pcnA*	nicotinamidase	-1.094	5.92E-09
PA5098	*hutH*	histidine ammonia-lyase	-1.155	9.81E-05
PA5099	probable transporter	NA	-1.342	1.46E-06
PA5100	*hutU*	urocanase	-1.430	5.48E-09
PA5104	conserved hypothetical protein	NA	-1.216	4.60E-04
PA5105	*hutC*	NA	-1.182	4.74E-09
PA5106	conserved hypothetical protein	conserved hypothetical protein	-1.646	3.63E-14
PA5112	*estA*	NA	-1.056	5.48E-09
PA5401	hypothetical protein	NA	-1.229	3.09E-05
PA5507	hypothetical protein	NA	-1.021	6.97E-07

Supplementary Table B.

Detailed list of Δ*lasR* mutant transcripts with significant differences in abundance: polymicrobial cultures (+) versus monospecies conditions (-)

Gene	Name	Product	log_2 FC	Adjusted p-value
PA0050	hypothetical protein	NA	-1.385	1.74E-06
PA0080	*tssJ1*	TssJ1	-1.551	2.35E-04
PA0083	*tssB1*	TssB1	-1.327	1.74E-03
PA0089	*tssG1*	TssG1	-1.354	2.10E-02
PA0090	*clpV1*	ClpV1	-1.592	4.12E-03
PA0108	*coIII*	cytochrome c oxidase	-1.41	4.92E-04
PA0109	hypothetical protein	NA	-1.359	1.52E-05
PA0120	probable transcriptional regulator	NA	-1.542	9.19E-03
PA0121	hypothetical protein	NA	-1.749	1.23E-03

Gene	Name	Product	log_2 FC	Adjusted p-value
PA0134	probable guanine deaminase	probable guanine deaminase	-1.754	6.46E-05
PA0160	hypothetical protein	NA	2.793	5.81E-06
PA0171	*siaB*	NA	1.408	9.20E-05
PA0172	*siaA*	NA	1.962	5.45E-08
PA0179	probable two-component response regulator	probable two-component response regulator	-1.714	1.13E-08
PA0200	hypothetical protein	NA	-1.898	2.81E-03
PA0205	probable permease of ABC transporter	probable permease of ABC transporter	-1.56	5.62E-04
PA0207	probable transcriptional regulator	NA	-1.308	1.26E-03
PA0218	probable transcriptional regulator	NA	-1.826	8.52E-06
PA0359	hypothetical protein	NA	-1.587	2.84E-11
PA0365	*laoB*	NA	-1.467	4.50E-08
PA0366	*laoC*	NA	-2.07	1.29E-13
PA0382	*micA*	NA	1.65	2.12E-06
PA0388	hypothetical protein	NA	-1.406	4.69E-07
PA0416	*chpD*	NA	1.471	5.01E-04
PA0424	*mexR*	multidrug resistance operon repressor MexR	-1.423	3.53E-04
PA0491	probable transcriptional regulator	NA	-1.724	3.37E-04
PA0492	conserved hypothetical protein	NA	-1.463	2.67E-03
PA0523	*norC*	nitric-oxide reductase subunit C	-1.385	1.45E-02
PA0529	conserved hypothetical protein	NA	1.641	3.43E-03
PA0530	probable class III pyridoxal phosphate-	probable class III pyridoxal phosphate-	1.757	1.87E-04

Gene	Name	Product	log_2 FC	Adjusted p-value
	dependent aminotransferase	dependent aminotransferase		
PA0531	probable glutamine amidotransferase	NA	1.682	7.81E-05
PA0534	*pauB1*	NA	-2.997	1.57E-06
PA0535	transcriptional regulator	NA	-2.112	5.70E-06
PA0578	conserved hypothetical protein	NA	1.469	7.24E-07
PA0586	conserved hypothetical protein	NA	-1.486	2.10E-16
PA0587	conserved hypothetical protein	NA	-1.704	8.51E-16
PA0588	conserved hypothetical protein	NA	-1.987	1.29E-13
PA0596	hypothetical protein	hypothetical protein	-1.415	2.01E-05
PA0603	*agtA*	AgtA	1.92	3.55E-04
PA0608	probable phosphoglycolate phosphatase	probable phosphoglycolate phosphatase	1.385	1.84E-06
PA0610	*prtN*	NA	-1.715	7.07E-07
PA0656	probable HIT family protein	NA	-1.442	2.05E-06
PA0673	hypothetical protein	NA	-1.495	3.95E-03
PA0716.2	*xisF4*	NA	-3.047	3.00E-02
PA0717	hypothetical protein of bacteriophage Pf1	NA	-3.067	2.88E-02
PA0718	hypothetical protein of bacteriophage Pf1	NA	-3.609	7.90E-03
PA0719	hypothetical protein of bacteriophage Pf1	NA	-4.641	6.71E-04
PA0720	helix destabilizing protein of bacteriophage Pf1	NA	-5.979	7.84E-05
PA0721	*pfsE*	NA	-4.546	4.45E-03

Gene	Name	Product	log_2 FC	Adjusted p-value
PA0722	hypothetical protein of bacteriophage Pf1	NA	-4.251	1.98E-03
PA0723	*coaB*	NA	-5.476	5.98E-04
PA0724	probable coat protein A of bacteriophage Pf1	NA	-3.227	2.22E-03
PA0725	hypothetical protein of bacteriophage Pf1	NA	-2.148	9.79E-04
PA0726	hypothetical protein of bacteriophage Pf1	NA	-2.313	1.48E-04
PA0727	Pf replication initiator protein	NA	-2.284	3.32E-04
PA0728	probable bacteriophage integrase	NA	-1.577	2.43E-03
PA0830	hypothetical protein	NA	-1.764	5.95E-10
PA0836	*ackA*	acetate kinase	-1.847	5.44E-05
PA0840	probable oxidoreductase	NA	1.431	5.66E-07
PA0862	hypothetical protein	NA	-1.437	4.00E-11
PA0865	*hpd*	4-hydroxyphenylpyruvate dioxygenase	-2.171	1.85E-04
PA0871	*phhB*	NA	-1.475	3.19E-05
PA0872	*phhA*	phenylalanine-4-hydroxylase	-2.077	3.59E-11
PA0907	*alpA*	NA	-2.372	6.52E-05
PA0914	hypothetical protein	NA	1.611	5.03E-05
PA0915	conserved hypothetical protein	NA	1.337	3.15E-04
PA0918	cytochrome b561	NA	-1.424	3.25E-07
PA0942	probable transcriptional regulator	NA	-1.384	3.75E-09
PA0978	conserved hypothetical protein	NA	1.579	6.84E-04

Gene	Name	Product	log_2 FC	Adjusted p-value
PA0984	colicin immunity protein	NA	-1.439	1.12E-03
PA0986	conserved hypothetical protein	NA	-1.744	5.52E-10
PA1003	*mvfR*	Transcriptional regulator MvfR	-1.492	8.86E-12
PA1029	hypothetical protein	NA	-1.739	1.80E-04
PA1030	hypothetical protein	NA	-1.804	1.97E-05
PA1073	*braD*	branched-chain amino acid transport protein BraD	-1.318	8.30E-04
PA1074	*braC*	branched-chain amino acid transport protein BraC	-1.957	2.97E-08
PA1137	probable oxidoreductase	NA	-1.664	1.61E-04
PA1138	probable transcriptional regulator	NA	-1.352	3.26E-05
PA1151	*imm2*	NA	-1.544	8.68E-06
PA1183	*dctA*	C4-dicarboxylate transport protein	1.778	1.37E-08
PA1194	probable amino acid permease	NA	1.4	2.95E-05
PA1196	*ddaR*	NA	-1.695	2.03E-03
PA1210	conserved hypothetical protein	NA	-1.854	3.81E-07
PA1223	probable transcriptional regulator	NA	-1.323	6.30E-05
PA1229	probable transcriptional regulator	NA	-1.412	1.72E-04
PA1239	hypothetical protein	NA	-1.636	5.84E-05
PA1240	probable enoyl-CoA hydratase/isomerase	NA	-1.738	1.66E-04
PA1256	*lhpO*	NA	-1.565	5.02E-04
PA1260	*lhpP*	NA	-2.695	2.46E-09
PA1261	*lhpR*	NA	-1.564	1.76E-04

Gene	Name	Product	log_2 FC	Adjusted p-value
PA1265	hypothetical protein	NA	1.782	4.08E-02
PA1267	*lhpB*	D-hydroxyproline dehydrogenase beta-subunit	1.894	3.03E-02
PA1285	probable transcriptional regulator	NA	-2.64	1.04E-08
PA1286	probable major facilitator superfamily (MFS) transporter	NA	-2.44	2.09E-08
PA1289	hypothetical protein	NA	-1.907	1.00E-05
PA1290	probable transcriptional regulator	NA	-1.726	2.06E-03
PA1299	conserved hypothetical protein	NA	1.493	1.57E-06
PA1300	*hxuI*	NA	1.719	1.19E-05
PA1301	*hxuR*	NA	1.598	3.21E-03
PA1317	*cyoA*	cytochrome o ubiquinol oxidase subunit II	2.541	8.93E-07
PA1318	*cyoB*	cytochrome o ubiquinol oxidase subunit I	2.494	9.54E-08
PA1319	*cyoC*	cytochrome o ubiquinol oxidase subunit III	2.603	3.09E-08
PA1320	*cyoD*	cytochrome o ubiquinol oxidase subunit IV	2.706	1.13E-07
PA1321	*cyoE*	cytochrome o ubiquinol oxidase protein CyoE	2.693	3.75E-09
PA1413	probable transcriptional regulator	NA	-1.439	7.66E-04
PA1414	hypothetical protein	NA	-1.808	3.16E-04
PA1421	*gbuA*	guanidinobutyrase	-1.304	6.04E-06
PA1423	*bdlA*	BdlA	-2.094	1.73E-08
PA1479	*ccmE*	NA	1.342	5.49E-04
PA1480	*ccmF*	NA	1.708	4.30E-05
PA1481	*ccmG*	NA	1.556	1.49E-04

Gene	Name	Product	log_2 FC	Adjusted p-value
PA1482	*ccmH*	NA	1.769	3.11E-05
PA1483	*cycH*	NA	1.876	8.83E-05
PA1499	conserved hypothetical protein	conserved hypothetical protein	-1.375	1.86E-02
PA1500	probable oxidoreductase	probable oxidoreductase	-1.96	9.22E-06
PA1502	*gcl*	glyoxylate carboligase	-1.843	4.16E-06
PA1515	*alc*	allantoicase	-1.793	2.05E-05
PA1516	hypothetical protein	NA	-2.213	7.39E-05
PA1517	conserved hypothetical protein	NA	-2.535	4.63E-06
PA1518	conserved hypothetical protein	conserved hypothetical protein	-1.777	4.78E-05
PA1519	probable transporter	NA	-1.357	3.21E-08
PA1531	hypothetical protein	NA	1.561	2.46E-09
PA1537	probable short-chain dehydrogenase	NA	-1.766	3.27E-06
PA1538	probable flavin-containing monooxygenase	NA	-1.927	2.75E-09
PA1553	*ccoO1*	Cytochrome c oxidase	1.326	1.18E-03
PA1554	*ccoN1*	Cytochrome c oxidase	1.435	5.95E-10
PA1561	*aer*	aerotaxis receptor Aer	-1.454	5.98E-04
PA1601	probable aldehyde dehydrogenase	NA	-1.815	9.72E-05
PA1602	probable oxidoreductase	probable oxidoreductase	-2.185	2.02E-07
PA1603	probable transcriptional regulator	NA	-2.183	1.25E-11
PA1604	hypothetical protein	NA	-2.035	7.62E-12
PA1628	probable 3-hydroxyacyl-CoA dehydrogenase	probable 3-hydroxyacyl-CoA dehydrogenase	-1.525	3.69E-05
PA1629	probable enoyl-CoA	NA	-1.566	1.30E-06

Gene	Name	Product	log_2 FC	Adjusted p-value
	hydratase/isomerase			
PA1639	hypothetical protein	NA	1.4	2.95E-04
PA1649	probable short-chain dehydrogenase	NA	1.569	3.07E-03
PA1673	*mhr*	NA	-1.572	2.69E-03
PA1688	hypothetical protein	NA	1.775	7.78E-06
PA1689	conserved hypothetical protein	NA	1.464	2.02E-04
PA1766	hypothetical protein	NA	1.451	1.07E-04
PA1771	*estX*	NA	1.895	5.63E-06
PA1774	*crfX*	NA	1.329	8.55E-07
PA1775	*cmpX*	NA	1.47	4.50E-06
PA1789	hypothetical protein	NA	-1.689	4.08E-04
PA1824	conserved hypothetical protein	NA	1.319	2.35E-03
PA1835	hypothetical protein	NA	-1.595	2.83E-06
PA1848	probable major facilitator superfamily (MFS) transporter	NA	1.51	4.54E-03
PA1853	probable transcriptional regulator	NA	2.22	5.20E-09
PA1854	conserved hypothetical protein	NA	3.305	2.21E-21
PA1855	hypothetical protein	NA	3.48	6.05E-06
PA1856	probable cytochrome oxidase subunit	probable cytochrome oxidase subunit	2.219	6.70E-06
PA1864	probable transcriptional regulator	NA	-2.308	2.49E-05
PA1883	probable NADH-ubiquinone/plastoquinone oxidoreductase	probable NADH-ubiquinone/plastoquinone oxidoreductase	-1.509	1.85E-04

Gene	Name	Product	log_2 FC	Adjusted p-value
PA1884	transcriptional regulator	NA	-1.303	2.77E-02
PA1885	conserved hypothetical protein	NA	-2.436	8.10E-08
PA1888	hypothetical protein	NA	-1.431	1.78E-09
PA1926	Uncharacterized protein	NA	1.326	1.73E-08
PA1930	probable chemotaxis transducer	probable chemotaxis transducer	-1.308	1.02E-05
PA1946	*rbsB*	binding protein component precursor of ABC ribose transporter	-2.024	1.08E-18
PA1947	*rbsA*	ribose transport protein RbsA	-2.355	8.12E-12
PA1982	*exaA*	quinoprotein ethanol dehydrogenase	1.561	4.32E-02
PA2008	*fahA*	fumarylacetoacetase	-1.561	3.44E-03
PA2009	*hmgA*	homogentisate 1	-2.619	2.40E-07
PA2012	*liuD*	methylcrotonyl-CoA carboxylase	-1.326	2.57E-04
PA2013	*liuC*	putative 3-methylglutaconyl-CoA hydratase	-1.631	1.19E-05
PA2014	*liuB*	methylcrotonyl-CoA carboxylase	-1.952	1.99E-07
PA2015	*liuA*	putative isovaleryl-CoA dehydrogenase	-2.6	6.32E-07
PA2016	*liuR*	NA	-2.618	1.53E-05
PA2042	probable transporter (membrane subunit)	NA	1.916	1.19E-05
PA2043	hypothetical protein	NA	1.635	5.62E-04
PA2064	*pcoB*	NA	1.565	5.02E-03
PA2099	probable short-chain dehydrogenase	NA	-1.41	2.21E-03
PA2100	probable transcriptional regulator	NA	-1.502	4.02E-03

Gene	Name	Product	log_2 FC	Adjusted p-value
PA2102	hypothetical protein	NA	-1.559	2.54E-04
PA2103	probable molybdopterin biosynthesis protein MoeB	probable molybdopterin biosynthesis protein MoeB	-1.404	4.23E-04
PA2118	*ada*	NA	1.549	4.25E-04
PA2128	*cupA1*	NA	3.605	5.39E-03
PA2129	*cupA2*	NA	5.186	1.88E-04
PA2130	*cupA3*	NA	3.85	3.26E-03
PA2131	*cupA4*	NA	4.902	6.17E-04
PA2132	*cupA5*	NA	5.203	2.35E-05
PA2133	Cyclic-guanylate-specific phosphodiesterase	NA	4.303	1.68E-03
PA2134	hypothetical protein	NA	3.191	7.34E-03
PA2136	hypothetical protein	NA	-1.854	1.40E-06
PA2187	hypothetical protein	NA	-1.362	2.34E-03
PA2202	probable amino acid permease	NA	1.621	1.20E-04
PA2220	probable transcriptional regulator	NA	-1.378	3.02E-03
PA2221	conserved hypothetical protein	NA	-1.64	9.93E-04
PA2238	*pslH*	PslH	1.645	8.63E-06
PA2239	*pslI*	PslI	1.505	4.04E-05
PA2240	*pslJ*	PslJ	1.758	5.95E-10
PA2242	*pslL*	hypothetical protein	1.403	3.40E-07
PA2245	*pslO*	NA	-1.627	2.32E-03
PA2247	*bkdA1*	2-oxoisovalerate dehydrogenase (alpha subunit)	-3.924	1.91E-21
PA2248	*bkdA2*	2-oxoisovalerate dehydrogenase (beta subunit)	-3.636	3.64E-12
PA2249	*bkdB*	branched-chain alpha-keto acid dehydrogenase (lipoamide component)	-2.92	4.22E-10

Gene	Name	Product	log_2 FC	Adjusted p-value
PA2250	*lpdV*	lipoamide dehydrogenase-Val	-2.529	1.63E-12
PA2277	*arsR*	NA	-1.804	2.18E-06
PA2292	hypothetical protein	NA	-1.687	5.24E-05
PA2297	probable ferredoxin	NA	-1.306	2.47E-03
PA2298	probable oxidoreductase	NA	-1.702	1.05E-04
PA2299	probable transcriptional regulator	NA	-1.639	5.71E-05
PA2322	*gntP*	NA	-2.197	6.49E-04
PA2323	*gapN*	GapN	-2.236	4.49E-04
PA2372	hypothetical protein	NA	-1.336	6.43E-06
PA2411	probable thioesterase	NA	2.592	4.91E-02
PA2413	*pvdH*	L-2	2.306	1.95E-02
PA2424	*pvdL*	NA	1.601	3.76E-02
PA2440	hypothetical protein	NA	1.347	4.00E-02
PA2442	*gcvT2*	glycine cleavage system protein T2	1.532	1.85E-03
PA2443	*sdaA*	L-serine dehydratase	1.345	8.06E-03
PA2444	*glyA2*	serine hydroxymethyltransferase	1.703	8.82E-04
PA2479	*dsbR*	NA	-1.343	4.50E-06
PA2485	hypothetical protein	NA	-1.355	2.28E-03
PA2497	probable transcriptional regulator	NA	-1.302	3.67E-06
PA2501	hypothetical protein	NA	-1.417	2.97E-02
PA2521	*czcB*	NA	-1.443	3.48E-02
PA2531	probable aminotransferase	probable aminotransferase	1.445	5.53E-04
PA2550	probable acyl-CoA dehydrogenase	probable acyl-CoA dehydrogenase	1.859	2.54E-06
PA2555	probable AMP-binding enzyme	probable AMP-binding enzyme	-1.357	6.10E-06
PA2557	probable AMP-binding enzyme	NA	-1.32	4.31E-05

Gene	Name	Product	log_2 FC	Adjusted p-value
PA2566.1	Uncharacterized protein	NA	-1.348	2.24E-04
PA2577	probable transcriptional regulator	NA	-1.407	1.07E-05
PA2589	hypothetical protein	NA	-1.574	1.15E-05
PA2590	hypothetical protein	NA	-1.6	4.51E-07
PA2611	*cysG*	siroheme synthase	1.35	4.11E-05
PA2645	*nuoJ*	NADH dehydrogenase I chain J	1.355	1.17E-05
PA2646	*nuoK*	NADH dehydrogenase I chain K	1.321	1.50E-05
PA2647	*nuoL*	NADH dehydrogenase I chain L	1.437	3.90E-06
PA2648	*nuoM*	NADH dehydrogenase I chain M	1.506	3.51E-07
PA2649	*nuoN*	NADH dehydrogenase I chain N	1.548	5.63E-06
PA2665	*fhpR*	NA	-1.853	3.18E-07
PA2729	hypothetical protein	NA	1.44	4.92E-06
PA2753	hypothetical protein	NA	-1.605	3.60E-03
PA2754	conserved hypothetical protein	NA	-1.503	1.59E-03
PA2756	hypothetical protein	NA	2.535	1.25E-11
PA2757	hypothetical protein	NA	2.329	2.98E-08
PA2769	hypothetical protein	NA	1.597	9.75E-05
PA2805	hypothetical protein	NA	-1.643	8.63E-06
PA2825	*ospR*	NA	-2.125	1.15E-04
PA2826	probable glutathione peroxidase	probable glutathione peroxidase	-2.463	3.34E-04
PA2827	conserved hypothetical protein	NA	-1.332	6.33E-04

Gene	Name	Product	log_2 FC	Adjusted p-value
PA2840	probable ATP-dependent RNA helicase	probable ATP-dependent RNA helicase	1.742	4.11E-05
PA2845	hypothetical protein	NA	-1.403	4.06E-02
PA2846	probable transcriptional regulator	NA	-1.517	2.08E-09
PA2878	hypothetical protein	NA	-1.335	4.12E-05
PA2886	*atuA*	NA	-1.319	1.85E-03
PA2910	conserved hypothetical protein	NA	1.782	8.64E-05
PA2931	*cifR*	NA	-1.888	2.37E-05
PA2932	*morB*	morphinone reductase	-1.995	3.63E-03
PA2937	hypothetical protein	NA	-2.853	2.72E-14
PA2938	probable transporter	NA	-1.961	2.54E-10
PA2941	hypothetical protein	NA	-1.8	1.95E-05
PA2964	*pabC*	4-amino-4-deoxychorismate lyase	1.612	2.75E-04
PA2968	*fabD*	malonyl-CoA-[acyl-carrier-protein] transacylase	1.481	4.63E-04
PA2969	*plsX*	fatty acid biosynthesis protein PlsX	1.7	4.15E-11
PA2998	*nqrB*	NA	1.427	4.48E-05
PA3063	*pelB*	PelB	1.589	8.40E-04
PA3066	hypothetical protein	NA	-1.335	2.04E-04
PA3067	probable transcriptional regulator	NA	-1.56	4.17E-04
PA3123	RidA subfamily protein	NA	-1.539	1.05E-03
PA3124	probable transcriptional regulator	NA	-1.371	1.39E-03
PA3132	probable hydrolase	NA	-1.641	3.02E-05
PA3133	*sawR*	NA	-1.584	4.47E-05

Gene	Name	Product	log_2 FC	Adjusted p-value
PA3165	*hisC2*	histidinol-phosphate aminotransferase	1.439	7.40E-06
PA3187	probable ATP-binding component of ABC transporter	probable ATP-binding component of ABC transporter	-1.564	4.32E-03
PA3190	probable binding protein component of ABC sugar transporter	probable binding protein component of ABC sugar transporter	-2.1	2.53E-03
PA3225	transcriptional regulator	NA	-1.371	2.04E-06
PA3306	hypothetical protein	NA	-1.39	9.64E-08
PA3307	hypothetical protein	NA	-1.546	5.88E-08
PA3308	*hepA*	NA	1.319	2.88E-11
PA3309	conserved hypothetical protein	NA	-1.665	9.93E-05
PA3310	conserved hypothetical protein	conserved hypothetical protein	-1.359	1.48E-04
PA3321	probable transcriptional regulator	NA	-1.331	1.26E-04
PA3323	conserved hypothetical protein	NA	-1.333	6.03E-06
PA3337	*rfaD*	ADP-L-glycero-D-mannoheptose 6-epimerase	-1.382	4.35E-03
PA3367	hypothetical protein	NA	1.337	9.93E-05
PA3394	*nosF*	NosF protein	1.318	1.05E-02
PA3395	*nosY*	NosY protein	1.752	4.51E-04
PA3396	*nosL*	NA	1.992	9.91E-04
PA3415	probable dihydrolipoamide acetyltransferase	probable dihydrolipoamide acetyltransferase	-1.864	5.06E-09
PA3416	probable pyruvate dehydrogenase E1 component	probable pyruvate dehydrogenase E1 component	-2.244	8.84E-14
PA3417	probable pyruvate	probable pyruvate	-2.477	1.29E-13

Gene	Name	Product	log_2 FC	Adjusted p-value
	dehydrogenase E1 component	dehydrogenase E1 component		
PA3418	*ldh*	leucine dehydrogenase	-2.519	4.22E-22
PA3424	hypothetical protein	NA	1.384	3.32E-02
PA3572	hypothetical protein	NA	-1.778	5.83E-06
PA3581	*glpF*	NA	-1.352	3.35E-07
PA3582	*glpK*	glycerol kinase	-1.864	1.19E-08
PA3584	*glpD*	glycerol-3-phosphate dehydrogenase	-2.202	3.65E-12
PA3614	hypothetical protein	NA	-1.536	7.25E-05
PA3630	*gfnR*	NA	-1.349	1.47E-05
PA3635	*eno*	enolase	1.476	4.17E-04
PA3636	*kdsA*	2-dehydro-3-deoxyphosphooctonate aldolase	1.469	1.62E-06
PA3677	*mexJ*	NA	-2.069	1.19E-16
PA3693	conserved hypothetical protein	NA	1.345	1.88E-04
PA3718	probable major facilitator superfamily (MFS) transporter	NA	-1.6	2.09E-09
PA3719	*armR*	antirepressor for MexR	-2.95	1.42E-12
PA3720	hypothetical protein	NA	-2.701	2.92E-45
PA3721	*nalC*	NalC	-1.48	2.33E-08
PA3723	probable FMN oxidoreductase	NA	-1.449	1.64E-06
PA3820	*secF*	secretion protein SecF	1.509	3.55E-05
PA3821	*secD*	secretion protein SecD	1.4	2.38E-07
PA3862	*dauB*	NAD(P)H-dependent anabolic L-arginine dehydrogenase	-1.5	2.99E-04
PA3863	*dauA*	FAD-dependent catabolic D-arginine dehydrogenase	-1.603	2.43E-06

Gene	Name	Product	log_2 FC	Adjusted p-value
PA3864	*dauR*	NA	-1.632	4.88E-05
PA3865	putative periplasmic lysine-	putative periplasmic lysine-	-2.762	4.71E-09
PA3865.1	pyocin S4 immunity protein	NA	-1.371	3.67E-05
PA3877	*narK1*	nitrite extrusion protein 1	-1.663	3.90E-04
PA3885	*tpbA*	NA	1.399	1.53E-02
PA3892	conserved hypothetical protein	NA	1.582	5.48E-04
PA3893	conserved hypothetical protein	NA	1.793	1.94E-05
PA3894	probable outer membrane protein precursor	NA	1.74	7.05E-04
PA3904	PAAR4	NA	2.426	2.12E-06
PA3914	*moeA1*	molybdenum cofactor biosynthetic protein A1	-1.48	1.10E-02
PA3919	conserved hypothetical protein	NA	-2.073	2.83E-06
PA3925	probable acyl-CoA thiolase	probable acyl-CoA thiolase	-1.5	1.44E-11
PA3971	hypothetical protein	NA	-1.554	3.25E-04
PA3972	probable acyl-CoA dehydrogenase	NA	-1.677	5.15E-07
PA3973	probable transcriptional regulator	NA	-1.874	4.68E-06
PA3988	*lptE*	NA	1.372	1.20E-04
PA3993	probable transposase	NA	1.543	1.63E-02
PA3995	probable transcriptional regulator	NA	-1.68	1.07E-06
PA4006	*nadD1*	nicotinate mononucleotide adenylyltransferase NadD1	1.309	2.62E-05
PA4033	*mucE*	NA	2.155	5.95E-10
PA4034	*aqpZ*	NA	2.23	8.58E-08

Gene	Name	Product	log_2 FC	Adjusted p-value
PA4050	*pgpA*	phosphatidylglycerophosphatase A	1.4	7.91E-08
PA4070	probable transcriptional regulator	NA	-1.735	1.57E-12
PA4071	hypothetical protein	NA	-1.482	3.17E-03
PA4090	hypothetical protein	NA	-1.384	9.13E-03
PA4107	*efhP*	NA	-1.34	8.31E-03
PA4108	cyclic di-GMP phosphodiesterase	NA	-1.998	5.93E-08
PA4139	hypothetical protein	NA	2.098	9.46E-06
PA4181	hypothetical protein	NA	-2.15	2.40E-09
PA4182	hypothetical protein	NA	-1.997	4.59E-13
PA4196	*bfiR*	NA	-1.318	7.01E-03
PA4197	*bfiS*	NA	-1.553	1.18E-03
PA4198	probable AMP-binding enzyme	NA	-1.904	2.14E-04
PA4202	*nmoA*	nitronate monooxygenase NmoA	-1.582	5.51E-09
PA4203	*nmoR*	NA	-1.706	2.01E-04
PA4204	*ppgL*	NA	-1.319	8.37E-03
PA4224	*pchG*	pyochelin biosynthetic protein PchG	2.369	1.87E-02
PA4229	*pchC*	NA	2.786	9.98E-03
PA4230	*pchB*	salicylate biosynthesis protein PchB	2.915	1.41E-02
PA4231	*pchA*	salicylate biosynthesis isochorismate synthase	1.667	1.01E-02
PA4238	*rpoA*	DNA-directed RNA polymerase alpha chain	1.337	1.83E-04
PA4243	*secY*	secretion protein SecY	1.405	1.13E-04
PA4288	probable transcriptional regulator	NA	-2.898	4.04E-08

Gene	Name	Product	log_2 FC	Adjusted p-value
PA4289	probable transporter	NA	-2.189	1.39E-12
PA4309	*pctA*	chemotactic transducer PctA	-2.05	7.11E-14
PA4353	conserved hypothetical protein	NA	-1.313	9.57E-06
PA4354	conserved hypothetical protein	NA	-2.001	3.87E-03
PA4359	conserved hypothetical protein	NA	-1.692	3.26E-05
PA4363	*iciA*	NA	-1.489	1.13E-04
PA4364	hypothetical protein	NA	-4.71	4.20E-24
PA4365	*lysE*	NA	-3.258	3.12E-20
PA4368	hypothetical protein	NA	-1.45	1.16E-10
PA4428	*sspA*	NA	1.444	4.51E-06
PA4463	conserved hypothetical protein	NA	-1.54	3.97E-04
PA4479	*mreD*	NA	1.57	7.93E-05
PA4480	*mreC*	NA	1.563	5.59E-11
PA4485	conserved hypothetical protein	NA	1.332	2.67E-03
PA4523	hypothetical protein	NA	-1.893	7.83E-08
PA4535	hypothetical protein	NA	-1.34	2.64E-06
PA4577	hypothetical protein	NA	-1.498	3.90E-04
PA4596	*esrC*	NA	-3.021	2.64E-11
PA4610	hypothetical protein	NA	-1.797	7.61E-04
PA4611	hypothetical protein	NA	-2.017	9.49E-04
PA4633	probable chemotaxis transducer	probable chemotaxis transducer	-2.122	5.19E-20
PA4657	hypothetical protein	NA	-1.649	5.13E-05
PA4658	hypothetical protein	NA	-1.978	9.17E-05
PA4664	*prmC*	NA	1.634	5.55E-05
PA4672	peptidyl-tRNA hydrolase	NA	1.63	1.60E-14

Gene	Name	Product	log_2 FC	Adjusted p-value
PA4673	conserved hypothetical protein	NA	1.404	2.52E-07
PA4674	Antitoxin HigA	NA	-1.883	6.08E-04
PA4674.1	*higB*	NA	-1.802	1.19E-04
PA4683	hypothetical protein	NA	1.748	5.85E-08
PA4739	conserved hypothetical protein	NA	1.64	5.98E-04
PA4809	*fdhE*	NA	1.347	1.09E-03
PA4810	*fdnI*	nitrate-inducible formate dehydrogenase	1.485	1.18E-04
PA4828	conserved hypothetical protein	NA	-2.289	5.23E-04
PA4829	*lpd3*	dihydrolipoamide dehydrogenase 3	-2.479	4.16E-06
PA4830	hypothetical protein	NA	-1.973	9.82E-04
PA4831	probable transcriptional regulator	NA	-1.387	2.39E-02
PA4832	probable short-chain dehydrogenase	NA	-1.883	6.02E-04
PA4837	*cntO*	NA	-1.315	5.78E-05
PA4846	*aroQ1*	3-dehydroquinate dehydratase	1.594	3.54E-12
PA4847	*accB*	biotin carboxyl carrier protein (BCCP)	1.496	7.65E-04
PA4848	*accC*	biotin carboxylase	1.338	2.06E-03
PA4854	*purH*	phosphoribosylaminoimidazolecarboxamide formyltransferase	1.323	5.81E-06
PA4855	*purD*	phosphoribosylamine--glycine ligase	1.386	6.25E-04
PA4865	*ureA*	urease gamma subunit	1.4	1.03E-02
PA4866	putative phosphinothricin acetyltransferase	putative phosphinothricin acetyltransferase	2.15	3.05E-05

Gene	Name	Product	log_2 FC	Adjusted p-value
PA4867	*ureB*	urease beta subunit	2.105	7.91E-06
PA4868	*ureC*	urease alpha subunit	1.681	1.62E-04
PA4898	*opdK*	NA	-2.269	3.45E-11
PA4902	probable transcriptional regulator	NA	-1.906	3.62E-12
PA4903	probable major facilitator superfamily (MFS) transporter	NA	-2.028	4.01E-05
PA4904	*vanA*	vanillate O-demethylase oxygenase subunit	-1.332	4.16E-03
PA4910	branched chain amino acid ABC transporter ATP binding protein	branched chain amino acid ABC transporter ATP binding protein	-1.46	5.09E-06
PA4911	probable permease of ABC branched-chain amino acid transporter	probable permease of ABC branched-chain amino acid transporter	-1.599	5.96E-05
PA4913	probable binding protein component of ABC transporter	probable binding protein component of ABC transporter	-2.196	5.72E-13
PA4916	*nrtR*	NA	-1.314	9.98E-03
PA4965	hypothetical protein	NA	1.339	4.37E-04
PA4966	hypothetical protein	NA	1.681	1.69E-04
PA4979	probable acyl-CoA dehydrogenase	NA	-1.766	4.13E-05
PA4980	probable enoyl-CoA hydratase/isomerase	probable enoyl-CoA hydratase/isomerase	-1.961	1.52E-05
PA5002	*dnpA*	NA	1.364	2.85E-05
PA5027	hypothetical protein	NA	-1.854	9.15E-04
PA5071	conserved hypothetical protein	NA	1.418	1.02E-08

Gene	Name	Product	log_2 FC	Adjusted p-value
PA5095	probable permease of ABC transporter	probable permease of ABC transporter	-1.471	5.82E-07
PA5096	probable binding protein component of ABC transporter	probable binding protein component of ABC transporter	-1.556	5.48E-08
PA5097	probable amino acid permease	NA	-1.676	1.64E-09
PA5098	*hutH*	histidine ammonia-lyase	-2.104	4.51E-14
PA5099	probable transporter	NA	-3.097	1.32E-17
PA5100	*hutU*	urocanase	-3.415	4.89E-35
PA5104	conserved hypothetical protein	NA	-2.011	5.92E-07
PA5105	*hutC*	NA	-2.492	5.50E-22
PA5106	conserved hypothetical protein	conserved hypothetical protein	-3.476	1.51E-42
PA5112	*estA*	NA	-1.636	2.83E-06
PA5117	*typA*	NA	1.371	1.08E-06
PA5153	amino acid (lysine/arginine/ ornithine/histidine/octopine) ABC transporter periplasmic binding protein	NA	-1.563	4.31E-06
PA5183.1	*rsmN*	NA	-1.419	1.20E-03
PA5220	hypothetical protein	NA	1.469	2.27E-04
PA5221	probable FAD-dependent monooxygenase	probable FAD-dependent monooxygenase	1.44	1.16E-03
PA5232	conserved hypothetical protein	NA	-1.681	1.88E-03
PA5264	hypothetical protein	NA	-1.417	5.91E-07
PA5275	conserved hypothetical protein	NA	-1.431	1.40E-05
PA5354	*glcE*	glycolate oxidase subunit GlcE	-1.658	3.67E-02
PA5356	*glcC*	NA	-1.377	2.09E-04
PA5400	probable electron transfer	NA	-1.682	4.62E-02

Gene	Name	Product	log_2 FC	Adjusted p-value
	flavoprotein alpha subunit			
PA5401	hypothetical protein	NA	-1.954	8.01E-05
PA5475	hypothetical protein	NA	-1.817	4.22E-05
PA5506	hypothetical protein	NA	-1.338	5.23E-03
PA5507	hypothetical protein	NA	-1.662	4.92E-05
PA5568	conserved hypothetical protein	conserved hypothetical protein	1.498	3.00E-12

Supplementary Table C.

Detailed list of transcripts with significant differences in abundance: monospecies $PAO1_{MW}$ cultures (+) versus monospecies Δ*lasR* mutant cultures (-)

Gene	Name	Product	log2 FC	Adjusted p-value
PA1430	*lasR*	transcriptional regulator LasR	5.551577	3.26E-45
PA1431	*rsaL*	NA	1.767839	0.022466
PA1432	*lasI*	autoinducer synthesis protein LasI	3.591374	6.13E-11
PA1433	conserved hypothetical protein	NA	1.696242	0.006615

Supplementary Table D.

Detailed list of transcripts with significant differences in abundance: polymicrobial $PAO1_{MW}$ cultures (+) versus polymicrobial Δ*lasR* mutant cultures (-)

Gene	Name	Product	log_2 FC	Adjusted p-value
PA0039	hypothetical protein	NA	-1.071	3.82E-03
PA0046	hypothetical protein	NA	-1.022	3.98E-05
PA0085	*hcp1*	Hcp1	-1.367	7.35E-03
PA0119	probable dicarboxylate transporter	probable dicarboxylate transporter	-1.279	1.63E-02
PA0136	probable ATP-binding component of ABC transporter	NA	1.232	1.31E-02

Gene	Name	Product	log_2 FC	Adjusted p-value
PA0155	*pcaR*	NA	1.412	1.07E-05
PA0160	hypothetical protein	NA	-2.585	7.99E-07
PA0161	hypothetical protein	NA	-2.048	6.36E-12
PA0162	*opdC*	NA	-1.518	6.27E-06
PA0169	*siaD*	SiaD	-1.260	8.23E-06
PA0170	*siaC*	NA	-1.050	1.20E-03
PA0171	*siaB*	NA	-1.493	7.29E-08
PA0173	probable methylesterase	probable methylesterase	1.478	1.76E-02
PA0227	probable CoA transferase	probable CoA transferase	1.483	1.97E-02
PA0359	hypothetical protein	NA	1.003	1.33E-05
PA0451	conserved hypothetical protein	NA	1.103	2.58E-02
PA0503	probable biotin synthesis protein BioC	probable biotin synthesis protein BioC	1.715	2.33E-07
PA0506	probable acyl-CoA dehydrogenase	NA	1.125	7.01E-03
PA0529	conserved hypothetical protein	NA	-1.062	4.14E-04
PA0532	hypothetical protein	NA	-1.278	3.02E-04
PA0535	transcriptional regulator	NA	1.636	1.97E-03
PA0563	conserved hypothetical protein	NA	-1.118	2.67E-07
PA0604	*agtB*	AgtB	-1.081	6.25E-04
PA0672	*hemO*	NA	-1.225	3.94E-02
PA0717	hypothetical protein of bacteriophage Pf1	NA	-1.014	1.55E-02
PA0826	hypothetical protein	NA	-1.227	4.68E-08
PA0839	probable transcriptional regulator	NA	-1.052	9.67E-05
PA0859	hypothetical protein	NA	1.171	9.67E-05
PA0874	hypothetical protein	NA	-2.284	6.27E-06

Gene	Name	Product	log_2 FC	Adjusted p-value
PA0887	*acsA*	acetyl-coenzyme A synthetase	-1.533	5.22E-03
PA0913	*mgtE*	NA	-1.063	3.80E-03
PA0922	hypothetical protein	NA	-1.197	4.59E-07
PA0978	conserved hypothetical protein	NA	-1.755	8.05E-06
PA1051	probable transporter	NA	-1.012	7.69E-03
PA1159	probable cold-shock protein	NA	-1.041	2.55E-05
PA1183	*dctA*	C4-dicarboxylate transport protein	-1.131	5.15E-04
PA1235	probable transcriptional regulator	NA	1.246	3.00E-02
PA1239	hypothetical protein	NA	1.618	2.11E-05
PA1240	probable enoyl-CoA hydratase/isomerase	NA	1.567	9.22E-04
PA1250	aprI	NA	1.190	2.08E-03
PA1251	probable chemotaxis transducer	NA	1.048	1.44E-02
PA1317	*cyoA*	cytochrome o ubiquinol oxidase subunit II	-1.917	5.83E-06
PA1318	*cyoB*	cytochrome o ubiquinol oxidase subunit I	-1.758	2.12E-05
PA1319	*cyoC*	cytochrome o ubiquinol oxidase subunit III	-1.660	2.33E-04
PA1320	*cyoD*	cytochrome o ubiquinol oxidase subunit IV	-1.683	4.03E-04
PA1321	*cyoE*	cytochrome o ubiquinol oxidase protein CyoE	-1.230	1.52E-02
PA1342	*aatJ*	putative acidic amino acid ABC transporter substrate-binding protein	-1.072	1.86E-03
PA1369	hypothetical protein	NA	-1.126	4.91E-07

Gene	Name	Product	log_2 FC	Adjusted p-value
PA1413	probable transcriptional regulator	NA	1.111	6.65E-04
PA1430	*lasR*	transcriptional regulator LasR	5.295	5.61E-90
PA1431	*rsaL*	NA	1.493	1.37E-03
PA1432	*lasI*	autoinducer synthesis protein LasI	3.607	4.33E-17
PA1433	conserved hypothetical protein	NA	2.338	1.27E-09
PA1445	*fliO*	flagellar protein FliO	1.039	2.73E-03
PA1494	*muiA*	NA	1.289	2.61E-03
PA1539	hypothetical protein	NA	-1.239	6.33E-04
PA1540	conserved hypothetical protein	NA	-1.048	1.34E-03
PA1541	probable drug efflux transporter	NA	-1.729	1.58E-09
PA1545	hypothetical protein	NA	-1.180	5.00E-03
PA1601	probable aldehyde dehydrogenase	NA	1.031	1.93E-02
PA1610	*fabA*	beta-hydroxydecanoyl -ACP dehydrase	-1.412	7.10E-13
PA1626	probable major facilitator superfamily (MFS) transporter	NA	1.165	1.85E-03
PA1713	*exsA*	transcriptional regulator ExsA	-1.198	1.79E-03
PA1785	*nasT*	NA	1.035	2.95E-02
PA1835	hypothetical protein	NA	1.082	9.91E-07
PA1856	probable cytochrome oxidase subunit	probable cytochrome oxidase subunit	-1.012	2.33E-04
PA1884	transcriptional regulator	NA	1.396	1.92E-02
PA1885	conserved hypothetical protein	NA	1.314	6.28E-03

Gene	Name	Product	log_2 FC	Adjusted p-value
PA1942	hypothetical protein	NA	1.032	2.02E-05
PA1947	*rbsA*	ribose transport protein RbsA	1.091	8.06E-04
PA1970	hypothetical protein	NA	1.195	7.44E-09
PA1982	*exaA*	quinoprotein ethanol dehydrogenase	-1.917	4.79E-03
PA1983	*exaB*	NA	-1.872	3.53E-02
PA2109	hypothetical protein	NA	1.833	1.85E-02
PA2217	probable aldehyde dehydrogenase	probable aldehyde dehydrogenase	1.044	3.14E-03
PA2268	hypothetical protein	NA	1.995	4.52E-04
PA2277	*arsR*	NA	1.246	6.85E-03
PA2302	*ambE*	NA	1.293	1.62E-04
PA2303	*ambD*	NA	2.227	1.09E-04
PA2304	*ambC*	NA	1.452	6.85E-03
PA2305	*ambB*	NA	1.464	5.12E-04
PA2355	probable FMNH2-dependent monooxygenase	NA	1.083	2.91E-02
PA2386	*pvdA*	NA	-2.763	1.80E-02
PA2392	*pvdP*	NA	-1.320	1.85E-02
PA2393	putative dipeptidase	NA	-1.873	3.89E-03
PA2394	*pvdN*	NA	-1.476	1.80E-02
PA2396	*pvdF*	NA	-1.456	3.38E-03
PA2398	*fpvA*	NA	-1.717	1.86E-03
PA2402	*pvdI*	NA	-1.106	4.19E-02
PA2412	conserved hypothetical protein	conserved hypothetical protein	-3.471	2.25E-02
PA2425	*pvdG*	NA	-1.616	3.88E-02
PA2426	*pvdS*	NA	-2.459	1.45E-03
PA2462	hypothetical protein	NA	-1.037	4.80E-04
PA2478	*dsbD*	NA	1.027	6.01E-03
PA2485	hypothetical protein	NA	1.004	5.03E-04
PA2487	hypothetical protein	NA	1.196	1.25E-05

Gene	Name	Product	log_2 FC	Adjusted p-value
PA2488	probable transcriptional regulator	NA	1.085	2.19E-04
PA2521	*czcB*	NA	1.614	2.86E-02
PA2539	conserved hypothetical protein	NA	-1.131	3.50E-03
PA2540	conserved hypothetical protein	NA	-1.022	1.72E-04
PA2570	*lecA*	LecA	-1.548	1.24E-06
PA2587	*pqsH*	probable FAD-dependent monooxygenase	1.881	2.31E-06
PA2605	conserved hypothetical protein	conserved hypothetical protein	1.212	2.84E-02
PA2667	*mvaU*	NA	-1.137	1.07E-05
PA2668	hypothetical protein	NA	-1.108	3.98E-05
PA2716	probable FMN oxidoreductase	NA	1.031	1.14E-02
PA2729	hypothetical protein	NA	-1.056	1.44E-04
PA2730	hypothetical protein	NA	-1.021	1.75E-06
PA2731	Uncharacterized protein	NA	-1.053	1.42E-04
PA2756	hypothetical protein	NA	-1.216	4.33E-04
PA2762	hypothetical protein	NA	-1.076	8.58E-04
PA2819	hypothetical protein	NA	-1.961	3.01E-06
PA2825	*ospR*	NA	1.224	1.29E-02
PA2880	hypothetical protein	NA	-1.060	5.07E-04
PA2891	*atuF*	geranyl-CoA carboxylase	1.270	1.78E-05
PA2903	*cobJ*	precorrin-3 methylase CobJ	1.088	3.36E-02
PA2904	*cobI*	precorrin-2 methyltransferase CobI	1.188	1.97E-02
PA2910	conserved hypothetical protein	NA	-1.571	1.96E-04
PA2933	probable major facilitator	NA	1.671	1.90E-02

Gene	Name	Product	log_2 FC	Adjusted p-value
	superfamily (MFS) transporter			
PA2935	hypothetical protein	NA	1.477	2.86E-02
PA2937	hypothetical protein	NA	1.086	2.31E-02
PA2947	*cobE*	CobE	1.343	2.77E-02
PA3035	probable glutathione S-transferase	probable glutathione S-transferase	1.579	5.51E-04
PA3037	hypothetical protein	NA	1.020	9.45E-04
PA3063	*pelB*	PelB	-1.150	1.29E-02
PA3067	probable transcriptional regulator	NA	1.081	6.61E-03
PA3132	probable hydrolase	NA	1.309	3.55E-05
PA3133	*sawR*	NA	1.182	9.67E-05
PA3140	hypothetical protein	NA	-1.156	4.90E-09
PA3143	transposase	NA	-1.091	3.18E-08
PA3145	*wbpL*	NA	-1.134	4.54E-09
PA3146	*wbpK*	NA	-1.075	6.97E-07
PA3147	*wbpJ*	NA	-1.096	4.41E-06
PA3148	*wbpI*	UDP-N-acetylglucosamine 2-epimerase WbpI	-1.086	2.42E-05
PA3149	*wbpH*	NA	-1.042	6.77E-04
PA3181	2-keto-3-deoxy-6-phosphogluconate aldolase	2-keto-3-deoxy-6-phosphogluconate aldolase	1.404	2.30E-03
PA3182	*pgl*	6-phosphogluconolactonase	1.711	8.06E-04
PA3193	*glk*	glucokinase	1.146	1.43E-03
PA3291	*tli1*	NA	-1.013	1.60E-02
PA3309	conserved hypothetical protein	NA	1.038	2.14E-02
PA3314	probable ATP-binding component of ABC transporter	probable ATP-binding component of ABC transporter	1.265	5.83E-03

Gene	Name	Product	log_2 FC	Adjusted p-value
PA3321	probable transcriptional regulator	NA	1.421	2.24E-03
PA3410	*hasI*	NA	-1.373	2.92E-04
PA3415	probable dihydrolipoamide acetyltransferase	probable dihydrolipoamide acetyltransferase	1.130	4.95E-02
PA3436	hypothetical protein	NA	2.278	1.92E-17
PA3476	*rhlI*	autoinducer synthesis protein RhlI	1.553	2.46E-05
PA3493	conserved hypothetical protein	NA	1.082	3.19E-02
PA3530	*bfd*	NA	-1.245	2.08E-03
PA3575	hypothetical protein	NA	1.059	1.04E-03
PA3677	*mexJ*	NA	1.370	5.45E-09
PA3681	hypothetical protein	NA	1.001	2.08E-03
PA3718	probable major facilitator superfamily (MFS) transporter	NA	1.251	2.51E-07
PA3719	*armR*	antirepressor for MexR	2.271	2.14E-09
PA3720	hypothetical protein	NA	1.385	4.37E-09
PA3727	hypothetical protein	NA	-1.056	2.29E-02
PA3729	conserved hypothetical protein	NA	-1.270	4.03E-06
PA3730	hypothetical protein	NA	-1.019	5.15E-03
PA3765	hypothetical protein	NA	1.344	2.03E-02
PA3862	*dauB*	NAD(P)H-dependent anabolic L-arginine dehydrogenase	1.670	1.24E-06
PA3863	*dauA*	FAD-dependent catabolic D-arginine dehydrogenase	1.672	1.35E-08
PA3864	*dauR*	NA	1.139	9.67E-05

Gene	Name	Product	log_2 FC	Adjusted p-value
PA3865	putative periplasmic lysine-	putative periplasmic lysine-	1.817	8.18E-09
PA3905	*tecT*	NA	1.967	2.09E-04
PA3907	*tseT*	NA	1.308	3.19E-02
PA3908	*tsiT*	NA	1.661	9.22E-04
PA3925	probable acyl-CoA thiolase	probable acyl-CoA thiolase	1.254	1.80E-08
PA3928	hypothetical protein	NA	1.079	3.06E-02
PA3933	*betT3*	NA	-1.064	1.63E-02
PA4033	*mucE*	NA	-1.053	9.88E-04
PA4139	hypothetical protein	NA	-1.065	3.26E-02
PA4181	hypothetical protein	NA	2.365	6.36E-12
PA4182	hypothetical protein	NA	2.170	2.87E-16
PA4183	hypothetical protein	NA	1.026	5.36E-03
PA4197	*bfiS*	NA	1.117	1.28E-02
PA4202	*nmoA*	nitronate monooxygenase NmoA	1.515	8.91E-10
PA4203	*nmoR*	NA	1.334	1.95E-03
PA4219	*ampO*	NA	-5.000	1.71E-02
PA4229	*pchC*	NA	-3.392	2.54E-04
PA4230	*pchB*	salicylate biosynthesis protein PchB	-3.801	1.53E-02
PA4231	*pchA*	salicylate biosynthesis isochorismate synthase	-1.387	1.75E-02
PA4357	conserved hypothetical protein	NA	1.538	5.70E-03
PA4362	hypothetical protein	NA	1.066	4.86E-02
PA4363	*iciA*	NA	1.414	4.58E-03
PA4364	hypothetical protein	NA	3.270	1.03E-08
PA4365	*lysE*	NA	2.440	3.81E-08
PA4467	hypothetical protein	NA	-1.021	3.01E-03
PA4468	*sodM*	NA	-1.138	2.10E-02
PA4495	hypothetical protein	NA	1.451	8.91E-10

Gene	Name	Product	log_2 FC	Adjusted p-value
PA4581	*rtcR*	NA	1.040	1.56E-05
PA4623	hypothetical protein	NA	1.324	1.96E-05
PA4746	conserved hypothetical protein	NA	-1.074	9.17E-07
PA4829	*lpd3*	dihydrolipoamide dehydrogenase 3	1.364	1.64E-02
PA4830	hypothetical protein	NA	1.210	3.97E-02
PA4832	probable short-chain dehydrogenase	NA	1.195	1.44E-02
PA4846	*aroQ1*	3-dehydroquinate dehydratase	-1.057	1.24E-06
PA4859	probable permease of ABC transporter	probable permease of ABC transporter	1.099	1.16E-02
PA4988	*waaA*	3-deoxy-D-manno-octulosonic-acid (KDO) transferase	1.195	1.86E-03
PA5020	probable acyl-CoA dehydrogenase	probable acyl-CoA dehydrogenase	-1.065	4.52E-04
PA5042	*pilO*	NA	-1.133	1.27E-03
PA5092	*hutI*	imidazolone-5-propionate hydrolase HutI	1.008	6.06E-03
PA5098	*hutH*	histidine ammonia-lyase	1.299	9.22E-04
PA5125	*ntrC*	two-component response regulator NtrC	1.123	2.14E-09
PA5157	probable transcriptional regulator	NA	1.146	1.37E-03
PA5158	probable outer membrane protein precursor	NA	1.186	3.02E-03
PA5291	*betT2*	NA	-1.337	3.42E-05
PA5374	*betI*	NA	-1.193	2.09E-04
PA5375	*betT1*	NA	-1.094	2.03E-07
PA5408	hypothetical protein	NA	1.342	2.71E-02
PA5553	*atpC*	ATP synthase epsilon chain	-1.053	4.16E-02